

# **DAMAGE MITIGATION STRATEGIES**

## **for**

# **NON-STRUCTURAL INFILL WALLS**

A thesis submitted in partial fulfilment of the  
requirements for the Degree of  
Doctor of Philosophy in Civil Engineering  
by

**Ali Sahin Tasligedik**

Supervised by  
Professor Stefano Pampanin

Department of Civil and Natural Resources Engineering  
University of Canterbury  
Christchurch, New Zealand

January 2014



© Copyright 2014 by Ali Sahin Tasligedik  
All Rights Reserved





*This thesis is dedicated to*  
*The people who helped me shape my life and career at important cross roads:*  
*My dear parents Ibrahim Tasligedik and Zeynep Tasligedik*  
*Prof. Dr. Stefano Pampanin*  
*Prof. Dr. Polat Gulkan*  
*Prof. Dr. Tugrul Tankut*



## **ABSTRACT**

In most design codes, infill walls are considered as non-structural elements and thus are typically neglected in the design process. The observations made after major earthquakes (Duzce 1999, L'Aquila 2009, Christchurch 2011) have shown that even though infill walls are considered to be non-structural elements, they interact with the structural system during seismic actions. In the case of heavy infill walls (i.e. clay brick infill walls), the whole behaviour of the structure may be affected by this interaction (i.e. local or global structural failures such as soft storey mechanism). In the case of light infill walls (i.e. non-structural drywalls), this may cause significant economical losses. To consider the interaction of the structural system with the 'non-structural' infill walls at design stage may not be a practical approach due to the complexity of the infill wall behaviour. Therefore, the purpose of the reported research is to develop innovative technological solutions and design recommendations for low damage non-structural wall systems for seismic actions by making use of alternative approaches.

Light (steel/timber framed drywalls) and heavy (unreinforced clay brick) non-structural infill wall systems were studied by following an experimental/numerical research programme. Quasi-static reverse cyclic tests were carried out by utilizing a specially designed full scale reinforced concrete frame, which can be used as a reusable bare frame. In this frame, two RC beams and two RC columns were connected by two un-bonded post tensioning bars, emulating a jointed ductile frame system (PRESSSS technology). Due to the rocking behaviour at the beam-column joint interfaces, this frame was typically a low damage structural solution, with the post-tensioning guaranteeing a linear elastic behaviour. Therefore, this frame could be repeatedly used in all of the tests carried out by changing only the infill walls within this frame. Due to the linear elastic behaviour of this structural bare frame, it was possible to extract the exact behaviour of the infill walls from the global results. In other words, the only parameter that affected the global results was given by the infill walls.

For the test specimens, the existing practice of construction (as built) for both light and heavy non-structural walls was implemented. In the light of the observations taken during these tests, modified low damage construction practices were proposed and tested. In total, seven tests were carried out:

- 1) Bare frame , in order to confirm its linear elastic behaviour.
- 2) As built steel framed drywall specimen FIF1-STFD (Light)
- 3) As built timber framed drywall specimen FIF2-TBFD (Light)
- 4) As built unreinforced clay brick infill wall specimen FIF3-UCBI (Heavy)
- 5) Low damage steel framed drywall specimen MIF1-STFD (Light)
- 6) Low damage timber framed drywall specimen MIF2-TBFD (Light)
- 7) Low damage unreinforced clay brick infill wall specimen MIF5-UCBI (Heavy)

The tests of the as built practices showed that both drywalls and unreinforced clay brick infill walls have a low serviceability inter-storey drift limit (0.2-0.3%). Based on the observations, simple modifications and details were proposed for the low damage specimens. The details proved to be working effectively in lowering the damage and increasing the serviceability drift limits. For drywalls, the proposed low damage solutions do not introduce additional cost, material or labour and they are easily applicable in real buildings. For unreinforced clay brick infill walls, a light steel sub-frame system was suggested that divides the infill panel zone into smaller individual panels, which requires additional labour and some cost. However, both systems can be engineered for seismic actions and their behaviour can be controlled by implementing the proposed details. The performance of the developed details were also confirmed by the numerical case study analyses carried out using Ruaumoko 2D on a reinforced concrete building model designed according to the NZ codes/standards. The results have confirmed that the implementation of the proposed low damage solutions is expected to significantly reduce the non-structural infill wall damage throughout a building.

## **ACKNOWLEDGEMENTS**

I would like to express my deepest gratitude to my primary supervisor Professor Stefano Pampanin. Without his vision and support, this research would not be possible. During my studies, he not only treated me as a supervisor, but also as a part of a big family at the University of Canterbury.

Although I have four older brothers back at home in Turkey, if I were to name someone in New Zealand to call a big brother, he would be Dr. Umut Akguzel. Not because he is one of the other very few Turkish in Christchurch, but because of his wisdom and support throughout my study. I have always respected his suggestions and advices, which were always useful and helpful.

I am also thankful to Professor Polat Gulkan and Professor Tugrul Tankut who have supported and encouraged my decision for choosing New Zealand for my doctoral studies. They affected my life at a very important cross road that I faced.

I also would like to express my gratitude to the Foundation for Research, Science and Technology (FRST) and the Ministry of Science and Innovation (MSI) through the Natural Hazard Research Platform (NHRP) for financially supporting this research as part of the projects “Non-Structural Elements in Building Seismic Performance” and “Improved Seismic Performance of Non-Structural Elements” respectively. The scholarships given by these organizations were crucial for me to carry out my studies at UC.

I am also very grateful to carry out my research in the structures laboratory where Robert Park and Thomas Paulay carried out their research in the past. Their unforgettable image and inspiration in structural engineering and reinforced concrete research has always been one of the greatest motivations for me in the darkest times.

Moreover, the help of the valuable technical staff working in this valuable laboratory is also appreciated. I would like to thank all the technicians who were involved in this research, namely: Gavin Keats (The appointed technician for the research), Mosese

Fifita, John Maley (Lab manager), Stuart Toase, Peter Coursey (Instrumentation and Software), David MacPherson (Technical services manager), Tim Perigo, Bob Wilsea-Smith and Nigel Dixon. Without their technical knowledge and experience, the designs on paper would not be realized.

I wish to extend my acknowledgement to Hans Gerlich and Bruce Levey (Winstone Wallboards Ltd.) for providing the material, labour and practical advice during the design and preparation of the as built and low damage drywalls. Cooperating with the industry was one of the major factors for achieving the reported results in a short period of time. Their cooperation and help will always be remembered and appreciated. I am also thankful to the Austral Bricks for providing the clay bricks used in the clay brick infill wall specimens.

I wish to thank Fidiria Tan for her support in the last year of my PhD when things were sometimes frustrating. Even when in dark times, she was a continuing source of light.

Finally, I wish to thank New Zealand for giving me the chance to be in this beautiful country. New Zealand has become my home away from Turkey. From the day I set foot in this country, I never felt like a foreigner. Seeing the historical ties that we share due to the war in Gallipoli made me realize how close the two nations are connected. I still feel the friendly connections built on Ataturk's speech for the lives lost in Gallipoli:

*Those heroes that shed their blood and lost their lives  
You are now lying in the soil of a friendly country. Therefore, rest in peace  
There is no difference between the Johnnies and the Mehmets to us where they lie side by side  
Here in this country of ours  
You, the mothers who sent their sons from far away countries  
Wipe away your tears  
Your sons are now lying in our bosom and are in peace  
After having lost their lives on this land, they have become our sons as well*

*Mustafa Kemal Ataturk (1934)*

*I thank New Zealand for showing me the same affection in every aspect of daily life*

## TABLE OF CONTENTS

<b>ABSTRACT .....</b>	<b>I</b>
<b>ACKNOWLEDGEMENTS.....</b>	<b>III</b>
<b>TABLE OF CONTENTS .....</b>	<b>V</b>
<b>LIST OF FIGURES .....</b>	<b>IX</b>
<b>LIST OF TABLES.....</b>	<b>XXV</b>
<b>LIST OF VIDEOS.....</b>	<b>XXV</b>
<b>NOTATION.....</b>	<b>XXVII</b>
<b>1 INTRODUCTION .....</b>	<b>3</b>
1.1 EVOLUTION OF CONSTRUCTION PRACTICE IN NEW ZEALAND .....	5
1.2 DEFINITIONS OF LIGHT AND HEAVY PARTITIONS .....	10
1.3 SCOPE.....	10
1.4 OBJECTIVES .....	13
1.5 THESIS OUTLINE .....	15
1.6 REFERENCES .....	16
<b>2 DRYWALLS: LITERATURE AND LESSONS LEARNT FROM EARTHQUAKES.....</b>	<b>21</b>
2.1 LITERATURE REVIEW.....	21
2.2 LESSONS LEARNT FROM THE CHRISTCHURCH EARTHQUAKES: DRYWALL PARTITIONS .....	28
2.3 REFERENCES .....	32
<b>3 UNREINFORCED CLAY BRICK INFILL WALLS: LITERATURE AND LESSONS LEARNT FROM EARTHQUAKES.....</b>	<b>37</b>
3.1 LITERATURE REVIEW.....	37
3.1.1 <i>Experimental Considerations for Heavy Infills: Focusing on Behaviour Modification by Strengthening and Ductility Changes to the Infill Panel Zone .....</i>	<i>37</i>
3.1.2 <i>Numerical Considerations for Heavy Infills: Focusing on the Modifications on the Dynamic Properties of Structures .....</i>	<i>44</i>
3.2 LESSONS LEARNT FROM THE CHRISTCHURCH EARTHQUAKES: HEAVY MASONRY INFILL WALLS 47	
3.3 REFERENCES .....	53
<b>4 EXPERIMENTAL PROGRAMME .....</b>	<b>57</b>
4.1 TEST SETUP.....	57
4.2 TEST SPECIMENS.....	60
4.3 MATERIALS .....	61

4.4	DESIGN OF THE BARE FRAME.....	62
4.4.1	Calculation of the Infill Wall Capacity .....	64
4.4.2	Shear and Moment Capacities of the RC Columns and RC Beams .....	67
4.5	CONSTRUCTION OF THE BARE FRAME .....	70
4.6	INSTRUMENTATION .....	72
4.7	TEST RESULTS .....	73
4.8	NUMERICAL MODEL CALIBRATION .....	74
4.9	REFERENCES.....	75
<b>5</b>	<b>AS BUILT DRYWALL TESTS.....</b>	<b>79</b>
5.1	AS BUILT STEEL FRAMED DRYWALL: FIF1-STFD .....	79
5.1.1	Construction.....	79
5.1.2	Standard Finishing of the Drywall.....	81
5.1.3	Instrumentation.....	82
5.1.4	Test Results .....	83
5.1.5	Numerical Model Calibration .....	89
5.2	AS BUILT TIMBER FRAMED DRYWALL: FIF2-TBFD .....	92
5.2.1	Construction.....	92
5.2.2	Instrumentation.....	94
5.2.3	Test Results .....	95
5.2.4	Numerical Model Calibration .....	103
5.3	OBSERVATIONS, ENERGY DISSIPATION AND EFFECTIVE STIFFNESS PROPERTIES OF THE AS BUILT STEEL AND TIMBER FRAMED DRYWALL SPECIMENS .....	106
5.3.1	Observations and Comparisons .....	106
5.3.2	Energy Dissipation and Stiffness Degradation Properties.....	107
5.4	CONCLUSIONS.....	108
5.5	REFERENCES.....	110
<b>6</b>	<b>LOW DAMAGE DRYWALL TESTS.....</b>	<b>113</b>
6.1	LOW DAMAGE STEEL FRAMED DRYWALL: MIF1-STFD .....	113
6.1.1	Development and Construction.....	113
6.1.2	Finishing of the Drywall.....	116
6.1.3	Instrumentation.....	117
6.1.4	Test Results .....	119
6.1.5	Numerical Model Calibration .....	124
6.2	LOW DAMAGE TIMBER FRAMED DRYWALL: MIF2-TBFD .....	126
6.2.1	Development and Construction.....	126
6.2.2	Finishing of the Drywall.....	129
6.2.3	Instrumentation.....	130
6.2.4	Test Results .....	130
6.2.5	Numerical Model Calibration .....	135



6.3	OBSERVATIONS, ENERGY DISSIPATION AND EFFECTIVE STIFFNESS PROPERTIES OF THE LOW DAMAGE STEEL AND TIMBER FRAMED DRYWALLS .....	137
6.3.1	<i>Observations and Comparisons</i> .....	137
6.3.2	<i>Energy Dissipation and Stiffness Degradation Properties</i> .....	138
6.4	JOINT DETAILS OF THE GENERALIZED LOW DAMAGE NON-STRUCTURAL DRYWALL SOLUTION	139
6.5	CONCLUSIONS.....	139
6.6	REFERENCES .....	140
<b>7</b>	<b>AS BUILT UNREINFORCED CLAY BRICK INFILL WALL TEST .....</b>	<b>143</b>
7.1	AS BUILT UNREINFORCED CLAY BRICK INFILL WALL: FIF3-UCBI.....	143
7.1.1	<i>Construction</i> .....	143
7.1.2	<i>Finishing of the Wall</i> .....	145
7.1.3	<i>Instrumentation</i> .....	146
7.1.4	<i>Test Results</i> .....	146
7.1.5	<i>Numerical Model Calibration</i> .....	153
7.2	OBSERVATIONS, ENERGY DISSIPATION AND EFFECTIVE STIFFNESS PROPERTIES OF THE AS BUILT UNREINFORCED CLAY BRICK INFILL WALL .....	154
7.2.1	<i>Observations and Comparisons</i> .....	154
7.2.2	<i>Energy Dissipation and Stiffness Degradation Properties</i> .....	155
7.3	CONCLUSIONS.....	156
7.4	REFERENCES .....	159
<b>8</b>	<b>LOW DAMAGE UNREINFORCED CLAY BRICK INFILL WALL TESTS .....</b>	<b>163</b>
8.1	LOW DAMAGE UNREINFORCED CLAY BRICK INFILL WALL: MIF5-UCBI.....	163
8.1.1	<i>Development and Design</i> .....	163
8.1.2	<i>Construction</i> .....	168
8.1.3	<i>Instrumentation</i> .....	170
8.1.4	<i>Test Results</i> .....	171
8.1.5	<i>Numerical Model Calibration</i> .....	175
8.2	OBSERVATIONS, ENERGY DISSIPATION AND EFFECTIVE STIFFNESS PROPERTIES OF THE LOW DAMAGE UNREINFORCED CLAY BRICK INFILL WALL.....	177
8.2.1	<i>Observations and Comparisons</i> .....	177
8.2.2	<i>Energy Dissipation and Stiffness Degradation Properties</i> .....	179
8.3	CONCLUSIONS.....	181
8.4	REFERENCES .....	182
<b>9</b>	<b>NUMERICAL CASE STUDIES .....</b>	<b>187</b>
9.1	CASE STUDY BUILDING: 10 STOREY NZS 3101 COMPLIANT REDBOOK BUILDING.....	187
9.2	APPLIED EARTHQUAKES .....	189
9.3	RESULTS FOR AS BUILT AND LOW DAMAGE DRYWALLS .....	192

9.4	RESULTS FOR AS BUILT AND LOW DAMAGE UNREINFORCED CLAY BRICK INFILL WALLS.....	197
9.5	CONCLUSIONS.....	203
9.6	REFERENCES.....	204
<b>10</b>	<b>GENERAL DESIGN RECOMMENDATIONS, CONCLUSIVE REMARKS AND SUGGESTIONS FOR FUTURE STUDIES .....</b>	<b>209</b>
10.1	GENERAL DESIGN RECOMMENDATIONS FOR THE LOW DAMAGE NON-STRUCTURAL WALL SOLUTIONS .....	209
10.2	CONCLUSIVE REMARKS.....	212
10.2.1	<i>Steel and Timber Framed Drywalls: As Built Practice and Low Damage Solutions.....</i>	<i>212</i>
10.2.2	<i>Unreinforced Clay Brick Infill Walls: As Built Practice and Low Damage Solution.....</i>	<i>213</i>
10.2.3	<i>Observations from the Numerical Case Study Building .....</i>	<i>215</i>
10.3	RECOMMENDATIONS FOR FUTURE STUDIES .....	216
	<b>REFERENCES .....</b>	<b>221</b>
	<b>APPENDICES.....</b>	<b>229</b>
	A-ADDITIONAL PHOTOS FOR THE BARE FRAME.....	229
	B-ADDITIONAL PHOTOS FOR THE AS BUILT STEEL FRAMED DRYWALL SPECIMEN FIF1-STFD .....	231
	C-ADDITIONAL PHOTOS FOR THE AS BUILT TIMBER FRAMED DRYWALL SPECIMEN FIF2-TBFD .....	235
	D-ADDITIONAL PHOTOS FOR THE AS BUILT UNREINFORCED CLAY BRICK INFILL WALL SPECIMEN FIF3-UCBI.....	239
	E-ADDITIONAL PHOTOS FOR THE LOW DAMAGE STEEL FRAMED DRYWALL SPECIMEN MIF1-STFD .....	243
	F-ADDITIONAL PHOTOS FOR THE LOW DAMAGE TIMBER FRAMED DRYWALL SPECIMEN MIF2-TBFD .....	247
	G-ADDITIONAL PHOTOS FOR THE LOW DAMAGE UNREINFORCED CLAY BRICK INFILL WALL SPECIMEN MIF5-UCBI.....	251
	H-NUMERICAL MODEL OF THE CASE STUDY BUILDING IN RUAUMOKO 2D WITH AS BUILT STEEL FRAME STRUTS .....	257

## LIST OF FIGURES

FIGURE 1.1. NAPIER EARTHQUAKE 1931 (SOURCE: CHRISTCHURCH CITY LIBRARY) .....	3
FIGURE 1.2. COST BREAKDOWN OF OFFICE BUILDINGS, HOTELS AND HOSPITALS FROM TAGHAVI AND MIRANDA [2] .....	4
FIGURE 1.3. A) CLAY BRICK, B) CONCRETE BLOCK, C) DRYWALL (LIGHT GAUGE STEEL FRAMED).....	4
FIGURE 1.4. THE OBSERVATIONS FOR THE PGC BUILDING AFTER 4 <sup>TH</sup> SEPTEMBER 2010 DARFIELD EARTHQUAKE (PHOTO BY TASLIGEDIK, A.S.) .....	5
FIGURE 1.5. INFILL WALL TYPES AND POSSIBLE OBSERVED DEFICIENCIES (SINCE THE SURVEY IS EXTERIOR ONLY, NO INFORMATION COULD BE GIVEN REGARDING THE PARTITIONS USED INSIDE THE BUILDINGS) .....	6
FIGURE 1.6. SOME EXAMPLE BUILDINGS WITH UNREINFORCED CLAY BRICK INFILL WALLS IN CHRISTCHURCH CBD A) 8 CATHEDRAL SQ., B) 159 MANCHESTER ST., C) 210 HEREFORD ST., D) 172 MANCHESTER ST. ....	8
FIGURE 1.7. A) UNREINFORCED MASONRY INFILL, B) LIGHT STEEL/TIMBER FRAMED WALL, C) REINFORCED GROUTED BRICK MASONRY, D) REINFORCED HOLLOW MASONRY .....	9
FIGURE 1.8. SAMPLE HYSTERESIS CURVES, A) DUCTILE WALL BY PAULAY AND PRIESTLEY [11], B) STRENGTHENING OF INFILLED FRAMES BY OZDEN ET AL. [12] .....	11
FIGURE 1.9. CONCEPTUAL EXPLANATION OF LOW DAMAGE-LOW INTERACTING SOLUTIONS, A) A SAMPLE BASE SHEAR VS. LATERAL DRIFT ENVELOPE CURVE FOR INFILLED AND BARE FRAMES (ORIGINAL GRAPH FOR BARE AND INFILLED FRAME IS TAKEN FROM MAGENES AND PAMPANIN 2004 [10], B) CONCEPTUAL REPRESENTATION OF MINIMIZED INTERACTION, MINIMIZED DAMAGE SOLUTIONS .....	13
FIGURE 1.10. BEHAVIOUR OF DIFFERENT MASONRY INFILL WALL TYPES, A) DIAGONAL CRACKING MECHANISM OF AS BUILT MASONRY INFILL (UNDESIRE), B) BEHAVIOUR OF MODIFIED INFILL WALLS WITH SLIDING DETAILS TO INCREASE DEFORMATION CAPACITY (UNDESIRE), C) BEHAVIOUR OF INFILL WALLS CONSTRUCTED AS MULTIPLE CANTILEVER WALLS WITH DESIGN GAP (DESIRED AND FOLLOWED ANALOGY IN THIS RESEARCH) NOTE: THE PLOTS SHOW AXIAL FORCE AT THE DIAGONAL STRUT VS. INTER-STOREY DRIFT .....	14
FIGURE 2.1. SAMPLE FORCE DEFLECTION HYSTERESIS CURVE FOR DIAGONALLY BRACED STEEL FRAME DRYWALLS BY ADHAM ET. AL. [25] (1990).....	24
FIGURE 2.2. TEST SPECIMEN BY McMULLIN AND MERRICK [27] (2001) .....	24
FIGURE 2.3. TEST SETUP USED BY LEE ET. AL. [28] AND THE TOTAL LATERAL FORCE VS. STORY DRIFT CURVE FOR A DRYWALL WITHOUT OPENING (2006) .....	25
FIGURE 2.4. HYSTERETIC BEHAVIOUR OF A TYPICAL DRYWALL SPECIMEN BY McMULLIN AND MERRICK [29] (2007).....	26
FIGURE 2.5. EXPERIMENTAL AND NUMERICAL COMPARISON OF THE REVERSE CYCLIC BEHAVIOUR OF THE PARTITIONS BY FILIATRAULT ET. AL. [30] (2010) .....	26
FIGURE 2.6. NOVEL SLIDING FRICTIONAL CONNECTION FOR DRYWALLS BY ARAYA-LETELIER AND MIRANDA [32] (2012).....	27

FIGURE 2.7. DAMAGE OBSERVATION AFTER 22 <sup>ND</sup> FEBRUARY 2011 CHRISTCHURCH EARTHQUAKE:	
INTERFACE CRACKING AMONG ADJACENT LININGS .....	29
FIGURE 2.8. DAMAGE OBSERVATION AFTER 22 <sup>ND</sup> FEBRUARY 2011 CHRISTCHURCH EARTHQUAKE: A)	
INTERFACE CRACKING AMONG ADJACENT LININGS, B) BROKEN GYPSUM LINING.....	29
FIGURE 2.9. DAMAGE OBSERVATION AFTER 22 <sup>ND</sup> FEBRUARY 2011 CHRISTCHURCH EARTHQUAKE: A)	
INTERFACE CRACKING AMONG ADJACENT LININGS, B) BROKEN GYPSUM LINING.....	29
FIGURE 2.10. DAMAGE OBSERVATION AFTER 22 <sup>ND</sup> FEBRUARY 2011 CHRISTCHURCH EARTHQUAKE:	
INTERFACE CRACKING AMONG ADJACENT LININGS .....	30
FIGURE 2.11. DAMAGE OBSERVATION AFTER 22 <sup>ND</sup> FEBRUARY 2011 CHRISTCHURCH EARTHQUAKE: A)	
LINING CRACKING DUE TO TIGHTLY FIXED WINDOW CORNER, B) LINING CRACKING DUE TO TIGHTLY FIXED BEAM CORNER .....	30
FIGURE 2.12. DAMAGE OBSERVATION AFTER 22 <sup>ND</sup> FEBRUARY 2011 CHRISTCHURCH EARTHQUAKE: A)	
SEPARATION FROM THE PERPENDICULAR WALL, B) INTERFACE CRACKING AMONG ADJACENT LININGS .....	30
FIGURE 2.13. DAMAGE OBSERVATION AFTER 22 <sup>ND</sup> FEBRUARY 2011 CHRISTCHURCH EARTHQUAKE:	
INTERFACE CRACKING AMONG ADJACENT LININGS .....	31
FIGURE 2.14. DAMAGE OBSERVATION AFTER 22 <sup>ND</sup> FEBRUARY 2011 CHRISTCHURCH EARTHQUAKE: A)	
INTERFACE CRACKING AMONG ADJACENT LININGS, B) LINING CRACKING AT TIGHTLY FIXED DOOR CORNER.....	31
FIGURE 2.15. DAMAGE OBSERVATION AFTER 22 <sup>ND</sup> FEBRUARY 2011 CHRISTCHURCH EARTHQUAKE: A)	
BROKEN GYPSUM LINING, B) UNDERLYING STEEL FRAMING SYSTEM .....	31
FIGURE 3.1. A) ARMATURE CROSS-WALL STRUCTURE AT THE EPICENTRE AFTER DUZCE 1999	
EARTHQUAKE IN TURKEY (NO DAMAGE), B) ARMATURE CROSS WALL STRUCTURE IN PAKISTAN (THE	
DAMAGE TO THE ADJACENT URM BUILDING IS SEVERE COMPARED TO THE ARMATURE CROSS-	
WALL, C) ARMATURE CROSS-WALL APPLIED IN PRACTICE TO AN RC STRUCTURE IN 1965. THE	
BUILDING SUFFERED SOFT STOREY AT GROUND LEVEL AFTER 1965 SAN SALVADOR EARTHQUAKE.	
HOWEVER, PROGRESSIVE PANCAKE WAS PREVENTED DUE TO THE INFILL WALL'S BEING INTACT	
WITH THE SUB-FRAMING.....	38
FIGURE 3.2. IN-PLANE QUASI-STATIC RESPONSE OF INFILLED RC FRAMES BY CALVI AND BOLOGNINI [39]	
(2001) .....	39
FIGURE 3.3. EXPERIMENTAL TESTING OF A SINGLE STOREY, ONE AND TWO BAY STEEL FRAMES INFILLED	
WITH UNREINFORCED MASONRY WALLS BY MOSALAM ET. AL. [40], A) HYSTERESIS ENVELOPES OF	
THE SPECIMENS (S2-N-II: WITHOUT OPENING, S2-SYM AND S2-ASYM: SYMMETRICAL AND	
ASYMMETRICAL OPENINGS), B) EFFECT OF OPENINGS IN CRACKING PATTERNS, THE SPECIMENS FROM	
TOP TO BOTTOM: S2-N-II, S2-SYM, S2-ASYM (1997) .....	39
FIGURE 3.4. EXPERIMENTAL TESTING OF A FULL SCALE, THREE STOREY, RC FLAT SLAB FRAME STRUCTURE	
FROM PUJOL AND FICK [41], A) COMPARISON OF HYSTERESIS CURVES OF BARE AND INFILLED	
FRAME, B) CRACK MAP AT THE END OF THE TEST .....	40
FIGURE 3.5. EXPERIMENTAL TESTING OF A SINGLE-STOREY, SINGLE-BAY STEEL FRAME INFILLED WITH	
UNREINFORCED CLAY BRICKS FROM TASNIMI AND MOHEBKHAH [42], A) CRACKS AND ACTIVATED	

STRESS FIELDS AT INFILL WALL, B) LOAD-DISPLACEMENT ENVELOPES AND COMPARISON OF THE RATIO OF ENERGY DISSIPATION TO DISPLACEMENT ( $2\Delta$ ) PER CYCLE .....	42
FIGURE 3.6. EXPERIMENTAL TESTING OF A STEEL FRAME WITH FRICTION SLIDING FUSES BY MOHAMMADI AND AKRAMI [21], A) DETAIL OF THE SPECIMEN AND THE SLIDER, B) HYSTERESIS CURVE OBTAINED FROM ONE OF THE SPECIMENS, C) PHOTOGRAPHIC VIEW OF THE SPECIMENS.....	43
FIGURE 3.7. A) SIWIS ISOLATOR DETAIL, B) ANALYTICAL LOAD DEFLECTION CURVE COMPARED TO EXPERIMENTAL BARE FRAME CURVE (FROM ALIAARI AND MEMARI [19, 20]).....	44
FIGURE 3.8. A) SENSITIVITY OF FUNDAMENTAL PERIOD WITH RESPECT TO SELECTED PARAMETERS, B) ARCHITECTURE OF ARTIFICIAL NEURAL NETWORK (ANN) MODEL USED FOR SENSITIVITY ANALYSIS FROM (KOSE, [43]).....	45
FIGURE 3.9. COMPARISON OF NUMERICAL EXPRESSIONS PROPOSED BY RICCI ET. AL. [44] AND OTHER RESEARCHERS WITH EXPERIMENTAL OBSERVATIONS (THE PROPOSED EXPRESSION STAYS WITHIN THE ZONE BOUNDED BY THE EXPERIMENTAL OBSERVATIONS) .....	46
FIGURE 3.10. ANALYTICAL WORK OF HASHEMI AND HASSANZADEH [45], A) VIEW FROM A CORNER OF THE BUILDING (STEEL BRACES AND BRICK INFILLS CAN BE SEEN), B) ENERGY DISSIPATED BY EACH COMPONENT IN THE STRUCTURE.....	46
FIGURE 3.11. OBSERVED DAMAGE ON MASONRY INFILLS AFTER THE 22 <sup>ND</sup> FEBRUARY 2011 CHRISTCHURCH EARTHQUAKE, A) DIAGONAL CRACKING, B) CLOSE UP VIEW OF THE DIAGONAL CRACKING.....	47
FIGURE 3.12. OBSERVED DAMAGE ON MASONRY INFILLS AFTER THE 22 <sup>ND</sup> FEBRUARY 2011 CHRISTCHURCH EARTHQUAKE, A) SLIDING SHEAR CRACK, B) OVERALL CORNER DAMAGE.....	47
FIGURE 3.13. OBSERVED DAMAGE ON MASONRY INFILLS AFTER THE 22 <sup>ND</sup> FEBRUARY 2011 CHRISTCHURCH EARTHQUAKE, A-B) DIAGONAL CRACKING.....	48
FIGURE 3.14. OBSERVED DAMAGE ON MASONRY INFILLS AFTER THE 22 <sup>ND</sup> FEBRUARY 2011 CHRISTCHURCH EARTHQUAKE, A) DIAGONAL CRACKING, B) DAMAGE TO COLUMN DUE TO INFILL .....	48
FIGURE 3.15. OBSERVED DAMAGE ON MASONRY INFILLS AFTER THE 22 <sup>ND</sup> FEBRUARY 2011 CHRISTCHURCH EARTHQUAKE, A) SLIDING SHEAR AND COLUMN DAMAGE, B) SLIDING SHEAR AND DIAGONAL CRACK .....	48
FIGURE 3.16. OBSERVED DAMAGE ON MASONRY INFILLS AFTER THE 22 <sup>ND</sup> FEBRUARY 2011 CHRISTCHURCH EARTHQUAKE, A) CORNER CRUSHING, B) STEPPED CRACKS .....	49
FIGURE 3.17. OBSERVED DAMAGE ON MASONRY INFILLS AFTER THE 22 <sup>ND</sup> FEBRUARY 2011 CHRISTCHURCH EARTHQUAKE, A-B) DIAGONAL CRACK.....	49
FIGURE 3.18. OBSERVED DAMAGE ON MASONRY INFILLS AFTER THE 22 <sup>ND</sup> FEBRUARY 2011 CHRISTCHURCH EARTHQUAKE, A) DIAGONAL CRACK, B) SHORT COLUMN.....	49
FIGURE 3.19. OBSERVED DAMAGE ON MASONRY INFILLS AFTER THE 22 <sup>ND</sup> FEBRUARY 2011 CHRISTCHURCH EARTHQUAKE, A) CORNER CRUSHING, B) DIAGONAL CRACKING .....	50
FIGURE 3.20. OBSERVED DAMAGE ON MASONRY INFILLS AFTER THE 22 <sup>ND</sup> FEBRUARY 2011 CHRISTCHURCH EARTHQUAKE, A-B) SLIDING SHEAR CRACK .....	50
FIGURE 3.21. OBSERVED DAMAGE ON MASONRY INFILLS AFTER THE 22 <sup>ND</sup> FEBRUARY 2011 CHRISTCHURCH EARTHQUAKE, A-B) DIAGONAL CRACK.....	50

FIGURE 3.22. OBSERVED DAMAGE ON MASONRY INFILLS AFTER THE 22ND FEBRUARY 2011	
CHRISTCHURCH EARTHQUAKE, A) DIAGONAL CRACK, B) VERTICAL SPLITTING.....	51
FIGURE 3.23. OBSERVED DAMAGE ON MASONRY INFILLS AFTER THE 22ND FEBRUARY 2011	
CHRISTCHURCH EARTHQUAKE, A) CORNER CRUSHING, B) DIAGONAL CRACKING.....	51
FIGURE 3.24. OBSERVED DAMAGE ON MASONRY INFILLS AFTER THE 22ND FEBRUARY 2011	
CHRISTCHURCH EARTHQUAKE, A) SHORT COLUMN, B) DIAGONAL CRACKING.....	51
FIGURE 3.25. OBSERVED DAMAGE ON MASONRY INFILLS AFTER THE 22ND FEBRUARY 2011	
CHRISTCHURCH EARTHQUAKE, A) SEPARATION, B) DIAGONAL CRACKING .....	52
FIGURE 3.26. OBSERVED DAMAGE ON MASONRY INFILLS AFTER THE 22ND FEBRUARY 2011	
CHRISTCHURCH EARTHQUAKE, A-B) DIAGONAL CRACKING .....	52
FIGURE 3.27. OBSERVED DAMAGE ON MASONRY INFILLS AFTER THE 22ND FEBRUARY 2011	
CHRISTCHURCH EARTHQUAKE, A) DIAGONAL CRACKING, B) DIAGONAL CRACKING AND SLIDING ON TOP.....	52
FIGURE 3.28. OBSERVED DAMAGE ON MASONRY INFILLS AFTER THE 22ND FEBRUARY 2011	
CHRISTCHURCH EARTHQUAKE, A) SHORT COLUMN, B) OUT-OF-PLANE FAILURE OF THE CLAY BRICK INFILL WALL .....	53
FIGURE 4.1. TEST SETUP AND BEAM-TO-COLUMN CONNECTION DETAILING .....	58
FIGURE 4.2. PHOTOGRAPHIC VIEW OF THE SETUP .....	58
FIGURE 4.3. APPLIED DRIFT HISTORY .....	59
FIGURE 4.4. GENERAL INSTRUMENTATION SCHEME .....	60
FIGURE 4.5. A) STRESS-STRAIN PROPERTY OF THE STEEL (AVERAGE OF 3 BARS), B) CONCRETE CYLINDER TEST RESULTS (AVERAGE OF 6 CYLINDERS) ON THE TESTING DAY OF THE BARE FRAME.....	61
FIGURE 4.6. FAILURE TYPES FOR FRAMES FULLY INFILLED WITH UNREINFORCED CLAY BRICKS.....	62
FIGURE 4.7. LOCAL AND GLOBAL FAILURES CAUSED BY THE INFILL WALLS, A-B) CORNER CRUSHING RESULTING IN SHORT COLUMN EFFECT AND RESULTING INCREASED SHEAR DEMAND ON COLUMNS, C) GLOBAL SOFT STOREY COLLAPSE MECHANISM (PHOTOS ARE FROM MAGENES AND PAMPANIN [10]).....	63
FIGURE 4.8. GEOMETRICAL DIMENSIONS USED IN THE UNREINFORCED CLAY BRICK INFILL STRUT FORMULATIONS AND CALCULATIONS.....	65
FIGURE 4.9. CLAY BRICK MATERIAL DATA BY KAUSHIK ET. AL. [50], A) BRICK COMPRESSIVE STRENGTH BY DIFFERENT MANUFACTURERS, B) MODULUS OF ELASTICITY VS. COMPRESSIVE STRENGTH, C) CLAY BRICK COMPRESSIVE STRESS VS. STRAIN, D) MORTAR STRESS VS. STRAIN.....	66
FIGURE 4.10. MEMBER FORCE DIAGRAMS UNDER 520 kN TOTAL LATERAL LOADING ON THE FRAME WITH DIAGONAL STRUT, A) AXIAL FORCE, B) SHEAR FORCE.....	68
FIGURE 4.11. MEMBER FORCE DIAGRAMS UNDER 520 kN TOTAL LATERAL LOADING ON THE BARE FRAME, A) SHEAR FORCE, B) MOMENT.....	68
FIGURE 4.12. MEMBER DETAILS, A) RC COLUMNS, B) RC BEAMS .....	69
FIGURE 4.13. MOMENT CURVATURE GRAPHS OF THE RESULTING SECTIONS, A) RC COLUMNS, B) RC BEAMS.....	69

FIGURE 4.14. CONSTRUCTION SEQUENCE OF THE BARE FRAME AND COMPLETED VIEW (FOR OUT-OF-PLANE ROLLERS AND PIN SUPPORT DETAILS, REFER TO FIGURE 4.15).....	71
FIGURE 4.15. OUT OF PLANE ROLLERS AND PIN SUPPORTS OF THE SETUP.....	71
FIGURE 4.16. INSTRUMENTATION SCHEME FOR BARE FRAME AND PHOTO OF THE INSTRUMENTATION AT THE LOWER BEAM COLUMN CONNECTION .....	72
FIGURE 4.17. BARE FRAME TEST RESULTS .....	73
FIGURE 4.18. SKETCH OF THE NUMERICAL MODEL OF BARE FRAME IMPLEMENTED IN RUAUMOKO 2D.....	74
FIGURE 4.19. A) COMPARISON OF NUMERICAL FORCE DISPLACEMENT CURVE TO THE EXPERIMENTAL FORCE DISPLACEMENT, B) EFFECTIVE STIFFNESS VS. INTER-STOREY DRIFT PLOT OF THE BARE FRAME (THE SLIGHT DROP IN THE EFFECTIVE STIFFNESS IS CAUSED BY THE LOSSES OCCURRING IN THE POST-TENSIONING DURING THE TEST).....	75
FIGURE 5.1. AS BUILT STEEL FRAMED DRYWALL FIF1-STFD, A) STEEL TRACK, B) STEEL STUD, C) ANCHORS USED FROM TOP TO BOTTOM: TOP TWO ARE USED FOR STEEL-TO-CONCRETE, THE LAST ONE IS PHILLIPS SELF DRILLING SCREW USED FOR STEEL-TO-STEEL .....	79
FIGURE 5.2. CONSTRUCTION SEQUENCE OF AS BUILT STEEL FRAMED DRYWALL FIF1-STFD AND CLOSE-UP DETAILS OF THE PERIMETER CONNECTIONS.....	80
FIGURE 5.3. AS BUILT STEEL FRAMED DRYWALL FIF1-STFD, A) CONNECTION BETWEEN STEEL TRACK AND CONCRETE, B) CONNECTION BETWEEN STEEL STUD AND TRACK, C) CONNECTION BETWEEN GYPSUM LINING AND STEEL FRAME .....	81
FIGURE 5.4. STANDARD FINISHING FOR DRYWALLS, A) PAPER TAPE, B) PLASTER, C) APPLICATION .....	81
FIGURE 5.5. INSTRUMENTATION OF THE AS BUILT STEEL FRAMED DRYWALL SPECIMEN FIF1-STFD .....	82
FIGURE 5.6. DAMAGE PROGRESS AND THE TOTAL DAMAGE MAP AT THE END OF THE TEST FOR AS BUILT STEEL FRAMED DRYWALL SPECIMEN FIF1-STFD.....	84
FIGURE 5.7. DAMAGE AT THE END OF THE TEST OF AS BUILT STEEL FRAMED DRYWALL SPECIMEN FIF1-STFD .....	85
FIGURE 5.8. DAMAGE MECHANISM FOR AS BUILT STEEL FRAMED DRYWALL FIF1-STFD.....	86
FIGURE 5.9. TEST RESULTS FOR AS BUILT STEEL FRAMED DRYWALL SPECIMEN FIF1-STFD .....	87
FIGURE 5.10. MOST SIGNIFICANT POTENTIOMETER MEASUREMENTS TAKEN FOR HORIZONTAL AND VERTICAL MOVEMENTS IN THE INFILL PANEL ZONE FOR AS BUILT STEEL FRAMED DRYWALL FIF1-STFD (LOCATIONS OF THE POTENTIOMETERS ARE SHOWN ABOVE).....	88
FIGURE 5.11. AS BUILT STEEL FRAMED DRYWALL FIF1-STFD, A) LATERAL FORCE EXERTED ON THE INFILL PANEL ZONE OBTAINED BY SUBTRACTING THE BARE FRAME FROM THE TOTAL, B) DIAGONAL FORCE EXERTED ON THE INFILL PANEL, PROJECTION OF A) IN DIAGONAL DIR. ....	88
FIGURE 5.12. WAYNE STEWART DEGRADING STIFFNESS MODEL FROM RUAUMOKO 2D BY CARR [51] .....	89
FIGURE 5.13. THE NUMERICAL MODEL OF AS BUILT STEEL FRAMED DRYWALL FIF1-STFD FOR RUAUMOKO 2D.....	91
FIGURE 5.14. HYSTERESIS BEHAVIOUR OF THE NUMERICAL MODEL COMPARED TO THE EXPERIMENTAL RESULT FOR AS BUILT STEEL FRAMED DRYWALL FIF1-STFD .....	91
FIGURE 5.15. AS BUILT TIMBER FRAMED DRYWALL FIF2-TBFD, A) USED TIMBER ELEMENTS TO CONSTRUCT THE TIMBER FRAMING, B) USED ANCHOR TYPES .....	92

FIGURE 5.16. CONSTRUCTION SEQUENCE OF AS BUILT TIMBER FRAMED DRYWALL SPECIMEN FIF2-TBFD AND CLOSE-UP DETAILS OF THE PERIMETER CONNECTIONS .....	93
FIGURE 5.17. AS BUILT TIMBER FRAMED DRYWALL FIF2-TBFD, A) CONNECTION BETWEEN TIMBER AND CONCRETE, B) CONNECTION BETWEEN TIMBER ELEMENTS, C) CONNECTION BETWEEN GYPSUM LINING AND TIMBER FRAME.....	94
FIGURE 5.18. INSTRUMENTATION OF THE AS BUILT TIMBER FRAMED DRYWALL SPECIMEN FIF2-TBFD...	95
FIGURE 5.19. DAMAGE PROGRESS AND THE TOTAL DAMAGE MAP AT THE END OF THE AS BUILT TIMBER FRAMED DRYWALL TEST FIF2-TBFD .....	96
FIGURE 5.20. DAMAGE AT THE END OF THE AS BUILT TIMBER FRAMED DRYWALL TEST FIF2-TBFD .....	97
FIGURE 5.21. A) DAMAGE MECHANISM FOR AS BUILT TIMBER FRAMED DRYWALL FIF2-TBFD, B) FAILED ANCHOR COMPARED TO AN INTACT TIMBER TO CONCRETE ANCHOR.....	98
FIGURE 5.22. ANCHOR SPECIFICATIONS GIVEN BY RED HEAD [54].....	99
FIGURE 5.23. TEST RESULTS FOR THE AS BUILT TIMBER FRAMED DRYWALL SPECIMEN FIF2-TBFD .....	101
FIGURE 5.24. THE MOST SIGNIFICANT POTENTIOMETER MEASUREMENTS TAKEN FOR HORIZONTAL AND VERTICAL MOVEMENTS IN THE INFILL PANEL ZONE FOR AS BUILT TIMBER FRAMED DRYWALL FIF2-TBFD (FOR THE LOCATION OF THE POTENTIOMETERS, REFER TO FIGURE 5.5).....	102
FIGURE 5.25. AS BUILT TIMBER FRAMED DRYWALL FIF2-TBFD, A) LATERAL FORCE EXERTED ON THE INFILL PANEL ZONE OBTAINED BY SUBTRACTING THE BARE FRAME FROM THE TOTAL, B) DIAGONAL FORCE EXERTED ON THE INFILL PANEL ZONE, PROJECTION OF A) IN DIAGONAL DIRECTION.....	102
FIGURE 5.26. THE NUMERICAL MODEL OF AS BUILT TIMBER FRAMED DRYWALL FIF2-TBFD FOR RUAUMOKO 2D .....	104
FIGURE 5.27. HYSTERESIS BEHAVIOUR OF THE NUMERICAL MODEL COMPARED TO THE EXPERIMENTAL RESULT FOR AS BUILT TIMBER FRAMED DRYWALL FIF2-TBFD .....	105
FIGURE 5.28. THE ENVELOPE CURVES OF THE BARE FRAME, AS BUILT STEEL FRAMED DRYWALL SPECIMEN FIF1-STFD AND TIMBER FRAMED DRYWALL SPECIMEN FIF2-TBFD.....	106
FIGURE 5.29. AVERAGE DISSIPATED ENERGY ( $E_D$ ) AND AVERAGE EQUIVALENT VISCOUS DAMPING ( $\Xi_{EQ}$ ) WITH RESPECT TO INTER-STOREY DRIFT FOR AS BUILT STEEL FRAMED DRYWALL SPECIMEN FIF1-STFD AND AS BUILT TIMBER FRAMED DRYWALL SPECIMEN FIF2-TBFD .....	107
FIGURE 5.30. STIFFNESS DEGRADATION FOR AS BUILT STEEL FRAMED DRYWALL SPECIMEN FIF1-STFD AND AS BUILT TIMBER FRAMED DRYWALL SPECIMEN FIF2-TBFD WITH RESPECT TO THE INTER-STOREY DRIFT, PLOTTED USING TOTAL LATERAL FORCE (LEFT AXIS) AND USING THE LATERAL FORCE EXERTED BY THE INFILL WALL (RIGHT AXIS) .....	108
FIGURE 6.1. DAMAGE AT THE FASTENERS OBSERVED AT AS BUILT STEEL FRAMED DRYWALL FIF1-STFD .....	113
FIGURE 6.2. MODIFICATIONS TO THE AS BUILT STEEL FRAMED DRYWALL PRACTICE .....	114
FIGURE 6.3. CONNECTION DETAILS USED IN LOW DAMAGE STEEL FRAMED DRYWALL SPECIMEN MIF1-STFD .....	115
FIGURE 6.4. A) FORMATION OF THE SPECIAL H-STUDS USED IN LOW DAMAGE STEEL FRAMED DRYWALL, B) COMPLETED FIRE RATED H- STUD TO BE USED AT THE FIRE-RATED INTERNAL CONNECTION, C)	



COMPLETED NON FIRE RATED H-STUD TO BE USED AT THE NON-FIRE-RATED INTERNAL CONNECTION .....	115
FIGURE 6.5. CONSTRUCTION SEQUENCE OF LOW DAMAGE STEEL FRAMED DRYWALL SPECIMEN MIF1-STFD, FOR DETAILS REFER TO FIGURE 6.3 .....	116
FIGURE 6.6. CLOSE UPS OF THE CONNECTIONS OF LOW DAMAGE STEEL FRAMED DRYWALL SPECIMEN MIF1-STFD, A) EXTERNAL FIRE RATED CONNECTION, B-C) FRICTION FITTED STUD, D-E) FIRE RATED H-STUD, F) LININGS CONNECTED TO NON-FIRE RATED H-STUD, G-H) INTERNAL AND EXTERNAL GAPS .....	117
FIGURE 6.7. A) FINISHING SCHEME, B) ALUMINIUM L-TRIM SPECIFICATION, USED AT THE EDGE OF THE EXTERNAL GYPSUM LININGS (GIB-WWW.GIB.CO.NZ) .....	117
FIGURE 6.8. INSTRUMENTATION OF THE LOW DAMAGE STEEL FRAMED DRYWALL SPECIMEN MIF1-STFD .....	118
FIGURE 6.9. DAMAGE MAP AT THE END OF TEST OF LOW DAMAGE STEEL FRAMED DRYWALL MIF1-STFD .....	119
FIGURE 6.10. DAMAGE AT THE END OF THE TEST OF LOW DAMAGE STEEL FRAMED DRYWALL SPECIMEN MIF1-STFD .....	120
FIGURE 6.11. BEHAVIOUR OF LOW DAMAGE STEEL FRAMED DRYWALL SPECIMEN MIF1-STFD .....	120
FIGURE 6.12. TEST RESULTS FOR THE LOW DAMAGE STEEL FRAMED DRYWALL SPECIMEN MIF1-STFD .....	121
FIGURE 6.13. LOWER AND UPPER POTENTIOMETER READINGS AT THE EXTERNAL GAPS AND THE LOCATIONS OF THE POTENTIOMETERS FOR LOW DAMAGE STEEL FRAMED DRYWALL SPECIMEN MIF1-STFD .....	122
FIGURE 6.14. LOWER AND UPPER POTENTIOMETER READINGS AT THE INTERNAL GAPS FOR LOW DAMAGE STEEL FRAMED DRYWALL MIF1-STFD (FOR POTENTIOMETER LOCATIONS, REFER TO FIGURE 6.13) .....	122
FIGURE 6.15. POTENTIOMETER MEASUREMENTS TAKEN AT THE GAPS (MIF1-STFD, FOR LOCATIONS REFER TO FIGURE 6.13) A) EXTERIOR GAPS, B) INTERIOR GAPS .....	123
FIGURE 6.16. LOW DAMAGE STEEL FRAMED DRYWALL MIF1-STFD, A) LATERAL FORCE EXERTED ON THE INFILL PANEL ZONE OBTAINED BY SUBTRACTING THE BARE FRAME FROM THE TOTAL, B) DIAGONAL FORCE EXERTED ON THE INFILL PANEL, PROJECTION OF A) IN DIAGONAL DIRECTION .....	124
FIGURE 6.17. THE NUMERICAL MODEL OF THE LOW DAMAGE STEEL FRAMED DRYWALL SPECIMEN MIF1-STFD FOR RUAUMOKO 2D .....	125
FIGURE 6.18. HYSTERESIS BEHAVIOUR OF THE NUMERICAL MODEL COMPARED TO THE EXPERIMENTAL RESULT FOR LOW DAMAGE STEEL FRAMED DRYWALL SPECIMEN MIF1-STFD .....	125
FIGURE 6.19. ANCHOR PULL OUT OF THE EXTERNAL STUD IN LOW DAMAGE STEEL FRAMED DRYWALL SPECIMEN MIF1-STFD .....	126
FIGURE 6.20. FOR LOW DAMAGE TIMBER FRAMED DRYWALL; MODIFICATIONS TO THE AS BUILT TIMBER FRAMED DRYWALL TO ACHIEVE A LOW DAMAGE SOLUTION FOR TIMBER FRAMED DRYWALL (MODIFICATIONS WERE MADE CONSIDERING ALSO THE BEHAVIOUR OF THE LOW DAMAGE STEEL FRAMED DRYWALL MIF1-STFD) .....	127

FIGURE 6.21. CONNECTION DETAILS USED IN LOW DAMAGE TIMBER FRAMED DRYWALL SPECIMEN MIF2-TBFD .....	127
FIGURE 6.22. CONSTRUCTION SEQUENCE OF THE LOW DAMAGE TIMBER FRAMED DRYWALL SPECIMEN MIF2-TBFD (FOR DETAILS REFER TO FIGURE 6.21).....	128
FIGURE 6.23. LOW DAMAGE TIMBER FRAMED DRYWALL SPECIMEN MIF2-TBFD, A-B) FIRE RATED EXTERNAL STUD AND INSTALLATION, C) GYPSUM LINING IS NOT FASTENED TO THE FIRE RATED STUD ON RC COLUMN, D-E) FRICTION FITTED STUDS INTO THE STEEL CHANNELS .....	129
FIGURE 6.24. FINISHING SCHEME OF THE LOW DAMAGE TIMBER FRAMED DRYWALL SPECIMEN MIF2-TBFD .....	129
FIGURE 6.25. DAMAGE MAP AT THE END OF THE TEST FOR LOW DAMAGE TIMBER FRAMED DRYWALL SPECIMEN MIF2-TBFD .....	130
FIGURE 6.26. DAMAGE PHOTOS AT THE END OF THE TEST (MIF2-TBFD) .....	131
FIGURE 6.27. BEHAVIOUR MECHANISM FOR THE LOW DAMAGE TIMBER FRAMED DRYWALL SPECIMEN MIF2-TBFD .....	132
FIGURE 6.28. TEST RESULTS FOR THE LOW DAMAGE TIMBER FRAMED DRYWALL SPECIMEN MIF2-TBFD .....	132
FIGURE 6.29. LOWER AND UPPER POTENTIOMETER READINGS AT THE EXTERNAL GAPS AND THE LOCATIONS OF THE POTENTIOMETERS (MIF2-TBFD) .....	133
FIGURE 6.30. LOWER AND UPPER POTENTIOMETER READINGS AT THE INTERNAL LINING JOINTS (MIF2-TBFD, FOR POTENTIOMETER LOCATIONS, REFER TO FIGURE 6.29) .....	134
FIGURE 6.31. POTENTIOMETER MEASUREMENTS TAKEN AT THE MID HEIGHT OF THE WALL FOR THE LOW DAMAGE TIMBER FRAMED DRYWALL SPECIMEN MIF2-TBFD, A) EXTERIOR GAPS, B) INTERIOR GAPS (FOR LOCATIONS REFER TO FIGURE 6.29) .....	134
FIGURE 6.32. LOW DAMAGE TIMBER FRAMED DRYWALL MIF2-TBFD, A) LATERAL FORCE EXERTED ON THE INFILL PANEL ZONE OBTAINED BY SUBTRACTING THE BARE FRAME FROM THE TOTAL, B) DIAGONAL FORCE EXERTED ON THE INFILL PANEL, PROJECTION OF A) IN DIAGONAL DIR. (MIF2-TBFD) .....	135
FIGURE 6.33. THE NUMERICAL MODEL OF THE LOW DAMAGE TIMBER FRAMED DRYWALL SPECIMEN MIF2-TBFD FOR RUAUMOKO 2D .....	136
FIGURE 6.34. THE HYSTERESIS BEHAVIOUR OF THE NUMERICAL MODEL COMPARED TO THE EXPERIMENTAL RESULT FOR THE LOW DAMAGE TIMBER FRAMED DRYWALL SPECIMEN MIF2-TBFD .....	136
FIGURE 6.35. COMPARISON OF THE AS BUILT AND LOW DAMAGE DRYWALL SPECIMEN GLOBAL FORCE-DISPLACEMENT ENVELOPES, A) AS BUILT STEEL FRAMED DRYWALL SPECIMEN FIF1-STFD AND LOW DAMAGE STEEL FRAMED DRYWALL SPECIMEN MIF1-STFD, B) AS BUILT TIMBER FRAMED DRYWALL SPECIMEN FIF2-TBFD AND LOW DAMAGE TIMBER FRAMED DRYWALL SPECIMEN MIF2-TBFD ..	137
FIGURE 6.36. AVERAGE DISSIPATED ENERGY ( $E_D$ ) AND AVERAGE EQUIVALENT VISCOUS DAMPING ( $\varepsilon_{EQ}$ ) WITH RESPECT TO INTER-STORY DRIFT FOR LOW DAMAGE STEEL MIF1-STFD SPECIMEN AND TIMBER FRAMED DRYWALL MIF2-TBFD SPECIMEN .....	138
FIGURE 6.37. STIFFNESS DEGRADATION COMPARISONS OF AS BUILT AND LOW DAMAGE SOLUTIONS FOR STEEL FRAMED (FIF1-STFD, MIF1-STFD) AND TIMBER FRAMED DRYWALLS (FIF2-TBFD, MIF2-	

TBFD), PLOTTED USING TOTAL LATERAL FORCE (LEFT AXIS) AND THE LATERAL FORCE EXERTED BY THE INFILL WALL (RIGHT AXIS).....	138
FIGURE 6.38. PROPOSED LOW DAMAGE NON-STRUCTURAL DRYWALL CONNECTION DETAILS .....	139
FIGURE 7.1. A) DAMAGE PHOTOS FROM ST. ELMO COURTS BUILDING AFTER 22 FEBRUARY 2011 CHRISTCHURCH EARTHQUAKE, B) DIAGONAL CRACKING AT GROUND LEVEL, C) THE REVEALED WALL TIE USED IN THE UNREINFORCED CLAY BRICK CAVITY WALL (DOUBLE SKINNED WALL) .....	143
FIGURE 7.2. USED CLAY BRICK TYPE (70×75×220 MM), PORTLAND CEMENT AND FINE SAND .....	144
FIGURE 7.3. THE CONSTRUCTION OF THE DOUBLE SKINNED UNREINFORCED CLAY BRICK INFILL WALL, AS BUILT UNREINFORCED CLAY BRICK INFILL WALL FIF3-UCBI.....	145
FIGURE 7.4. COMPLETED UNREINFORCED CLAY BRICK INFILL WALL BEFORE THE WHITE PAINT WAS APPLIED FIF3-UCBI.....	145
FIGURE 7.5. INSTRUMENTATION OF THE AS BUILT UNREINFORCED CLAY BRICK INFILL WALL SPECIMEN FIF3-UCBI .....	146
FIGURE 7.6. DAMAGE PROGRESS OF THE AS BUILT CLAY BRICK INFILL WALL SPECIMEN FIF3-UCBI.....	148
FIGURE 7.7. DAMAGE PHOTOS AT THE END OF THE AS BUILT UNREINFORCED CLAY BRICK INFILL WALL TEST FIF3-UCBI.....	149
FIGURE 7.8. DAMAGE MECHANISM FOR AS BUILT UNREINFORCED CLAY BRICK INFILL WALL SPECIMEN FIF3-UCBI .....	150
FIGURE 7.9. TEST RESULTS FOR AS BUILT UNREINFORCED CLAY BRICK INFILL WALL SPECIMEN FIF3-UCBI, A) GLOBAL FORCE VS. INTER-STOREY DRIFT HYSTERESIS, B) POST TENSIONING AND BEAM ELONGATION VS. INTER-STOREY DRIFT .....	151
FIGURE 7.10. THE POTENTIOMETER READINGS TAKEN DURING THE TESTING OF THE AS BUILT UNREINFORCED CLAY BRICK INFILL WALL SPECIMEN FIF3-UCBI (POTENTIOMETER LOCATIONS HAS ALSO BEEN GIVEN ABOVE) .....	152
FIGURE 7.11. AS BUILT UNREINFORCED CLAY BRICK INFILL WALL SPECIMEN FIF3-UCBI, A) LATERAL FORCE EXERTED ON THE INFILL PANEL ZONE OBTAINED BY SUBTRACTING THE BARE FRAME FROM THE TOTAL, B) DIAGONAL FORCE EXERTED ON THE INFILL PANEL ZONE, PROJECTION OF A) IN DIAGONAL DIR.....	152
FIGURE 7.12. THE NUMERICAL MODEL OF AS BUILT UNREINFORCED CLAY BRICK INFILL WALL FOR RUAUMOKO 2D (FULLY INFILLED IN THE INFILL PANEL ZONE).....	153
FIGURE 7.13. HYSTERESIS BEHAVIOUR OF THE NUMERICAL MODEL COMPARED TO THE EXPERIMENTAL RESULT FOR AS BUILT UNREINFORCED CLAY BRICK INFILL WALL SPECIMEN FIF3-UCBI.....	154
FIGURE 7.14. THE ENVELOPE CURVES OF THE BARE FRAME AND AS BUILT UNREINFORCED CLAY BRICK INFILL WALL SPECIMEN FIF3-UCBI.....	155
FIGURE 7.15. AVERAGE VISCOUS DAMPING AND AVERAGE DISSIPATED ENERGY WITH RESPECT TO INTER-STOREY DRIFT FOR AS BUILT UNREINFORCED CLAY BRICK INFILL WALL SPECIMEN FIF3-UCBI ....	156
FIGURE 7.16. STIFFNESS DEGRADATION WITH RESPECT TO THE INTER-STOREY DRIFT, PLOTTED USING TOTAL LATERAL FORCE (LEFT AXIS) AND USING THE LATERAL FORCE EXERTED BY THE INFILL WALL (RIGHT AXIS) FOR AS BUILT UNREINFORCED CLAY BRICK INFILL WALL SPECIMEN FIF3-UCBI .....	156

FIGURE 7.17. SUMMARY OF THE UNREINFORCED CLAY BRICK INFILL WALL SPECIMEN FIF3-UCBI BEHAVIOUR.....	158
FIGURE 8.1. COMPARISON OF BASE SHEAR VS. DRIFT FOR BARE FRAMES AND CLAY BRICK INFILLED FRAMES BY MAGENES AND PAMPANIN [10] .....	163
FIGURE 8.2. ARMATURE CROSS WALLED STRUCTURE AT EPICENTRE AFTER THE DUZCE 1999 EARTHQUAKE IN TURKEY FROM LANGENBACH [37] .....	164
FIGURE 8.3. CHANGE OF GOVERNING FAILURE MODES OF CLAY BRICK INFILLS RELATIVE TO CHANGE IN THICKNESS $t_w=70$ TO $90$ MM AND CHANGE IN MORTAR STRENGTH $0.3$ TO $3.1$ MPa (THE MATERIAL DATA HAS BEEN TAKEN FROM KAUSHIK ET. AL. [50] AND N STANDS FOR THE VERTICAL AXIAL LOAD ON THE CLAY BRICK INFILL WALL IN kN).....	165
FIGURE 8.4. DEVELOPED LOW DAMAGE SOLUTION FOR UNREINFORCED CLAY BRICK INFILL WALL SPECIMEN MIF5-UCBI WITH FOUR 10 MM WIDTH ISOLATION GAPS BETWEEN THE INDIVIDUAL INFILL PANELS.....	166
FIGURE 8.5. USED LIGHT GAUGE STEEL CHANNEL SECTION BY USG [64] ( $50 \times 75 \times 0.75$ MM WAS CHOSEN) .....	166
FIGURE 8.6. CAPACITY CHECK FOR THE STUD MEMBERS BETWEEN THE TOP AND BOTTOM STEEL CHANNELS (CALCULATIONS WERE CARRIED OUT FOR A SINGLE SKIN OF THE INFILL WALL) .....	167
FIGURE 8.7. CAPACITY CHECK FOR THE RC ANCHORS AT TOP AND BOTTOM STEEL CHANNELS (CALCULATIONS WERE CARRIED OUT FOR A SINGLE SKIN OF THE INFILL WALL AND IT HAS BEEN ASSUMED THAT THE WHOLE WEIGHT OF THE INFILL PANEL ZONE WILL BE CARRIED BY THE CONSTRUCTED STEEL SUB-FRAME) .....	167
FIGURE 8.8. DETAILS OF THE LOW DAMAGE SOLUTION FOR DOUBLE SKINNED UNREINFORCED CLAY BRICK INFILL WALL SPECIMEN MIF5-UCBI .....	168
FIGURE 8.9. POLYURETHANE JOINT SEALANT APPLICATION (FIRE RATED SIKAFLEX CONSTRUCTION AP) .....	168
FIGURE 8.10. CONSTRUCTION PROCESS OF THE LOW DAMAGE UNREINFORCED CLAY BRICK INFILL WALL SPECIMEN MIF5-UCBI.....	169
FIGURE 8.11. LOW DAMAGE UNREINFORCED CLAY BRICK INFILL WALL SPECIMEN MIF5-UCBI, A) CONNECTION OF STUD TO THE TOP TRACK, B) THE LOWER RIGHT CORNER OF THE INFILL PANEL ZONE AFTER THE CONSTRUCTION STARTED, C) GENERAL VIEW DURING THE CONSTRUCTION .....	169
FIGURE 8.12. LOW DAMAGE UNREINFORCED CLAY BRICK INFILL WALL SPECIMEN MIF5-UCBI, A) POLYETHYLENE FOAM INSTALLATION, B-C) EXTERNAL AND INTERNAL JOINTS AFTER THE POLYURETHANE JOINT SEALANT APPLICATION, D) GENERAL VIEW AFTER THE CONSTRUCTION WAS FINISHED .....	170
FIGURE 8.13. INSTRUMENTATION OF THE LOW DAMAGE UNREINFORCED CLAY BRICK INFILL WALL SPECIMEN MIF5-UCBI.....	170
FIGURE 8.14. DAMAGE PROGRESS OF THE LOW DAMAGE UNREINFORCED CLAY BRICK INFILL WALL SPECIMEN MIF5-UCBI.....	171
FIGURE 8.15. DAMAGE PHOTOS OF LOW DAMAGE UNREINFORCED CLAY BRICK INFILL WALL SPECIMEN MIF5-UCBI AT THE END OF THE TEST .....	172

FIGURE 8.16. A) BEHAVIOUR OF THE LOW DAMAGE UNREINFORCED CLAY BRICK INFILL WALL SPECIMEN MIF5-UCBI, B) THE DEFORMATION OF POLYURETHANE JOINT SEALANT AT +2.5% DRIFT LEVEL.	173
FIGURE 8.17. TEST RESULTS FOR LOW DAMAGE UNREINFORCED CLAY BRICK INFILL WALL SPECIMEN MIF5-UCBI, A) GLOBAL FORCE VS. INTER-STOREY DRIFT HYSTERESIS, B) POST TENSIONING AND BEAM ELONGATION VS. INTER-STOREY DRIFT.	174
FIGURE 8.18. A) LATERAL FORCE EXERTED ON THE INFILL PANEL ZONE OBTAINED BY SUBTRACTING THE BARE FRAME FROM THE TOTAL, B) DIAGONAL FORCE EXERTED ON THE INFILL PANEL ZONE, PROJECTION OF A) IN DIAGONAL DIR.	174
FIGURE 8.19. POTENTIOMETER READINGS TAKEN AT THE SHOWN LOCATIONS, A-B) UPLIFT AT BOTTOM AND TOP, C) RELATIVE VERTICAL DEFORMATION BETWEEN THE PANEL A AND B, THE PANEL B AND C, D) SLIDING AT TOP AND BOTTOM OF THE INFILL WALL.	175
FIGURE 8.20. THE NUMERICAL MODEL OF LOW DAMAGE UNREINFORCED CLAY BRICK INFILL WALL SPECIMEN MIF4-UCBI FOR RUAUMOKO 2D (STRUT MODEL WITH A $\pm$ GAP TO ACCOUNT FOR THE VERTICAL ISOLATION JOINTS)	176
FIGURE 8.21. HYSTERESIS BEHAVIOUR OF THE NUMERICAL MODEL COMPARED TO THE EXPERIMENTAL RESULT FOR LOW DAMAGE UNREINFORCED CLAY BRICK INFILL WALL SPECIMEN MIF5-UCBI	177
FIGURE 8.22. THE ENVELOPE CURVES OF THE BARE FRAME, AS BUILT AND LOW DAMAGE UNREINFORCED CLAY BRICK INFILL WALL SPECIMENS (FIF3-UCBI AND MIF5-UCBI) ALONG WITH THE KEY DRIFT VALUES	178
FIGURE 8.23. AXIAL DIAGONAL STRUT STRAINS WITH RESPECT TO ASPECT RATIO OF THE INFILL PANEL ZONE AND IMPOSED DRIFT LEVELS GIVEN BY MAGENES AND PAMPANIN [10] AND THE MODIFICATION TO INCORPORATE THE GAP SYSTEM IN THE LOW DAMAGE INFILL WALL SOLUTION (D=1.5% IN THE SHOWN CASE ABOVE), A) AS BUILT CLAY BRICK INFILL WALLS, B) LOW DAMAGE SOLUTION	179
FIGURE 8.24. THE LOW DAMAGE UNREINFORCED CLAY BRICK INFILL WALL COMPARED TO AS BUILT (MIF5-UCBI AND FIF3-UCBI), A) AVERAGE DISSIPATED ENERGY VS. THE INTER-STOREY DRIFT, B) AVERAGE EQUIVALENT VISCOUS DAMPING.	180
FIGURE 8.25. STIFFNESS DEGRADATION VS. INTER-STOREY DRIFT COMPARED TO AS BUILT SPECIMEN, PLOTTED USING THE TOTAL LATERAL FORCE (LEFT AXIS) AND USING THE LATERAL FORCE EXERTED BY THE INFILL WALL (RIGHT AXIS),	180
FIGURE 8.26. CONCEPTUAL ADDED EXTERNAL DISSIPATION OPTIONS FOR THE SUGGESTED LOW DAMAGE SOLUTION FOR UNREINFORCED CLAY BRICK INFILL WALL PANELS (INSTEAD OF CLAY BRICKS, TIMBER WALLS CAN ALSO BE USED AS INFILL WALLS)	181
FIGURE 9.1. THE PLAN AND ELEVATION VIEW OF THE MODELLED EXTERIOR BARE FRAME	188
FIGURE 9.2. THE DETAILS AND THE MOMENT CURVATURE OF THE RC BEAMS FROM BULL AND BRUNSDON [66]	188
FIGURE 9.3. THE DETAILS, THE AXIAL FORCE-MOMENT INTERACTION AND MOMENT CURVATURE DIAGRAMS OF THE RC COLUMNS FROM BULL AND BRUNSDON [66]	189

FIGURE 9.4. RECORDED GROUND ACCELERATION DATA, ACCELERATION AND DISPLACEMENT RESPONSE SPECTRUM FOR EQ1, EQ2, EQ3, EQ4 AND EQ9, EQ10, EQ11, EQ12 (SET COMPATIBLE WITH 500 YEAR RETURN PERIOD SPECTRUM) .....	191
FIGURE 9.5. RECORDED GROUND ACCELERATION DATA, ACCELERATION AND DISPLACEMENT RESPONSE SPECTRUM FOR EQ5, EQ6, EQ7, EQ8 AND EQ13, EQ14, EQ15, EQ16 (SET COMPATIBLE WITH 2500 YEAR RETURN PERIOD SPECTRUM) .....	192
FIGURE 9.6. COMPARISON OF AS BUILT AND LOW DAMAGE DRYWALL SOLUTIONS USING EQ1-EQ4 AND EQ9-EQ12 (SET COMPATIBLE WITH 500 YEAR RESPONSE SPECTRUM) .....	193
FIGURE 9.7. COMPARISON OF AS BUILT AND LOW DAMAGE DRYWALL SOLUTIONS USING EQ5, EQ6, EQ7, EQ8 AND EQ13, EQ14, EQ15, EQ16 (SET COMPATIBLE WITH 2500 YEAR SPECTRUM).....	194
FIGURE 9.8. DISTRIBUTION OF THE DAMAGE PERCENTAGE FOR AS BUILT STEEL AND TIMBER FRAMED DRYWALLS FOR 1/500 YEAR AND 1/2500 YEAR EVENTS.....	196
FIGURE 9.9. INTER-STOREY DRIFT PROFILE COMPARISONS USING EQ1-EQ4 AND EQ9-EQ12, SOFT STOREY MECHANISM AT AS-BUILT AND BARE FRAME IN EQ11 (SET COMPATIBLE WITH 500 YEAR SPECTRUM) .....	197
FIGURE 9.10. INTER-STOREY DRIFT COMPARISONS USING EQ5-EQ8 AND EQ13-EQ16, SOFT STOREY MECHANISM AT AS BUILT AND BARE FRAME IN EQ7, EQ14 AND EQ15 (SET COMPATIBLE WITH 2500 YEAR SPECTRUM).....	198
FIGURE 9.11. DISTRIBUTION OF THE DAMAGE PERCENTAGE FOR AS BUILT UNREINFORCED CLAY BRICK INFILL WALLS FOR 1/500 YEAR AND 1/2500 YEAR EVENTS.....	199
FIGURE 9.12. INTER-STOREY DRIFT PROFILES FOR THE RC FRAME WITH THE BARE FRAME, AS BUILT AND LOW DAMAGE OPTIONS USING EQ7, EQ11, EQ14 AND EQ15 (WHICH CAUSE SOFT STOREY MECHANISMS FOR EITHER BARE FRAME OR THE AS BUILT OPTION ESPECIALLY IN EQ14: AS BUILT SOFT STOREY MECHANISM PREVENTED AND DRIFTS WERE PULLED FROM ABOUT 6.5% TO 4% BY THE LOW DAMAGE SOLUTION) .....	204
FIGURE 10.1. DESIGN RECOMMENDATIONS FOR LOW DAMAGE DRYWALLS (EITHER STEEL OR TIMBER FRAMED) .....	210
FIGURE 10.2. DESIGN RECOMMENDATIONS FOR LOW DAMAGE UNREINFORCED CLAY BRICK INFILL WALLS .....	211
FIGURE 10.3. POSSIBLE DISSIPATION OPTIONS FOR FUTURE STUDIES .....	218
FIGURE 0.1. A) REINFORCING CAGE, B) CASTING.....	229
FIGURE 0.2. A) BARE FRAME SPECIMEN BF, B) THE REACTION FRAME .....	229
FIGURE 0.3. INSTRUMENTATION LAYOUT AT THE JOINTS .....	230
FIGURE 0.4. DATA COLLECTION AND CONTROL SYSTEM .....	230
FIGURE 0.5. A) STEEL STUD INSTALLATION, B) CUTTING THE GYPSUM LINING.....	231
FIGURE 0.6. GYPSUM LINING INSTALLATION .....	231
FIGURE 0.7. PAPER TAPE APPLICATION FOR THE FINISHING OF THE GYPSUM LINING INTERFACES.....	231
FIGURE 0.8. AS BUILT STEEL FRAMED DRYWALL SPECIMEN FIF1-STFD AFTER THE FINISHING .....	232
FIGURE 0.9. AS BUILT STEEL FRAMED DRYWALL SPECIMEN FIF1-STFD, A) 0.1% DRIFT, B) 0.2% DRIFT .....	232

FIGURE 0.10. AS BUILT STEEL FRAMED DRYWALL SPECIMEN FIF1-STFD, A) 0.3% DRIFT, B) 0.4% DRIFT	232
FIGURE 0.11. AS BUILT STEEL FRAMED DRYWALL SPECIMEN FIF1-STFD, A) 0.5% DRIFT, B) 0.75% DRIFT	233
FIGURE 0.12. AS BUILT STEEL FRAMED DRYWALL SPECIMEN FIF1-STFD, A) 1.0% DRIFT, B) 1.25% DRIFT	233
FIGURE 0.13. AS BUILT STEEL FRAMED DRYWALL SPECIMEN FIF1-STFD, A) 1.5% DRIFT, B) 2.0% DRIFT	233
FIGURE 0.14. AS BUILT STEEL FRAMED DRYWALL SPECIMEN FIF1-STFD AT 2.5% DRIFT (END OF THE TEST)	234
FIGURE 0.15. AS BUILT TIMBER FRAMED DRYWALL SPECIMEN FIF2-TBFD: INSTALLATION OF THE TIMBER ELEMENTS	235
FIGURE 0.16. AS BUILT TIMBER FRAMED DRYWALL SPECIMEN FIF2-TBFD: INSTALLATION OF THE TIMBER-TO-CONCRETE ANCHORS	235
FIGURE 0.17. AS BUILT TIMBER FRAMED DRYWALL SPECIMEN FIF2-TBFD, INSTALLATION OF THE GYPSUM LININGS	235
FIGURE 0.18. AS BUILT TIMBER FRAMED DRYWALL SPECIMEN FIF2-TBFD, A) 0.1% DRIFT, B) 0.2% DRIFT	236
FIGURE 0.19. AS BUILT TIMBER FRAMED DRYWALL SPECIMEN FIF2-TBFD, A) 0.3% DRIFT, B) 0.4% DRIFT	236
FIGURE 0.20. AS BUILT TIMBER FRAMED DRYWALL SPECIMEN FIF2-TBFD, A) 0.5% DRIFT, B) 0.75% DRIFT	236
FIGURE 0.21. AS BUILT TIMBER FRAMED DRYWALL SPECIMEN FIF2-TBFD, A) 1.0% DRIFT, B) 1.25% DRIFT	237
FIGURE 0.22. AS BUILT TIMBER FRAMED DRYWALL SPECIMEN FIF2-TBFD, A) 1.5% DRIFT, B) 2.0% DRIFT	237
FIGURE 0.23. AS BUILT TIMBER FRAMED DRYWALL SPECIMEN FIF2-TBFD AT 2.5% DRIFT (END OF TEST)	237
FIGURE 0.24. AS BUILT UNREINFORCED CLAY BRICK INFILL WALL SPECIMEN: CONSTRUCTION OF THE CLAY BRICKS	239
FIGURE 0.25. AS BUILT UNREINFORCED CLAY BRICK INFILL WALL SPECIMEN FIF3-UCBI, A) SAW CUTTING THE CLAY BRICKS WHEREVER REQUIRED, B) WALL TIES BETWEEN THE TWO SKINS OF CLAY BRICKS	239
FIGURE 0.26. FOUR COURSE LAID CLAY BRICKS AT THE LOWER CORNERS OF THE INFILL PANEL ZONE	239
FIGURE 0.27. AS BUILT UNREINFORCED CLAY BRICK INFILL WALL SPECIMEN FIF3-UCBI, A) +0.75% DRIFT (PUSH), B) -0.75% DRIFT (PULL)	240
FIGURE 0.28. AS BUILT UNREINFORCED CLAY BRICK INFILL WALL SPECIMEN FIF3-UCBI, A) +1.0% DRIFT (PUSH), B) -1.0% DRIFT (PULL)	240
FIGURE 0.29. AS BUILT UNREINFORCED CLAY BRICK INFILL WALL SPECIMEN FIF3-UCBI, A) +1.25% DRIFT (PUSH), B) -1.25% DRIFT (PULL)	240

FIGURE 0.30. AS BUILT UNREINFORCED CLAY BRICK INFILL WALL SPECIMEN FIF3-UCBI, A) +1.5% DRIFT (PUSH), B) -1.5% DRIFT (PULL) .....	241
FIGURE 0.31. AS BUILT UNREINFORCED CLAY BRICK INFILL WALL SPECIMEN FIF3-UCBI, A) +2.0% DRIFT (PUSH), B) -2.0% DRIFT (PULL) .....	241
FIGURE 0.32. AS BUILT UNREINFORCED CLAY BRICK INFILL WALL SPECIMEN FIF3-UCBI, A) +2.5% DRIFT (PUSH), B) -2.5% DRIFT (PULL) .....	241
FIGURE 0.33. LOW DAMAGE STEEL FRAMED DRYWALL SPECIMEN MIF1-STFD, A) INSTALLATION OF THE FIRE-RATED EXTERIOR STUDS, B) INSTALLATION OF THE INTERIOR STUDS AND THE GYPSUM LINING .....	243
FIGURE 0.34. LOW DAMAGE STEEL FRAMED DRYWALL SPECIMEN MIF1-STFD: FRICTION FITTED INTERIOR FIRE-RATED STUD .....	243
FIGURE 0.35. LOW DAMAGE STEEL FRAMED DRYWALL SPECIMEN MIF1-STFD: INSTALLATION OF THE GYPSUM LINING TO THE STEEL STUDS (NO SCREW TO THE STEEL TRACK) .....	243
FIGURE 0.36. LOW DAMAGE STEEL FRAMED DRYWALL SPECIMEN MIF1-STFD, A) EXTERIOR GAP OF 15 MM AT THE EDGE OF THE GYPSUM LINING, B) INTERIOR GAP OF 5 MM AND BOTTOM GAP OF 13 MM AT THE EDGES OF THE GYPSUM LININGS .....	244
FIGURE 0.37. FINISHED LOW DAMAGE STEEL FRAMED DRYWALL SPECIMEN MIF1-STFD.....	244
FIGURE 0.38. LOW DAMAGE STEEL FRAMED DRYWALL SPECIMEN MIF1-STFD AT +2.0% DRIFT: PULL-OUT OF THE EXTERIOR STUDS OF THE DRYWALL.....	245
FIGURE 0.39. LOW DAMAGE STEEL FRAMED DRYWALL SPECIMEN MIF1-STFD AT -2.0% DRIFT: PULL-OUT OF THE EXTERIOR STUDS OF THE DRYWALL .....	245
FIGURE 0.40. LOW DAMAGE STEEL FRAMED DRYWALL SPECIMEN MIF1-STFD AT +2.5% DRIFT .....	246
FIGURE 0.41. LOW DAMAGE STEEL FRAMED DRYWALL SPECIMEN MIF1-STFD AT -2.5% DRIFT .....	246
FIGURE 0.42. LOW DAMAGE TIMBER FRAMED DRYWALL SPECIMEN MIF2-TBFD, A) CONSTRUCTION OF THE TIMBER FRAME WITHIN THE STEEL TRACKS, B) FRICTION FITTED TIMBER STUDS INTO STEEL CHANNELS.....	247
FIGURE 0.43. LOW DAMAGE TIMBER FRAMED DRYWALL SPECIMEN MIF2-TBFD, A) INSTALLATION OF THE EXTERIOR FIRE-RATED TIMBER STUD ON THE TIGHT RC COLUMN (FIRE RATING GIVEN BY THE TWO STRIPS OF GYPSUM BOARDS), B) INSTALLED FIRE-RATED STEEL TRACK ON TOP AND FIRE-RATED EXTERIOR STUD ON THE RIGHT RC COLUMN .....	247
FIGURE 0.44. LOW DAMAGE TIMBER FRAMED DRYWALL SPECIMEN MIF2-TBFD ABOUT TO BE COMPLETED .....	248
FIGURE 0.45. LOW DAMAGE TIMBER FRAMED DRYWALL SPECIMEN MIF2-TBFDAT +2.5% DRIFT (PUSH) .....	248
FIGURE 0.46. LOW DAMAGE TIMBER FRAMED DRYWALL SPECIMEN MIF2-TBFDAT -2.5% DRIFT (PULL) .....	249
FIGURE 0.47. CONSTRUCTION OF THE LOW DAMAGE UNREINFORCED CLAY BRICK INFILL WALL SPECIMEN MIF5-UCBI.....	251
FIGURE 0.48. LOW DAMAGE UNREINFORCED CLAY BRICK INFILL WALL SPECIMEN MIF5-UCBI, A) THE SUB-FRAME SYSTEM, B) THE CLAY BRICKS INFILLED WITHIN THE SUB-FRAME .....	251



FIGURE 0.49. LOW DAMAGE UNREINFORCED CLAY BRICK INFILL WALL SPECIMEN MIF5-UCBI: THE INSTALLATION OF THE POLYETHYLENE FOAM.....	252
FIGURE 0.50. LOW DAMAGE UNREINFORCED CLAY BRICK INFILL WALL SPECIMEN MIF5-UCBI AFTER THE INSTALLATION OF THE POLYURETHANE STRUCTURAL JOINT SEALANT.....	252
FIGURE 0.51. COMPLETED LOW DAMAGE UNREINFORCED CLAY BRICK INFILL WALL SPECIMEN MIF5- UCBI .....	252
FIGURE 0.52. LOW DAMAGE UNREINFORCED CLAY BRICK INFILL WALL SPECIMEN MIF5-UCBI AT +1.5% DRIFT .....	253
FIGURE 0.53. LOW DAMAGE UNREINFORCED CLAY BRICK INFILL WALL SPECIMEN MIF5-UCBI AT -1.5% DRIFT .....	253
FIGURE 0.54. LOW DAMAGE UNREINFORCED CLAY BRICK INFILL WALL SPECIMEN MIF5-UCBI AT +2.0% DRIFT .....	254
FIGURE 0.55. LOW DAMAGE UNREINFORCED CLAY BRICK INFILL WALL SPECIMEN MIF5-UCBI AT -2.0% DRIFT .....	254
FIGURE 0.56. LOW DAMAGE UNREINFORCED CLAY BRICK INFILL WALL SPECIMEN MIF5-UCBI AT +2.5% DRIFT .....	255
FIGURE 0.57. LOW DAMAGE UNREINFORCED CLAY BRICK INFILL WALL SPECIMEN MIF5-UCBI AT -2.5% DRIFT .....	255



## LIST OF TABLES

TABLE 1.1. NZ TYPICAL DIMENSIONS FOR THE WALL TYPES IN FIGURE 1.7.....	9
TABLE 2.1. DESCRIPTION OF WALL PANELS BY FREEMAN IN [22] (1971).....	22
TABLE 2.2. DESCRIPTION OF PARTITION TEST SPECIMENS BY RIHAL IN [23] (1980) .....	23
TABLE 2.3. DAMAGE PROGRESSION REPORTED BY RESTREPO AND LANG [31] (2011) .....	27
TABLE 3.1. SUMMARY OF DAMAGE ACCORDING TO DRIFT LEVELS ACCORDING TO PUJOL AND FICK [41].	40
TABLE 4.1. SUMMARY OF THE TEST SPECIMENS.....	61
TABLE 4.2. SUMMARY OF MATERIAL STRENGTHS.....	62
TABLE 4.3. VALUES OF K1 AND K2 GIVEN BY BERTOLDI ET. AL. [49] .....	64
TABLE 4.4. UNREINFORCED CLAY BRICK DIAGONAL STRUT FAILURE STRENGTHS USING 500 kPa MORTAR STRENGTH (A TYPICALLY ASSUMED MORTAR STRENGTH VALUE).....	67
TABLE 4.5. UNREINFORCED CLAY BRICK DIAGONAL STRUT FAILURE STRENGTHS USING 3100 kPa MORTAR STRENGTH VALUE GIVEN BY KAUSHIK ET. AL. [50] .....	67
TABLE 9.1. SECTION SIZES OF THE MODELLED BUILDING .....	187
TABLE 9.2. LIST OF THE EARTHQUAKES .....	190
TABLE 9.3. SUMMARY FOR THE PERCENTAGE OF THE DAMAGE TO NON-STRUCTURAL WALLS IN THE MODEL BUILDING .....	195
TABLE 9.4. SUMMARY OF THE PERCENTAGE OF THE DAMAGE TO NON-STRUCTURAL WALLS IN THE MODEL BUILDING .....	199
TABLE 9.5. NUMERICAL SUMMARY OF THE INTER-STOREY DRIFT PROFILES FOR EQ1-EQ8 .....	201
TABLE 9.6. NUMERICAL SUMMARY OF THE INTER-STOREY DRIFT PROFILES FOR EQ9-EQ16.....	202
TABLE 10.1. SUMMARY OF THE NON-STRUCTURAL WALL DAMAGE IN THE BUILDING RESULTING FROM THE NUMERICAL ANALYSES OF THE BUILDING .....	216

## LIST OF VIDEOS

	Construction	Testing
<b>FIF1-STFD</b> As built steel framed drywall	<a href="http://youtu.be/EHINFs6vfIQ">http://youtu.be/EHINFs6vfIQ</a>	<a href="http://youtu.be/FgU3c0zfkM8">http://youtu.be/FgU3c0zfkM8</a>
<b>FIF2-TBFD</b> As built timber framed drywall	<a href="http://youtu.be/WAV7m4_E-0">http://youtu.be/WAV7m4_E-0</a>	<a href="http://youtu.be/vGsYnFtr6CI">http://youtu.be/vGsYnFtr6CI</a>
<b>MIF1-STFD</b> Low damage steel framed drywall	<a href="http://youtu.be/FXShuxRWPdg">http://youtu.be/FXShuxRWPdg</a>	<a href="http://youtu.be/Qw5eRRnWbvY">http://youtu.be/Qw5eRRnWbvY</a>
<b>MIF2-TBFD</b> Low damage timber framed drywall	<a href="http://youtu.be/NlxsYaKRdvw">http://youtu.be/NlxsYaKRdvw</a>	<a href="http://youtu.be/KXYVw5iyzho">http://youtu.be/KXYVw5iyzho</a>
<b>FIF3-UCBI</b> As built unreinforced clay brick infill	<a href="http://youtu.be/4xRWa77iZfE">http://youtu.be/4xRWa77iZfE</a>	<a href="http://youtu.be/804H7uckzgE">http://youtu.be/804H7uckzgE</a>
<b>MIF5-UCBI</b> Low damage unreinforced clay brick infill	Not recorded	<a href="http://youtu.be/1h97J9YgFSI">http://youtu.be/1h97J9YgFSI</a>



## NOTATION

$A$	: Shear area of anchorage (timber-to-concrete anchor)
$A_o$	: Area of opening in an infill panel
$A_p$	: Area of infill panel
$A_{sw}$	: Total area of the transverse steel supplied at a section
$b_{wm}$	: Modified equivalent diagonal strut width due to opening
$b_w$	: Compression strut width
$D$	: Design inter-storey drift
$D_i$	: Previous drift amplitude
$D_{i+1}$	: Next drift amplitude
$\Delta_G$	: The required gap width to accommodate the design inter-storey drift
$\delta$	: As built unreinforced clay brick infill wall drift level in the formulation of Magenes and Pampanin (2004)
$d$	: Effective depth of an RC section
$d_w$	: Diagonal strut length (from centroidal points)
$E_w$	: Modulus of elasticity for the diagonal strut
$E_{wh}$	: Modulus of elasticity of the masonry infill in horizontal
$E_{wv}$	: Modulus of elasticity of the masonry infill in vertical
$E_c$	: Approximate modulus of elasticity for concrete
$E_D$	: Energy dissipated at a cycle
$E_{SO}$	: Maximum strain energy at a cycle
$\varepsilon_w$	: Strut strain in the formulation of Magenes and Pampanin (2004)
$F_u^+$	: Calibrated yield strength of the diagonal strut in Wayne Stewart degrading stiffness rule
$f_{uf}$	: Ultimate flexural strength
$f_{yw}$	: Yielding strength of the transverse steel
$f'_w$	: Compressive strength of masonry
$f_{wu}$	: Sliding shear strength of mortar joints
$f_y$	: Yield strength of steel
$f'_c$	: Concrete compressive strength
$f_{ws}$	: Shear strength from diagonal compression test

---

$G$	: Shear modulus of the masonry infill
$h$	: Inter-storey height (from centroidal points)
$h_c, h_w, H$	: Infill wall clear height (From the faces of the RC beams)
$H_B$	: The building height
$I_p$	: Moment of inertia for the columns
$I$	: Moment of inertia of any given section
$K_1, K_2$	: Calibrated coefficients
$KX$	: Calibrated stiffness of the diagonal strut in Wayne Stewart degrading stiffness rule
$L$	: Infill wall length in the formulation of Magenes and Pampanin (2004)
$\lambda$	: Relative stiffness between the infill and the frame
$l_C$	: Clear story height
$l_O$	: Opening height in the infill wall
$M_B$	: Bending moment at the bottom of the column
$M_T$	: Bending moment at the top of the column
$\nu$	: Poisson's ratio
$R_F$	: Reduction factor for equivalent diagonal strut width due to opening
$\sigma_w$	: Equivalent diagonal strut strength
$\sigma_v$	: Vertical stress on the wall
$\theta$	: Angle between the diagonal strut and the horizontal
$\tau_u$	: Ultimate shear strength
$t_w$	: Thickness of the infill wall
$V_s$	: Supplied shear capacity by the steel
$V_{sc}$	: Supplied shear capacity by the steel in column members
$V_{sb}$	: Supplied shear capacity by the steel in beam members
$V_u$	: Ultimate shear capacity per anchorage
$\xi_{eq}$	: Equivalent viscous damping
$w$	: Uniformly distributed load

*Note: the used notations are also given where they are used for ease of reference while reading*

# CHAPTER 1

## INTRODUCTION

*Aerodynamically, the bumble bee shouldn't be able to fly,  
but the bumble bee doesn't know it so it goes on flying anyway.*

*Mary Kay Ash*





## 1 INTRODUCTION

The design of reinforced concrete structures for seismic actions has become a major research area in the last few decades, gaining more interest and recognition around the world and even more so with each catastrophic earthquake that takes place. The 1931 Napier earthquake in New Zealand initiated significant changes towards reinforced concrete construction after many years of unreinforced masonry construction practice in the country (Figure 1.1). Earthquakes have been major causes of change towards the understanding of earthquake engineering globally, as it is with New Zealand. The current main philosophy behind seismic design methods is collapse prevention and life safety, which focuses on preventing the full collapse of a structure and the loss of life. According to this design philosophy, some damage is allowed in discrete parts of a structure up to an extent, such as plastic hinges at beam ends. However, most of the researches in structural engineering focus on the structural skeleton itself. The interaction of the structural skeleton and the non-structural components that are in contact is, in comparison, a relatively neglected topic.



**Figure 1.1.** Napier Earthquake 1931 (Source: Christchurch city library)

As new building design methodologies and technologies are developed, structures can now be built to survive moderate-to-severe seismic events. Although structures are able to survive such events, the resulting damage to non-structural components may prevent the immediate usage of a building after an earthquake. In addition, the resulting cost and downtime may exert a serious burden for the economy and the society. Recent researches have shown that the costs related to the failure of non-structural components in a building may easily exceed the replacement cost of the whole building [1]. As shown in Figure 1.2, the costs associated with the loss of the non-structural components approximately constitute 62% for offices, 70% for hotels,

48% for hospitals [2]. By examining these figures, it can be concluded that prevention of damage to non-structural components is an important concern for the seismic performance of new buildings.

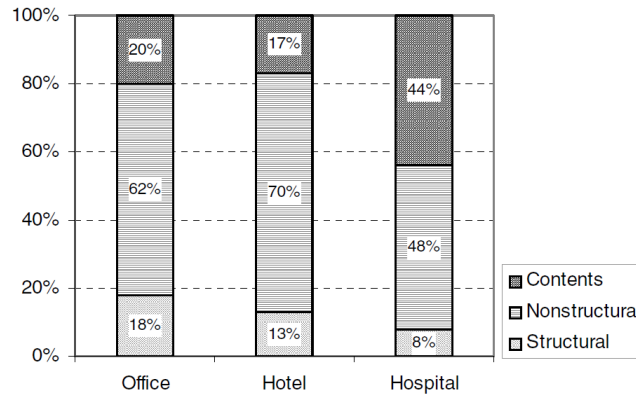


**Figure 1.2.** Cost breakdown of office buildings, hotels and hospitals from Taghavi and Miranda [2]

Non-structural components consist of a large variety of building parts: Partitions, ceilings, power/gas lines, water and sewage systems. Among these, the partition walls are one of the major elements that interact with the structural system and suffer damage due to the imposed drifts on the structure. In this reported PhD work, partition walls are the main area of interest.

Non-structural partition wall practice differs in every country depending on individual preferences. They can mainly be constructed by using unreinforced clay bricks, reinforced concrete block masonry or drywall systems. The materials for these most common practices are shown in Figure 1.3.

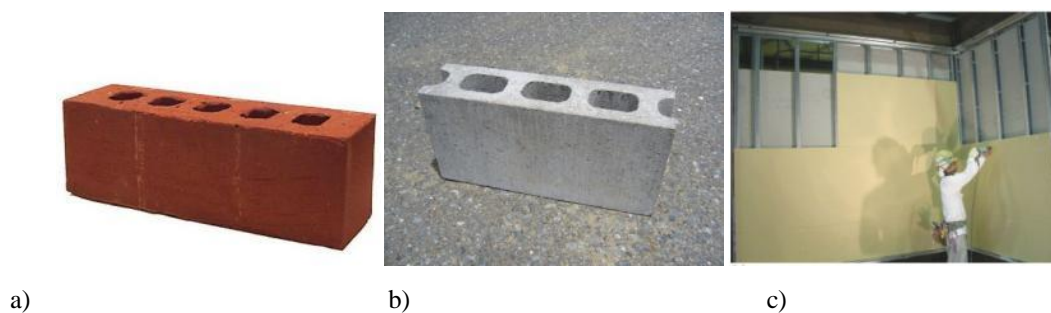



**Figure 1.3.** a) Clay brick, b) Concrete block, c) Drywall (Light gauge steel framed)

### 1.1 Evolution of Construction Practice in New Zealand

The Napier Earthquake in 1931 showed the susceptibility of unreinforced masonry (URM) buildings and resulted in the development of the first construction standards, which favoured the use of reinforced concrete (RC) construction [3]. Prior to the 1930s, clay brick was a common construction material in New Zealand both for URM (as part of the structure) and for RC buildings (as non-seismic resisting walls or infill walls). However, between the 1930s and 1950s, concrete blocks replaced clay bricks as the more commonly used infills. These two types of heavy infill options, blocks or bricks, were mostly used as infill walls in the external frames of buildings before claddings became the popular way to “dress” a building. For internal frames, light-weight drywalls have been preferred in most cases since the introduction of gypsum plasterboard to New Zealand in 1927.

In order to create an inventory of pre-70s RC buildings, a structural survey/preliminary assessment for critical RC buildings in Christchurch City Business District (CBD) was carried out as part of an FRST-funded research project (FRST Retrofit, 2010). This survey was carried out right after the 4<sup>th</sup> September Darfield earthquake in 2010. A total of 64 buildings were inspected from exterior only without any drawings. Some of these buildings, one of which collapsed (PGC, Figure 1.4), suffered significant damage after the 22<sup>nd</sup> February Christchurch earthquake in 2011. As part of the survey, different types and configurations of infill types for these older vintage RC buildings were sampled. Figure 1.5 shows the distribution of different infill types and the common critical structural deficiencies in these buildings. Short column effect, a result of the presence of half-height infill walls or spandrel beams, is the most common type of critical weakness observed.

<b>(22) CAMBRIDGE 233</b>		
Number of Storeys	5	
Structure Type	R/C Frame	
Infill Type	Unknown	
Configuration	Vertical Irregularity	
Function	Office	
Possible Deficiencies	Soft Storey	
Observed Damage After 2010 Darfield Earthquake	-	

**Figure 1.4.** The observations for the PGC building after 4<sup>th</sup> September 2010 Darfield earthquake (Photo by Tasligedik, A.S.)

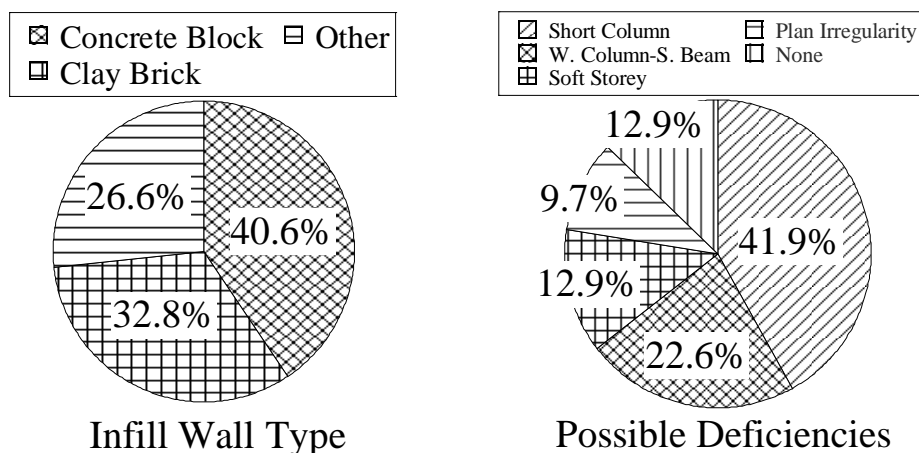


**Figure 1.5.** Infill wall types and possible observed deficiencies (Since the survey is exterior only, no information could be given regarding the partitions used inside the buildings)

In addition, the building code requirements in relation to the infill practice in New Zealand, starting from the NZS 95 [3] up to the present NZS 4230 [4] were reviewed to obtain a clear overview of the changes made to the practice over time. A summary of the major modifications in the building standards is reported below.

According to the standard NZS 95 Part V and VI (1935), panel walls should be constructed of stonework, brickwork, concrete or a combination of them and panel walls shall be properly secured to the concrete frame. Those panel walls can either be constructed of a single skin wall or a cavity wall (double skins with a cavity in between). Usually, the interior walls were constructed as single skin and the exterior walls were constructed as cavity walls for water proofing purposes. Surprisingly, NZS 95 also stated that it was possible to construct infill walls as reinforced brickwork, for increased lateral and out-of plane resistance against earthquake. Note that the definitions given before mentioning the reinforced brickwork referred to unreinforced masonry panel walls, which meant that the usage of unreinforced masonry infill panels were allowed in the code.

No separate standard specification for concrete bricks and concrete blocks existed until NZSS 595 (1952) [5] and it introduced the following definitions:

- ‘Concrete brick’ means a solid or hollow concrete masonry unit of nominal dimensions of 9 in. in length (228.6 mm), 4.25 in. in width (107.95 mm), and 3 in. in depth (76.2 mm)

- ‘Concrete block’ means a solid or hollow concrete masonry unit, any one of the nominal dimensions of which differs from the corresponding dimensions of a concrete brick

In 1964, many important definitions for practices in wall construction were made in NZSS 1900 [6]:

- ‘Infilling Panels’ means any wall between beams, columns, or floors which by virtue of its position and construction is subject to induced and/or applied loadings (Figure 1.7a)
- ‘Partition Wall’ means a wall which by virtue of its position and construction does not contribute to the strength or rigidity of a structure (Figure 1.7b)
- ‘Reinforced Grouted Brick Masonry’ means a construction of two or more skins of brick between which reinforcing steel is embedded in grout (Figure 1.7c)
- ‘Reinforced Hollow Masonry’ means masonry of cellular units having reinforcement in filled cells (Figure 1.7d)
- ‘Reinforced Masonry’ means any masonry in which reinforcing steel is so bedded and bonded that the two materials act together in resisting forces
- ‘Shear Wall’ means a structural wall which because of its position and shape, makes a major contribution to the rigidity and strength of a building

An observation was made after the examination of the 1960s structures; there were still many buildings with unreinforced clay brick infill walls although the first concrete block and brick standard was passed down in 1952 (Figure 1.6). On the other hand, after the introduction of NZSS 1900:1964, use of concrete block masonry flourished, and the number of projects that used concrete block masonry as infill increased. In addition, in those years, a new type of seismic resisting system, which relied on reinforced concrete block masonry for lateral stiffness and strength, without RC framing, was also introduced and widely used [7].

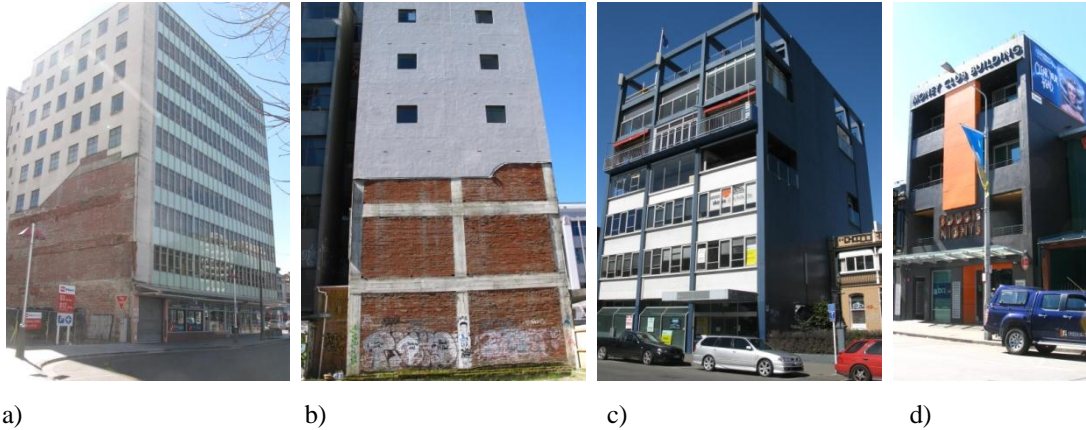


**Figure 1.6.** Some example buildings with unreinforced clay brick infill walls in Christchurch CBD: a) 8 Cathedral Sq., b) 159 Manchester St., c) 210 Hereford St., d) 172 Manchester St.

In NZS 4230:2004, the word ‘masonry’ was used for many types of infill wall or wall construction materials. ‘Masonry Unit’ was defined as ‘a preformed component intended for use in reinforced concrete masonry construction with cells laid in the vertical direction and with face-shell-bedded joints’. It should be noted that NZS 4230:2004 superseded NZS 4230P [8] with few changes considering the infill walls. Therefore, it can be deduced that the first standard to give guidelines for the design of infill walls in reinforced concrete frames was NZS 4230P:1985 and with only few changes in the 2004 edition, largely remains the current state-of-the-art.

Currently in New Zealand, partition walls, or non-structural infill walls, are mostly light steel/timber framed drywalls. These walls can also be used in exterior frames of a building in combination with many available cladding options. The first examples of drywalls were manufactured and used in 1927 and have been popular in New Zealand. The specifications for these non-structural wall types are given by the manufacturers and the main parameters are dependent on acoustic and thermal insulation capabilities of the walls without any comments on their seismic capabilities. Light steel framed drywalls are specified as non-load bearing elements and are the preferred drywall type to be used in commercial buildings. On the other hand, timber framed drywalls are specified as load bearing elements due to their structural use in residential construction, but their use as non-structural walls in buildings are still allowed [9]. For many parts of the world, such as southern Europe, Mid-East Asia, and South America, the use of unreinforced masonry bricks/blocks as infill walls is still a major element of infill practices.



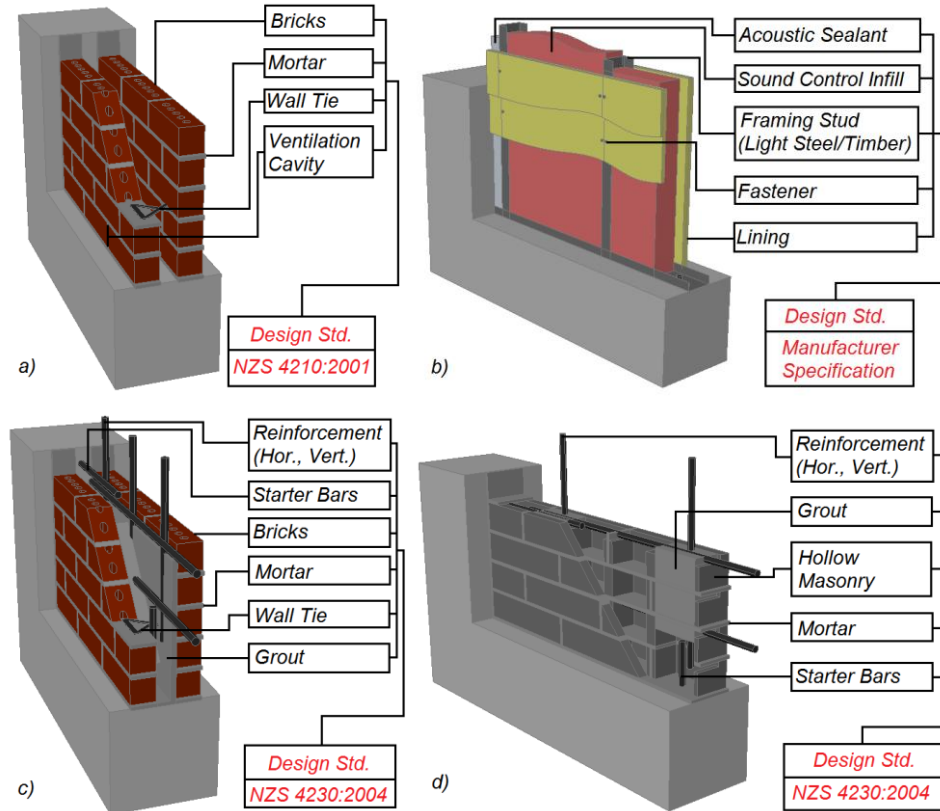


**Figure 1.7.** a) Unreinforced Masonry Infill, b) Light Steel/Timber Framed Wall, c) Reinforced Grouted Brick Masonry, d) Reinforced Hollow Masonry

**Table 1.1.** NZ Typical dimensions for the wall types in Figure 1.7

Infill Type	$t_m$ (mm)	$d_{wth}, d_{wtv}$ (mm)	$d_{ves}, h_{ve}$ (mm)				$t_m$ : Mortar Thickness
a) Unreinforced Masonry	$\leq 10$	$\leq 600, 400$	$\leq 800, 75$				$d_{wth}$ : Wall Tie Spacing in Horizontal $d_{wtv}$ : Wall Tie Spacing in Vertical $d_{vc}$ : Ventilation Cavity Spacing $h_{vc}$ : Ventilation Cavity Height
b) Light Steel/Timber Framed Wall	$d_{fs}$ (mm)	$t_e$ (mm)	$h_w$ (mm)	$t_{sci}$ (mm)	$t_l$ (mm)	$d_f$ (mm)	$d_{fs}$ : Framing Stud Spacing $t_e$ : Expansion Gap at the Top of the Frame $h_w$ : Wall Height $t_{sci}$ : Sound Control Infill Thickness $t_l$ : Thickness of Linings $d_f$ : Fastener Spacing
c) Reinforced Grouted Brick Masonry	$t_m$ (mm)	$d_{wth}, d_{wtv}$ (mm)	$t_w$ (mm)	$\phi$ (mm)	$S$ (mm)		
	$\leq 10$	$\leq 600, 400$	$\geq 140$	$\geq 12$	$\leq 400$		
d) Reinforced Hollow Masonry	$\leq 10$		$\geq 140$	$\geq 12$	$\leq 400$		

For More Information Refer to the Related Standards Shown in the Figures

Due to their popularity overseas and in New Zealand, the light gauge steel framed drywalls, timber framed drywalls and unreinforced clay brick infill walls were studied in the reported PhD work. Therefore, they will be the main focus of the reported work. However, the results and analogies can be extended to any other type of infill walls.

## 1.2 Definitions of Light and Heavy Partitions

*Heavy* and *light* are used in order to qualitatively describe different issues that may arise due to the failure of each component;

- Heavy: Failure of which may threaten life safety of people and may affect the structural response due to their high strength and stiffness. Therefore, heavy has been used in order to refer to such materials (i.e. Concrete blocks, clay bricks, concrete claddings/panels)
- Light: Failure of which may not necessarily cause life safety issues, but rather economical issues. Therefore, light refers to such materials (i.e. Drywalls)

## 1.3 Scope

By virtue of their material properties and behaviour, different types of partition walls raise different issues during and after a moderate-to-severe seismic event. Partition walls constructed of heavy masonry brick/block materials increase the lateral stiffness and contribute to lateral load resisting capacity of the structure. This effect is valid until the infilled frame reaches its load bearing capacity. After this point, a sudden strength degradation is observed with increasing displacement demands, which may likely cause local or global failure mechanisms in a structure [10]. During a seismic event, a structure should be able to sustain its strength with increasing displacements, or ductility [11] (a ductile wall behaviour is shown in Figure 1.8a). Extensive research has been carried out worldwide focusing on strengthening of infill walls over the years. As observed in most of these studies, the brittle nature of infill partition walls could not be prevented, or this issue was not addressed at all. In Figure 1.8b, hysteresis curves for bare frame, infilled frame, strengthened infilled frames have been shown as an example [12]. Therefore, the behaviour of an infilled frame is usually a brittle one when heavy materials are used such as concrete block or clay brick. After a moderate-to-severe seismic event, these materials may pose as a significant threat to life safety of people inside and outside a building as well as a threat to global stability of the structure itself.



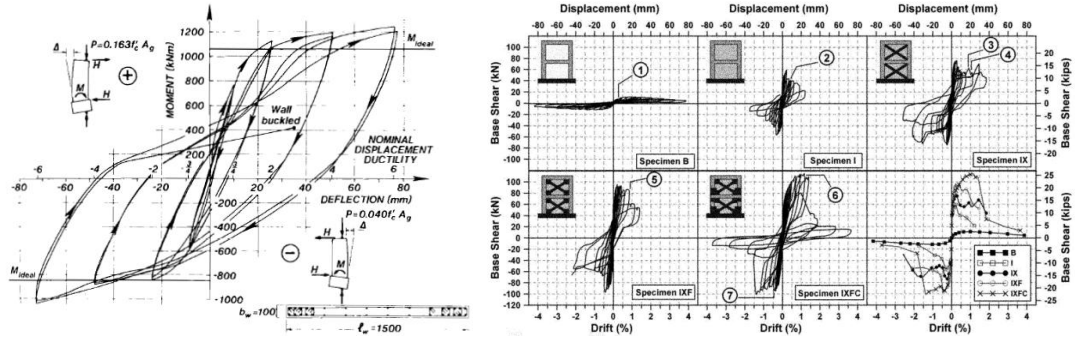


**Figure 1.8.** Sample hysteresis curves: a) Ductile wall by Paulay and Priestley [11], b) Strengthening of infilled frames by Ozden et al. [12]

Although partition walls constructed of drywalls with light steel or timber framing are weak enough not to modify the lateral load capacity of a structure, the interaction with the surrounding frame may cause extensive non-structural wall damage, or even impairing the serviceability of a structure. Thus, these types of light partition walls have potential economical impacts.

In most of international design codes, infill walls and partitions, heavy or light, have been considered as “non-structural elements” and thus tend to be mostly neglected in the structural design process. However, the observations made after major earthquakes have shown that even though infill walls might be considered to be “non-structural” elements, their interaction with the structural system during seismic actions can modify the overall bare frame system response, potentially leading to unexpected and undesired failure mechanisms at high drift demands ([10, 13-18]). These mechanisms can be either at a local level (e.g. shear failure in captive columns, damage to joint region) or at a global level affecting the structure’s seismic response (e.g. soft storey mechanism). On the other hand, under low-to-moderate shaking intensity, infills can provide additional stiffness and strength to the building before reaching their capacity, which is followed by a brittle failure mechanism. The positive or negative effects of infills on the seismic response of a structure still represent a controversial topic among the research community.

A typical approach in modern code provisions is to either require the engineer to consider and model the interaction of the infills in the overall seismic response in the design phase, which is practically not carried out, or alternatively to provide adequate separation to minimize that interaction [4], which is more likely to be adapted by

practitioners. However, the separations may introduce other issues to be addressed such as acoustic, thermal and fire resistance.

Considering the above mentioned effects of ‘non-structural’ infill walls on life safety and global stability of the structure, code provisions are stated in Section 12.5 of NZS 4230:2004 [4]:

- a) When infill panels are constructed without full separation from the frame, the composite action must be considered in analysis and designed accordingly.
- b) It should be noted that even where sufficient separation is provided at the top and at the lateral ends of a panel, the panel will still tend to stiffen the supporting beam considerably, concentrating frame potential plastic hinge regions in short hinge lengths at each end, or forcing migration of hinges into columns, with a breakdown of the weak-beam, strong-column concept.

Although these two alternatives have been contemplated in NZS 4230, there is in general a lack of comprehensive guidelines to support the implementation. Therefore, the motivation of this research has focused on minimizing the interaction between the non-structural walls and the structural system in order to develop low damage solutions for both heavy and light partition/infill walls. This could only be achieved by developing state-of-the-art methods and solutions capable of surviving the earthquake induced drift demands, examples of such research and technologies are still a few [19-21]. However, the potential of applicability and use of such outcomes have gained importance after the seismic events in Christchurch in 2011.

During the progress of this research, Christchurch was hit by a series of strong seismic events starting from the main shock on 4<sup>th</sup> September 2010. Among them the 22<sup>nd</sup> February (aftershock) earthquake in 2011 was the most destructive one. Although the research was disrupted by these seismic events, they gave the author valuable opportunities to observe the behaviour of the buildings and non-structural elements in the Christchurch City Business District (CBD). These observations validated the necessity of this research and emphasized the susceptibility of vertical ‘non-structural’

elements to damage caused by seismic actions. These observations made it evident that further study was required on the subject.

#### 1.4 Objectives

The conceptual idea for minimizing damage can be achieved by altering the non-structural wall behaviour by using innovative details. The behaviour can be modified into a more favourable behaviour that can accommodate the deformations caused by seismic actions. Therefore, the damage to non-structural walls can be prevented or minimized. In order to show the resulting effect of the developed solutions, a sample envelope curve is shown in Figure 1.9a. In this conceptual figure, the solutions (Figure 1.9b) minimize the interaction between the structural and the non-structural systems. This shows that the behaviour modification pushes the original infilled frame behaviour towards the bare frame behaviour though it can never be exactly equal to the bare frame, resulting in modified frame response. Nonetheless, the desired modification is capable of resulting in minimized damage to non-structural walls as well as minimized non-structural wall and structural frame interaction (Figure 1.9a, b).

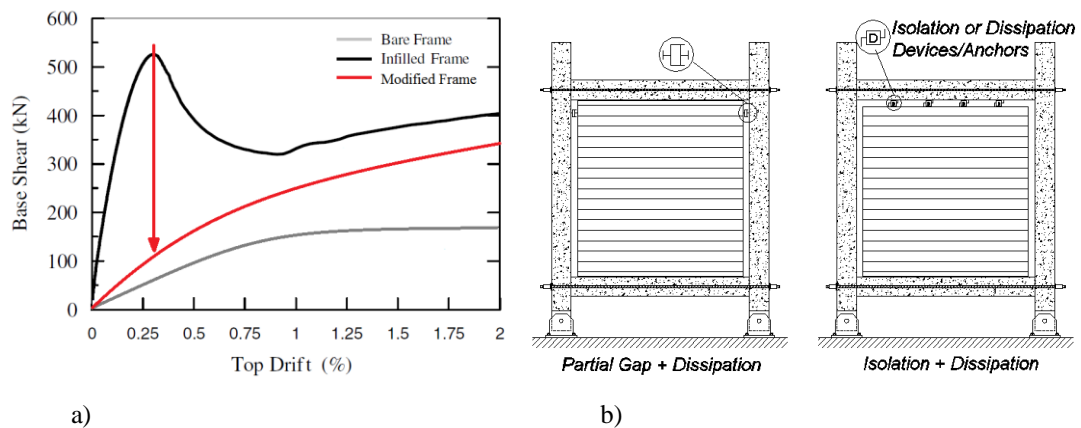


**Figure 1.9.** Conceptual explanation of low damage-low interacting solutions: a) A sample base shear vs. lateral drift envelope curve for infilled and bare frames (Original graph for bare and infilled frame is taken from Magenes and Pampanin 2004 [10], b) Conceptual representation of minimized interaction, minimized damage solutions

In Figure 1.10, the behaviour of three types of infill walls is compared in order to give the reader an opinion about how low damage, low interacting solutions can be achieved. Although these figures are for unreinforced clay brick infill walls, a similar analogy was used for non-structural drywalls and they will be presented in their

respective chapters. As it can be seen in Figure 1.10a, an existing as built masonry infill wall practice does not have much deformation capacity and results in brittle mechanisms, which is being addressed in the reported research. The solution in Figure 1.10b was already investigated by Mohammadi and Akrami [21]. However, this system may have significant out-of-plane issues, which may not be easily addressed in practical applications. Moreover, at high drift levels, the system had a possibility to induce shear failure in the columns. After studying the performances of different infill wall systems and the infill panel zone behaviour, a low damage infill wall system consisting of multiple cantilever panels were seemed more appropriate by the author. In order to give the reader an introductory overview, a rough sketch of the developed low damage system is shown in Figure 1.10c. More details about these low damage solutions are given in their respective chapters.

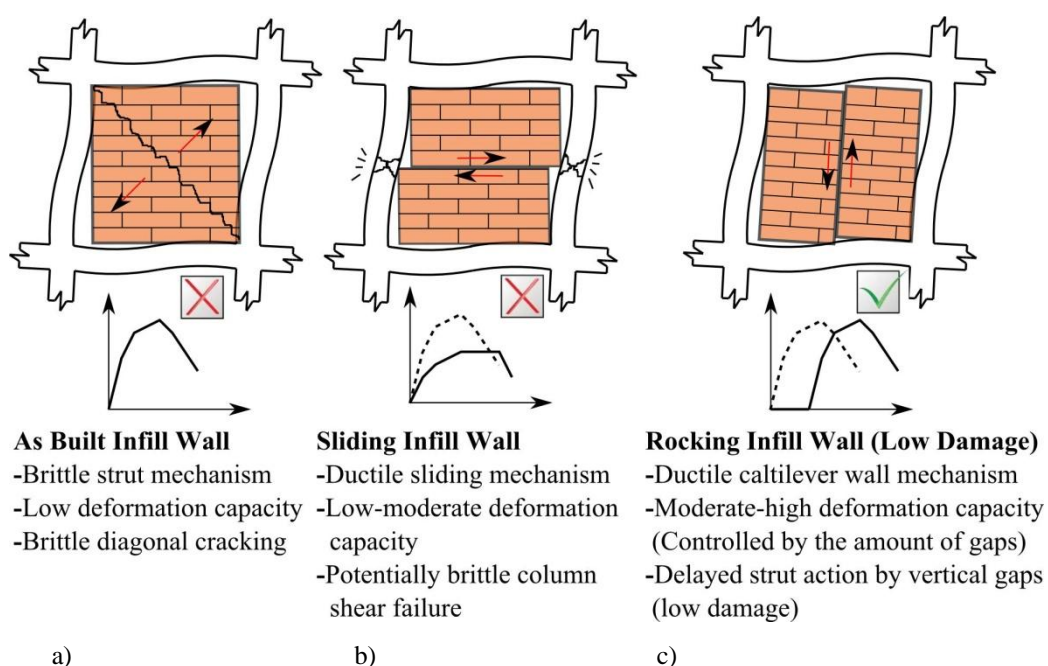


**Figure 1.10.** Behaviour of different masonry infill wall types: a) Diagonal cracking mechanism of as built masonry infill (undesired), b) Behaviour of modified infill walls with sliding details to increase deformation capacity (undesired), c) Behaviour of infill walls constructed as multiple cantilever walls with design gap (desired and followed analogy in this research) Note: The plots show axial force at the diagonal strut vs. inter-storey drift

Consequently, the objective of the reported research is the development of low damage solutions that are able to survive low-to-moderate earthquake induced drift demands for both heavy and light non-structural wall systems. In order to achieve the described

objective, the following research tasks were aimed to be accomplished at the end of the research:

- 1) Classify the main typologies of panels, panel to structure connections.
- 2) Obtain cyclic behaviour information of the most common NZ connection (panel-to-structure) typologies and proposals of enhanced solutions. It will be based on the literature as well as experimental data. Focus will be given to heavy unreinforced infill walls and light partition walls.
- 3) Analytically and experimentally evaluate the interactions and their effects on the overall system response.
- 4) Propose innovative solutions with reduced post-earthquake non-structural damage for newly designed buildings and enhanced seismic rehabilitation proposals for existing buildings.
- 5) Implement simplified analytical models for panels, panel-to-structure connections to predict the cyclic behaviour of the system.

### **1.5 Thesis Outline**

The thesis organization and the subjects that will be reported in the subsequent chapters are given below.

<b>Chapter 1</b>	-Introduction, Scope and Objectives Introduction to the concept and to the methodology of the reported work.
<b>Chapter 2</b>	-Drywalls: Literature and the Lessons Learnt from Earthquakes Summarized literature for drywalls and the observations made during 22 <sup>nd</sup> February 2011 Christchurch Earthquake.
<b>Chapter 3</b>	-Unreinforced Clay Brick Infill Walls: Literature and Lessons Learnt from Earthquakes Summary of researches focusing on behaviour modification caused by unreinforced clay brick infill walls and damage summary from February 2011 Christchurch earthquake.
<b>Chapter 4</b>	- Experimental Programme Introduction of the test setup and the test specimens

- Chapter 5** -As Built Drywall Tests  
The specimen details and test results of as built steel and timber framed drywalls are reported.
- Chapter 6** -Low Damage Drywall Tests  
The development and the details of the low damage solutions for steel and timber framed drywalls are reported along with the experimental results and observations.
- Chapter 7** -As Built Unreinforced Clay Brick Infill Wall Tests  
The specimen details and the test results of the as built unreinforced clay brick infill walls are reported.
- Chapter 8** -Low Damage Unreinforced Clay Brick Infill Wall Tests  
Developed innovative low damage solution for unreinforced clay brick infill walls is explained. The resulting details and the results of the test are reported.
- Chapter 9** -Numerical Case Study Building  
The Ruaumoko2D models of the as built and low damage non-structural wall types are implemented in a typical NZ reinforced concrete frame building model. The global performance of the developed low damage solutions and their effects on the global response are reported.
- Chapter 10** -General design recommendations and conclusive remarks  
In the light of the developed low damage solutions, general design recommendations are made. The conclusions of the reported work are summarized.

## 1.6 References

- [1] R. Villaverde, "Seismic Design of Secondary Structures: State of the Art," *Journal of Structural Engineering*, vol. 123, pp. 1011-1019, August 1997.
- [2] S. Taghavi and E. Miranda, "Response Assessment of Nonstructural Building Elements," *Pacific Earthquake Engineering Research Center*, September 2003.
- [3] NZS95, "New Zealand Standard of Model Building By-Law," vol. 95, ed: New Zealand Standard, 1935.
- [4] NZS4230, "Design of Reinforced Concrete Masonry Structures," vol. 4230, ed: New Zealand Standard, 2004.

- [5] NZSS595, "New Zealand Specification for Concrete Bricks and Blocks," vol. 595, ed: New Zealand Standard, 1952.
- [6] NZSS1900, "New Zealand Standard of Model Building Bylaw," vol. 1900, ed: New Zealand Standard, 1964.
- [7] I. L. Holmes, "Concrete Masonry Buildings in New Zealand," in 3rd World Conference on Earthquake Engineering, Auckland, New Zealand, pp. 244-255, 1965.
- [8] NZS4230P, "Provisional New Zealand Standard-The Design of Masonry Structures," vol. 4230P, ed: New Zealand Standard, 1985.
- [9] GIB, "GIB Noise Control Systems-Specifications for Drywalls," ed, 2006.
- [10] G. Magenes and S. Pampanin, "Seismic Response of Gravity-Load Design Frames with Masonry Infills," in 13th World Conference on Earthquake Engineering, Vancouver, B.C., Canada, 2004.
- [11] T. Paulay and M. J. N. Priestley, *Seismic Design of Reinforced Concrete and Masonry Buildings*: John Wiley and Sons, Inc., 1992.
- [12] S. Ozden, U. Akguzel, and T. Ozturan, "Seismic Strengthening of Infilled Reinforced Concrete Frames with Composite Materials," *ACI STRUCTURAL JOURNAL*, vol. 108, pp. 414-422, July-August 2011.
- [13] V. Bertero and S. Brokken, "Infills in Seismic Resistant Building," *Journal of Structural Engineering*, vol. 109, pp. 1337-1361, 06 June 1983.
- [14] M. Dolšek and P. Fajfar, "Soft Storey Effects in Uniformly Infilled Reinforced Concrete Frames," *Journal of Earthquake Engineering*, vol. 5, pp. 1-12, 2001.
- [15] M. Dolšek and P. Fajfar, "The Effect of Masonry Infills on the Seismic Response of a Four-Storey Reinforced Concrete Frame-A Deterministic Assessment," *Engineering Structures*, vol. 30, pp. 1991-2001, 2008.
- [16] M. N. Fardis and T. B. Panagiotakos, "Seismic Design and Response of Bare and Masonry-Infilled Reinforced Concrete Buildings. Part 11: Infilled Structures," *Journal of Earthquake Engineering*, vol. 1, pp. 475-503, 1997.
- [17] M. Galli, "Evaluation of the Seismic Response of Existing R.C. Frame Buildings with Masonry Infills," Master Degree in Earthquake Engineering Master Thesis, European School of Advanced Studies in Reduction of Seismic Risk (ROSE School), ROSE School, Pavia, 2006.
- [18] S. Personeni, P. M.D., A. Palermo, and S. Pampanin, "Numerical Investigations on the Seismic Response of Masonry Infilled Steel Frames," presented at the The 14th World Conference on Earthquake Engineering, Beijing, China, 2008.
- [19] M. Aliaari and A. M. Memari, "Experimental Evaluation of a Sacrificial Seismic Fuse Device for Masonry Infill Walls," *Journal of Architectural Engineering*, vol. 13, pp. 111-125, June 2007.
- [20] M. Aliaari and A. M. Memari, "Analysis of Masonry Infilled Steel Frames with Seismic Isolator Subframes," *Engineering Structures*, vol. 27, pp. 487-500, 2005.

- [21] M. Mohammadi and V. Akrami, "An Engineered Infilled Frame: Behavior and Calibration," *Journal of Constructional Steel Research*, vol. 66, pp. 842-849, 2010.



# CHAPTER 2

## DRYWALLS: LITERATURE and LESSONS LEARNT from EARTHQUAKES

*Bad times have a scientific value. These are occasions a good learner would not miss.*

*Ralph Waldo Emerson*



## 2 DRYWALLS: LITERATURE AND LESSONS LEARNT FROM EARTHQUAKES

### 2.1 Literature Review

Drywalls are currently the most common partition wall practice in use around the world. They are especially popular in developed countries such as New Zealand, United States and European countries. Because of their light weight compared to heavier options (i.e. clay bricks and concrete blocks), they are usually not considered to be part of the structural system. Although there are standardized regulations, there is generally no specific control during the construction and installation of these types of non-structural walls within a structure, unlike the structural systems. This lack of quality control can mainly be attributed to the misleading definition of non-structural elements, which seems to not trigger requirements for adequate check by structural engineers. In addition to that, the lack of innovative technologies and construction details for damage mitigation of drywalls contribute to the continuous observation of poor seismic performances. In spite of their extreme vulnerability to seismic events, this topic has not been studied extensively by researchers except for a few. In this section, most of the up to date researches are summarized.

Freeman [22] carried out dynamic tests on drywalls made of different materials and different connection types (e.g. stud to track connection by friction or pop-rivets) using a transportable racking test setup in 1971. This is probably the earliest research found giving information and findings about reverse cyclic behaviour and energy absorption properties of drywalls with different connection typologies. Rihal [23] followed a similar testing program with similar drywall types and connections in 1980. The tests were carried out using quasi-static loading protocol and confirmed the previous work of Freeman. The types of specimens tested by Freeman and Rihal are given in Table 2.1 and Table 2.2 respectively. In both researches, it should be noted that the gypsum boards of the specimens were attached to the runners (or tracks) even though they had friction fitted studs.

Wang [24] reported the cladding performance as a result of a joint project between US and Japan. The joint project focused on quasi-static testing of cladding and partitions in

a full scale six storey steel structure. In the research, US practice and Japan practice were compared. The significance of this research was that the tested vertical non-structural components were attached to a full scale frame structure.

**Table 2.1.** Description of wall panels by Freeman in [22] (1971)

Type Number	Wall Material	Stud Material	Wall Openings	Remarks	1st Report NVO-99-15	1st Report JAB-99-35	1st Report JAB-99-54
1	1/2" Gypsum wallboard (sheetrock)	3-5/8" Metal	None	Connection of stud to runner by friction	A-3	A-10 A-19	A-29 <sup>D</sup>
2	1/2" Gypsum wallboard	3-5/8" Metal	Door	Connection of stud to runner by friction	A-2	A-14	A-23 A-28 <sup>D</sup>
3	1/2" Gypsum wallboard	3-5/8" Metal	None	Connection of stud to runner by pop-rivets	A-4	A-12	A-30 <sup>D</sup> X-33 <sup>D+</sup>
4	1/2" Gypsum wallboard	3-5/8" Metal	Door	Connection of stud to runner by pop-rivets	A-5	A-15	A-31 <sup>D</sup>
5	1/2" Gypsum wallboard	2×4 wood	None	---	A-6	A-13	A-32 <sup>D</sup>
6	1/2" Gypsum wallboard	2×4 wood	Door	---	A-7	A-16	A-33 <sup>D</sup>
7	1/2" Plywood	2×4 wood	None	8 <sup>d</sup> nails at 12" centers	A-8	A-17 A-18	A-34 <sup>D</sup> A-35 <sup>D</sup>
8	8" Concrete Block*	---	None	No grout, no reinforcement	A-9	--	--
9	1/2" Gypsum wallboard	3-5/8" Metal	None	Same as Type 3 with wallboard screws to runners	--	A-11	A-27
10	Plywood and gypsum wallboard	2×4 wood	Window	One side plywood and one side wallboard	--	A-20	A-25 A-36 <sup>D</sup> A-37 <sup>D</sup>
11	Plaster and gypsum lath	2×4 wood	None	Plate and sill bolted to concrete	--	A-21	A-24 A-38 <sup>D+</sup> A-39 <sup>D+</sup>
12	Plaster and gypsum lath	2×4 wood	Door	Plate and sill bolted to concrete	--	A-22	A-26
17	3/8" plywood	2×4 wood	None	8d nails at 6" centers, blocking at mid-height	--	--	A-50 <sup>+</sup>

*D: Dynamic loading*

*+: Transportable rack system used*

**Table 2.2.** Description of partition test specimens by Rihal in [23] (1980)

No.	Partition Size/Ft.	Facing Material	Studs	Opening	Remarks	Date of Test
P1	8×8	3/8" plywood	2×4 wood	None	Trial specimen only.	Aug-79
P2	8×8	5/8" gypsum wallboard	3-5/8" metal	None	Facing panels placed vertically. Taped Joints. Connection of studs to runner at top by friction only	Oct-79
P2A	8×8	5/8" gypsum wallboard	3-5/8" metal	None	Same as P2, except connection between gypsum board and runner at top by drywall screws at 16" o.c.	Oct-79
P3	8×8	5/8" gypsum wallboard	3-5/8" metal	None	Same as P2, except no gap between studs and runner at top. Joints not taped.	Oct-79
P3A	8×8	5/8" gypsum wallboard	3-5/8" metal	None	Same as P2A, except no gap between studs and runner at top. Joints not taped	Oct-79
P4	8×8	5/8" gypsum wallboard	3-5/8" metal	None	Facing panels placed horizontally. Connection between gypboard and runner at top by drywall screws at 16" o.c. Joints not taped	Oct-79
P5	8×8	5/8" gypsum wallboard	3-5/8" metal	None	Facing panels placed vertically. Joints not taped. Different drywall screw layout.	Nov-79
P6	8×8	5/8" gypsum wallboard	3-5/8" metal	None	Same as P5 except joints are taped and different screw layout is used.	Nov-79
P7	8×8	5/8" gypsum wallboard	3-5/8" metal	Door opening	3'-0" × 6'-8" door opening. Wooden door frame	Jan-80
P8	8×8 overall	5/8" gypsum wallboard	3-5/8" metal	None	Partial height partition. Height of gypboard=6'-0". Facing panels placed vertically. Taped joints. Connection of studs to runner at top by friction only.	Jan-80
P8A	8×8	5/8" gypsum wallboard	3-5/8" metal	None	Condition similar to P8 except studs fully covered. Joints taped	Feb-80
P9	8×8	5/8" gypsum wallboard	3-5/8" metal	Window	3'-0" × 3'-0" window opening: wooden frame.	Mar-80
P10	8×8	5/8" gypsum wallboard	2-5/8" metal	Door	2'-8" × 6'-8" door opening: metal door frame: gypboard placed horizontally.	May-80
P11	8×8	5/8" gypsum wallboard	2-5/8" metal	Door	2'-8" × 6'-8" door opening: metal door frame: gypboard placed vertically.	Apr-80

Adham et. al. [25] tested 6 structural light gauge steel framed drywall specimens with diagonal straps in 1990. In this research, the drywalls were intended to be structural elements as in a residential house. The results showed that using steel diagonal struts increased both displacement and load capacity level at which the gypsum linings cracked (Figure 2.1).

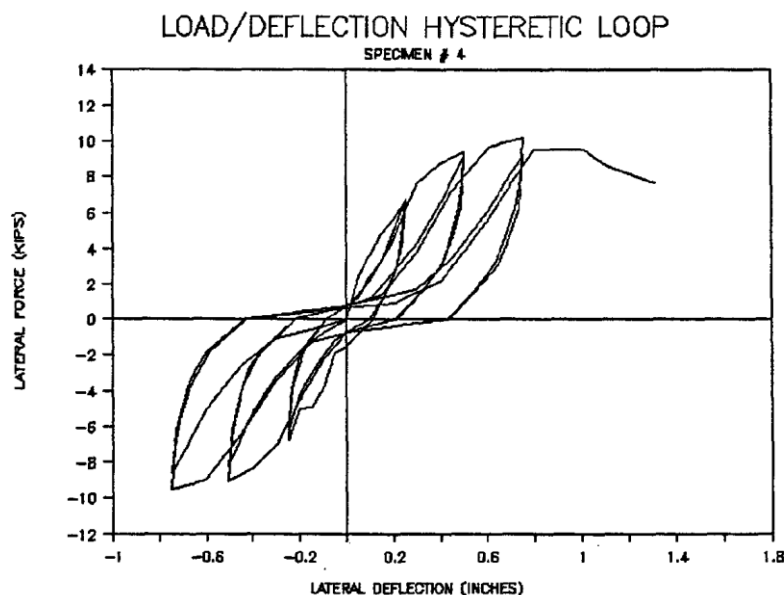


**Figure 2.1.** Sample force deflection hysteresis curve for diagonally braced steel frame drywalls by Adham et. al. [25] (1990)

Kanvinde and Deierlein [26] carried out an analytical research for the development of analytical models for the seismic performance of gypsum drywall partitions in 2006 using the experimental work reported by McMullin and Merrick in 2001 [27], where boundary members were used at the sides of the drywall in order to simulate the restraint provided by perpendicular walls in a real life scenario (Figure 2.2). In their study, Kanvinde and Deierlein showed that even when they were not designed as seismic elements, the gypsum drywalls' contribution to the lateral strength and stiffness in the wood-frame structures was significant.

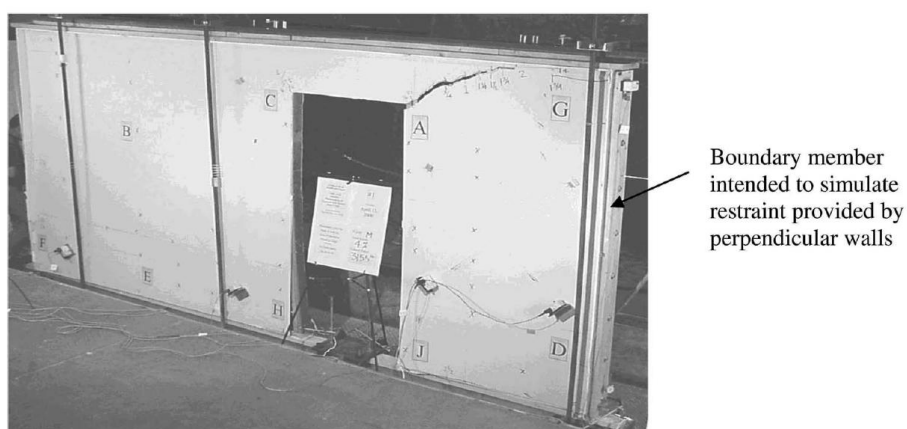


**Figure 2.2.** Test specimen by McMullin and Merrick [27] (2001)

Lee et. al. [28] tested 4 full-scale light gauge steel framed drywall partitions following Japan's practice within a modified racking test setup in 2006. The setup simulated the confinement caused by a surrounding frame without moment capacity, where four steel members were connected by four pins (Figure 2.3). Effects of a door and an intersecting wall were studied. It was reported that the damage typically concentrated to perimeter regions in contact with ceiling, floor or columns. Also, the dynamic loading did not cause any amplification in damage when compared to the quasi-static test. It was concluded that the repair cost after 2.0% inter-storey drift reached almost the initial cost of construction for a new drywall infill.

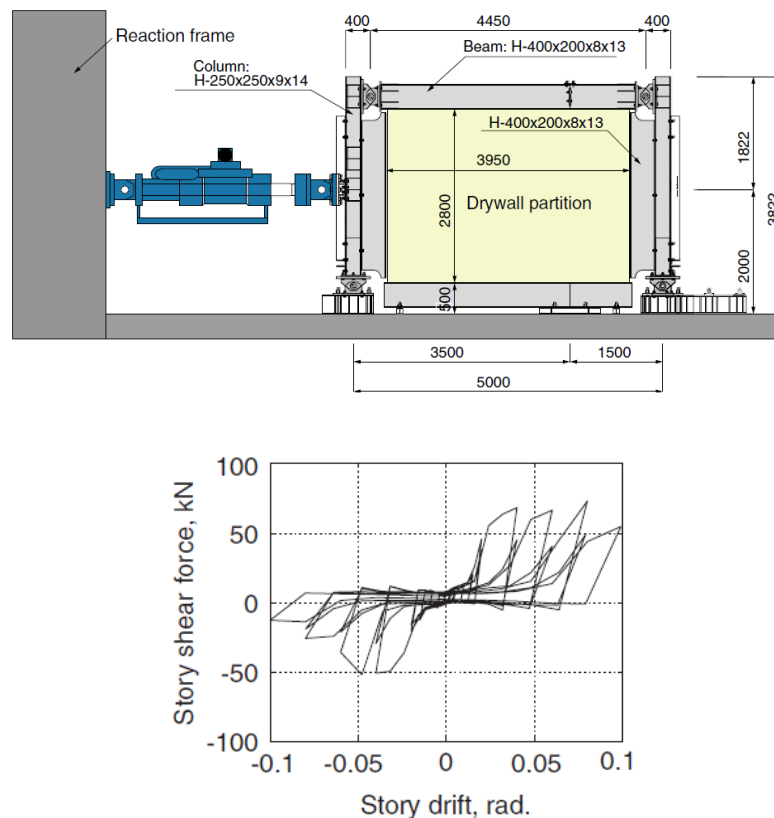


**Figure 2.3.** Test setup used by Lee et. al. [28] and the total lateral force vs. story drift curve for a drywall without opening (2006)

McMullin and Merrick [29] conducted 11 tests using *full scale timber framed drywalls* with diagonal straps as bracing elements in 2007. Tests were carried out using the racking test setup in Figure 2.2. Two failure modes were reported: i) Joint failure with the individual gypsum linings racking, ii) Pier rotation where all the gypsum linings in a pier rotated as a unit. Moreover, it was reported that the maximum load occurred at

drift levels between 0.68% and 1.87% with the initial cracking occurring at 0.25% drift level.

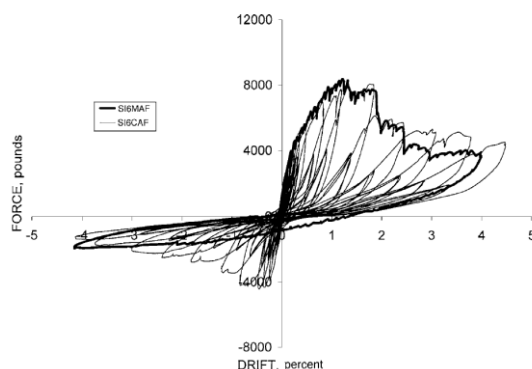


**Figure 2.4.** Hysteretic behaviour of a typical drywall specimen by McMullin and Merrick [29] (2007)

Filiatrault et. al. [30] (2010) tested 36 steel studded gypsum drywall partitions in a typical racking setup. It was concluded that using slip tracks and gaps at top end of the drywalls reduce the seismic damage of the drywall type where panels were attached in vertical orientation. However, it concentrated the damage to the vertical joints between the drywalls in the orthogonal direction. The hysteresis curves of two partitions and the test setup are shown in Figure 2.5. Although the research addressed the fragility of the existing drywalls with different connection types, it did not provide explicit suggestions on alternative low-damage details for such walls. Also, apparently the setup adopted in that research could not simulate the confinement effects exerted on non-structural walls from the surrounding frame, which is likely to affect the behaviour of such walls and their serviceability limits.

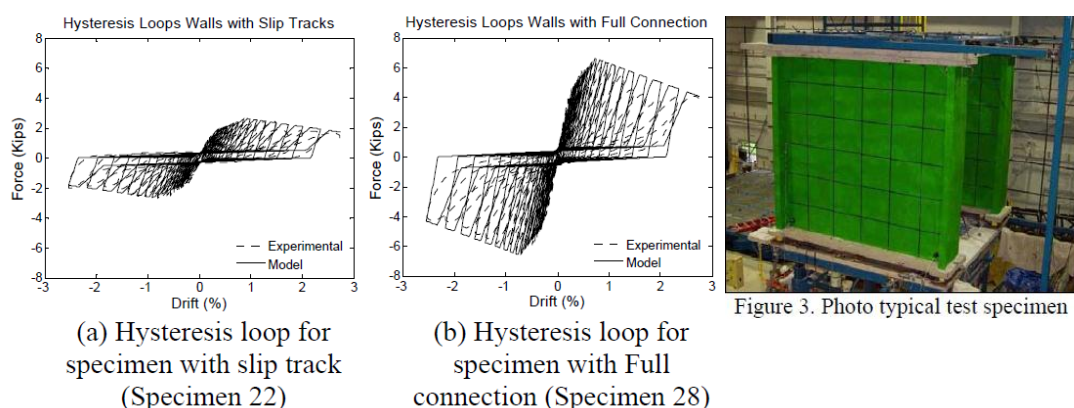


Figure 3. Photo typical test specimen

**Figure 2.5.** Experimental and numerical comparison of the reverse cyclic behaviour of the partitions and the used racking setup by Filiatrault et. al. [30] (2010)



Restrepo and Lang [31] tested two identical rooms consisting of light-gauge steel framed drywalls in 2011. Testing was carried out using two different quasi-static testing protocols. The objective was to study the sensitivity of loading protocol on damage progression, which was concluded to be very small. It was also concluded that drywalls were *prone to failure by slip occurring at top and bottom tracks the most* (Table 2.3).

**Table 2.3.** Damage progression reported by Restrepo and Lang [31] (2011)

Damage State	Damage Description	Drift Ratio (%)	
		Test Specimen 1	Test Specimen 2
DS1	Door Jamming	0.1	Not observed
	Screw embedding	0.25	0.4
	Gypsum board separation	0.28	0.28
DS2	Gypsum panel crushing	0.61	Not observed
DS3	Track slip	0.77	0.82
	Column wrap separation	0.82	1.08

Araya-Letelier and Miranda [32] addressed the same problem with drywalls and developed a novel sliding frictional connection in order to mitigate damage in 2012. While a conventional drywall specimen suffered damage around 0.1%, with this sliding frictional connection type, the specimen stayed damage-free until 1.52% drift.

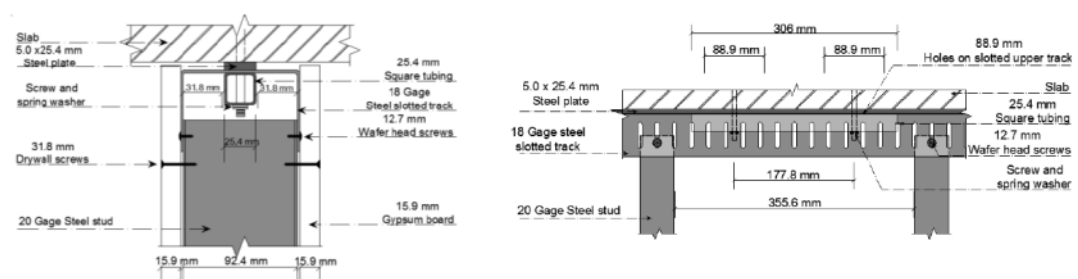


**Figure 2.6.** Novel sliding frictional connection for drywalls by Araya-Letelier and Miranda [32] (2012)

For self-centring systems, Eatherton and Hajjar [33] studied the residual drifts by considering the effect of non-structural elements in 2011. It was concluded that typical gypsum interior partitions reduce peak drift and experience strength degradation without significantly affecting the residual drifts.

## **2.2 Lessons Learnt from the Christchurch Earthquakes: Drywall Partitions**

Christchurch has recently been struck by an unusual sequence of earthquakes since 4<sup>th</sup> September 2010 ( $M_w$  7.1). The total number of earthquakes between September 2010 and September 2012 above  $M_w$  3.0, 4.0, 5.0 and 6.0 were reported as 4423, 958, 82, 9 respectively (EQC/GNS 2012) [34] with the most intensive and devastating one being 22<sup>nd</sup> February 2011 ( $M_w$  6.3, depth 5 km). More details on the 2010-2011 earthquake sequences and their wider impacts can be found in the two special bulletin issues published by the NZSEE [35, 36] (Darfield Earthquake Special Issue 2010; Christchurch Earthquake Special Issue 2011). During the sequence of strong aftershocks ( $M_w$  5+), one of the most common observations was that many of the modern buildings suffered moderate-to-extensive damage to drywalls that repeatedly needed extensive repair or complete replacement. This represented a severe economical burden required to bring the buildings back to serviceable condition for reoccupation considering the high costs associated with the loss of the non-structural components [2] (Percentage of the total cost of a building: 62% for offices, 70% for hotels, 48% for hospitals).

After the 22<sup>nd</sup> February 2011 Christchurch earthquake, significant damage to drywall partitions was observed in almost all of the buildings. In order to give an overview of the observed damage, the photographic records are reported in this section. The most common damage was cracking at interfaces among adjacent linings. Almost all of the buildings had drywall partitions cracking in this manner at a certain level. In addition, cracking at lining corners caused by tightly finished corners is another common damage observed (e.g. around the corners of windows or doors). In some cases, the linings detached from the underlying framing due to significant diagonal compression imposed on the linings, resulting in breaking at lining corners.



**Figure 2.7.** Damage observation after 22<sup>nd</sup> February 2011 Christchurch earthquake: Interface cracking among adjacent linings



**Figure 2.8.** Damage observation after 22<sup>nd</sup> February 2011 Christchurch earthquake: a) Interface cracking among adjacent linings, b) Broken gypsum lining

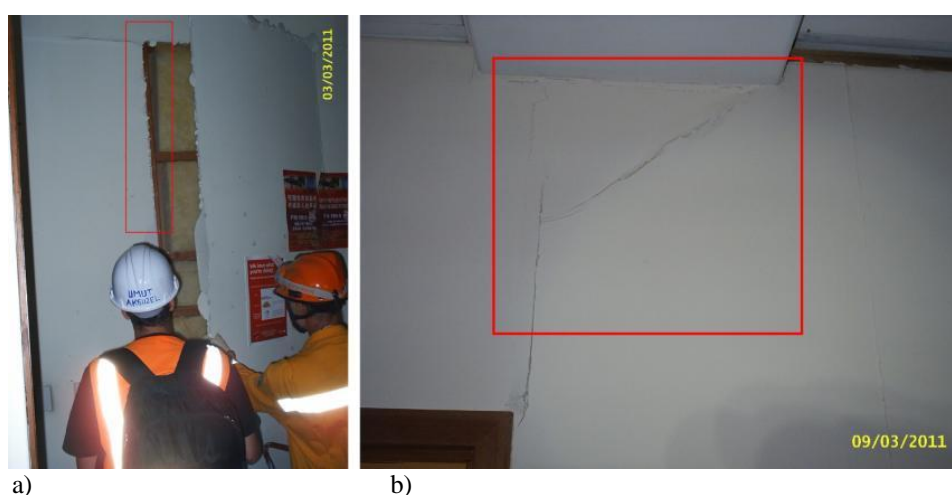


**Figure 2.9.** Damage observation after 22<sup>nd</sup> February 2011 Christchurch earthquake: a) Interface cracking among adjacent linings, b) Broken gypsum lining

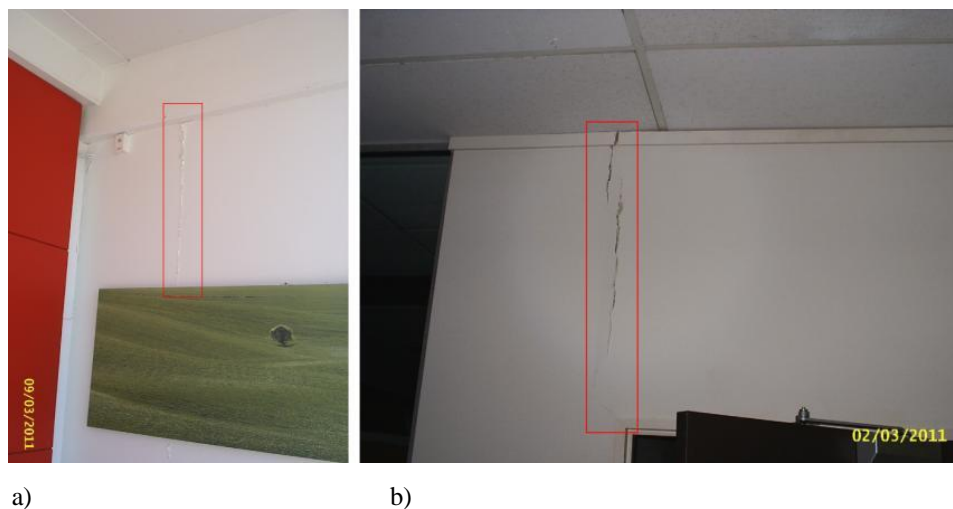


**Figure 2.10.** Damage observation after 22nd February 2011 Christchurch earthquake: Interface cracking among adjacent linings



**Figure 2.11.** Damage observation after 22nd February 2011 Christchurch earthquake: a) Lining cracking due to tightly fixed window corner, b) Lining cracking due to tightly fixed beam corner

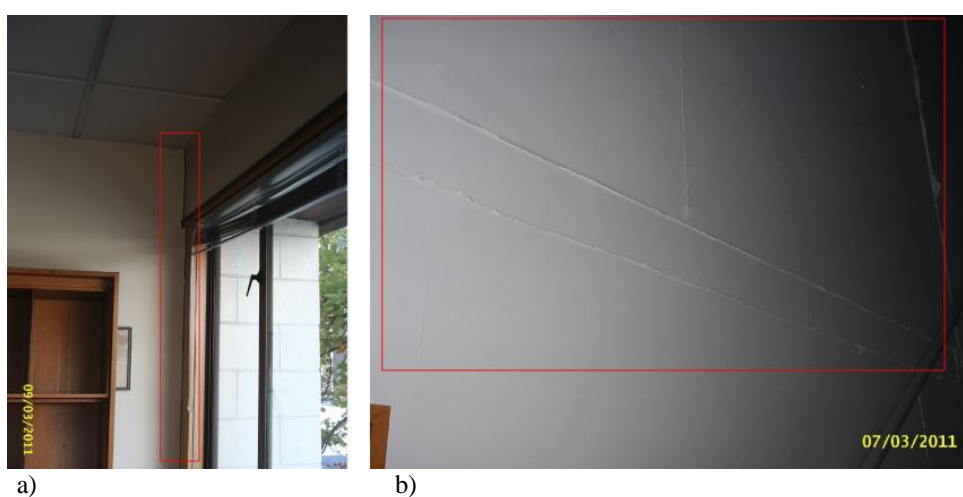
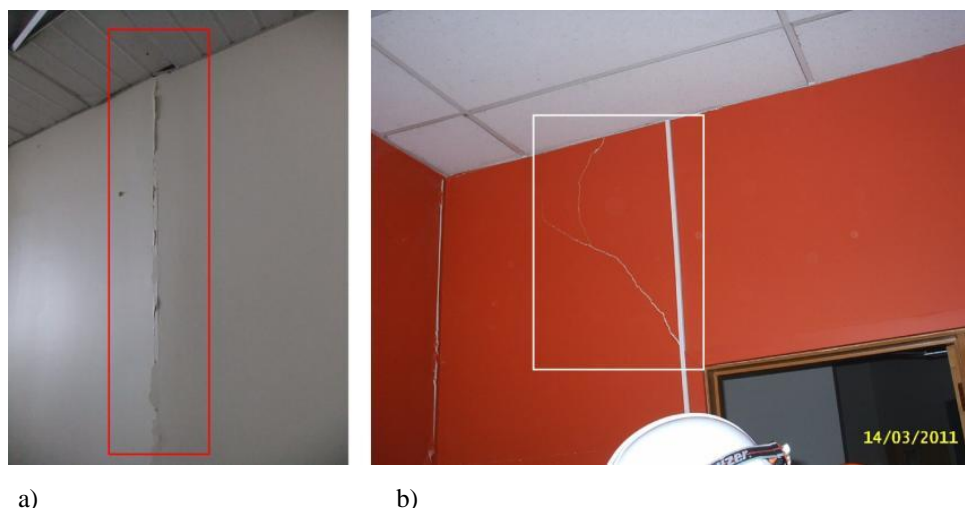


**Figure 2.12.** Damage observation after 22nd February 2011 Christchurch earthquake: a) Separation from the perpendicular wall, b) Interface cracking among adjacent linings



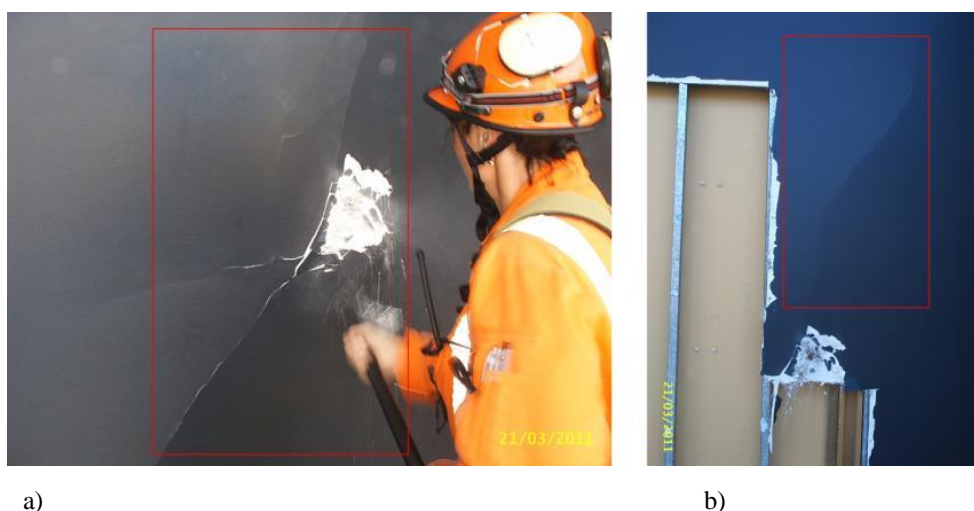
**Figure 2.13.** Damage observation after 22nd February 2011 Christchurch earthquake: Interface cracking among adjacent linings



a)

b)

**Figure 2.14.** Damage observation after 22nd February 2011 Christchurch earthquake: a) Interface cracking among adjacent linings, b) Lining cracking at tightly fixed door corner



a)

b)

**Figure 2.15.** Damage observation after 22nd February 2011 Christchurch earthquake: a) Broken gypsum lining, b) Underlying steel framing system

### **2.3 References**

- [2] S. Taghavi and E. Miranda, "Response Assessment of Nonstructural Building Elements," Pacific Earthquake Engineering Research Center September 2003.
- [22] S. A. Freeman, "Third Progress Report on Racking Tests of Wall Panels," University of California, Berkeley November, 1971.
- [23] S. S. Rihal, "Racking Tests of Non-Structural Building Partitions," California Polytechnic State University December 1980.
- [24] M. L. Wang, "Cladding Performance on a Full Scale Test Frame," Earthquake Spectra, vol. 3, pp. 119-172, 1987.
- [25] S. A. Adham, V. Avanesian, C. Hart, R. W. Anderson, J. Elmlinger, and J. Gregory, "Shear Wall Resistance of Lightgauge Steel Stud Wall Systems," Earthquake Spectra, vol. 6, pp. 1-14, 1990.
- [26] A. M. Kanvinde and G. G. Deierlein, "Analytical Models for the Seismic Performance of Gypsum Drywall Partitions," Earthquake Spectra, vol. 22, pp. 391-411, May 2006.
- [27] K. M. McMullin and D. S. Merrick, "Seismic Performance of Gypsum Walls-Experimental Test Program," 2001.
- [28] T. H. Lee, M. Kato, T. Matsumiya, K. Suita, and M. Nakashima, "Seismic Performance Evaluation of Non-Structural Components: Drywall Partitions," Earthquake Engineering and Structural Dynamics, 2006.
- [29] K. M. McMullin and D. S. Merrick, "Seismic Damage Thresholds for Gypsum Wallboard Partition Walls," Journal of Architectural Engineering, vol. 13, pp. 22-29, March 1, 2007.
- [30] A. Filiatrault, G. Mosqueda, R. Retamales, R. Davies, Y. Tian, and J. Fuchs, "Experimental Seismic Fragility of Steel Studded Gypsum Partition Walls and Fire Sprinkler Piping Subsystems," presented at the ASCE Structures Congress, Orlando, Florida, 2010.
- [31] J. I. Restrepo and A. F. Lang, "Study of Loading Protocols in Light-Gauge Stud Partition Walls," Earthquake Spectra, vol. 27, pp. 1169-1185, November 2011.
- [32] G. Araya-Letelier and E. Miranda, "Novel Sliding/Frictional Connections for Improved Seismic Performance of Gypsum Wallboard Partitions," in 15th World Conference on Earthquake Engineering, Lisbon, Portugal, 2012.

- [33] M. R. Eatherton and J. F. Hajjar, "Residual Drifts of Self-Centring Systems Including Effects of Ambient Building Resistance," *Earthquake Spectra*, vol. 27, pp. 719-744, August 2011.
- [34] EQC/GNS. (2012). *GeoNet-Geological Hazard Information for New Zealand*.
- [35] "Darfield Earthquake Special Issue," *Bulletin of the New Zealand Society for Earthquake Engineering*, vol. 43, December 2010.
- [36] "Christchurch Earthquake Special Issue," *Bulletin of the New Zealand Society for Earthquake Engineering*, vol. 44, December 2011.





# CHAPTER 3

## UNREINFORCED CLAY BRICK INFILL WALLS: LITERATURE and LESSONS LEARNT from EARTHQUAKES

*Nothing has such power to broaden the mind as the ability to investigate systematically  
and truly all that comes under thy observation in life.*

*Marcus Aurelius*



### 3 UNREINFORCED CLAY BRICK INFILL WALLS: LITERATURE AND LESSONS LEARNT FROM EARTHQUAKES

#### 3.1 Literature Review

In this part of the thesis, a filtered summary of a wide literature survey is reported. The aim of the survey was to find researches that studied the structural modifications caused by the changes at infill panel zone content. These researches helped the author understand the behaviour of the unreinforced masonry infill walls in a behaviour modification concept so that an innovative low damage seismic solution for unreinforced clay brick infill walls could be developed. The reported literature summary is just a portion of the referred research and throughout the reported work; references are given to other researches as required.

##### 3.1.1 *Experimental Considerations for Heavy Infills: Focusing on Behaviour Modification by Strengthening and Ductility Changes to the Infill Panel Zone*

Langenbach [37] considered old armature cross wall practices, typical in regions like Turkey, India and Pakistan, and their performances after seismic events. The author proposed modernized methods based on observations made after major earthquakes and expressed the importance of learning from past construction practices, which are considered to be obsolete. The considered ancient practice of armature cross wall is shown in Figure 3.1 along with an adapted version to a comparably modern building. According to the International Building Code [38], a cross-wall is defined as an interior partition wall that is not a shear wall but nonetheless provides structural support and hysteretic damping. The term “armature” refers to use of a “sub-frame” to subdivide the masonry walls. Armature cross-walls are thus infill masonry walls modified by the introduction of a sub-frame of studs and cross pieces and the deliberate use of a weak lime-based mortar. These studs and cross pieces would be securely attached to the RC frame, with bricks tightly packed in between. By generating less initial stiffness than standard infill masonry walls, multi-story frame can behave as a bare frame rather than an infilled RC frame. Therefore, cross-walls

reduce the problems and complexities caused by the frame infill interaction, which could lead to undesired local or global failure mechanisms as shear failure in columns or a soft storey mechanism. Moreover, the studs and cross pieces prevent the formation of an equivalent diagonal strut, while substantially increasing the out-of-plane resistance. The author also stated that weaker timber studs and crosses in the old types of armature cross walls did not get any damage after earthquakes and this can be attributed to subdivision of the infill panel into smaller panels using studs and horizontal members and a low strength mortar, which reduces the initial stiffness and prevent the formation of diagonal cracking due to prevention of equivalent diagonal strut formation. In addition, these modifications change the global behaviour of the structure to a more ductile one, which was stated by the author to be the cause of the desirable behaviour observed in these old structures.



**Figure 3.1.** a) Armature cross-wall structure at the epicentre after Duzce 1999 earthquake in Turkey (no damage), b) Armature cross wall structure in Pakistan (the damage to the adjacent URM building is severe compared to the armature cross-wall, c) Armature cross-wall applied in practice to an RC structure in 1965. The building suffered soft storey at ground level after 1965 San Salvador earthquake. However, progressive pancake was prevented due to the infill wall's being intact with the sub-framing.

Calvi and Bolognini [39] carried out testing on four RC frame types: bare frame (benchmark); infilled frame with unreinforced clay bricks (lateral hollow cores), infilled frame with clay bricks with horizontal reinforcement in mortar layers and infilled frame with clay bricks with reinforcing mesh on the surface. Quasi-static response of each type is shown in Figure 3.2. It can be concluded that the reinforcing mesh on the surface improved both in-plane and out-of-plane response of the infill wall the most effectively. It can also be observed that the hysteresis given by the reinforcing

mesh was more stable and ductile. The brittle failure of the infill material was prevented and a ductile post-peak response was achieved.

Mosalam et al. [40] carried out quasi-static testing of single-storey, one and two-bay steel frames infilled with unreinforced masonry walls with and without openings in 1997. An interesting observation regarding the effects of the infill walls on the global response was that openings in infill walls led to a more ductile behaviour and larger post-cracking force ratio compared to infill walls without openings. The hysteresis envelopes and effect of openings on cracking patterns have been shown in Figure 3.3.

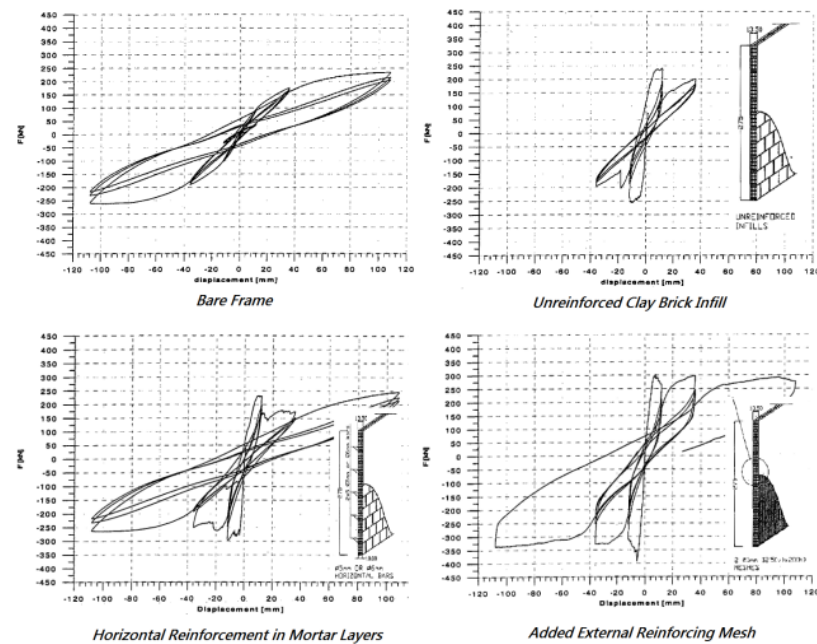


Figure 3.2. In-plane quasi-static response of infilled RC frames by Calvi and Bolognini [39] (2001)

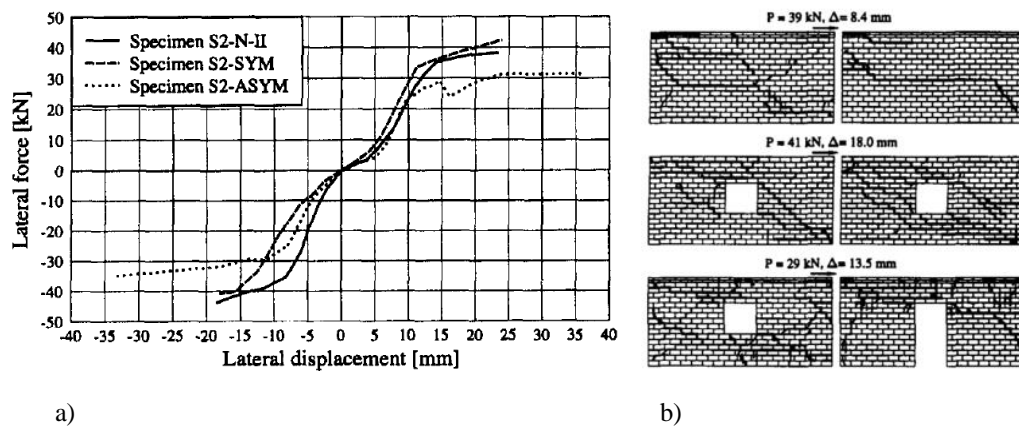
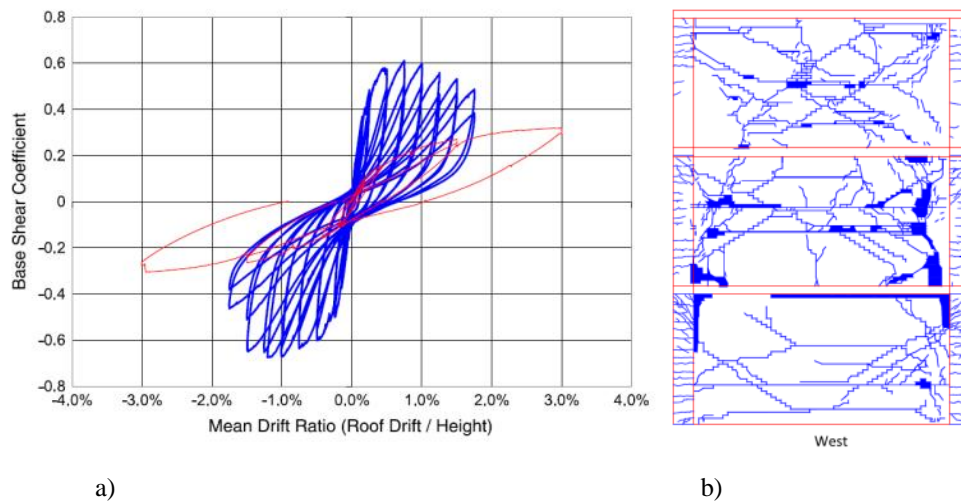


Figure 3.3. Experimental testing of a single storey, one and two bay steel frames infilled with unreinforced masonry walls by Mosalam et. al. [40]: a) Hysteresis envelopes of the specimens (S2-N-II: without opening, S2-SYM and S2-ASYM: symmetrical and asymmetrical openings), b) Effect of openings in cracking patterns, the specimens from top to bottom: S2-N-II, S2-SYM, S2-ASYM (1997)

Pujol and Fick [41] carried out reverse-cyclic quasi-static testing on a full-scale three storey-reinforced concrete flat slab building. The structure was tested as bare frame then as an infilled frame with unreinforced masonry bricks. The aim was to observe the effects of masonry infills on the structural response. Crack map at the end of the test and the comparison of the hysteresis curves of bare frame and infilled frame are shown in Figure 3.4. According to drift levels, the observations given by the authors are summarized in Table 3.1. In the conclusions, it was stated that the structure retained its capacity up to 1.5% drift, which is conflicting with the shown hysteresis curves, i.e. the post-peak response is decreasing after 0.8%-1.0% drift.



**Figure 3.4.** Experimental testing of a full scale, three storey, RC flat slab frame structure from Pujol and Fick [41]: a) Comparison of hysteresis curves of bare and infilled frame, b) Crack map at the end of the test

**Table 3.1.** Summary of damage according to drift levels according to Pujol and Fick [41]

Drift (%)	Observed Damage
0.15	Separation between infill wall and columns Cracks at infill wall
0.2	First abrupt drop in stiffness
0.25	Maximum crack width at infill wall is 4 mm
0.75	Length of separation increased from 1500, 2000 to 1800, 2000 mm Cracks at infill wall widened
1	Maximum crack width at infill wall is 10 mm

Tasnimi and Mohebkah [42] tested six full-scale, single-storey, single-bay steel frame specimens. The first reference test was a bare frame and the second reference test was an infilled frame without openings. The rest of the specimens had different orientations

of openings on the infill walls. The experimental results indicated that infill panels with and without openings can improve the seismic performance of steel frames with equal cumulative dissipated energy at ultimate state. The authors also concluded that the ductility of infill walls with openings is not always higher than the ones without openings. It was stated that the ductility of such frames depends on the failure mode of infill piers. The test results showed that infilled frames with openings experienced pier diagonal tension or toe crushing and have smaller ductility factors than infills without openings. In addition, a simple analytical method was proposed to estimate the maximum shear capacity of masonry infilled steel frames with openings. A reduction factor for the equivalent diagonal strut width was also proposed to account for openings (shown below). The modes of damage, comparison of load-displacement envelopes and the ratio of energy dissipation to displacement per cycle are shown in Figure 3.5.

$$b_{wm} = R_F \cdot b_w$$

$$\text{For } A_o < 0.4A_p, R_F = 1.49 \left( \frac{A_o}{A_p} \right)^2 - 2.238 \left( \frac{A_o}{A_p} \right) + 1$$

$$\text{For } A_o > 0.4A_p, R_F = 0$$

Where:  $b_w$  : Equivalent diagonal strut width  
 $b_{wm}$  : Modified equivalent diagonal strut width due to opening  
 $R_F$  : Reduction factor for equivalent diagonal strut width due to opening  
 $A_o$  : Area of opening  
 $A_p$  : Area of infill panel

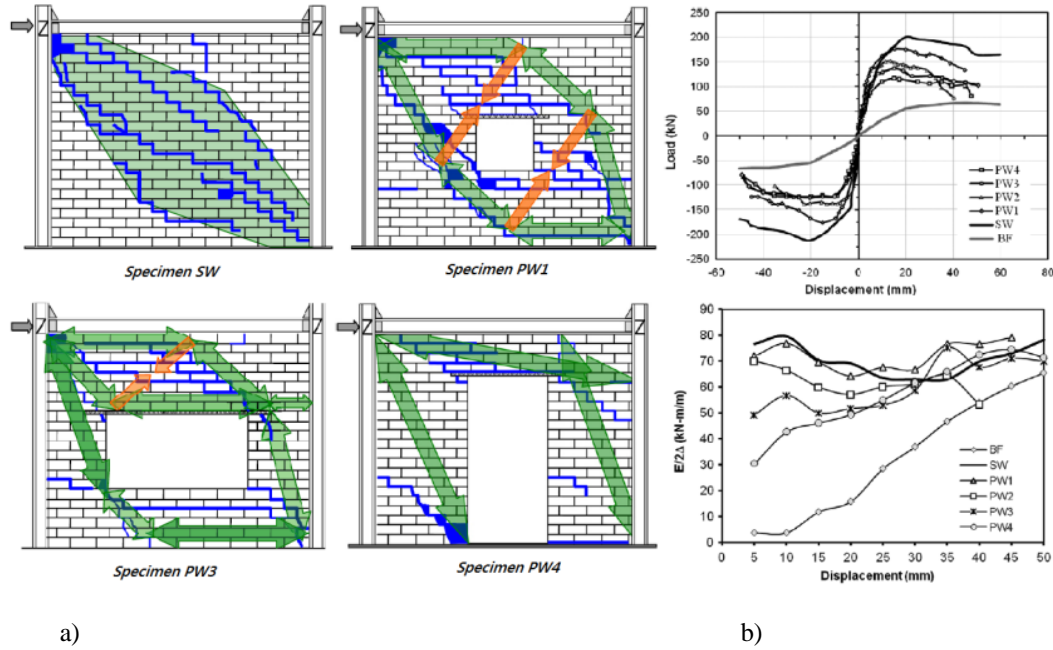


**Figure 3.5.** Experimental testing of a single-storey, single-bay steel frame infilled with unreinforced clay bricks from Tasnimi and Mohebkah [42]: a) Cracks and activated stress fields at infill wall, b) Load-displacement envelopes and comparison of the ratio of energy dissipation to displacement ( $2\Delta$ ) per cycle

Mohammadi and Akrami [21] experimentally investigated a method in order to change the infill wall behaviour to a ductile one. The concept was to introduce an element to the infill wall, referred to as friction sliding fuses (FSFs). Conceptually, the fuse acts before infill corner crushing and controls the infill so that it is not overloaded. As a result of that, deformation capacity increases and strength deterioration decreases. The achieved strength and ductility can be adjusted by controlling the friction between the surfaces. The infill can be made of either bricks or concrete. The infill type investigated in this research was a concrete infill, following on the authors' previous work where clay brick infill was used. Authors also observed that if the friction slider adjustment is not properly made, crushing at the lower boundary of the wall occurs. The details and a sample hysteresis curve obtained in this study are shown in Figure 3.6.



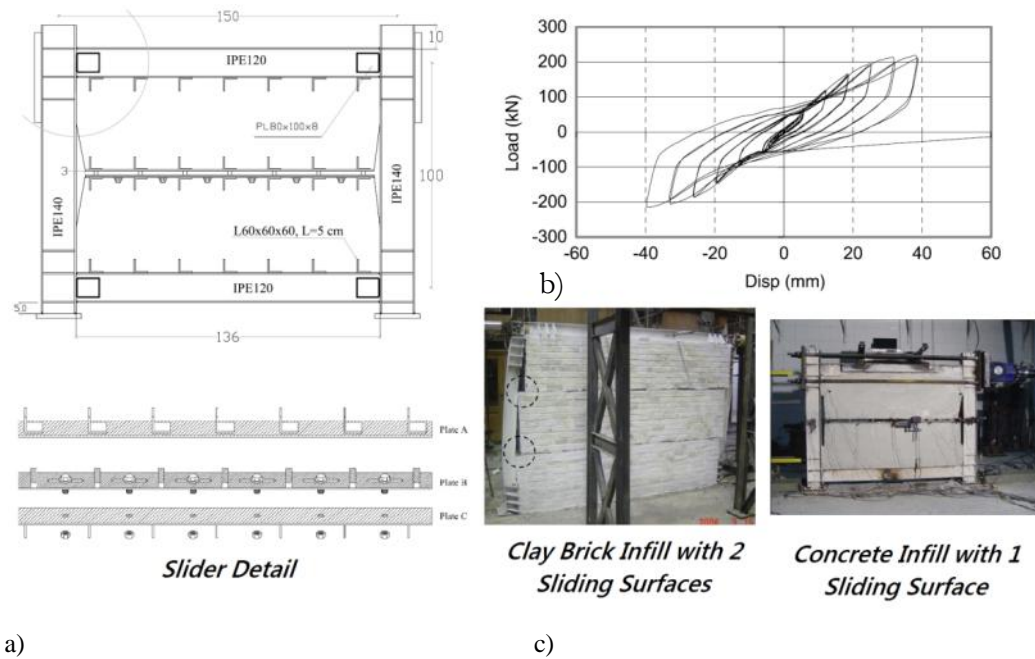


**Figure 3.6.** Experimental testing of a steel frame with friction sliding fuses by Mohammadi and Akrami [21]: a) Detail of the specimen and the slider, b) Hysteresis curve obtained from one of the specimens, c) Photographic view of the specimens

Aliaari and Memari [20] analytically investigated the performance of an isolation method for masonry infill walls. The system was named seismic infill wall isolator sub-frame (SIWIS). The system consisted of two vertical and one horizontal light-gauge steel studs connected to a surrounding frame. Then the isolator was to be placed between the sub-framing and the masonry infill. The isolator was designed to fail at a specified load limit after which the behaviour turned suddenly into bare frame behaviour (Figure 3.7). However, the method was later tested experimentally in 2007 [19] and it was observed that the SIWIS added a very brittle nature to the global behaviour, which may be considered to be an undesirable effect for such type of modifications.

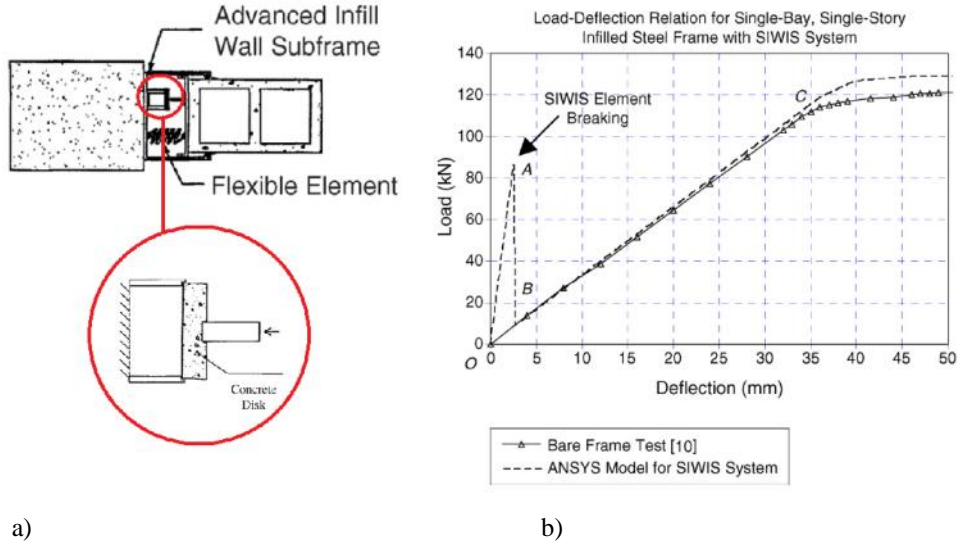


**Figure 3.7.** a) SIWIS isolator detail, b) Analytical load deflection curve compared to experimental bare frame curve (from Aliaari and Memari [19, 20])

### 3.1.2 Numerical Considerations for Heavy Infills: Focusing on the Modifications on the Dynamic Properties of Structures

Kose [43] analytically investigated the effects of different parameters on the fundamental period of RC buildings with infill walls. The studied parameters were the building height ( $H_B$ ), the number of bays ( $B$ ), the ratio shear walls' area to floor areas ( $S$ ), the ratio of infilled panels to the total number of panels ( $I$ ) and the type of frame ( $F$ ). The Following formula was proposed for the calculation of fundamental period ( $T$ ).

$$T = 0.0935 + 0.0301H_B + 0.0156B + 0.0039F - 0.1656S - 0.0232I, H (m), S(\%)$$

It was concluded that the number of floors is the primary parameter affecting the fundamental period. The percentage of the shear walls was identified as the second most important parameter. The percentage of infill walls and the number of bays almost had the same effect on the period Figure 3.8.

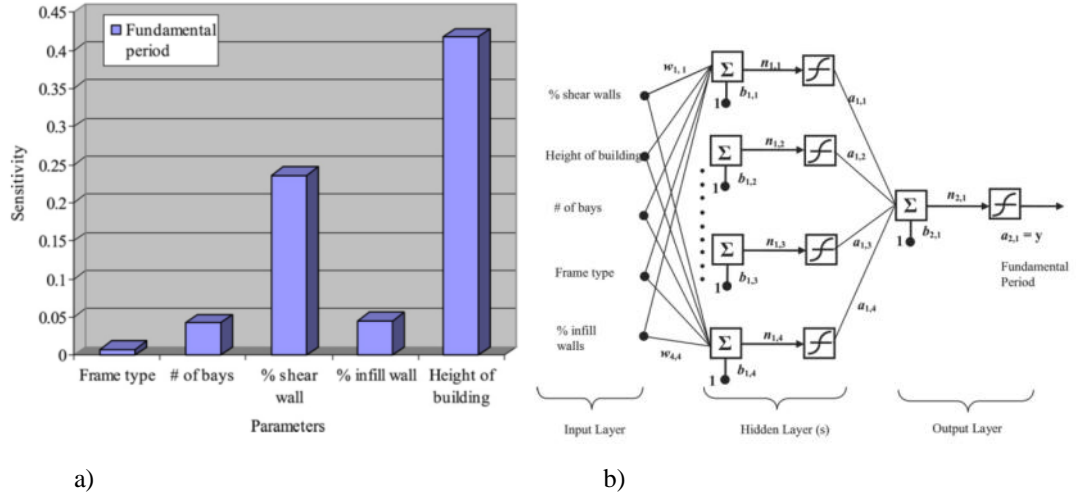


**Figure 3.8.** a) Sensitivity of fundamental period with respect to selected parameters, b) Architecture of artificial neural network (ANN) model used for sensitivity analysis from (Kose, [43])

Ricci et al. [44] carried out modal analyses on 3D-reinforced concrete frame building models with different geometrical properties (height, surface area, aspect ratio of the plan) and infill wall characteristics. Simplified formulas based on regression analyses were proposed. Furthermore, these expressions were compared to similar numerical expressions and experimental data. The authors suggested that analytical evaluation of the elastic period of infilled buildings had to be based on uncracked infill stiffness, or initial tangent stiffness. If another stiffness was assumed, the obtained numerical formulas overestimated the empirical data by 200% (Figure 3.9a). Moreover, assuming cracked stiffness at each storey did not represent the actual dynamic properties of a damaged infilled RC building. According to the authors, the distribution of damage at infill walls was not uniform along the height of the structure, but rather concentrated at the lowest storey (usually). As a result of the study, the following formulas were proposed by the authors:

$$\text{Cracked infills without openings} : T_x = 0.026H_B, T_y = 0.036H_B$$

$$\text{Cracked infill with openings} : T_x = 0.034H_B, T_y = 0.048H_B$$

$$\text{Simplified formula for infill without openings} : T = 0.031H_B \text{ (independent of dir.)}$$

$$\text{Simplified formula for infill with openings} : T = 0.041H_B \text{ (independent of dir.)}$$

Where:  $x$  and  $y$  : corresponds to longitudinal and transverse directions

$H_B$  : the building height

A plot of these expressions is shown in Figure 3.9b along with their comparison to experimental results from the literature.

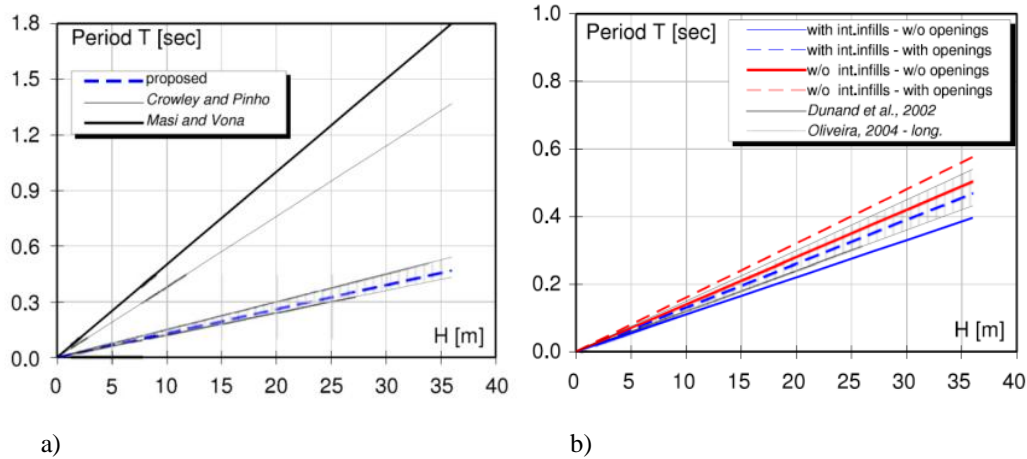


**Figure 3.9.** Comparison of numerical expressions proposed by Ricci et. al. [44] and other researchers with experimental observations (the proposed expression stays within the zone bounded by the experimental observations)

Hashemi and Hassanzadeh [45] analytically investigated the performance of a steel building with braces and brick infills. The considered building survived Bam earthquake in 2003. It was concluded that infill panels played a crucial role in preventing the structure from collapse. A view from the corner of the building is shown in Figure 3.10a, where steel sections and brick infills can be seen. Moreover, computed energy dissipated by each component in the structure is shown in Figure 3.10b, where the infills contribute to energy dissipation the most.

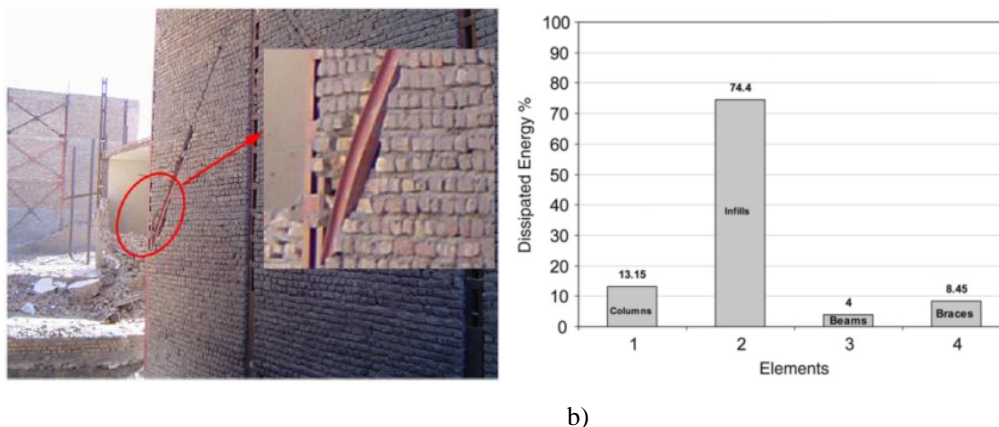


**Figure 3.10.** Analytical work of Hashemi and Hassanzadeh [45]: a) View from a corner of the building (Steel braces and brick infills can be seen), b) Energy dissipated by each component in the structure

### 3.2 Lessons Learnt from the Christchurch Earthquakes: Heavy Masonry Infill Walls

Although heavy masonry infill walls are not the most popular cladding type currently, there was a large number of building stock suffering damage to their heavy masonry infills after Christchurch earthquake in 22<sup>nd</sup> February 2011. The most common masonry infill type for old buildings was unreinforced clay brick infills. For newer buildings, reinforced grouted hollow masonry infill walls were the most common type. However, these two types of infill walls have very similar damage and failure mechanisms. The damage to these masonry infill walls is photographically summarized in this section.



**Figure 3.11.** Observed damage on masonry infills after the 22<sup>nd</sup> February 2011 Christchurch earthquake: a) Diagonal cracking, b) Close up view of the diagonal cracking



**Figure 3.12.** Observed damage on masonry infills after the 22nd February 2011 Christchurch earthquake: a) Sliding shear crack, b) Overall corner damage



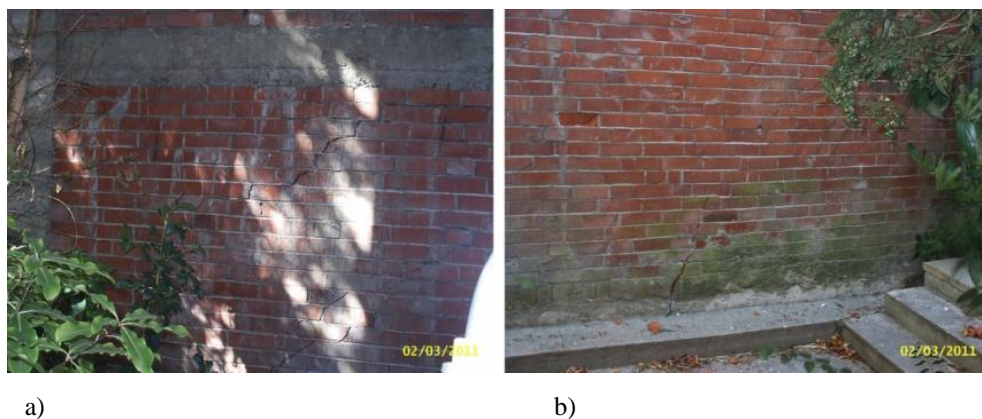


**Figure 3.13.** Observed damage on masonry infills after the 22nd February 2011 Christchurch earthquake: a-b) Diagonal cracking

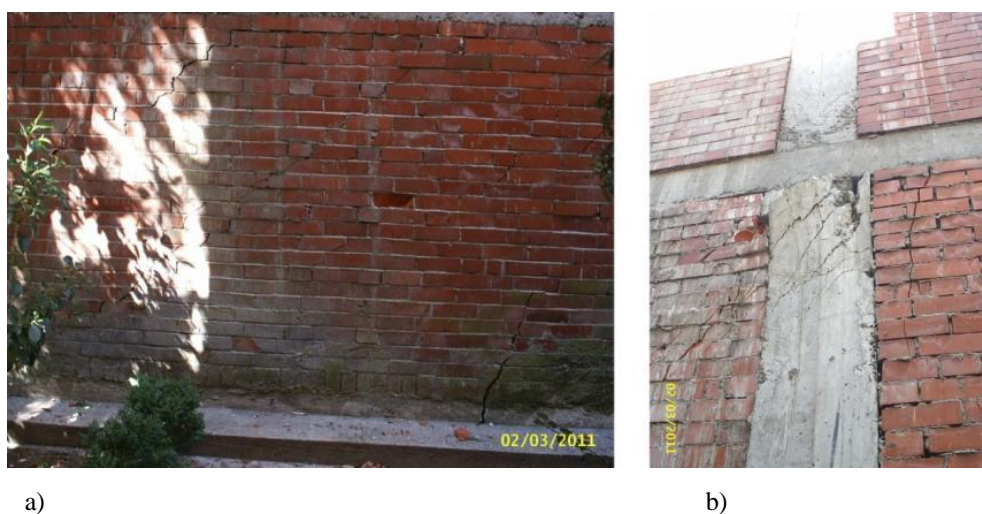


**Figure 3.14.** Observed damage on masonry infills after the 22nd February 2011 Christchurch earthquake: a) Diagonal cracking, b) Damage to column due to infill

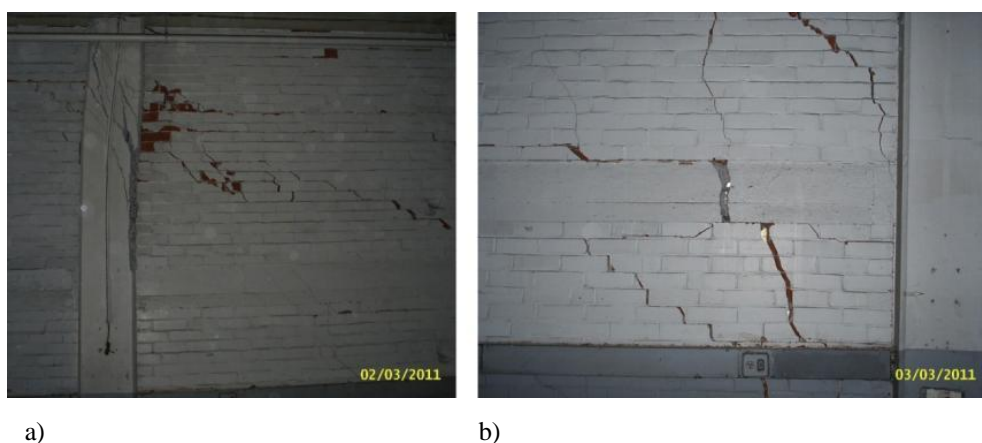


**Figure 3.15.** Observed damage on masonry infills after the 22nd February 2011 Christchurch earthquake: a) Sliding shear and column damage, b) Sliding shear and diagonal crack

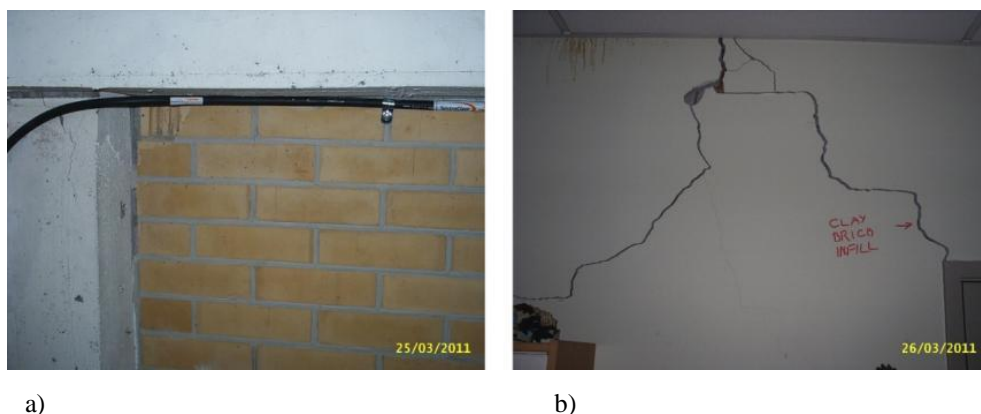


**Figure 3.16.** Observed damage on masonry infills after the 22nd February 2011 Christchurch earthquake: a) Corner crushing, b) Stepped cracks



**Figure 3.17.** Observed damage on masonry infills after the 22nd February 2011 Christchurch earthquake: a-b) Diagonal crack

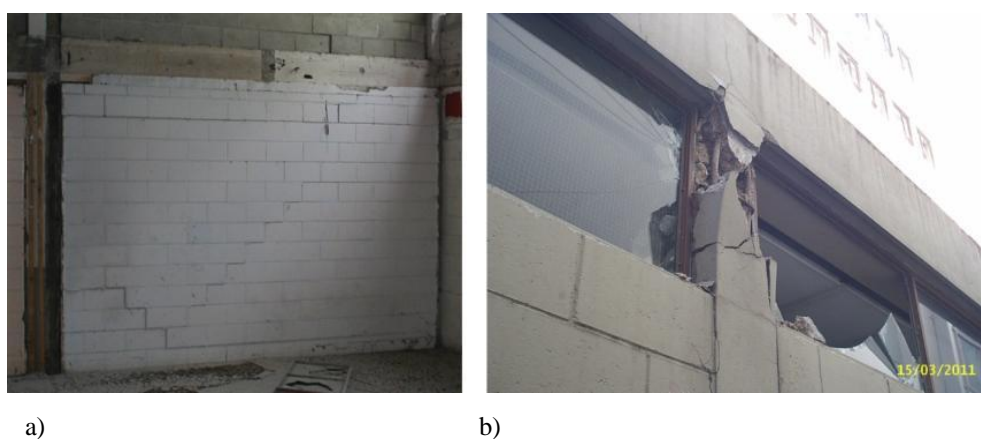


**Figure 3.18.** Observed damage on masonry infills after the 22nd February 2011 Christchurch earthquake: a) Diagonal crack, b) Short column

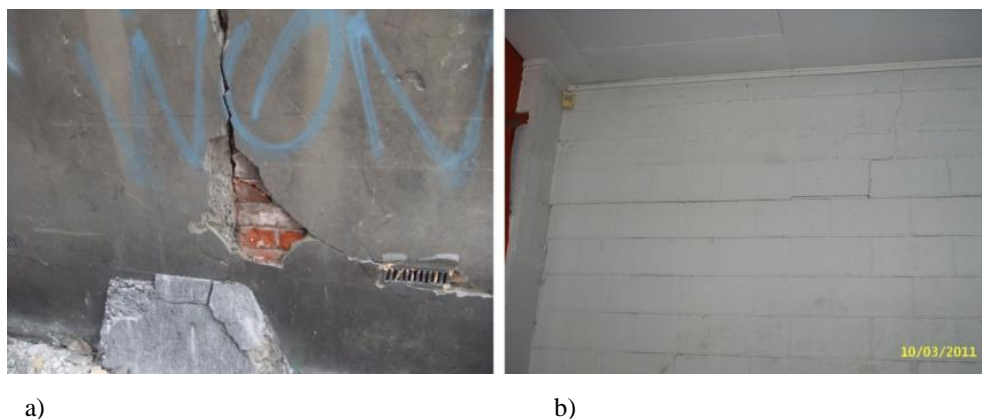


**Figure 3.19.** Observed damage on masonry infills after the 22nd February 2011 Christchurch earthquake: a) Corner crushing, b) Diagonal cracking



**Figure 3.20.** Observed damage on masonry infills after the 22nd February 2011 Christchurch earthquake: a-b) Sliding shear crack

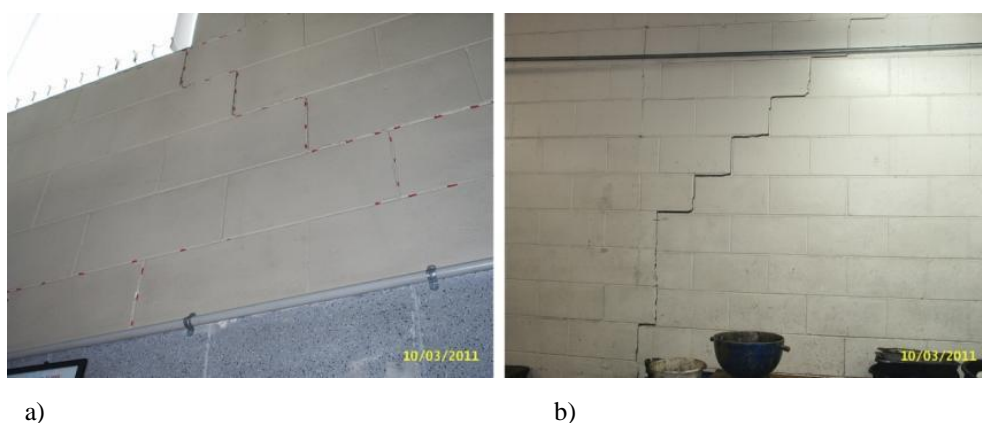


**Figure 3.21.** Observed damage on masonry infills after the 22nd February 2011 Christchurch earthquake: a-b) Diagonal crack



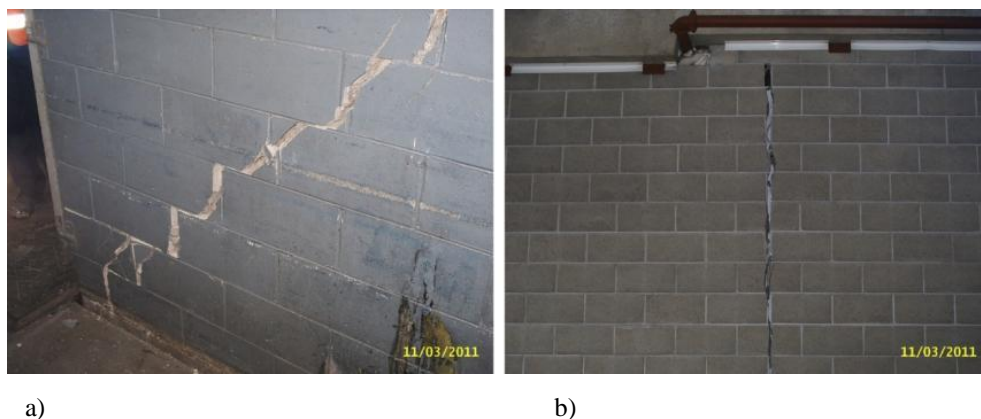


**Figure 3.22.** Observed damage on masonry infills after the 22nd February 2011 Christchurch earthquake: a) Diagonal crack, b) Vertical splitting

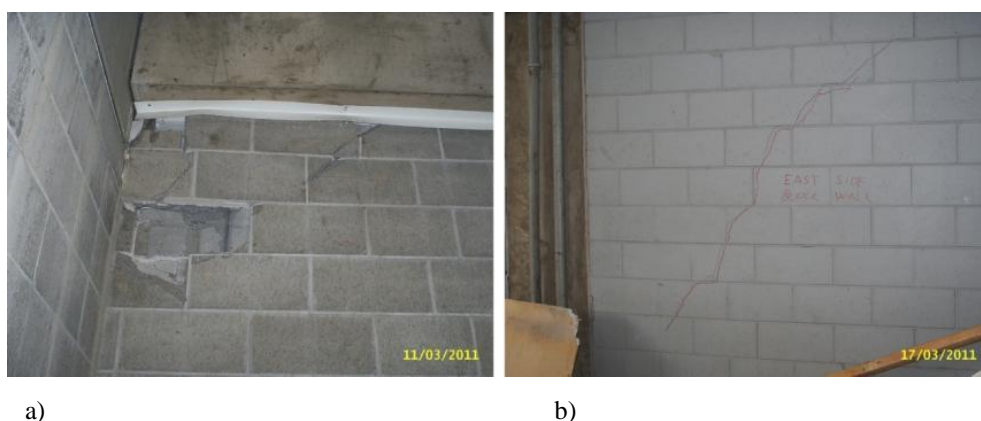


**Figure 3.23.** Observed damage on masonry infills after the 22nd February 2011 Christchurch earthquake: a) Corner crushing, b) Diagonal cracking



**Figure 3.24.** Observed damage on masonry infills after the 22nd February 2011 Christchurch earthquake: a) Short column, b) Diagonal cracking

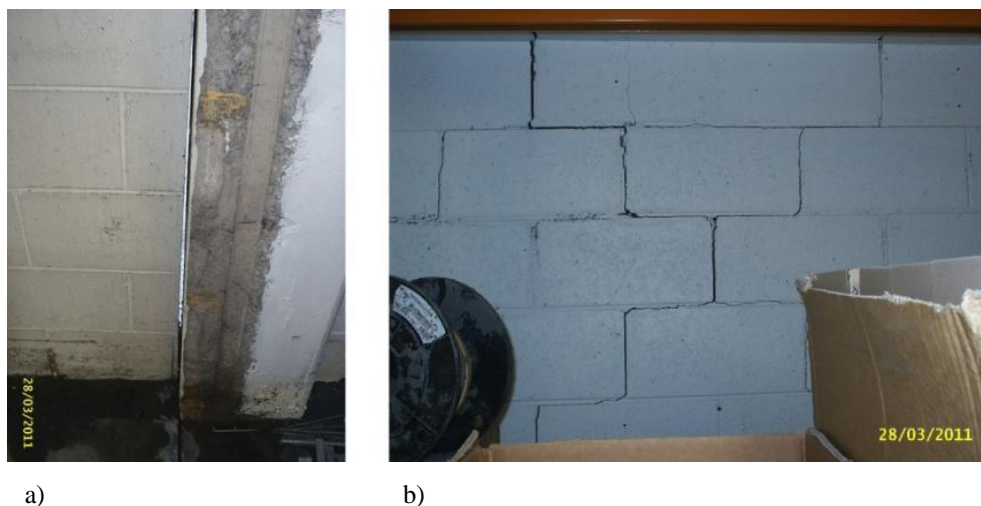


**Figure 3.25.** Observed damage on masonry infills after the 22nd February 2011 Christchurch earthquake: a) Separation, b) Diagonal cracking

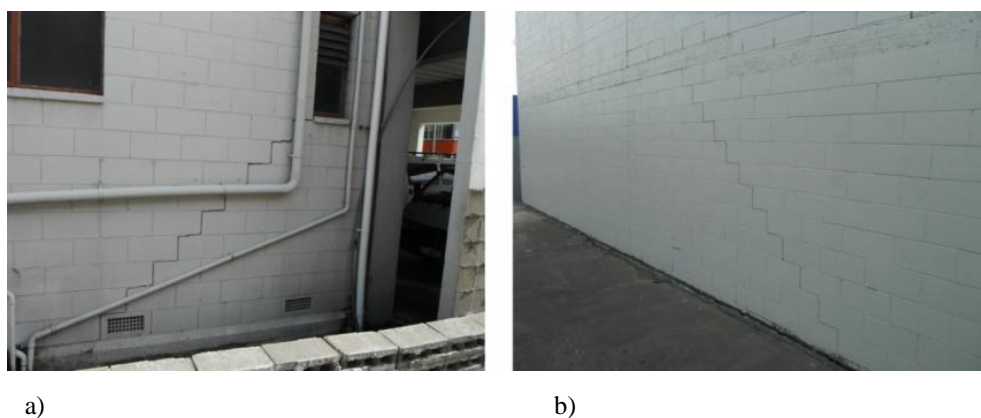


**Figure 3.26.** Observed damage on masonry infills after the 22nd February 2011 Christchurch earthquake: a-b) Diagonal cracking

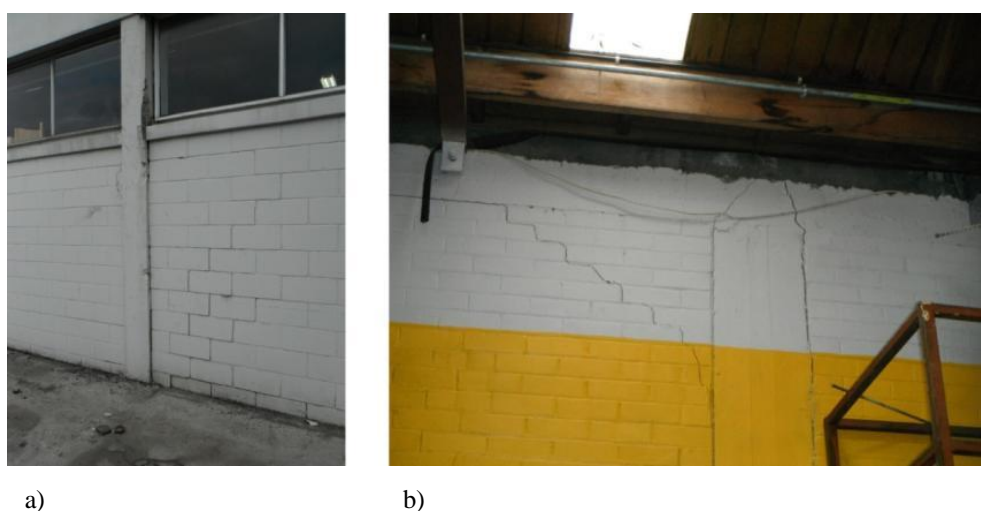


**Figure 3.27.** Observed damage on masonry infills after the 22nd February 2011 Christchurch earthquake: a) Diagonal cracking, b) Diagonal cracking and sliding on top

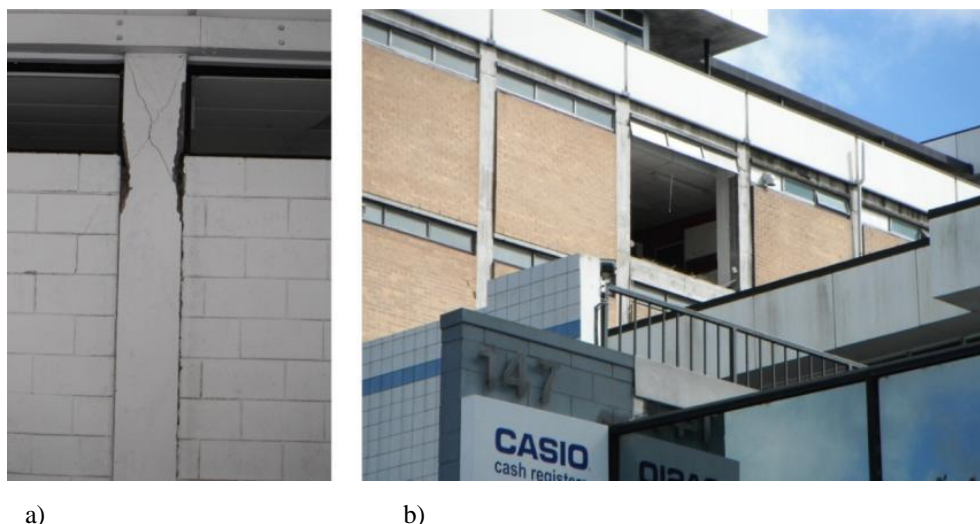


**Figure 3.28.** Observed damage on masonry infills after the 22nd February 2011 Christchurch earthquake: a) Short column, b) Out-of-plane failure of the clay brick infill wall

### 3.3 References

- [19] M. Aliaari and A. M. Memari, "Experimental Evaluation of a Sacrificial Seismic Fuse Device for Masonry Infill Walls," *Journal of Architectural Engineering*, vol. 13, pp. 111-125, June 2007.
- [20] M. Aliaari and A. M. Memari, "Analysis of Masonry Infilled Steel Frames with Seismic Isolator Subframes," *Engineering Structures*, vol. 27, pp. 487-500, 2005.
- [21] M. Mohammadi and V. Akrami, "An Engineered Infilled Frame: Behavior and Calibration," *Journal of Constructional Steel Research*, vol. 66, pp. 842-849, 2010.
- [37] R. Langenbach, "Learning from the Past to Protect the Future: Armature Crosswalls," *Engineering Structures*, vol. 30, pp. 2096-2100, 2008.
- [38] IBC, "INTERNATIONAL BUILDING CODE," ed: International Code Council, 2009.
- [39] G. M. Calvi and D. Bolognini, "Seismic Response of Reinforced Concrete Frames Infilled with Weakly Reinforced Masonry Panels," *Journal of Earthquake Engineering*, vol. 5, pp. 153-185, 2001.
- [40] K. M. Mosalam, R. N. White, and P. Gergely, "Static Response of Infilled Frames Using Quasi-Static Experimentation," *Journal of Structural Engineering*, vol. 123, pp. 1462-1469, 1997.

- [41] S. Pujol and D. Fick, "The Test of a Full-Scale Three-Story RC Structure with Masonry Infill Walls," *Engineering Structures*, vol. 32, pp. 3112-3121, 2010.
- [42] A. A. Tasnimi and A. Modebkhah, "Investigation on the Behavior of Brick-Infilled Steel Frames with Openings, Experimental and Analytical Approaches," *Engineering Structures*, vol. 33, pp. 968-980, 2011.
- [43] M. M. Kose, "Parameters Affecting the Fundamental Period of RC Buildings with Infill Walls," *Engineering Structures*, vol. 31, pp. 93-102, 2009.
- [44] P. Ricci, G. M. Verderame, and G. Manfredi, "Analytical Investigation of Elastic Period of Infilled RC MRF Buildings," *Engineering Structures*, vol. 33, pp. 308-319, 2011.
- [45] B. H. Hashemi and M. Hassanzadeh, "Study of Semi-Rigid Steel Braced Building Damaged in the Bam Earthquake " *Journal of Constructional Steel Research*, vol. 64, pp. 704-721, 2008.

# CHAPTER 4

## EXPERIMENTAL PROGRAMME

*The best scientist is open to experience and begins with romance - the idea that  
anything is possible.*

*Ray Bradbury*



## 4 EXPERIMENTAL PROGRAMME

In order to determine the cyclic performances of different non-structural infill wall types, a quasi static testing programme was followed. A specially designed full scale structural testing frame was utilized throughout the study. Within this testing frame, as built (existing) practices of light and heavy non-structural walls as well as the proposed low damage solutions were installed and tested. In this chapter, the details of the experimental programme are reported.

### 4.1 Test Setup

To test the reverse cyclic performances of non-structural infill walls, a reusable full scale reinforced concrete PRESSS frame [46] was specially designed to be utilized in the experimental programme. The structural frame, acting itself as the testing rig, consisted of two precast RC columns and beams ( $f'_c=50$  MPa,  $f_y=500$  MPa) connected by two D40 Macalloy 1030 unbonded post tensioning bars [47], one per each connection with a post tensioning force of 80 kN. The adoption of this structural system had the following benefits:

- 1) The precast RC frame behaved elastically and re-centred without undergoing any permanent damage and residual displacement. As such, it could be used multiple times with only the infill wall requiring to be substituted.
- 2) Since the behaviour of the frame always remained linear elastic, the behaviour of the infill walls could easily be extracted from the global behaviour.

In order to prevent different rates of beam elongations and the resulting clamping effect to the columns, pivot points were provided at the lower beam ends. Therefore, the beam elongation only occurred at the upper beam without any clamping effect on the columns. The resulting frame was connected to the strong floor by two pin supports. A hydraulic jack of 1000 kN capacity was used to impose in-plane displacements on the structural frame. In order to constrain the frame against out-of-plane deformations, four rollers (two on each side) were placed at the upper beam level. The deformed shape of the setup simulated the inter-storey drift at an inner



storey of a multi-storey structure. The test setup is schematically and photographically shown in Figure 4.1 and Figure 4.2 respectively.

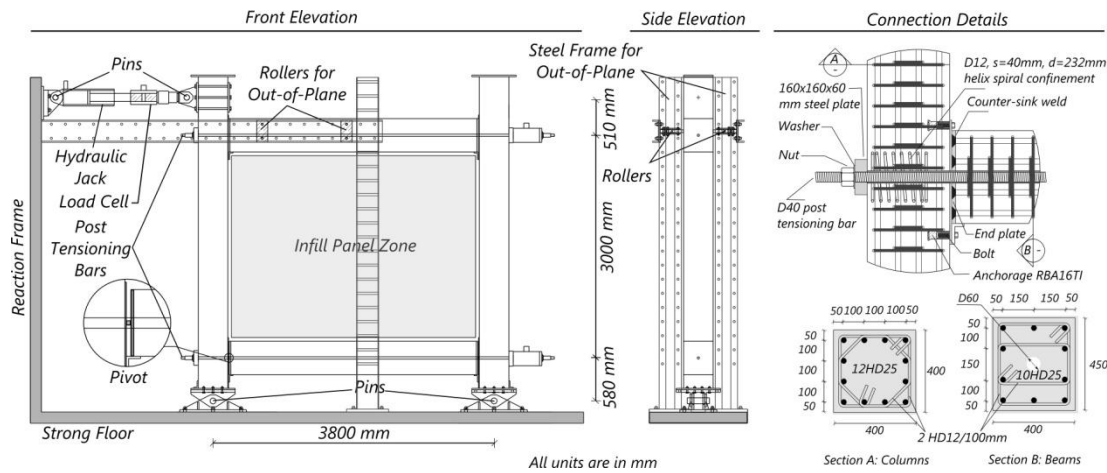


**Figure 4.1.** Test setup and the top beam-to-column connection detailing

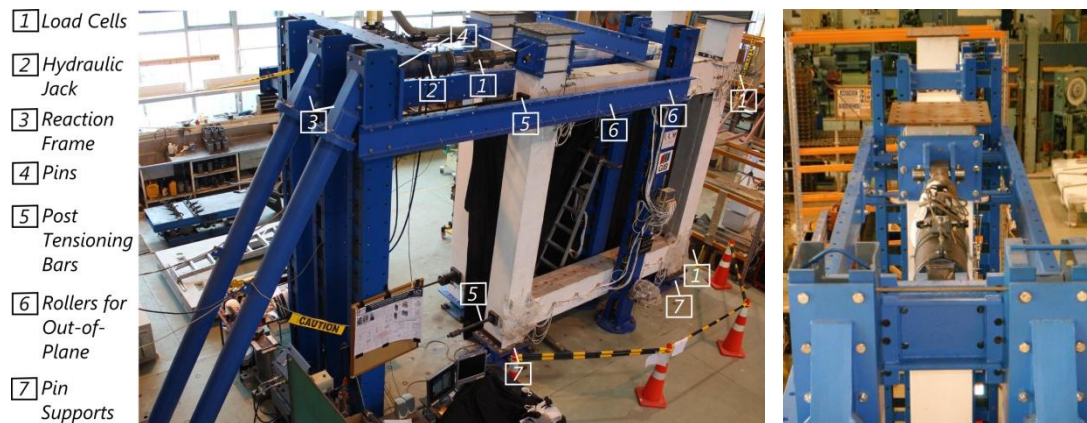


**Figure 4.2.** Photographic view of the setup

The columns and the beams were designed to resist the forces to be exerted by all of the different non-structural infill wall types, planned to be tested as part of the experimental campaign, namely as built drywalls and unreinforced clay bricks as well as the low damage solutions developed for each. The moment capacity of the connections was similar to that of a typical RC frame and it can be controlled by changing the post-tensioning force of the unbounded post-tensioning bars. The connections exhibited rocking type behaviour, i.e. gap opening/closing, and cause the initial post tensioning forces to increase with the applied drift increments. Due to this increase, an additional confinement requirement, as stated by ETA 07/0046 [47], was provided in the form of helix shaped confining reinforcement as suggested by ETA 07/0046. The details of the beam-column connection are given in Figure 4.1.



In terms of loading protocol, the recommendations of ACI374.1-05 [48] was followed with the simplification of not including the intermediate small cycles between two consecutive drift amplitude levels. For the selection of the applied drift levels, ACI374.1-05 requirement is as follows:

$$1.25 \cdot D_i \leq D_{i+1} \leq 1.5 \cdot D_i \quad (4.1)$$

where  $D_i$  : Previous drift amplitude

$D_{i+1}$  : Next drift amplitude

Following the above criterion, the drift history shown in Figure 4.3 was prepared and used in the tests.

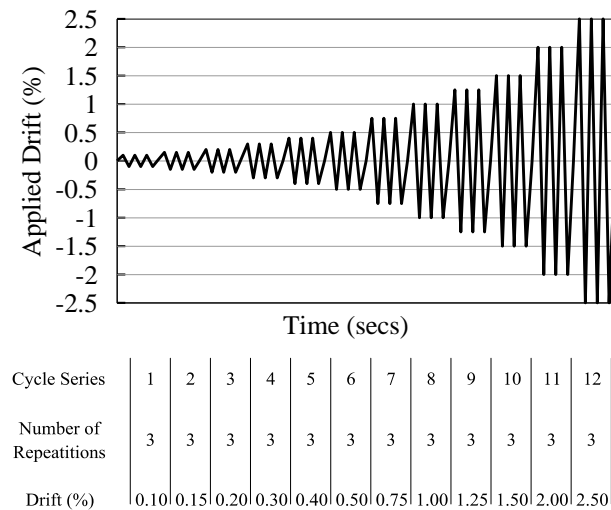


**Figure 4.3.** Applied drift history

All test specimens were monitored using 3 load cells, 5 rotary pods and 57 potentiometers. Among those, one rotary pod recorded the top deflection occurring at the level of the applied load and two were placed at the beam levels to be able to calculate the inter-storey drifts imposed on the structure (all of them were installed on the right RC column in Figure 4.4). The general layout of the instrumentation is shown in Figure 4.4. It should be noted that this layout is a general scheme developed for all wall types planned in the experimental campaign and not all of the instruments were essential in each test.

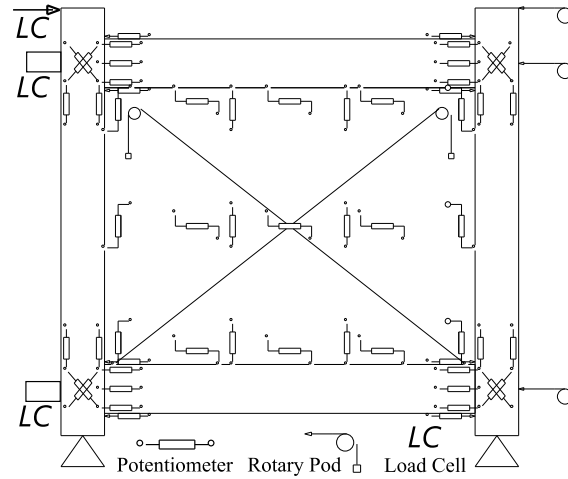


**Figure 4.4.** General instrumentation scheme

## 4.2 Test Specimens

Both heavy and light non-structural infill wall practices, i.e. steel and timber framed drywalls and unreinforced clay brick infill walls, were covered in the research. The construction details of each will be given in different chapters. These specimens are summarized in Table 4.1. The materials used for the construction of these wall types are given in the next section.

The notation used in naming the specimens is given below:

BF

FIFi-Type

MIFi-Type

where BF : Bare Frame

FIF : Fully Infilled Frame (Conventional/As built practice)

MIF : Modified Infilled Frame (Low damage solution)

i : Specimen number

Type : STFD for Steel Framed Drywall

TBFD for Timber Framed Drywall

UCBI for Unreinforced Clay Brick Infill wall

**Table 4.1.** Summary of the test specimens

Test No	Specimen	Explanation	Panel Thickness (mm)	Panel Length (mm)	Panel Height (mm)
Test 1	BF	Bare Frame	-	-	-
Test 2	FIF1-STFD	Conventional Steel Framed Drywall	120	3400	2550
Test 3	FIF2-TBFD	Conventional Timber Framed Drywall	120	3400	2550
Test 4	MIF1-STFD	Low Damage Steel Framed Drywall	120	3400	2550
Test 5	MIF2-TBFD	Low Damage Timber Framed Drywall	120	3400	2550
Test 6	FIF3-UCBI	Fully Infilled Unreinforced Clay Brick Masonry	140	3400	2550
Test 7	MIF5-UCBI	Low Damage Unreinforced Clay Brick Masonry	140	3400	2550

Note: Clay brick infill walls are built as double skinned cavity walls with an internal cavity of 10 mm.

If the gap is also considered, the total thickness of the infill becomes 150 mm

### 4.3 Materials

The reinforced concrete members were cast by the precast concrete company Stahlton in Christchurch, New Zealand. For the concrete, a self compacting concrete mix was used targeting a characteristic strength  $f'_c=50$  MPa on 28<sup>th</sup> day. As for the reinforcing steel, deformed steel with the characteristic yield strength  $f_y=500$  MPa was used. The stress strain plot for the steel and the concrete compressive strength test results on the testing day of the bare frame (average of 6 cylinders taken during the casting of the members) are shown in Figure 4.5 along with a summary shown in Table 4.2. The concrete cylinder specimens had 100 mm diameter and 200 mm height and the strength values were calculated accordingly.

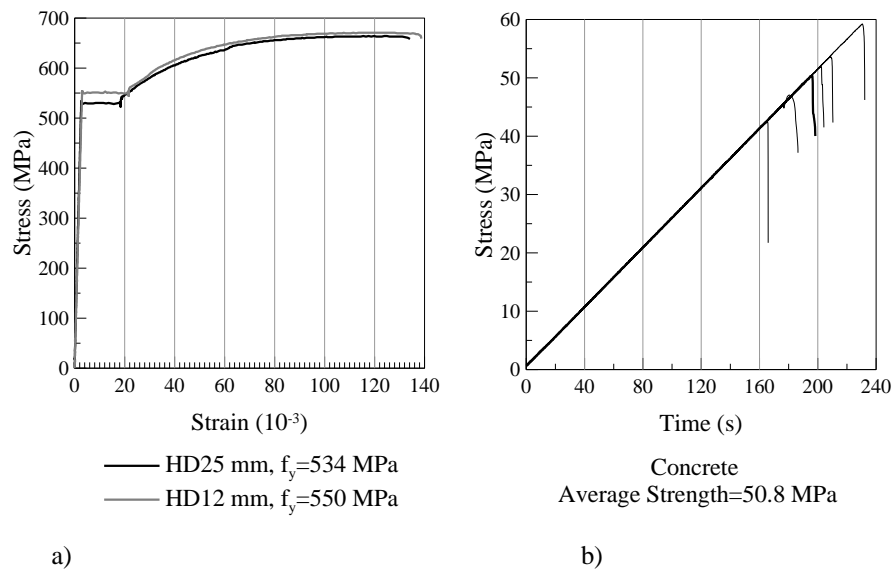


**Figure 4.5.** a) Stress-strain property of the steel (Average of 3 bars), b) Concrete cylinder test results (Average of 6 cylinders) on the testing day of the bare frame

**Table 4.2.** Summary of material strengths

Material	Average Characteristic Strength (MPa)
Concrete	50.8
Steel HD 25	534
Steel HD 12	550

#### 4.4 Design of the Bare Frame

Due to the intended repetitive usage of the test setup, the bare frame had to be designed for the worst possible case situation, i.e. inducing structural damage to the frame. The following considerations were made while designing the setup:

- Highest internal moments develop in the RC members when the bare frame is considered.
- Highest shear forces develop in the RC members when the frame with unreinforced clay brick infill wall is considered.
- There are basically four types of failure for fully infilled frames with unreinforced clay bricks; crushing at the centre, crushing at the corners, sliding shear, diagonal tension (Figure 4.6). Each of those failure modes may induce different local shear forces on the RC members, which may cause unexpected premature local failures in the RC framing.

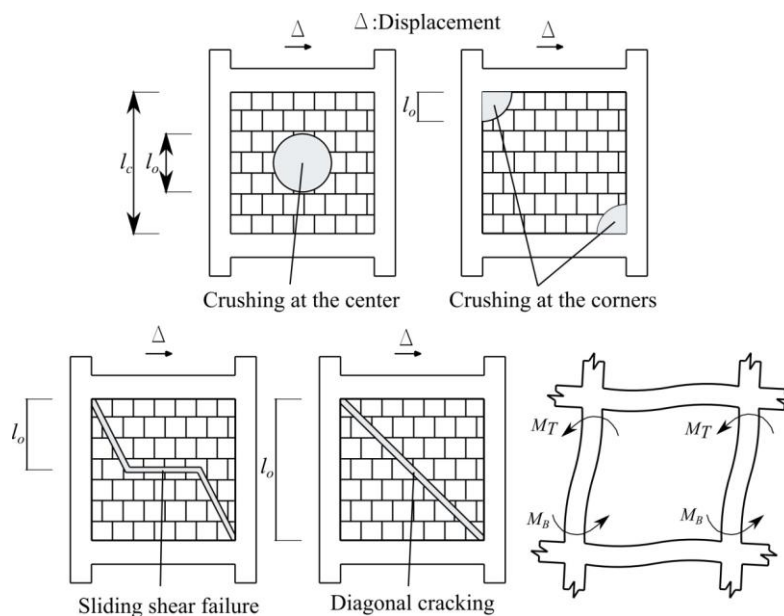


**Figure 4.6.** Failure types for frames fully infilled with unreinforced clay bricks

These different failure types may affect the shear demand transferred to the frame by changing the clear story height ( $l_c$ ) as suggested in the capacity design principles by Paulay and Priestley [11], which is shown in the equation below (The change in  $l_c$  by  $l_o$  resulting from different failure types of the infill is shown in Figure 4.6):

$$V_D = \frac{M_T + M_B}{l_c} \quad (4.2)$$

Where;  $M_T$  : Bending moment at the top of the column  
 $M_B$  : Bending moment at the bottom of the column  
 $l_c$  : Clear story height ( $=l_o$  for different infill failures)  
 $l_o$  : Opening height in Figure 4.6

In equation 2, the clear story height,  $l_c$ , may differ for each of the failure types depending on the expected failure modes as shown in Figure 4.6. In each of these failure modes, the clear height may be reduced due to the openings formed as a result of the failure of the clay brick infill and it may result in an increased shear demand on the columns, which may also cause diagonal compression struts to form at these locations. In Figure 4.7, some examples of column failures caused by the local and global failure of the infill walls are shown.

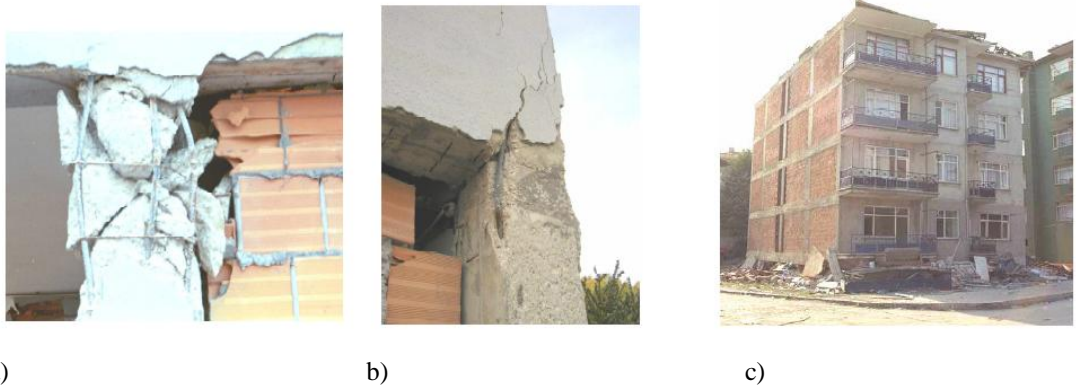


**Figure 4.7.** Local and global failures caused by the infill walls: a-b) Corner crushing resulting in short column effect and resulting increased shear demand on columns, c) Global soft storey collapse mechanism (Photos are from Magenes and Pampanin [10])

Due to these issues caused by the failure of the clay brick infill walls, in the design of the members of the RC frame, a conservative overdesign was necessary in order to utilize the test setup repetitively. The possibility of a certain level of cracking in the RC framing existed due to the low tensile strength of concrete in the unconfined cover region. However, the development of cracks was expected to cease in progress after testing the bare frame a couple of times whereby its behaviour would remain linear elastic at each test due to the self-centring provided by the post-tensioning bars.

#### 4.4.1 Calculation of the Infill Wall Capacity

The failure strength for each of the above mentioned failure types can be given by the following equations as reported by Bertoldi et. al. [49]:

$$\text{Crushing at the center} : \sigma_w = \frac{1.16f'_w \tan \theta}{K_1 + K_2 \lambda h} \quad (4.3)$$

$$\text{Corner crushing} : \sigma_w = \frac{1.12f'_w \sin \theta \cdot \cos \theta}{K_1 (\lambda h)^{-0.12} + K_2 (\lambda h)^{0.88}} \quad (4.4)$$

$$\text{Sliding shear} : \sigma_w = \frac{(1.2 \sin \theta + 0.45 \cos \theta) f_{wu} + 0.3 \sigma_v}{b_w / d_w} \quad (4.5)$$

$$\text{Diagonal cracking} : \sigma_w = \frac{0.6 f_{ws} + 0.3 \sigma_v}{b_w / d_w} \quad (4.6)$$

$$\lambda = \sqrt[4]{\frac{E_w t_w \sin(2\theta)}{4E_c I_p h_w}} \quad (4.7)$$

$$E_w = \left[ \frac{\cos^4 \theta}{E_{wh}} + \frac{\sin^4 \theta}{E_{wv}} + \cos^2 \theta \cdot \sin^2 \theta \cdot \left( \frac{1}{G} - 2 \cdot \frac{\nu}{E_{wv}} \right) \right] \quad (4.8)$$

$$b_w = \left( \frac{K_1}{\lambda h} + K_2 \right) d_w \quad (4.9)$$

**Table 4.3.** Values of K1 and K2 given by Bertoldi et. al. [49]

	$\lambda h < 3.14$	$3.14 < \lambda h < 7.85$	$\lambda h > 7.85$
$K_1$	1.3	0.707	0.47
$K_2$	-0.178	0.01	0.04

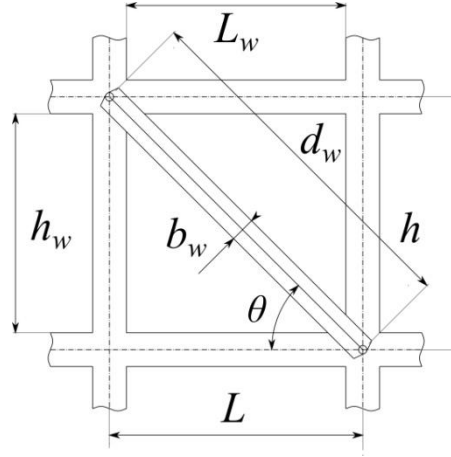


**Figure 4.8.** Geometrical dimensions used in the unreinforced clay brick infill strut formulations and calculations

- Where:
- $\sigma_w$  : Equivalent diagonal strut strength
  - $f'_w$  : Compressive strength of masonry
  - $f_{wu}$  : Sliding shear strength of mortar joints
  - $\sigma_v$  : Vertical stress on the wall
  - $f_{ws}$  : Shear strength from diagonal compression test
  - $K_1, K_2$  : Calibrated coefficients by Bertoldi et. al. [49]
  - $\lambda$  : Relative stiffness between the infill and the frame
  - $\theta$  : Angle between the diagonal strut and the horizontal
  - $h$  : Inter-storey height (from centroidal points)
  - $b_w$  : Compression strut width
  - $d_w$  : Diagonal strut length (from centroidal points)
  - $E_w$  : Modulus of elasticity for the diagonal strut
  - $E_{wh}$  : Modulus of elasticity of the masonry infill in horizontal
  - $E_{wv}$  : Modulus of elasticity of the masonry infill in vertical
  - $t_w$  : Thickness of the infill wall
  - $E_c$  : Approximate modulus of elasticity for concrete
  - $I_p$  : Moment of inertia for the columns
  - $h_w$  : Infill wall height
  - $G$  : Shear modulus of the masonry infill
  - $\nu$  : Poisson's ratio

For design purposes, the unreinforced clay brick material data reported by Kaushik et. al. [50] was used and are shown in Figure 4.9.

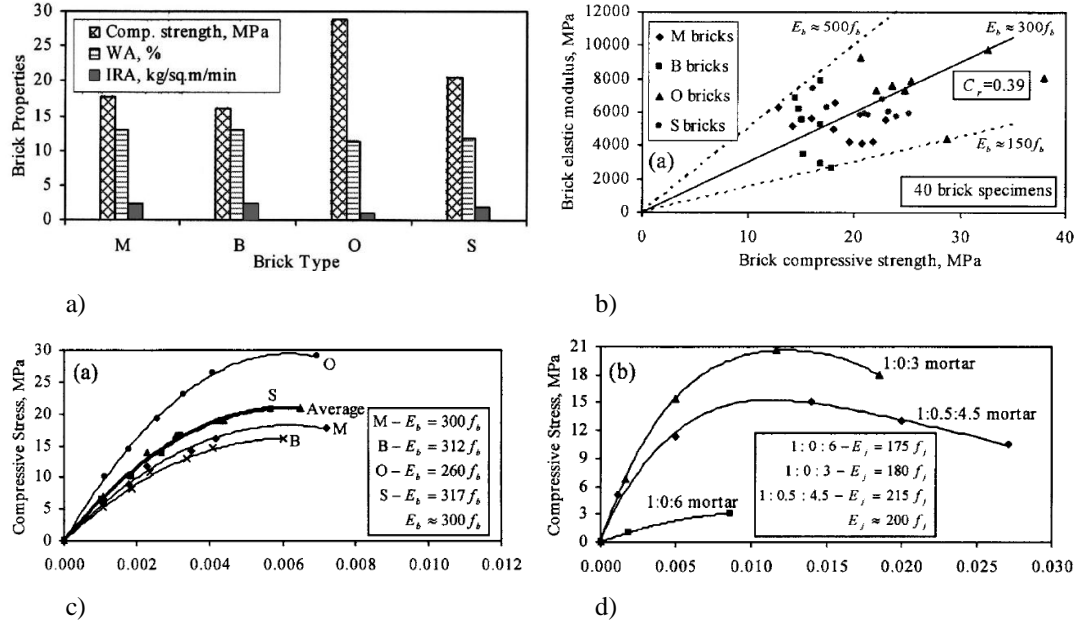


**Figure 4.9.** Clay brick material data by Kaushik et. al. [50]: a) Brick compressive strength by different manufacturers, b) Modulus of elasticity vs. compressive strength, c) Clay brick compressive stress vs. strain, d) Mortar stress vs. strain

When Kaushik's data was considered, the following could be extrapolated and assumed from the results in order to calculate the required material properties of the clay brick infills;

$$f'_w \approx 20 \text{ MPa (Compressive strength of the masonry)}$$

$$E_{wv} = 300f'_w \approx 6000 \text{ MPa (Modulus of elasticity of masonry in vertical)} \quad (4.10)$$

Using the data above, two capacity calculations were made for unreinforced clay brick infill wall. One with a typical mortar strength of 300 kPa, and the other one being 3100 kPa, as reported by Kaushik et. al. [50]. Table 4.4 and Table 4.5 show the tabulated results. It can be observed that the change in mortar strength does not cause a significant change in the governing failure mode, which is diagonal cracking or shear sliding that is expected to occur in the order of 250 kN diagonal strut force. However, due to the scattered material properties of clay bricks, these formulas only give an approximation rather than an exact estimation and were only used for an overall idea of the magnitude of the shear forces to be resisted by the columns and beams.



**Table 4.4.** Unreinforced clay brick diagonal strut failure strengths using 300 kPa mortar strength (A typically assumed mortar strength value)

INFILL PROPERTIES		FAILURE STRENGTHS	
hw (m)=	2.55 Infill Height	Compression at the center of the panel	
lw (m)=	3.4 Infill Length	$\sigma_w$ (kPa)= 11866.46	<b>1879.89 kN</b>
dw (m)=	4.85 Diagonal Length	fw= 9571.275	
tw (m)=	0.14 Infill Thickness	Compression at the corners	
h (m)=	3 Interstorey Height (CENTER TO CENTER)	$\sigma_w$ (kPa)= 8104.964	<b>1284 kN</b>
l (m)=	3.8 Span Length (CENTER TO CENTER)	Sliding shear	
Ewh (kPa)=	2773000 Masonry Panel Horizontal Modulus of E	$\sigma_w$ (kPa)= 1538.826	<b>243.782 kN</b>
Ewv (kPa)=	6000000 Masonry Panel vertical Modulus of E	Diagonal tension	
G (kPa)=	2500000 Shear Modulus	$\sigma_w$ (kPa)= 1594.411	<b>252.588 kN</b>
$\nu$ =	0.2		
Ec (kPa)=	21000000 Concrete Modulus		
bc (m)=	0.4 Column Width		
hc (m)=	0.4 Column Height		
fwh (kPa)=	1849 Compression Strength in the horizontal	Note: Clay brick material data except for the mortar are chosen considering Kaushik 2007. For mortar typical values from literature are assumed	
fwv (kPa)=	20000 Compression Strength in the vertical		
fwu (kPa)=	300 Mortar Joint Strength		
$\sigma_v$ (kPa)=	100 Vertical Compression Stress Due to Grav Loads		
fws (kPa)=	570 Shear Strength from Compression Diagonal Test		

**Table 4.5.** Unreinforced clay brick diagonal strut failure strengths using 3100 kPa mortar strength value given by Kaushik et. al. [50]

INFILL PROPERTIES		FAILURE STRENGTHS	
hw (m)=	2.55 Infill Height	Compression at the center of the panel	
lw (m)=	3.4 Infill Length	$\sigma_w$ (kPa)= 11866.46	<b>1879.89 kN</b>
dw (m)=	4.85 Diagonal Length	fw= 9571.275	
tw (m)=	0.14 Infill Thickness	Compression at the corners	
h (m)=	3 Interstorey Height (CENTER TO CENTER)	$\sigma_w$ (kPa)= 8104.964	<b>1284 kN</b>
l (m)=	3.8 Span Length (CENTER TO CENTER)	Sliding shear	
Ewh (kPa)=	2773000 Masonry Panel Horizontal Modulus of E	$\sigma_w$ (kPa)= 14701.11	<b>2328.96 kN</b>
Ewv (kPa)=	6000000 Masonry Panel vertical Modulus of E	Diagonal tension	
G (kPa)=	2500000 Shear Modulus	$\sigma_w$ (kPa)= 1594.411	<b>252.588 kN</b>
$\nu$ =	0.2		
Ec (kPa)=	21000000 Concrete Modulus		
bc (m)=	0.4 Column Width		
hc (m)=	0.4 Column Height		
fwh (kPa)=	1849 Compression Strength in the horizontal	Note: Clay brick material data and the mortar values are chosen considering Kaushik 2007	
fwv (kPa)=	20000 Compression Strength in the vertical		
fwu (kPa)=	3100 Mortar Joint Strength		
$\sigma_v$ (kPa)=	100 Vertical Compression Stress Due to Grav Loads		
fws (kPa)=	570 Shear Strength from Compression Diagonal Test		

#### 4.4.2 Shear and Moment Capacities of the RC Columns and RC Beams

The calculated strut failure force, in the range of 250 kN, can be reached under 520 kN total lateral load applied on the structure as shown in Figure 4.10a, which is a very rough estimation. Also, this results in shear forces developing in the order of 500 kN in the column and 300 kN in the beam elements. Therefore, the RC members were design to carry such magnitude of shear forces. The test specimen was idealized as a monolithic RC frame without taking into account the gap opening and closing action of the connections. This approach gives the highest expected member design moments

that can develop in the RC members so that a conservative design can be carried out, facilitating repetitive use of the test setup. The maximum moments that can be imposed on this idealized system is in the order of 480 kNm, which can be reduced by choosing different levels of post tensioning during the testing phase. However, the capacity supplied for columns and beams are in the order of 450 kNm (Figure 4.13), which was sufficient enough to resist even the most undesirable conditions for the bare frame.

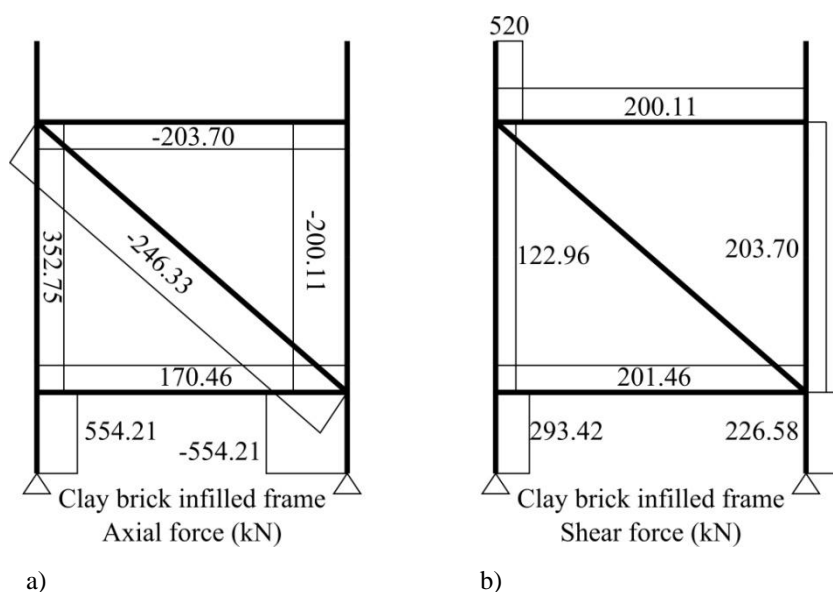


**Figure 4.10.** Member force diagrams under 520 kN total lateral loading on the frame with diagonal strut: a) Axial force, b) Shear force

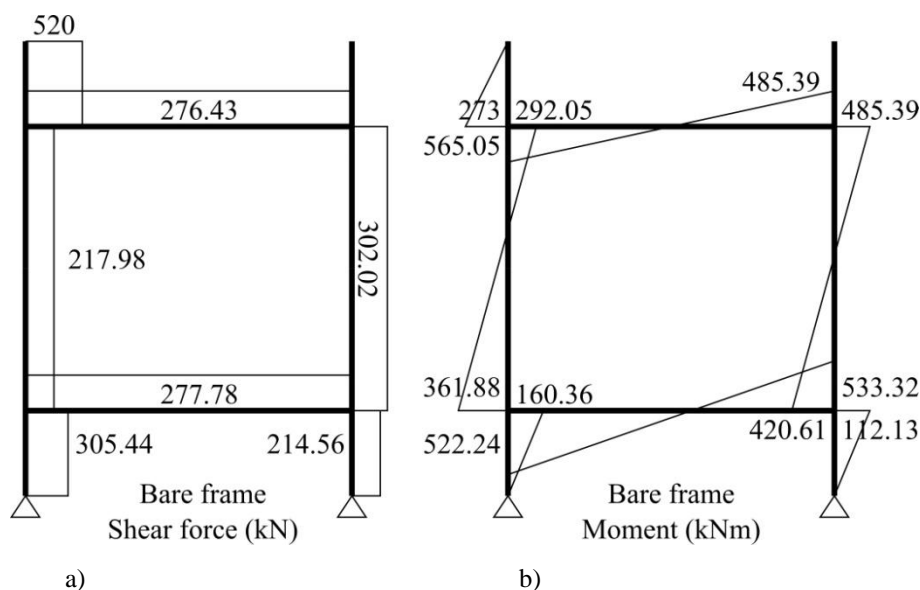


**Figure 4.11.** Member force diagrams under 520 kN total lateral loading on the bare frame: a) Shear force, b) Moment

While designing for shear, the highest expected shear force on the system was considered (520 kN). To account for the possible additional shear demand that can be caused by different failure modes of the clay brick infills, this number was multiplied by 1.5 and the contribution of concrete was neglected. Also, for ease of construction, the beams were reinforced for the same amount of shear demand as the columns. The resulting section details are shown in Figure 4.12.

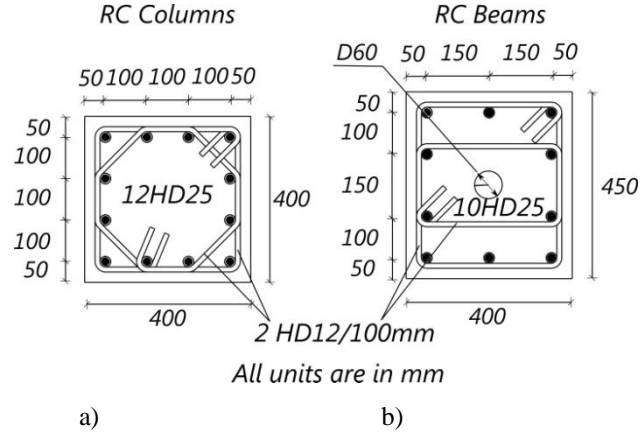


**Figure 4.12.** Member details: a) RC columns, b) RC beams

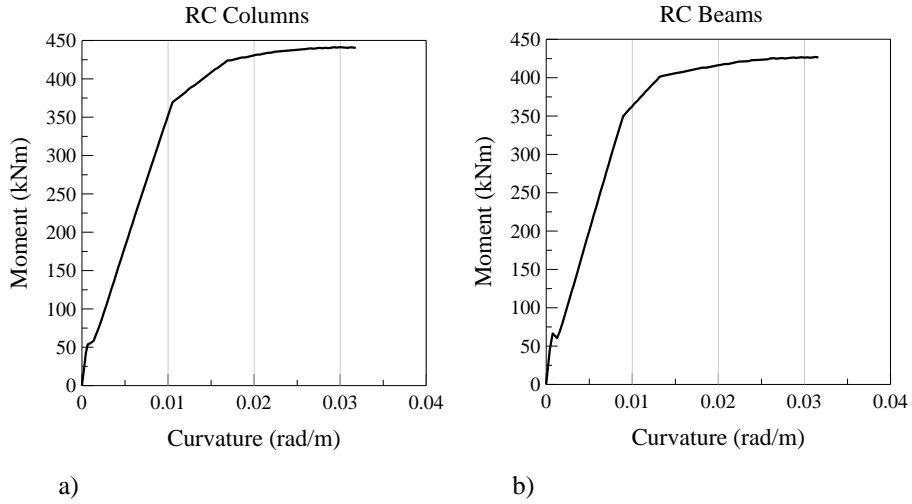


**Figure 4.13.** Moment curvature graphs of the resulting sections: a) RC columns, b) RC beams

The resulting shear capacities of the given sections can be calculated as (without taking concrete into account):

$$V_s = \frac{A_{sw}}{s} \cdot f_{yw} \cdot d \quad (4.11)$$

$$V_{sc} = \frac{4 \cdot \pi \cdot 12^2 / 4}{100} \cdot 500 \cdot 350 \times 10^{-3} = 792 \text{ kN} > 1.5 \cdot 520 = 780 \text{ kN}$$

$$V_{sb} = \frac{4 \cdot \pi \cdot 12^2 / 4}{100} \cdot 500 \cdot 400 \times 10^{-3} = 905 \text{ kN} > 1.5 \cdot 300 = 450 \text{ kN}$$

$V_s$  : Supplied shear capacity by the steel

$V_{sc}$  : Supplied shear capacity by the steel in column members

$V_{sb}$  : Supplied shear capacity by the steel in beam members

$f_{yw}$  : Yielding strength of the transverse steel

$d$  : Effective depth of the section

$A_{sw}$  : Total area of the transverse steel supplied at a section

#### 4.5 Construction of the Bare Frame

The bare frame (BF) is the structural part of the test setup and it was repeatedly used by only changing the infill panel content. In order to determine its reverse cyclic behaviour, the bare frame was tested as the first test specimen. The construction sequence of the bare frame is summarized in Figure 4.14.

The construction was carried out in four steps. In the first step, the pin supports were fixed to their positions and locked in place so that the rotation at pins was constrained. Then, two external steel columns were placed next to the pin supports, to which the reinforced concrete columns were secured for additional safety. In the second step, the lower reinforced concrete beam was placed onto the steel corbels provided on columns. In the third step, the upper beam was placed onto the upper steel corbels on the columns. This was followed by placing post tensioning bars at both beams with a small amount of post tensioning to hold the system together. In the fourth step, the two external steel columns were removed and the second out-of-plane steel column at the middle part of the specimen was installed and another steel beam was fixed between the reaction frame and this column. Lastly, the rollers were placed at the upper beam level in order to prevent out-of-plane deformation of the specimen. The details of the used rollers and pin supports are shown in Figure 4.15.

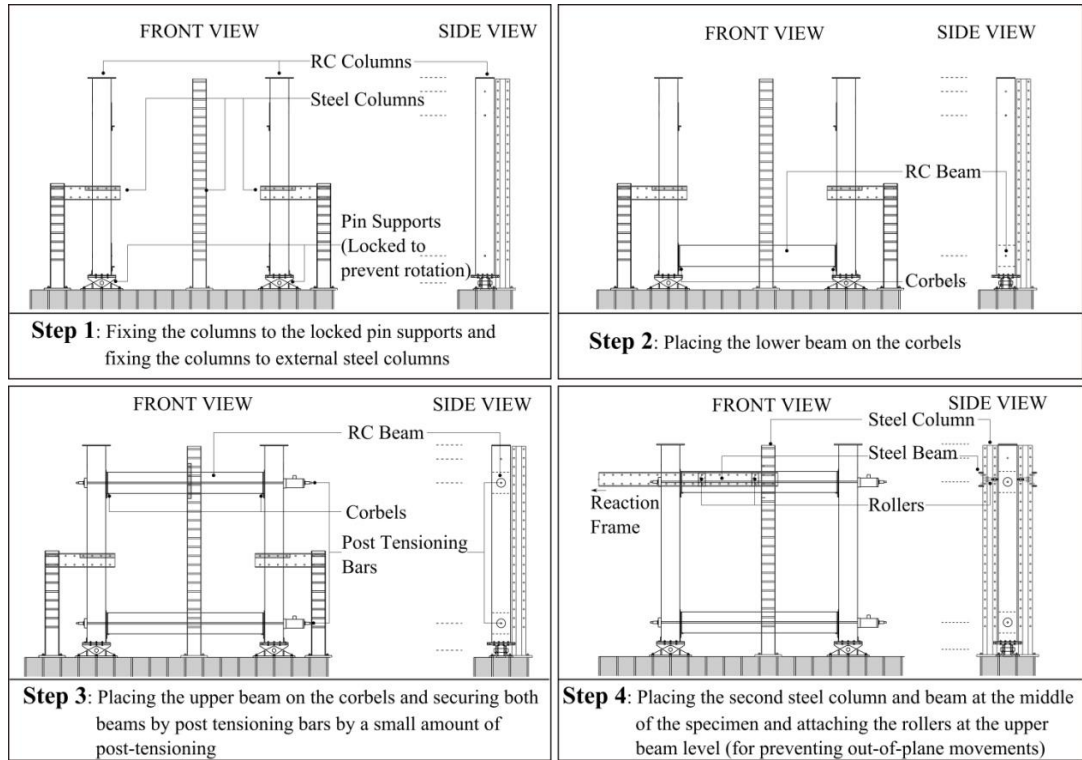


**Figure 4.14.** Construction sequence of the bare frame and completed view (For out-of-plane rollers and pin support details, refer to Figure 4.15)

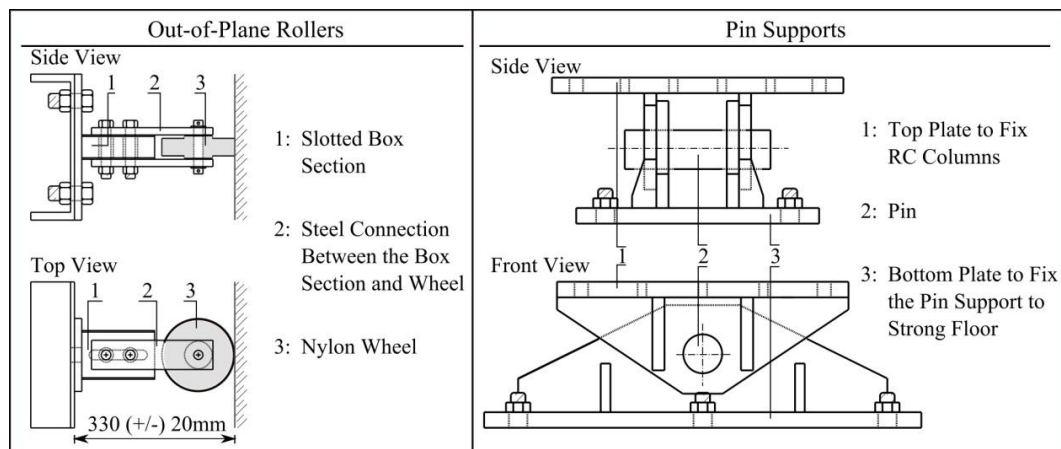


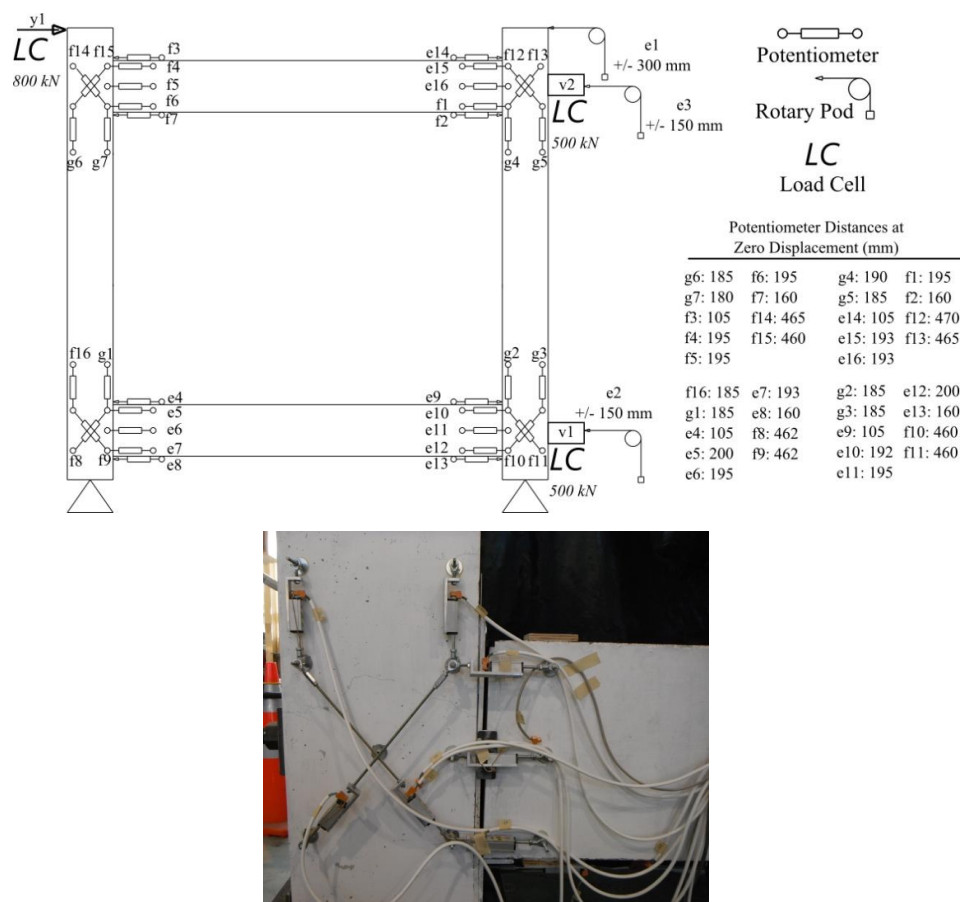
**Figure 4.15.** Out of plane rollers and pin supports of the setup

## 4.6 Instrumentation

The finished bare frame specimen was instrumented to measure:

- The rotations developing between beams and columns by using 30 mm potentiometers
- The bending at column ends by using 30 mm potentiometers
- Shear deformation at beam column joints by using 30 mm potentiometers
- Lateral deformations by using rotary pots at the level of the actuator ( $\pm 300$  mm) and the RC beams ( $\pm 150$  mm)
- Load cells at actuator (800 kN capacity) and the post tensioning bars (500 kN capacity)

These instruments are summarized in Figure 4.16. The numbers shown at each instrument designates the data logger channel numbers for that specific instrument.



#### 4.7 Test Results

The test was carried out on 17<sup>th</sup> October, 2011. The specimen was post-tensioned with a post-tensioning force of 80kN, which was roughly 10% of the yield strength of the post-tensioning bars. The drift history, which was previously given in Figure 4.3, was applied on the specimen. The testing took two days to complete. During the test, the bare frame behaved as expected, linear elastically with very minor flexural cracking at the cover concrete (Figure 4.17).

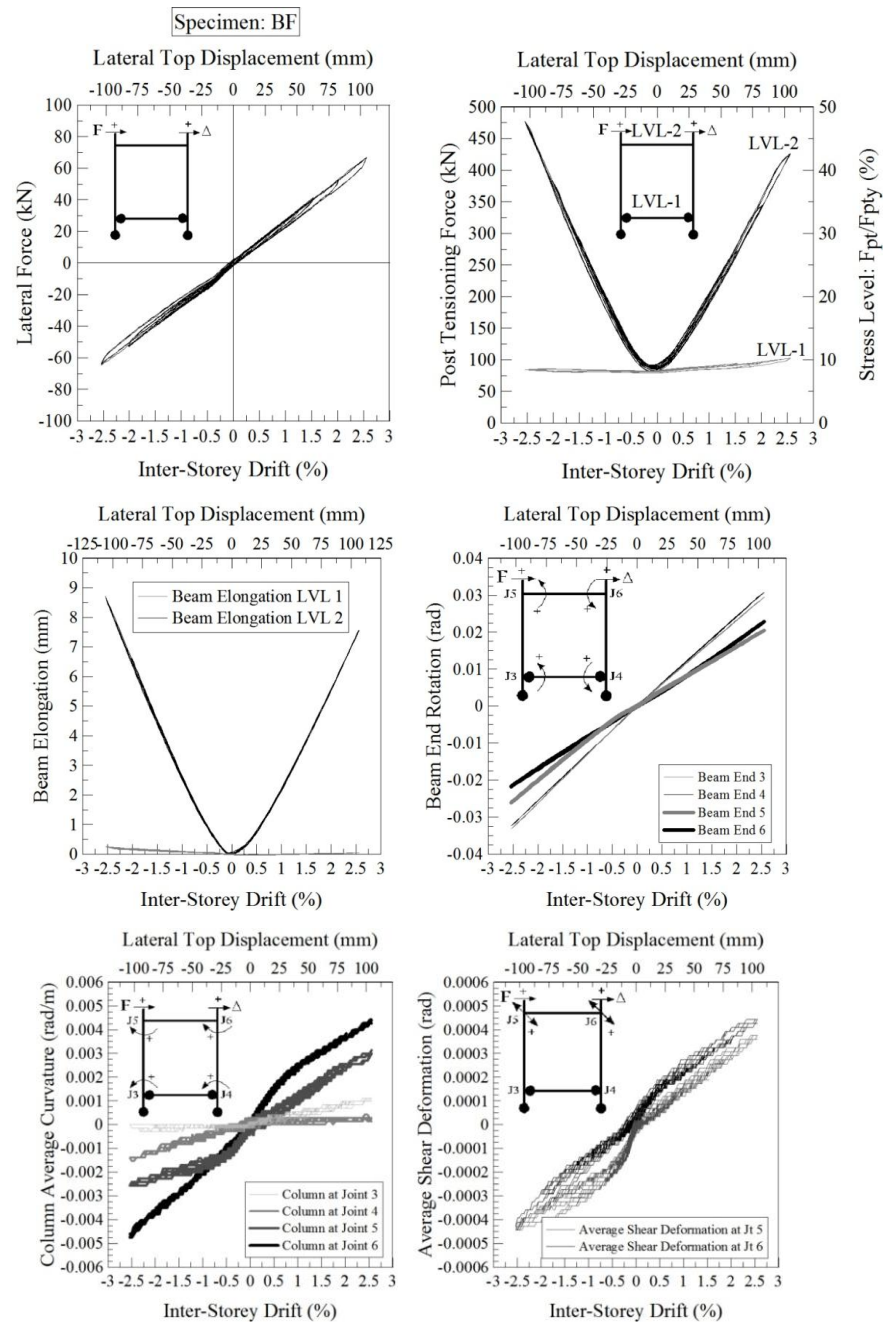
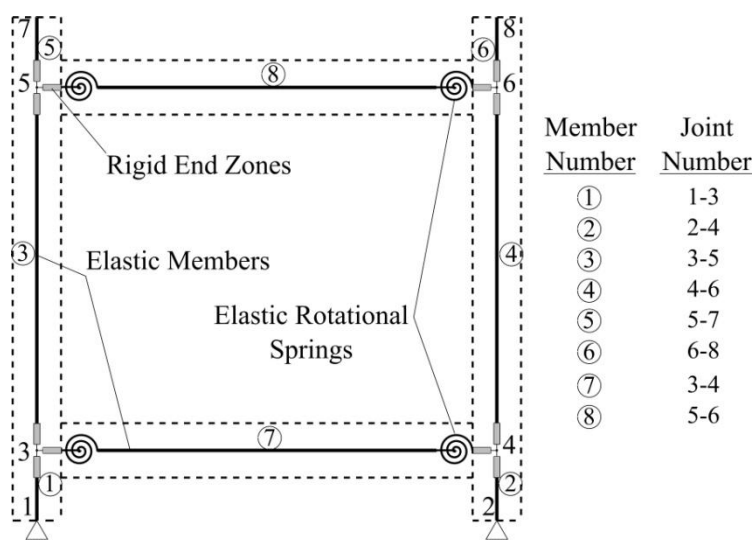


Figure 4.17. Bare Frame test results

In Figure 4.17, the lateral force and inter-storey drift graph shows the linear elastic behaviour of the bare frame without any dissipative properties, which means no damage. In addition, it can be seen that the provided pivot points at the ends of the first level beam prevented beam elongation effectively. Beam elongation only occurred at the upper beam level. Therefore, the bare frame behaved as intended and showed no damage at even 2.5% drift level.

#### 4.8 Numerical Model Calibration

In order to numerically calibrate the future infill wall models using the experimental results, the numerical bare frame model was required to be calibrated with the experimental bare frame result. Therefore, the bare frame model, to be utilized as is by only changing the infill wall panel content, was implemented in Ruaumoko 2D [51] using the following lumped plasticity model with elastic properties.



**Figure 4.18.** Sketch of the numerical model of bare frame implemented in Ruaumoko 2D

Since the bare frame remained linear elastic, all the components in the system were modelled as elastic elements without any inelastic response (Giberson beam elements for beams and concrete beam-column elements for columns). This is also valid for the rotational springs assigned at the beam ends due to the chosen low post-tensioning force value and early gap opening, i.e. to get an elastic response from the bare frame. The model was calibrated to match the experimental behaviour and compared to the experimental result (as shown in Figure 4.19a). In the rest of the research, this bare



frame model was used as is by incorporating different infill wall struts for different infill wall types.

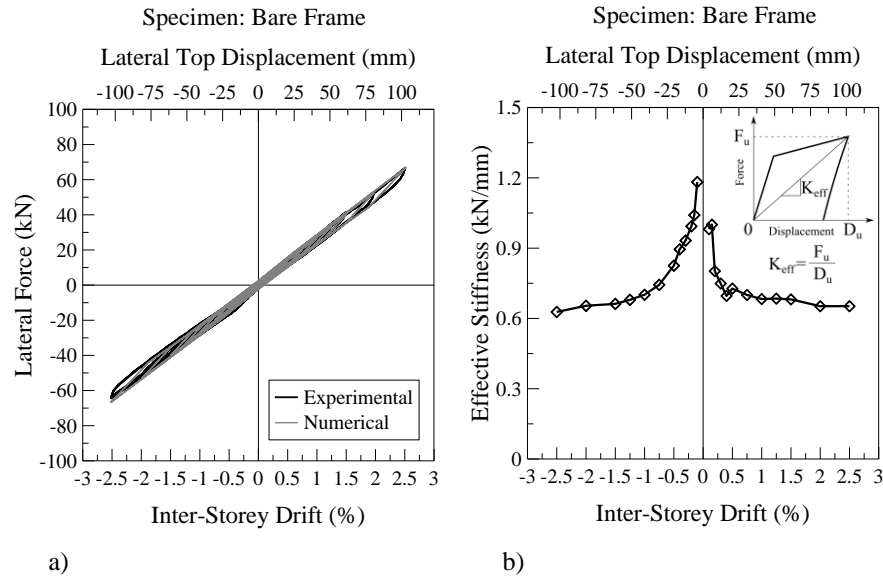


**Figure 4.19.** a) Comparison of numerical force displacement curve to the experimental force displacement, b) Effective stiffness vs. inter-storey drift plot of the bare frame (The slight drop in the effective stiffness is caused by the losses occurring in the post-tensioning during the test)

As can be seen in Figure 4.19b, the bare frame had almost constant effective stiffness (around 0.6 kN/mm), which made it possible to extract the future infill wall behaviour from the obtained global force displacement graphs. Therefore, the only parameter affecting the behaviour was given by the infill wall content, reducing the inherent complications given by the structural frames in other test setups [52].

## 4.9 References

- [10] G. Magenes and S. Pampanin, "Seismic Response of Gravity-Load Design Frames with Masonry Infills," in 13th World Conference on Earthquake Engineering, Vancouver, B.C., Canada, 2004.
- [11] T. Paulay and M. J. N. Priestley, *Seismic Design of Reinforced Concrete and Masonry Buildings*: John Wiley and Sons, Inc., 1992.
- [46] S. Pampanin, A. Palermo, and D. Marriott, *PRESSS Design Handbook*: NZ Concrete Society Inc., 2010.
- [47] Macalloy, "Macalloy 1030 Post Tensioning Kit, Internal Bonded or Unbonded Bar Post-Tensioning Kit Using High Tensile Plain Bar 25 to 40 mm and Ribbed

- Bar 25 to 50 mm in Accordance with European Technical Approval ETA-07/0046," EOTA, Kent/United Kingdom 08.10.2007.
- [48] ACI374.1-05, "Acceptance Criteria for Moment Frames Based on Structural Testing and Commentary," vol. 374.1-05, ed: American Concrete Institute, 2005.
- [49] S. H. Bertoldi, L. D. Decanini, and C. Gavarini, "Telai Tamponati Soggetti ad Azione Sismica, un Modello Semplificato: Confronto Sperimentale e Numerico (in Italian), ," presented at the Atti Del 6 Convegno Nazionale ANIDIS, 1993.
- [50] H. B. Kaushik, D. C. Rai, and S. K. Jain, "Stress-Strain Characteristics of Clay Brick Masonry under Uniaxial Compression," *Journal of Materials in Civil Engineering*, vol. 19, pp. 728-739, September 1, 2007.
- [51] A. J. Carr, "Ruaumoko 2D-Computer Program for Inelastic Time History Analysis of Structures," ed. Christchurch, New Zealand: University of Canterbury, 2013.
- [52] F. J. Crisafulli, "Seismic Behaviour of Reinforced Concrete Structures with Masonry Infills," PhD, Civil Engineering, University of Canterbury, Christchurch, 1997.

# CHAPTER 5

## AS BUILT DRYWALL TESTS

*Research is what I'm doing when I don't know what I'm doing.*

*Wernher von Braun*



## 5 AS BUILT DRYWALL TESTS

### 5.1 As Built Steel Framed Drywall: FIF1-STFD

#### 5.1.1 Construction

For the drywall framing, light gauge steel tracks and stud elements with 30×92×0.55 mm cross sectional dimensions were used (Figure 5.1a-b). Standard gypsum wallboards of 13 mm thickness were chosen as the lining. Three types of anchorages and fasteners used in this installation are shown in Figure 5.1c. Among them, the top two, e.g. steel-to-concrete fasteners, are typically used in fixing the steel elements to the surrounding structural frame. In this particular case, the second option with a predrilled and pre-installed capsule was selected due to ease of removal, which is an HRD frame anchor. The third anchor type is a Phillips-head self drilling screw for fixing the steel elements to each other.

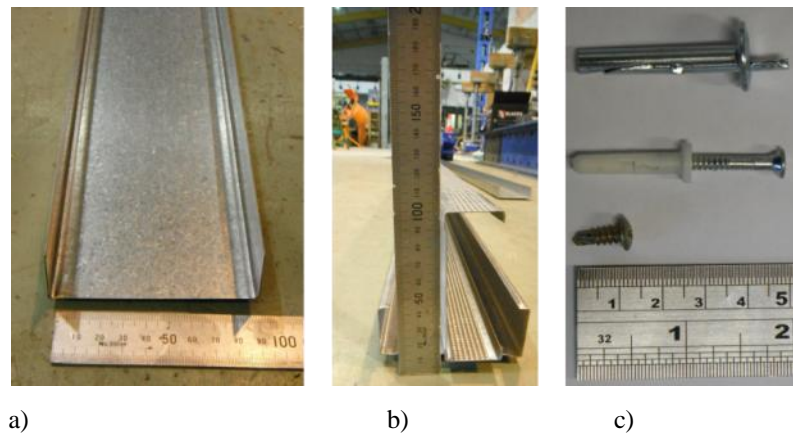


**Figure 5.1.** As built steel framed drywall FIF1-STFD: a) Steel track, b) Steel stud, c) Anchors used from top to bottom: Top two are used for steel-to-concrete, the last one is Phillips self drilling screw used for steel-to-steel

The construction started by fixing the steel tracks to the upper and the lower beams using the steel-to-concrete fasteners (Step 1 in Figure 5.2). Then the vertical steel studs were fitted into these tracks (Step 2 in Figure 5.2). In common practice, the contractors tend to fix these studs to the tracks using self drilling Phillips-head screws shown in Figure 5.3b. After the studs were fixed to the tracks, linings were attached on both sides using the self drilling drywall screws (Step 3 in Figure 5.2). The construction procedure is summarized in Figure 5.2 and the connections of the members are shown in Figure 5.3. The finishing on the drywall is summarized in Section 5.1.2.

Construction video: <http://youtu.be/EHINFs6vfIQ>

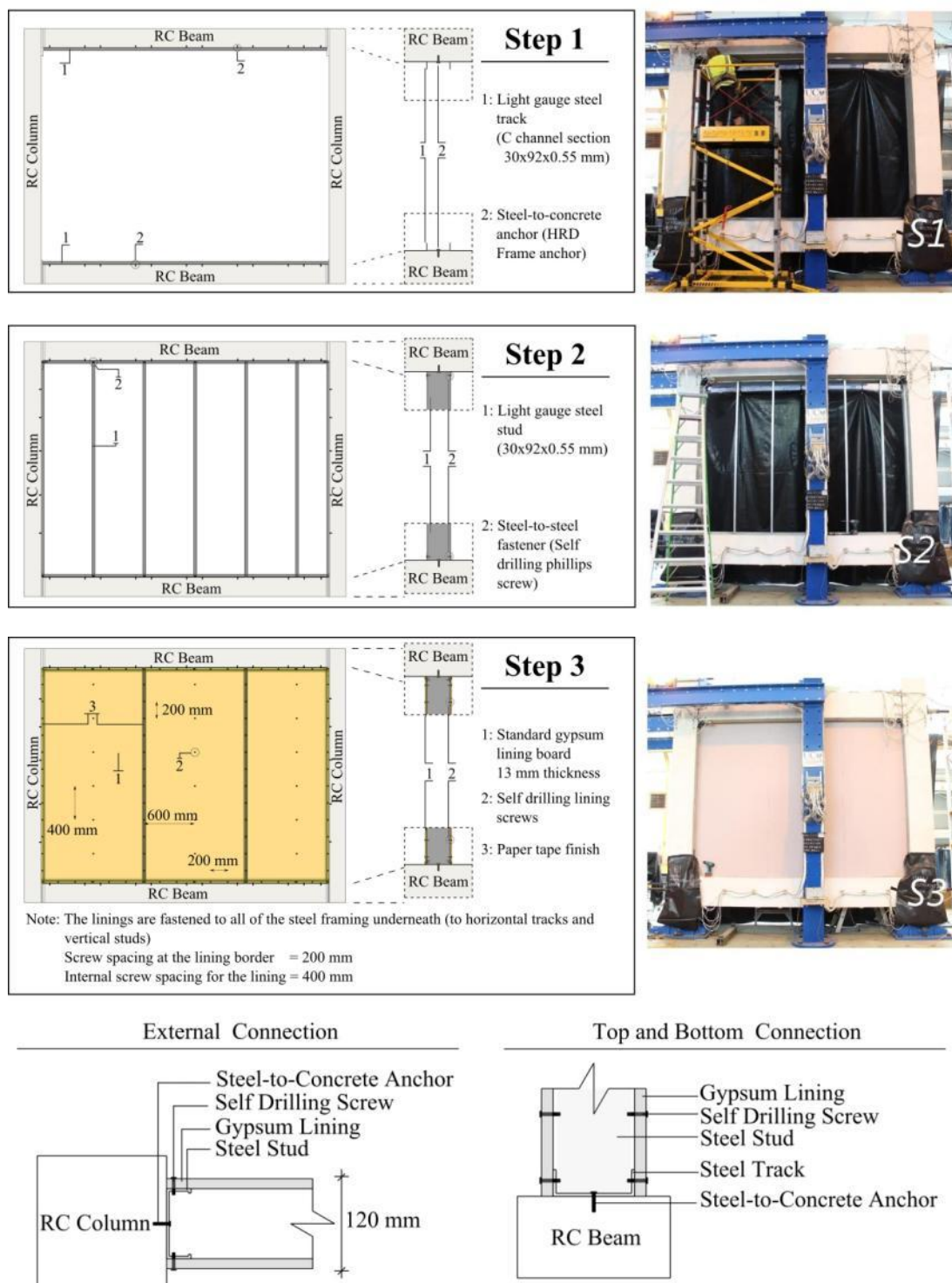


**Figure 5.2.** Construction sequence of as built steel framed drywall FIF1-STFD and close-up details of the perimeter connections (Note: The gypsum linings were installed on both sides of the wall)

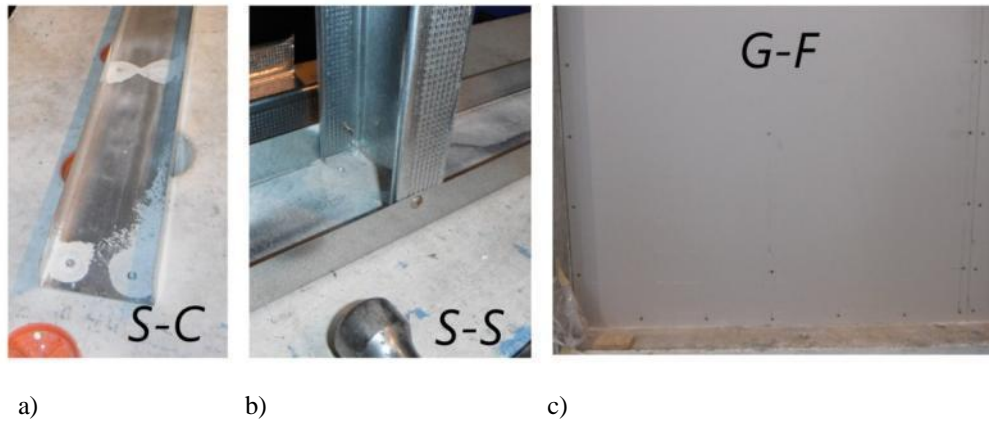


**Figure 5.3.** As built steel framed drywall FIF1-STFD: a) Connection between steel track and concrete, b) Connection between steel stud and track, c) Connection between gypsum lining and steel frame

### 5.1.2 Standard Finishing of the Drywall

For drywalls, the preferred method of finish is a flushed wall surface and square stops at wall ends. The finishing was done by applying the plaster at any of the desired lining-to-lining or lining-to-concrete interfaces. Then the paper tape was applied on the plaster using another thin layer of the plaster on the tape. The porous structure of the paper tape allows for the penetration of the plaster and provides a tight fixing to the lining. The used materials and the installation procedure are shown in Figure 5.4. After this phase, the specimens were painted using a thin coat of white paint to allow for ease of visibility for damage and crack marking.



**Figure 5.4.** Standard finishing for drywalls: a) Paper tape, b) Plaster, c) Application

### 5.1.3 Instrumentation

In order to measure the relative horizontal movement between the linings and the reinforced concrete beams, horizontal potentiometers were installed at the lower and upper lining-to-RC beam interfaces (g10, g11, g12, g16, h1, h2). In addition, potentiometers were installed at mid-height level between the linings (g13, g15) to measure possible lateral deformations among the linings. Vertical potentiometers were installed between the linings and RC columns to measure the corresponding relative deformation (h5, h9, h13, h8, h12, h16). Finally, four potentiometers were installed vertically between the bottom and top border of the linings A and C in order to measure possible uplift of the lining (h6, h7, h14, h15). The instrumentation is summarized in Figure 5.5. Potentiometers h10 and h11 were installed in order to capture the strain resulting from potential bowing at lining A and C.

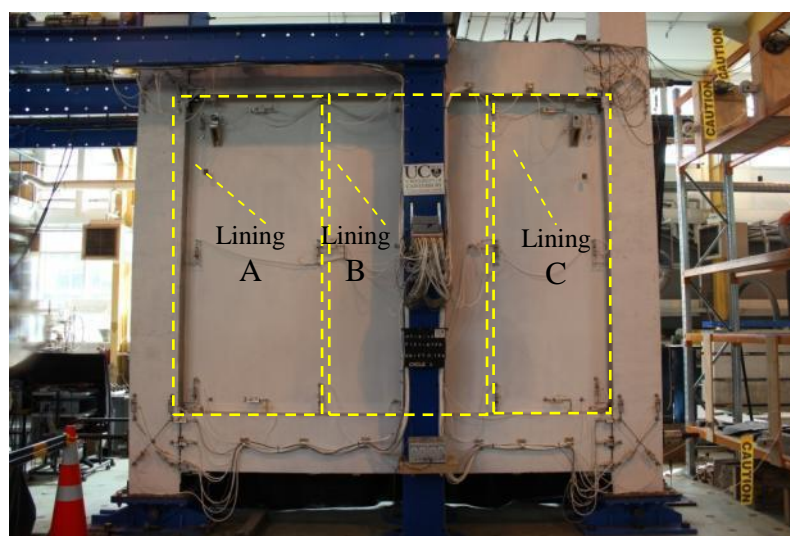
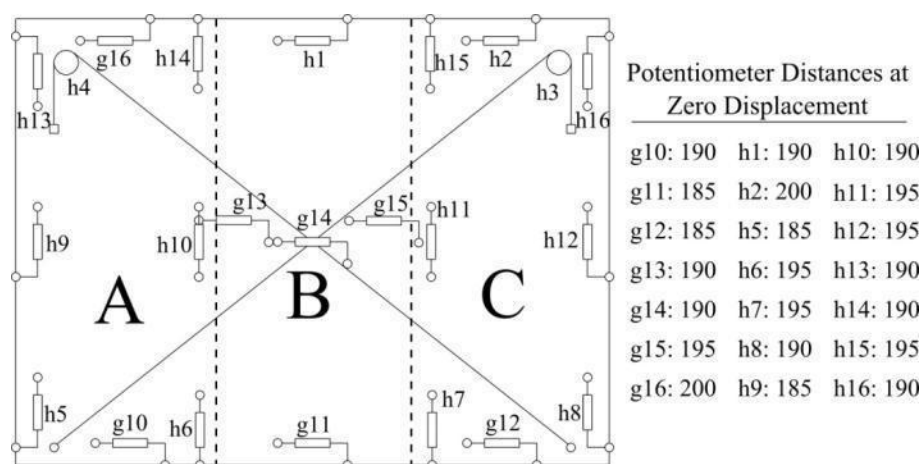


**Figure 5.5.** Instrumentation of the as built steel framed drywall specimen FIF1-STFD



#### **5.1.4 Test Results**

##### **5.1.4.1 Damage Observations**

The specimen was subjected to the previously given displacement history. At the initial cycle of 0.1% drift, there was no apparent damage to the drywall. At 0.15% drift, the first hairline cracking was observed along the perimeter of the drywall. At 0.2% drift, the first cracking at the interface between the lining A and lining B was observed (refer to Figure 5.5 for the naming of the linings). The observed damage up to this point was within tolerable levels. However, at 0.3% drift, the cracked vertical lining interface deformed significantly and started to push against the lining A and B resulting in bowing at the interface between the linings. At the same level of drift, initiation of minor damage to a few fasteners was also observed. 0.3% drift also corresponded to a slight strength loss, followed by a ductile post-yield behaviour. At 0.4% drift, the bowing damage at the lining A and B interface progressed further and lining A started to rock on the lower beam causing some toe crushing at the bottom right corner. Further damage concentrated mainly around lining A and lining B. From 0.3% onwards, the testing continued until 2.5% drift level without further loss in strength. The damage to the drywall was severe at the end of the test, serviceability loss occurring at 0.3% drift level. The stage-by-stage progress of damage on the specimen is schematically shown in Figure 5.6. The resulting physical damage on the drywall and the damage mechanism is summarized in Figure 5.7.

Video of the test: <http://youtu.be/FgU3c0zfkM8>

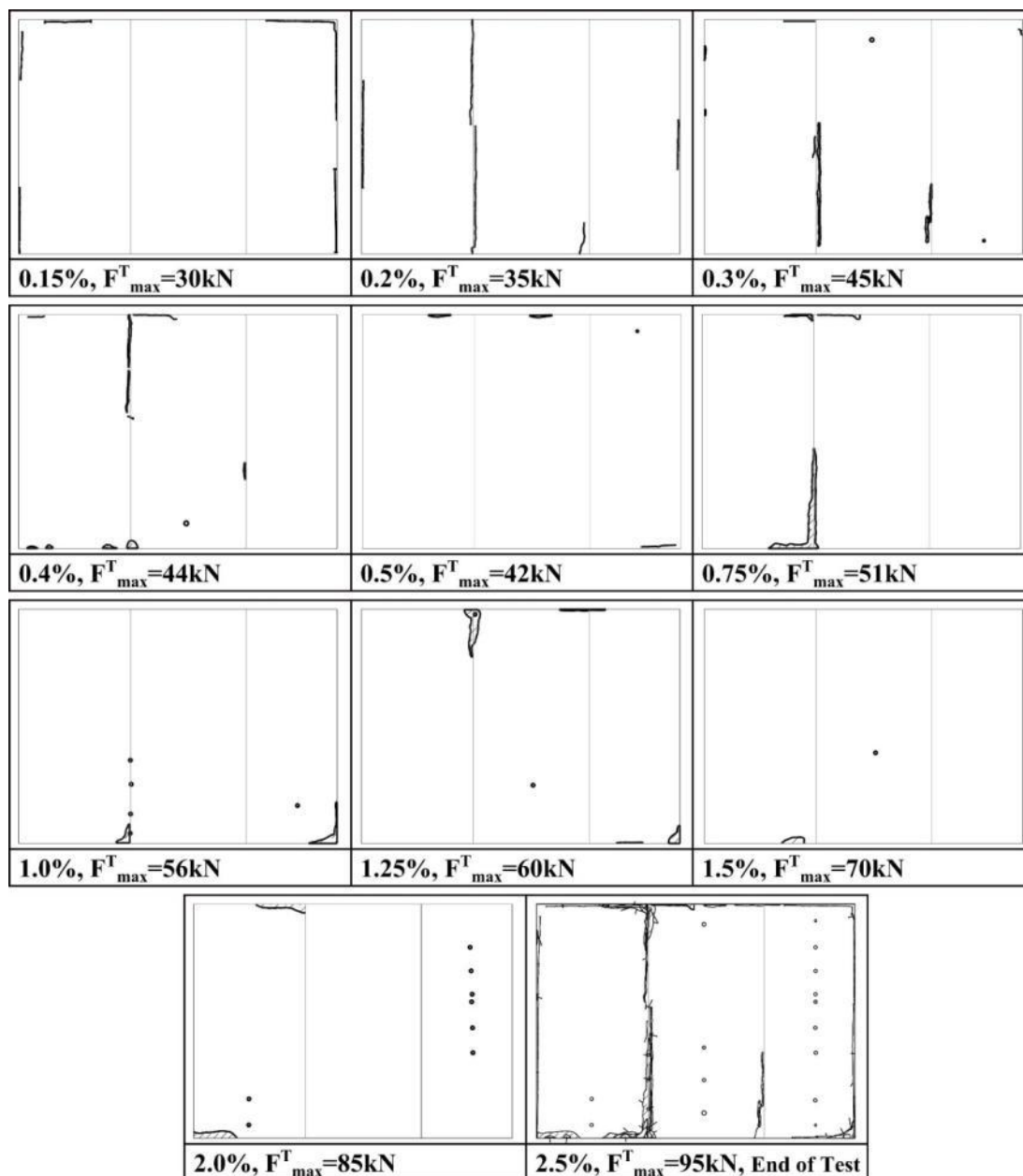


**Figure 5.6.** Damage progress and the total damage map at the end of the test for as built steel framed drywall specimen observed in the front face of the specimen FIF1-STFD



**Figure 5.7.** Damage at the end of the test of as built steel framed drywall specimen FIF1-STFD

#### 5.1.4.2 Behaviour Explanation

As seen in the photos of damage, the drywall suffered severe damage from 0.3% drift level onwards. At the end of the test, the damage was extensive (Figure 5.6). Most of the damage concentrated at the lining interfaces with the major one being between the lining A and lining B. The cause for concentration of the damage to the lining interfaces can be deduced with the aid of inspection of deformability of the underlying framing. As shown in Figure 5.3b, the steel framing was constructed by attaching the steel tracks and the studs with single screws. Because of this connection type, the studs had a degree of freedom to rotate at the stud ends, which caused the linings to rock and get damage at lining interfaces along with toe crushing (Figure 5.8).

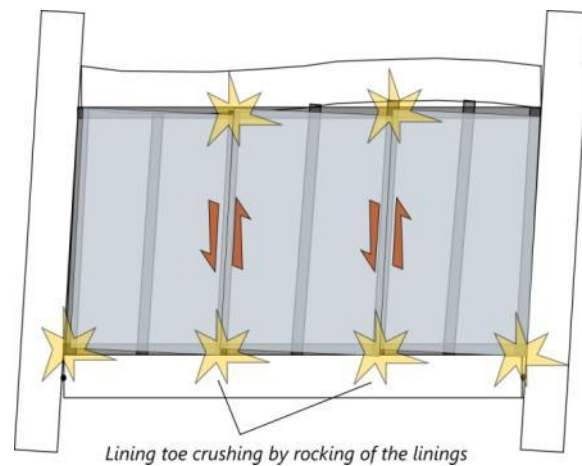


**Figure 5.8.** Damage mechanism for as built steel framed drywall FIF1-STFD

The hysteresis behaviour and other measurements taken are shown in Figure 5.9, Figure 5.10 and Figure 5.11. The significant horizontal displacement demand between the infill panel zone and the lower/upper RC beams are shown in Figure 5.10, where the potentiometers reached their maximum recording limit of  $\pm 15$  mm at 0.75% imposed drift level. In addition, the displacement demand imposed to the vertical potentiometers between the infill panel zone and the RC columns is also shown in Figure 5.10. As stated previously, most of the damage concentrated to lining-to-lining interfaces, suggesting a rocking behaviour at the linings. In this specimen (FIF1-STFD), lining A had the most pronounced rocking, and therefore the lateral potentiometer readings recorded at g10 and g16 (Lining A) were lower than g11, g12 and h1, h2 (Linings B and C). This suggests a more dominant rocking mechanism for Lining A and more dominant sliding for Linings B and C, which was confirmed by the recordings in Figure 5.10.

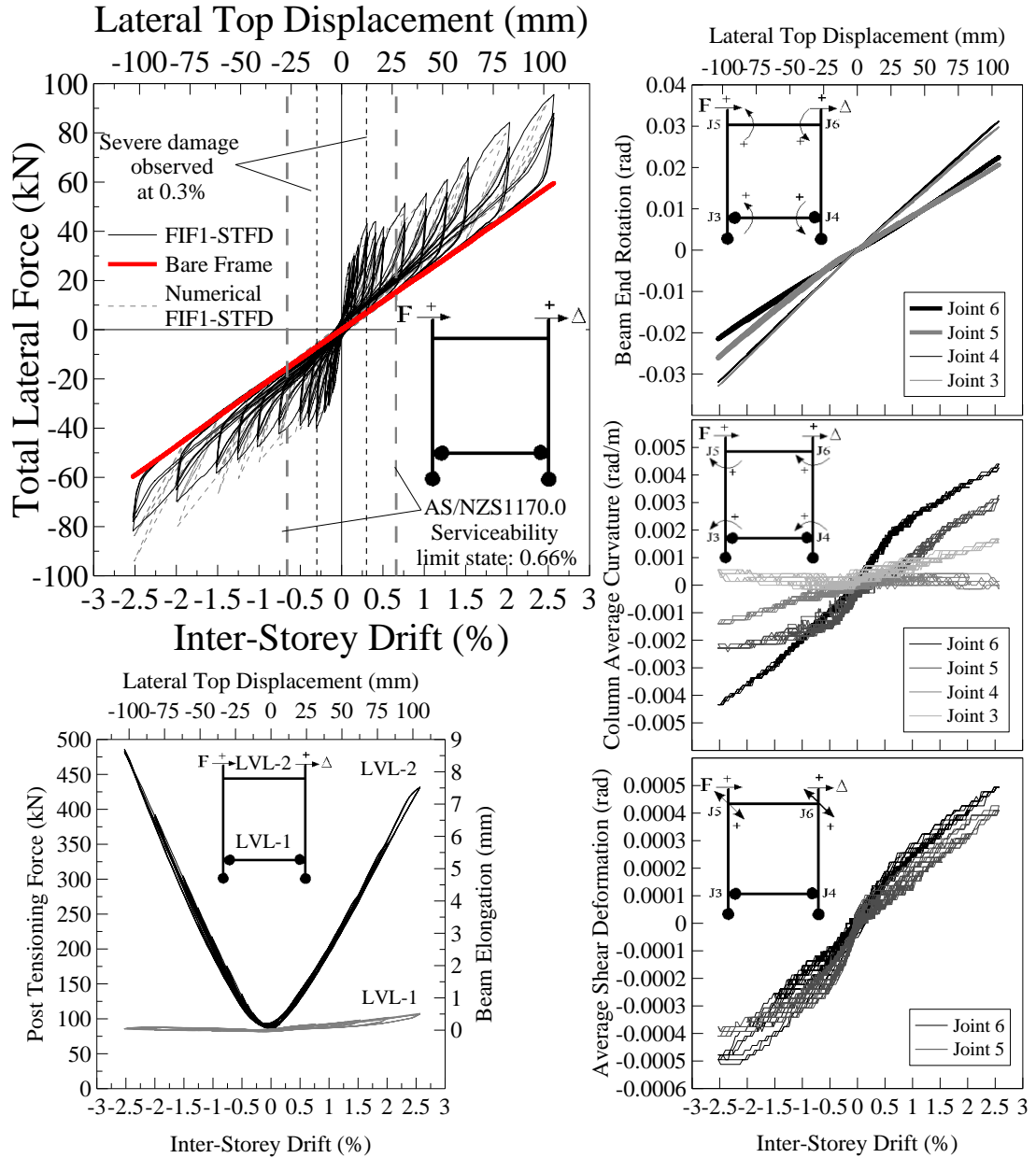


**Figure 5.9.** Test results for as built steel framed drywall specimen FIF1-STFD

The hysteresis behaviour of the infill content was extracted from the global behaviour and shown graphically for both horizontal and diagonal directions in the infill panel zone in Figure 5.11. As it can be noted, the as built steel framed drywall behaved very much in a ductile manner, sustaining its strength with increasing displacements.

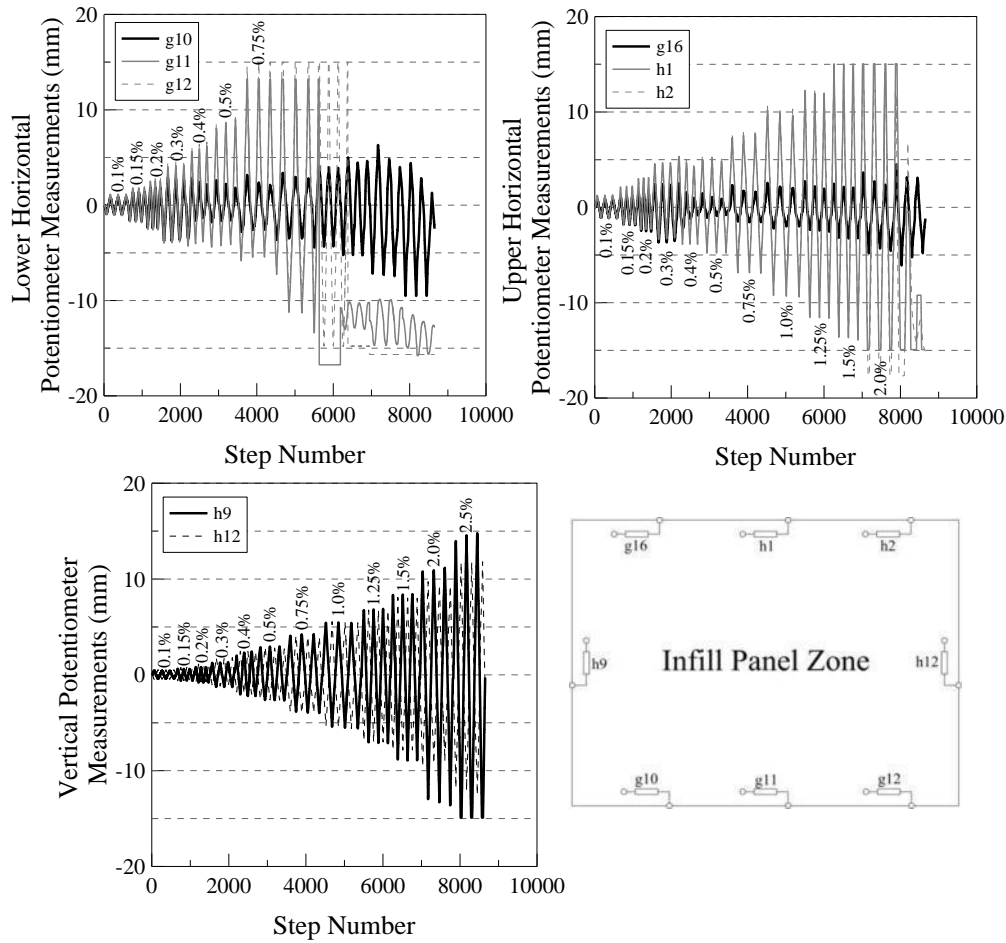


**Figure 5.10.** Most significant potentiometer measurements taken for horizontal and vertical movements in the infill panel zone for as built steel framed drywall FIF1-STFD (Locations of the potentiometers are shown above)

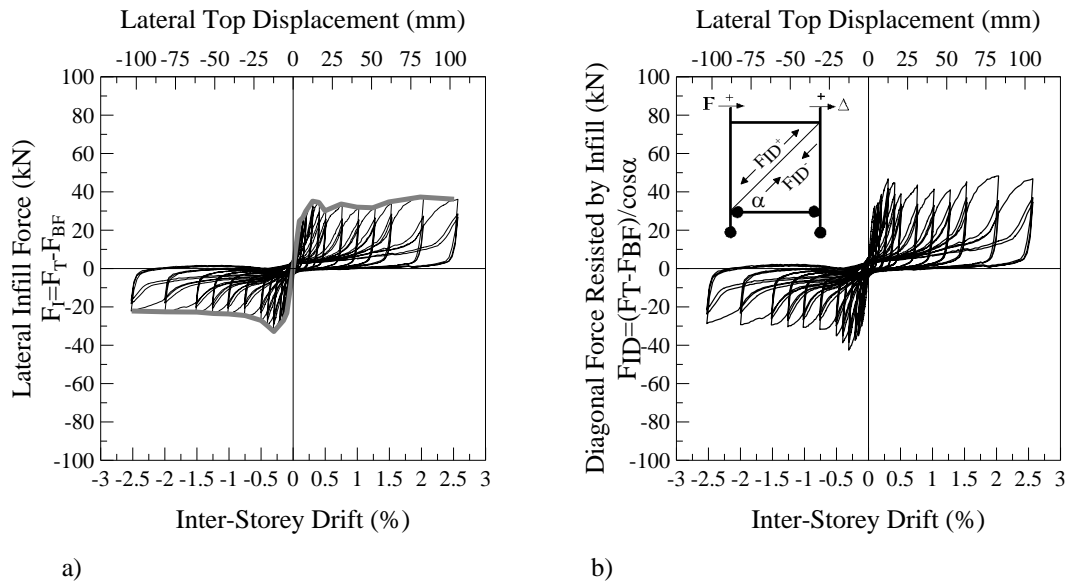
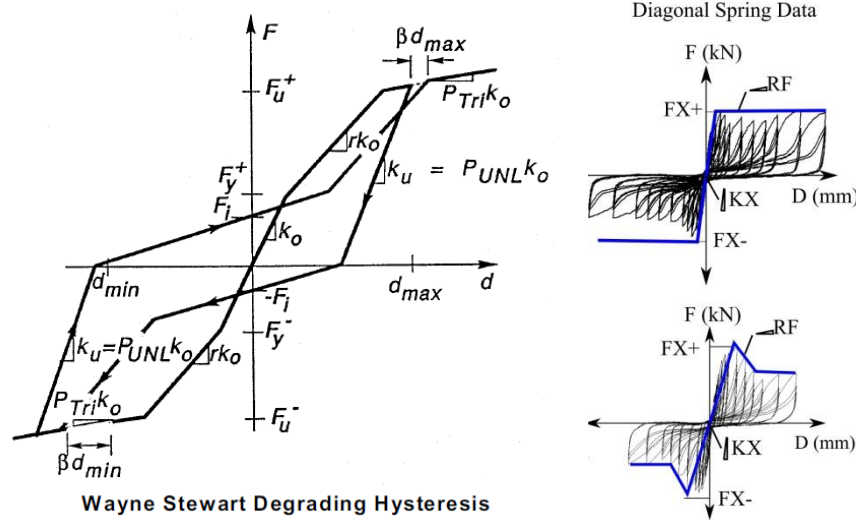


**Figure 5.11.** As built steel framed drywall FIF1-STFD: a) Lateral force exerted on the infill panel zone obtained by subtracting the bare frame from the total, b) Diagonal force exerted on the infill panel, projection of a) in diagonal dir.

### 5.1.5 Numerical Model Calibration

For numerical purposes, the experimental results were used to calibrate a diagonal spring added to the developed bare frame model in order to model the diagonal strut mechanism. Because of the significant pinching, as seen in Figure 5.11b, the hysteresis rule used to describe the behaviour of the strut was Wayne Stewart degrading stiffness model available in Ruaumoko 2D [51].



#### Key Parameters of Wayne Stewart Degrading Hysteresis

All to be calibrated to match the experimental results for as-built steel and timber framed drywalls. Then the same models will be adapted for the low damage options only by adding the slackness (GAP) parameters. Note that the elastic and post-yield strut stiffness are defined elsewhere in the models.

<b>FU</b>	Ultimate force or moment ( $> 0$ ):	Calibrated to match the experiments
<b>FI</b>	Intercept force or moment ( $> 0$ ):	Calibrated to match the experiments
<b>PTRI</b>	Tri-linear factor beyond ultimate force or moment :	N/A
<b>PUNL</b>	Unloading stiffness factor ( $> 1$ ):	Calibrated to match the experiments
<b>GAP+</b>	Initial slackness in positive axis, Diagonal gap ( $> 0$ ):	Introduced directly
<b>GAP-</b>	Initial slackness in negative axis, Diagonal gap ( $< 0$ ):	Introduced directly
<b>BETA</b>	Softening factor ( $\geq 1$ ):	Calibrated to match the experiments
<b>ALPHA</b>	Pinch power factor ( $\leq 1$ ):	Calibrated to match the experiments
<b>LOOP</b>	0 for the unmodified loop, 1 for the modified loop:	1 for all specimens

**Figure 5.12.** Wayne Stewart degrading stiffness model from Ruaumoko 2D by Carr [51]

For simplicity, a single diagonal strut was added to the existing bare frame model. The hysteresis rule was defined by calibrating the diagonal infill force-displacement data given in Figure 5.11b where the positive direction describes elongation of the spring and the negative direction describes compression of the spring. However, the same model can be adapted as two separate diagonal compression-only (no tension) struts placed in both diagonal directions by using the corresponding-data for each (positive or negative direction of loading). The calibrated model is shown in Figure 5.13. The

calibration was carried out to match the experimental results and the hysteresis curve given in Figure 5.14 was obtained. The parameters describing the model are also given in Figure 5.13 for use in full scale building models.

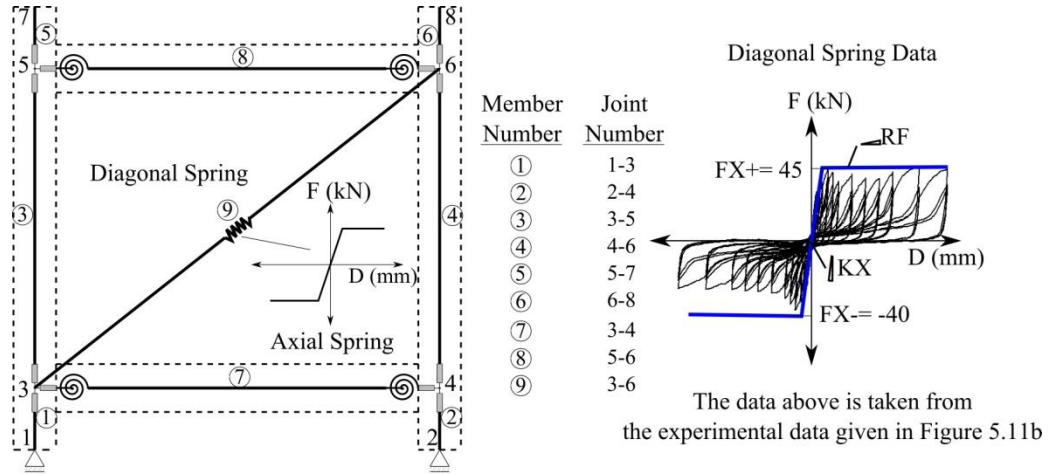
As previously shown in the damage mechanism of the steel framed drywall specimen (Figure 5.8), the failure mode of the steel framed drywall is governed by the deformation of the vertical lining interfaces due to the rocking of the linings. Therefore, it can be stated that the capacity is proportional with the non-structural wall height. Although the dimensions in a real building model may vary, the given experimental results in Figure 5.11b can be approximately adapted to real buildings for modelling and assessment purposes. For this, the following modification of the yield strength ( $F_u^+$ ) and stiffness ( $KX$ ), without change in drift, can be carried out (Modifies the yield strength and the resulting stiffness, only valid for as built steel framed drywalls):

$$(F_u^+)_{\text{RealSTFD}} = (F_u^+)_{\text{FIF1-STFD}} \cdot \frac{(h_c)_{\text{RealSTFD}}}{(h_c)_{\text{FIF1-STFD}}} \quad (5.1)$$

$$(KX)_{\text{RealSTFD}} = \frac{(F_u^+)_{\text{RealSTFD}}}{(F_u^+)_{\text{FIF1-STFD}} / (KX)_{\text{FIF1-STFD}}} \quad (5.2)$$

Where;  $(h_c)_{\text{FIF1-STFD}}$ : Clear height of the non-structural wall=2550 mm or 2.55 m  
 $(F_u^+)_{\text{FIF1-STFD}}$ : Calibrated Yield strength of the diagonal strut $\approx 1.13 \times 40$  kN  
 $(KX)_{\text{FIF1-STFD}}$ : Calibrated stiffness of the diagonal strut $\approx 15000$  kN/m  
 1.13 is the yield strength calibration coefficient as shown in Figure 5.13





Wayne Stewart Degrading Stiffness model data for Ruaumoko2D

!	N	MTYPE LABEL														
	5	SPRING STRUT														
!	12A BASIC SECTION PROPERTIES															
!	ITYPE	IHYST	ILOS	IDAMG	KX	KY	GJ	WGT	RF	RT	PSX	PSY	PSZ	THETA	ITRUSS	IOP
	1	9	0	0	15000	0	0	0	0.001	0	0	0	0	0	0	0
!	12C YIELD SURFACE															
!	FX+	FX-	FY+	FY-	MZ+	MZ-										
	45	-40	0	0	0	0										
!	FU	FI	PTRI	PUNL	GAP+	GAP-	BETA	ALPHA	LOOP							
	45	0	0	2	0	0	1.04	0.2	1							

1.13 x

Diagonal Strength

(40 kN)

Figure 5.13. The numerical model of as built steel framed drywall FIF1-STFD for Ruaumoko 2D

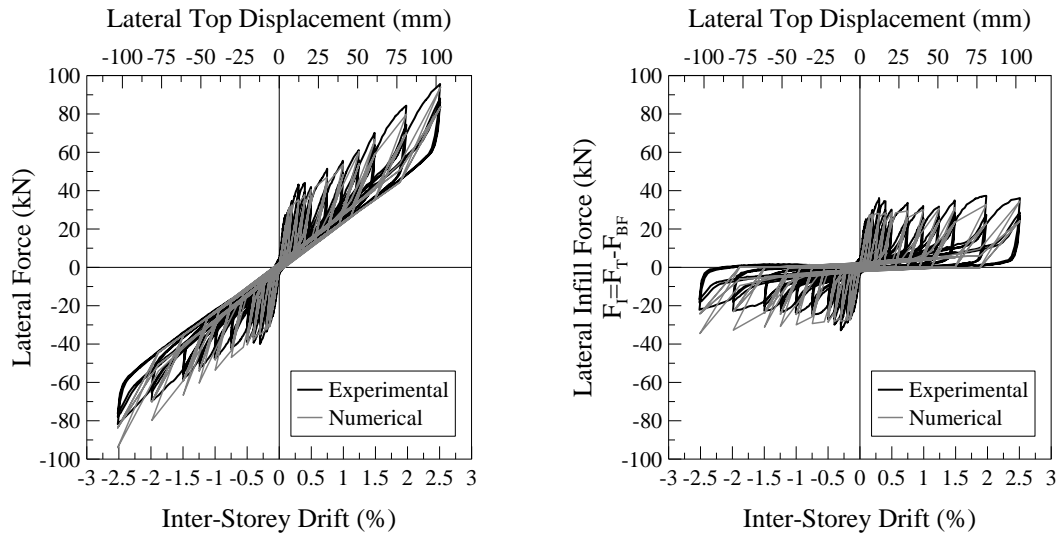
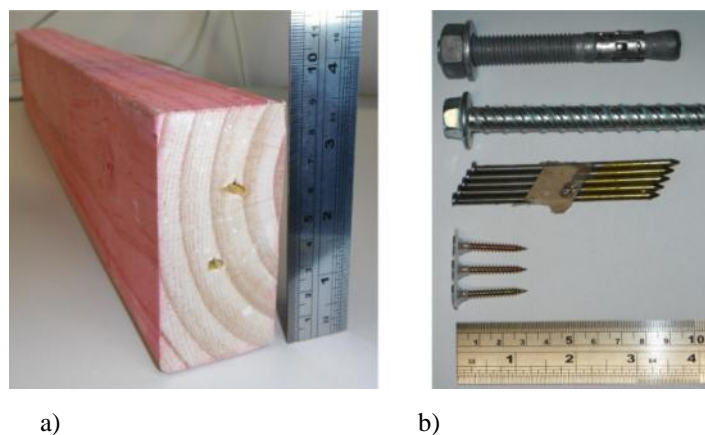


Figure 5.14. Hysteresis behaviour of the numerical model compared to the experimental result for as built steel framed drywall FIF1-STFD

## 5.2 As Built Timber Framed Drywall: FIF2-TBFD

### 5.2.1 Construction

In this drywall type, timber elements of 45×90 mm cross sectional dimensions were used for the construction of the underlying framing. The lining type was the same as the one used in the steel framed drywall (standard gypsum wallboard of 13 mm thickness). The materials and the anchor types of this drywall are summarized in Figure 5.15. In Figure 5.15b, either of the top two anchors is typically used to fix the border timber elements to the surrounding structural frame. In the reported work, the second anchor type, a self drilling HUS-H universal screw, was used due to ease of removal. The third type of anchors shown, nails, were used to fix the vertical and horizontal timber elements to each other. The last ones were self drilling screws for fixing the gypsum wallboards to the timber framing.



**Figure 5.15.** As built timber framed drywall FIF2-TBFD: a) Used timber elements to construct the timber framing, b) Used anchor types

The construction procedure for the timber framed drywalls is similar to the steel framed counterpart. The procedure started by fixing the timber elements at the borders (Figure 5.16-Step 1). Then the vertical elements were installed (Figure 5.16-Step 2). The horizontal timber elements were installed after the vertical elements were all in place (Figure 5.16-Step 3). Finally, the linings were attached to the formed timber framing (Figure 5.16-Step 4). Close up details of the connections used in the specimen are shown in Figure 5.17. The finishing of the drywall was completed in the same way as summarized in 5.1.2. Standard Finishing of the Drywall.

Construction video: [http://youtu.be/\\_WAV7m4\\_E-0](http://youtu.be/_WAV7m4_E-0)

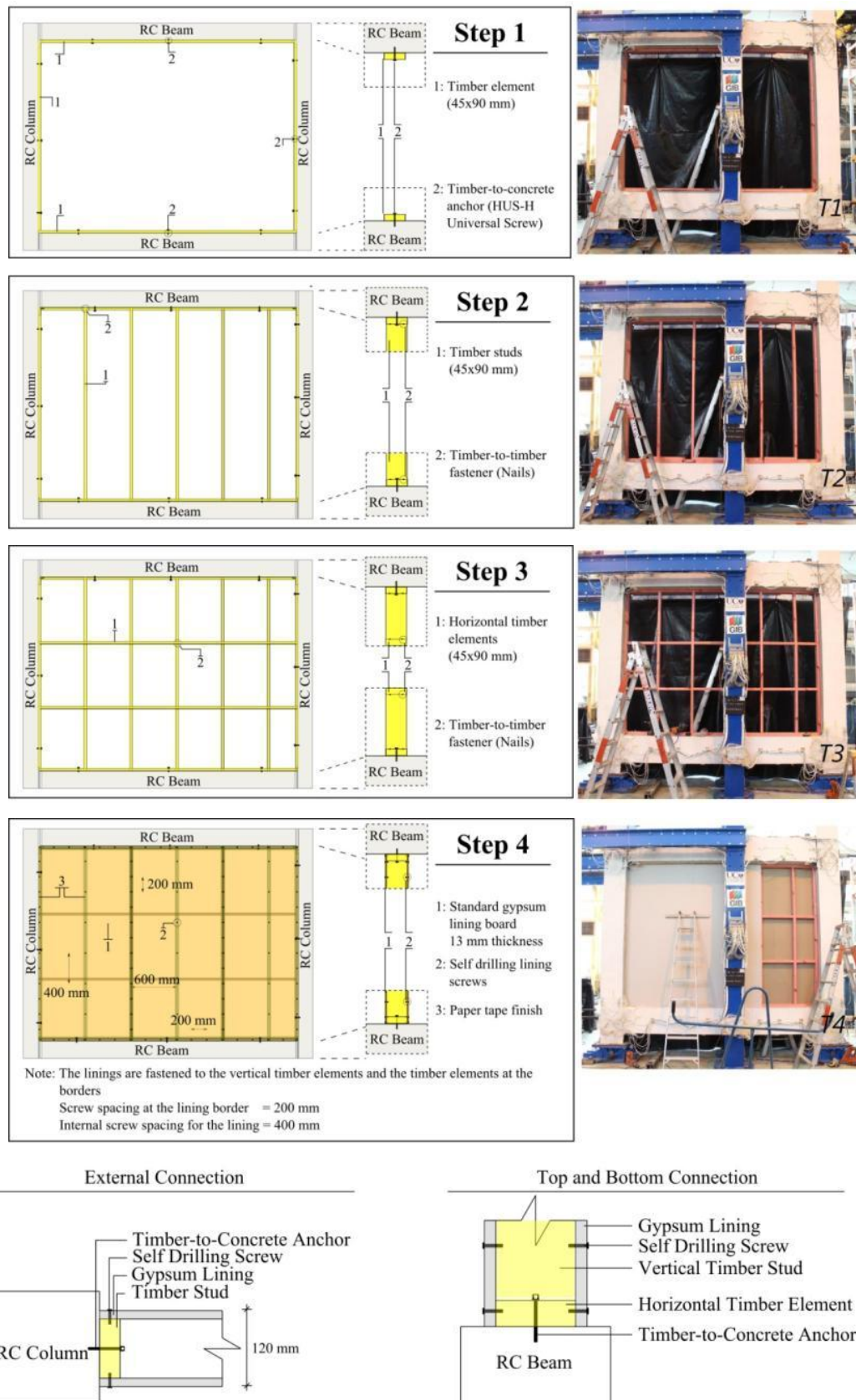


**Figure 5.16.** Construction sequence of as built timber framed drywall specimen FIF2-TBFD and close-up details of the perimeter connections

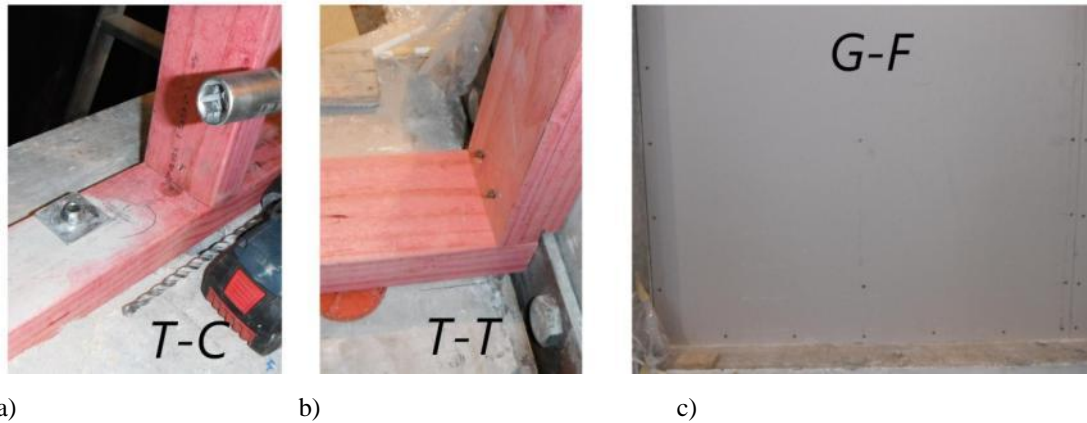


**Figure 5.17.** As built timber framed drywall FIF2-TBFD: a) Connection between timber and concrete, b) Connection between timber elements, c) Connection between gypsum lining and timber frame

### 5.2.2 Instrumentation

In order to measure the relative horizontal movement between the linings and the reinforced concrete beams, horizontal potentiometers were installed at the lower and upper lining-to-RC beam interfaces (g10, g12, g16, h2). As no significant deformations were measured in FIF1-STFD, the potentiometers installed at mid-height level between the linings were not installed for this specimen (g13, g14, g15). Vertical potentiometers were installed between the linings and RC columns to measure the corresponding relative deformation (h9, h12) as well as between the linings to measure the possible relative deformation (h10, h11). Finally, eight potentiometers were installed vertically between the lower and upper border of the linings A and C in order to measure possible rocking of the linings (h5, h6, h7, h8, h13, h14, h15, h16). The instrumentation scheme is graphically shown in Figure 5.18.



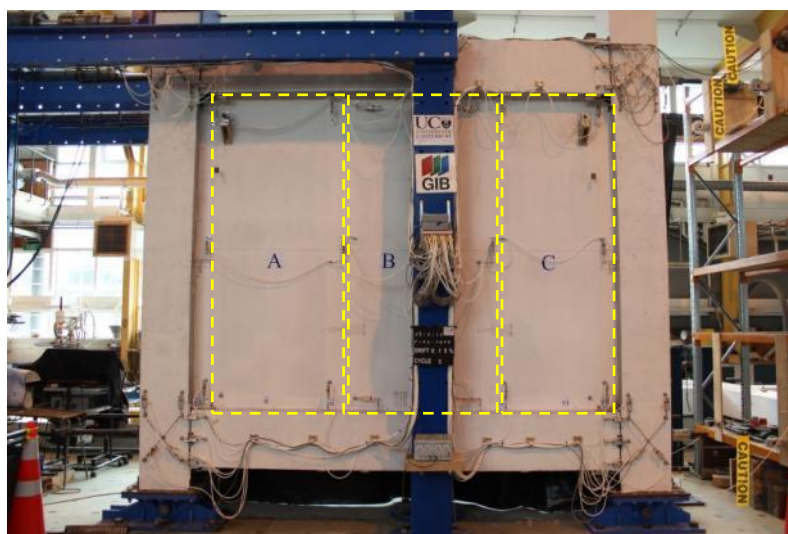
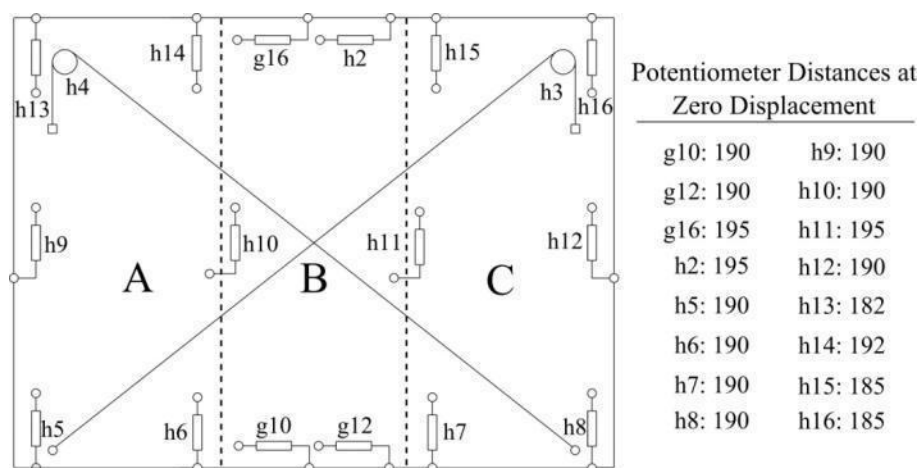


**Figure 5.18.** Instrumentation of the as built timber framed drywall specimen FIF2-TBFD

### 5.2.3 Test Results

#### 5.2.3.1 Damage Observations

The specimen was subjected to the same displacement history as the other tests. However, the behaviour of this specimen was rather different from its steel framed counterpart. At 0.1% drift, the first damage was observed in the form of perimeter cracking between the linings and the RC frame. After this, at 0.3%, minor crushing at the bottom right corner of the lining C initiated. The existing damage slightly progressed until 0.75% drift, at which severe corner crushing and corner bowing at linings were observed, which corresponded to a sudden loss in strength and a brittle behaviour. Therefore, there was a more significant strut effect, which affected the global behaviour and the failure mode. The damage progress is schematically

summarized in Figure 5.19. The observation of the damage at the end of the test is shown in Figure 5.20.

Video of the test: <http://youtu.be/vGsYnFtr6CI>

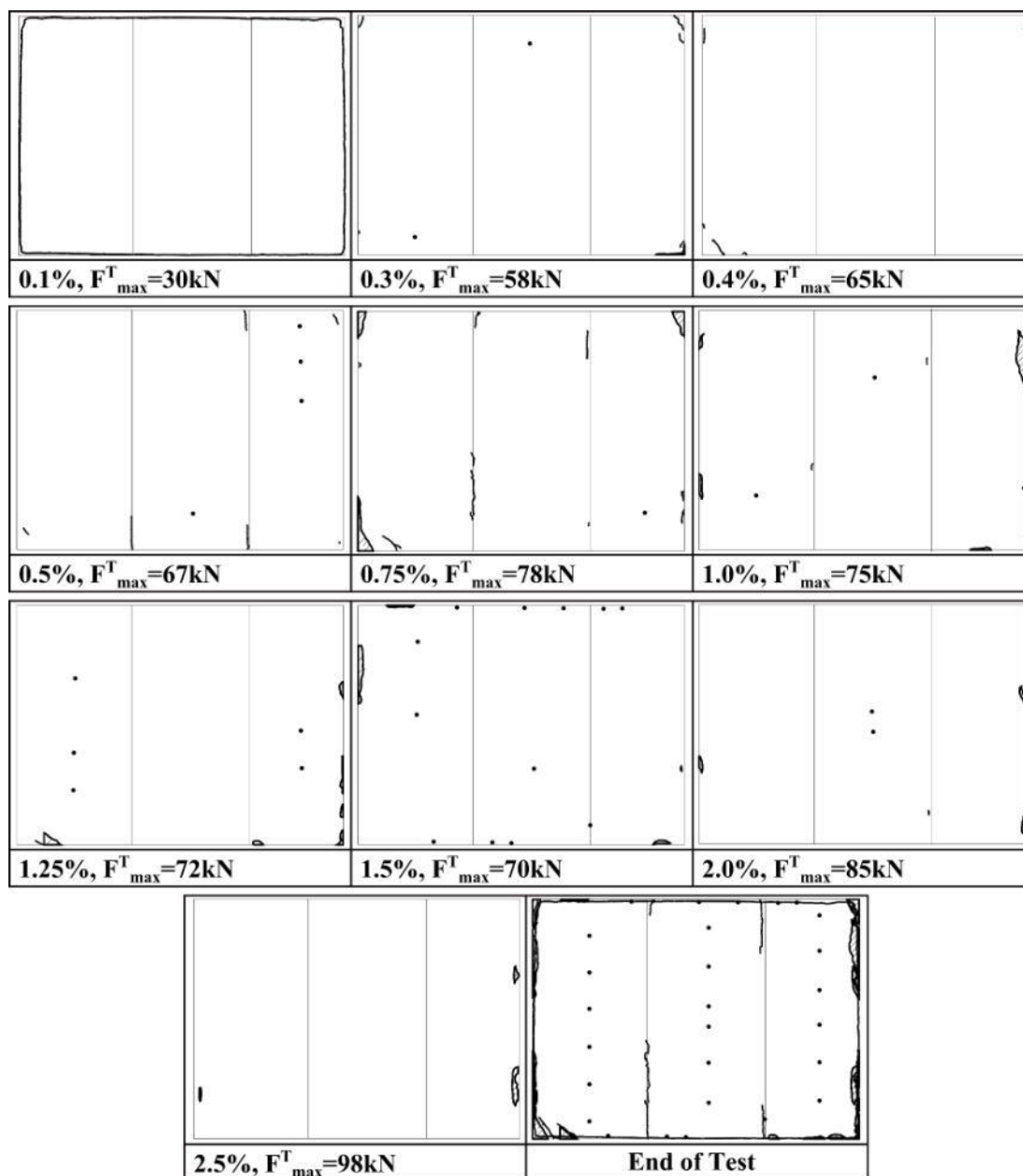


**Figure 5.19.** Damage progress and the total damage map at the end of the as built timber framed drywall test FIF2-TBFD

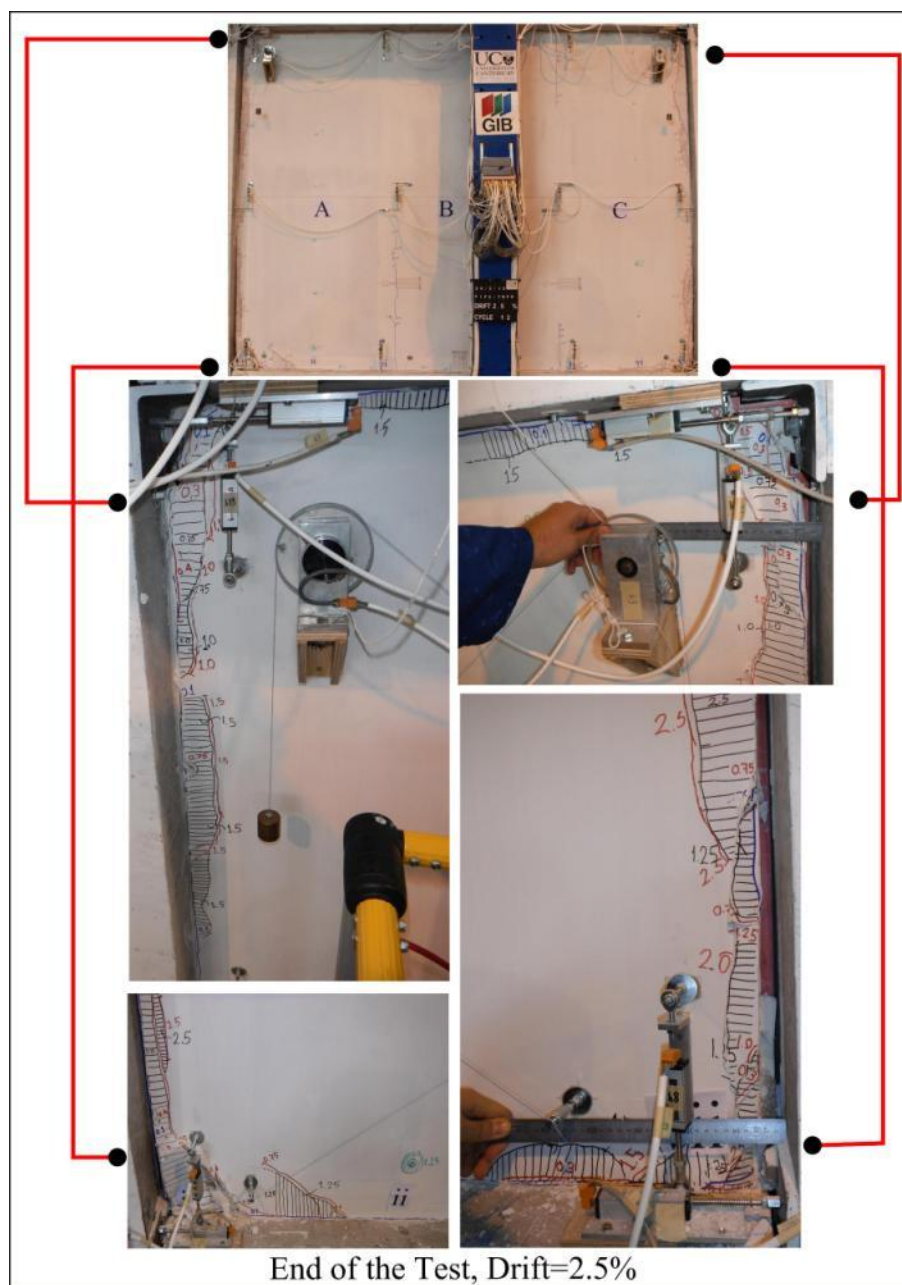


**Figure 5.20.** Damage at the end of the as built timber framed drywall test FIF2-TBFD

### 5.2.3.2 Behaviour Explanation

When the test was over and the deconstruction was carried out, it was found that the 3 anchors fixing the lateral timber member to the lower RC beam had failed in shear at the interface with the RC beam (Figure 5.21b).

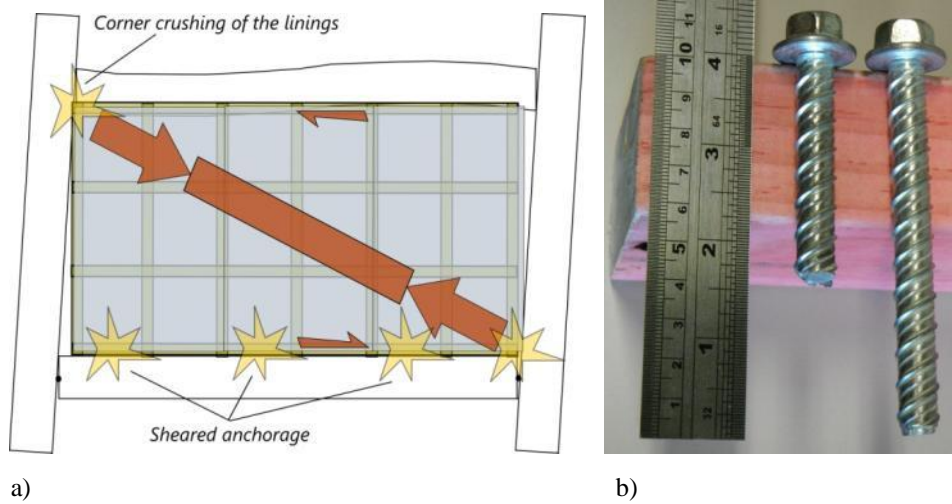


**Figure 5.21.** a) Damage mechanism for as built timber framed drywall FIF2-TBFD: b) Failed anchor compared to an intact timber to concrete anchor

Unlike the as built steel framed drywall specimen FIF1-STFD, the as built timber framed drywall specimen FIF2-TBFD behaved in a more brittle manner. The difference between the behaviour of the timber framed and the steel framed specimens can be attributed to the differences in the boundary conditions and the underlying frame systems: i) due to the additional horizontal timber elements, the timber framed system was stiffer, ii) this specimen had moment resisting connections among its elements and with the surrounding structural frame (Figure 5.17). The resulting shear failure observed at the timber-to-RC beam connections at the lower beam can be shown as a proof of the pronounced strut action and stiffness. This shear failure can also be associated to the brittle behaviour of the timber framed specimen.

When the shear capacity of these anchors are examined:

$$\text{by NZS3404 [53]} \quad \tau_u \cong 0.62 \cdot f_{uf} \quad (5.3)$$

$$V_u = \tau_u \cdot A \quad (5.4)$$

where  $\tau_u$  = Ultimate shear strength

$f_{uf}$  = Ultimate flexural strength  $\approx 480$  MPa for mild steel

$V_u$  = Ultimate shear capacity per anchorage

$A$  = Shear area of each anchorage ( $d=9.5$  mm)

$\tau_u \approx 0.62 \times 480 = 298$  MPa for mild steel considering code definition



$\tau_u \cong 230 - 240 \text{ MPa}$  , was extrapolated from the manufacturer's specification for the 9.5 mm diameter 88.9 mm embedment length considering 50 MPa concrete compressive strength (Figure 5.22)

PERFORMANCE TABLE							
<b>LDT Anchors</b>		<b>Ultimate Tension and Shear Values (Lbs/kN) in Concrete</b>					
ANCHOR DIA. In. (mm)	EMBEDMENT DEPTH In. (mm)	$f'_c = 2000 \text{ PSI (13.8 MPa)}$		$f'_c = 3000 \text{ PSI (20.7 MPa)}$		$f'_c = 4000 \text{ PSI (27.6 MPa)}$	
		TENSION Lbs. (kN)	SHEAR Lbs. (kN)	TENSION Lbs. (kN)	SHEAR Lbs. (kN)	TENSION Lbs. (kN)	SHEAR Lbs. (kN)
3/8 (9.5)	1-1/2 (38.1)	1,336 (5.9)	2,108 (9.4)	1,652 (7.3)	2,764 (12.3)	1,968 (8.8)	3,416 (15.2)
	2 (50.8)	1,492 (6.6)	3,036 (13.5)	2,024 (9.0)	3,228 (14.4)	2,552 (11.4)	3,420 (15.2)
	2-1/2 (63.5)	3,732 (16.6)	3,312 (14.7)	3,748 (16.7)	3,364 (15.0)	3,760 (16.7)	3,424 (15.2)
	3-1/2 (88.9)	5,396 (24.0)	3,312 (14.7)	6,624 (29.5)	3,368 (15.0)	7,852 (34.9)	3,428 (15.2)
1/2 (12.7)	2 (50.8)	3,580 (15.9)	5,644 (25.1)	3,908 (17.4)	6,512 (29.0)	4,236 (18.8)	7,380 (32.8)
	3-1/2 (88.9)	7,252 (32.3)	6,436 (28.6)	8,044 (35.8)	7,288 (32.4)	8,836 (39.3)	8,140 (36.2)
	4-1/2 (114.3)	10,176 (45.3)	7,384 (32.8)	10,332 (46.0)	7,968 (35.4)	10,488 (46.7)	8,552 (38.0)
5/8 (15.9)	2-3/4 (69.9)	5,276 (23.5)	8,656 (38.5)	6,560 (29.2)	11,064 (49.2)	7,844 (34.8)	13,476 (59.9)
	3-1/2 (88.9)	7,972 (35.5)	10,224 (45.5)	9,848 (43.8)	12,144 (54.0)	11,724 (52.2)	14,060 (62.5)
	4-1/2 (114.3)	11,568 (51.5)	12,316 (54.8)	13,432 (59.8)	13,580 (60.4)	16,892 (75.1)	14,840 (66.0)
3/4 (19.1)	3-1/4 (82.6)	6,876 (30.6)	7,140 (31.8)	9,756 (43.4)	10,728 (47.7)	12,636 (56.2)	14,316 (63.6)
	4-1/2 (114.3)	10,304 (45.8)	13,120 (58.4)	14,424 (64.2)	16,868 (75.0)	18,540 (82.5)	20,612 (91.7)
	5-1/2 (139.7)	13,048 (58.0)	17,908 (79.7)	18,156 (80.8)	21,718 (96.9)	23,268 (103.5)	25,652 (114.1)

**Figure 5.22.** Anchor specifications given by Red Head [54]

Considering the code definition:  $V_u = 298 \times 10^{-3} \cdot \pi \cdot 9.5^2 / 4 = 21 \text{ kN}$  per anchor

Considering the manufacturer's values  $V_u = 240 \times 10^{-3} \cdot \pi \cdot 9.5^2 / 4 = 17 \text{ kN}$  per anchor

There were 3 anchors connecting the bottom part of the timber framed infill to the RC beam. Therefore, the total shear carried by the three bolts was equal to:

$$\sum V_u = 21 \times 3 = 63 \text{ kN}, \text{ considering code definition}$$

$$\text{Or } \sum V_u = 17 \times 3 = 51 \text{ kN}, \text{ considering manufacturer's values}$$

These numbers are consistent with the measured force-deflection curve for the infill panel zone of the as built timber framed specimen FIF2-TBFD in Figure 5.25a. In this figure, the highest lateral force carried by the infill wall approximately corresponds to 60 kN. Therefore, it can be deduced that at 0.75% drift, the boundary anchors between the timber and lower beam progressively started to rupture under shear, which caused the observed brittle behaviour on the global response. After 0.75% drift, this resulted in an increased deformation demand between the wall and the lower RC beam. This demand resulted in crushing of the corner of the linings in the next cycles.

The hysteresis behaviour and potentiometer measurements are shown in Figure 5.23, Figure 5.24 and Figure 5.25. The significant horizontal displacement demand between the infill panel zone and the lower/upper RC beams are shown in Figure 5.24, where the potentiometers reached their maximum recording limit of  $\pm 15$  mm at 1.0% imposed drift level. In addition, the significant displacement imposed to the vertical potentiometers between the infill panel zone and the RC columns is also shown in Figure 5.24.

The horizontal potentiometer readings at the lower and upper boundaries of the infill panel zone shows that g10, g12 (lower boundary) g16 and h2 (upper boundary) recorded approximately the same deformation values suggesting rigid lateral translation of the drywall in the infill panel zone. It should be noted that in the as built timber framed specimen, the damage concentrated to the corners of the drywall with very minor lining-to-lining interface damage as summarized in Figure 5.19 and Figure 5.20. In other words, the drywall remained monolithic internally and the whole wall showed lateral rigid body translation. It can also be observed that the differential vertical displacement between the timber framed drywall and the adjacent RC column is smaller compared to the steel framed drywall. This can be supported by the vertical potentiometer measurements in Figure 5.24 (h9, h12), which confirms the higher rigidity and stiffness of the inner framing of the timber framed drywall.

The hysteresis behaviour of the infill content was extracted from the global behaviour and shown graphically for both horizontal and diagonal directions in the infill panel zone in Figure 5.25. As can be seen in Figure 5.25, as built timber framed drywall behaved in a brittle manner due to the shear failure of the anchors at the lower boundary of the wall, losing its strength with increasing displacements.

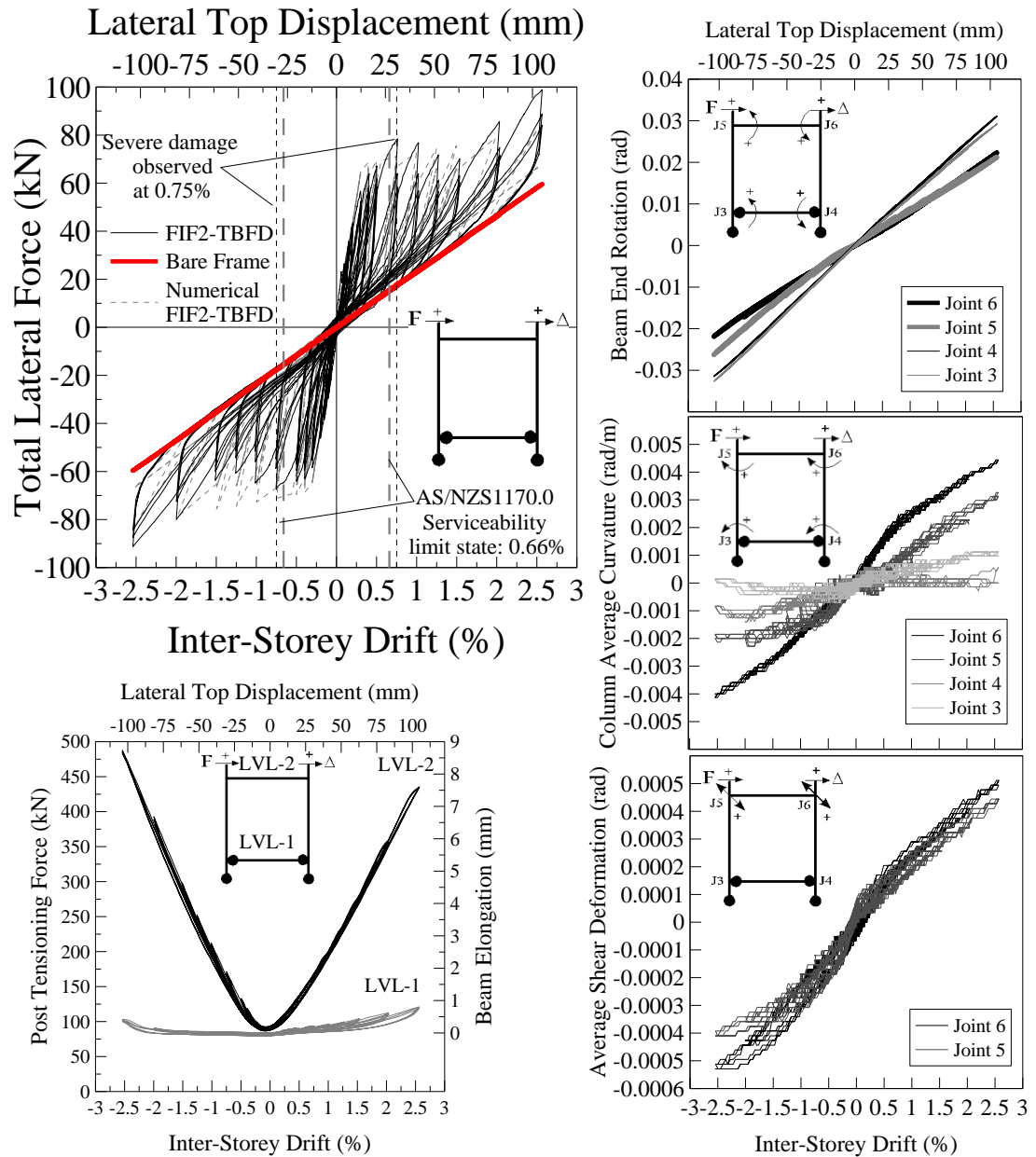


**Figure 5.23.** Test results for the as built timber framed drywall specimen FIF2-TBFD

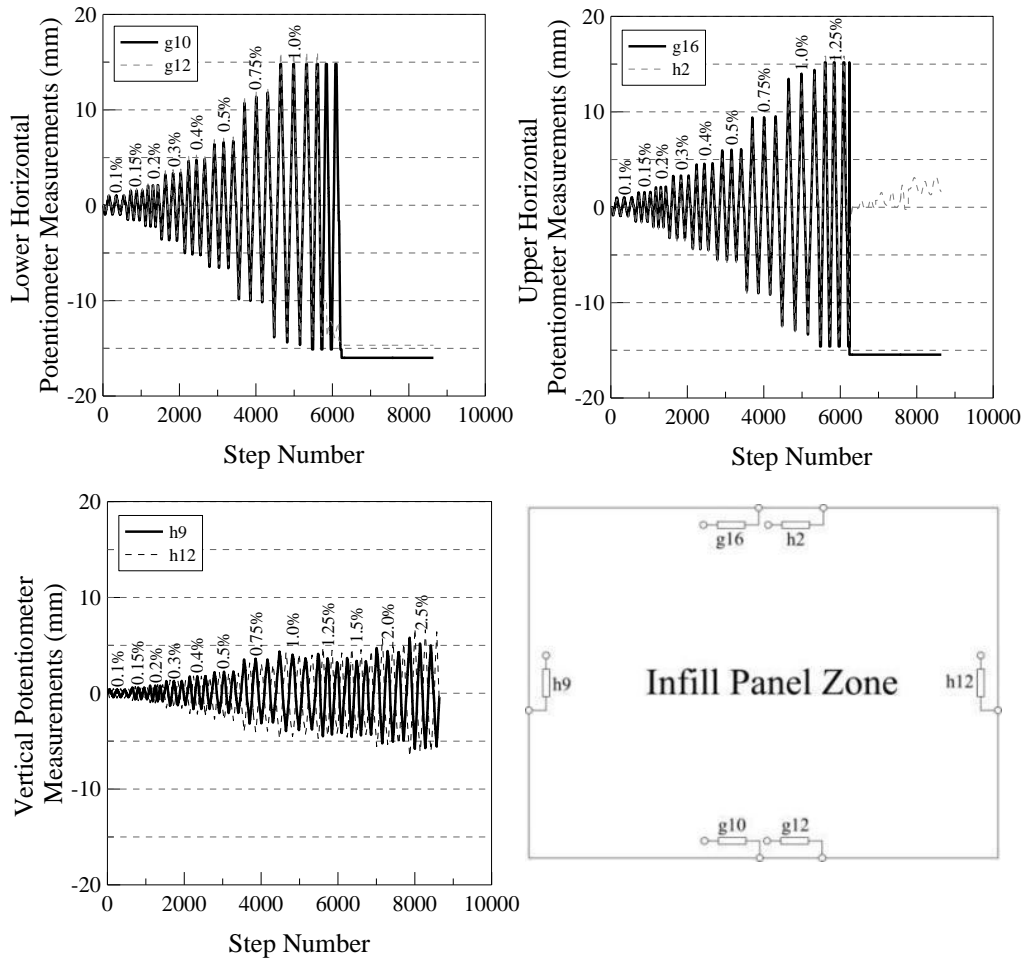


**Figure 5.24.** The most significant potentiometer measurements taken for horizontal and vertical movements in the infill panel zone for as built timber framed drywall FIF2-TBFD (For the location of the potentiometers, refer to Figure 5.5)

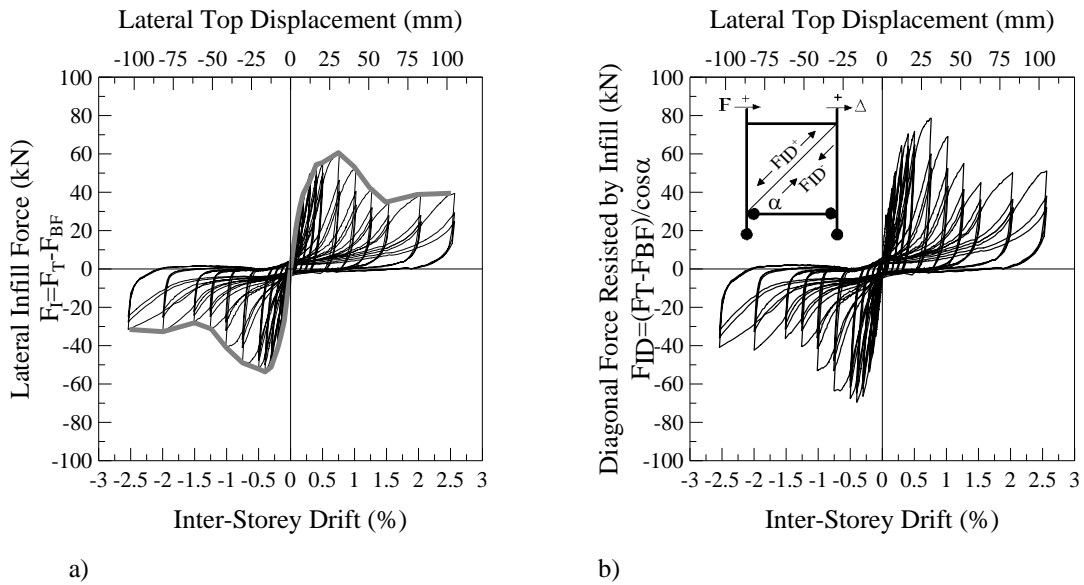


**Figure 5.25.** As built timber framed drywall FIF2-TBFD: a) Lateral force exerted on the infill panel zone obtained by subtracting the bare frame from the total, b) Diagonal force exerted on the infill panel zone, projection of a) in diagonal direction

#### 5.2.4 Numerical Model Calibration

The same diagonal spring model used for the as built steel framed drywall was modified by considering the behaviour of the as built timber frame drywall. The experimental results of the as built timber frame drywall FIF2-TBFD in Figure 5.25b was used to modify the implemented strut model.

The resulting model is shown in Figure 5.26. The model was calibrated to match the experimental results and the hysteresis curve shown in Figure 5.27 was obtained. The parameters describing the model are also shown in Figure 5.26 for use in full scale building models. However, the numbers given here need to be modified in a real building. Depending on the number of anchors used to fix the timber framing to either lower or upper beams, the shear failure force of the anchors will define the strength given by the infill in horizontal direction (Figure 5.25a). For the as built timber framed drywall FIF2-TBFD, the numerical shear failure force of the three anchors that were used to fix the timber framing to lower or upper RC beam ranged from 51-63 kN (Explained in 5.2.2), which confirmed the experimental observation given in Figure 5.25a. Then, this value can be projected to the diagonal direction of the related infill panel zone dividing by the *cosine* of the angle between the diagonal and the horizontal axes ( $\cos 41.42^\circ$ ). Therefore, the force values to be used in defining the range of parameters of the strut model can be obtained. The same model given here can also be adapted as two separate diagonal compression struts placed in both diagonal directions by using the corresponding data for each and assuming the struts do not carry any tension (compression only).

In the light of the explanation given above, the given calibrated strut model data for as built timber framed drywall specimen FIF2-TBFD can approximately be modified for a building as follows:

Assuming the number of anchors between the timber frame and the RC beam is directly proportional with the length of the wall, the peak diagonal strut strength ( $F_u^+$ ) and stiffness ( $KX$ ) can be approximately calculated by (only valid for timber framed drywalls);

$$(F_U^+)_{\text{RealTBFD}} = (F_U^+)_{\text{FIF 2-TBFD}} \cdot \frac{(L_c)_{\text{RealTBFD}}}{(L_c)_{\text{FIF 2-TBFD}}} \quad (5.5)$$

$$(KX)_{\text{RealTBFD}} = \frac{(F_U^+)_{\text{RealTBFD}}}{(F_U^+)_{\text{FIF 2-TBFD}} / (KX)_{\text{FIF 2-TBFD}}} \quad (5.7)$$

Where;  $(L_c)_{\text{RealTBFD}}$ : Length of the non-structural wall in a real structure

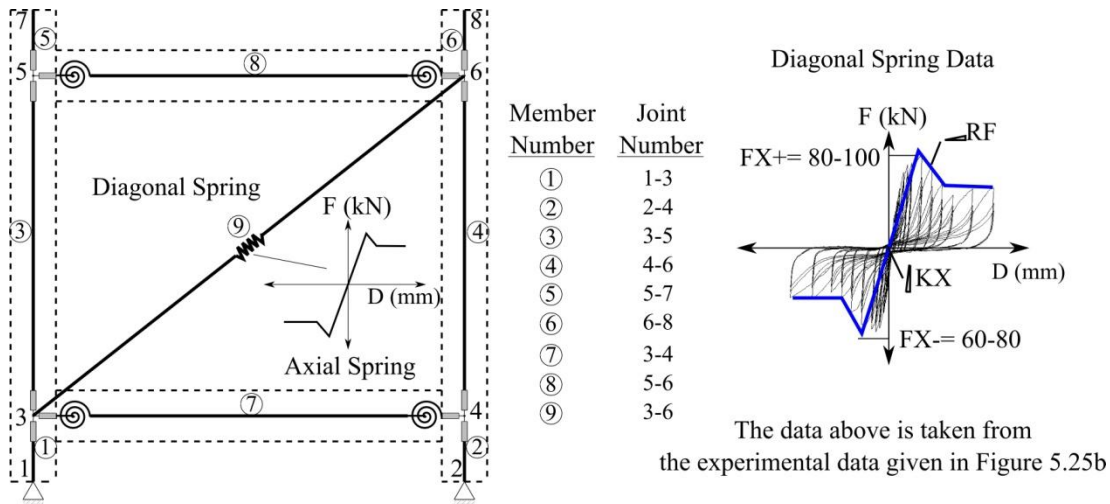
$(F_u^+)_{\text{RealTBFD}}$ : Peak strength of the diagonal strut in a real structure

$(L_c)_{\text{FIF2-TBFD}}$ : Length of the non-structural wall=3400 mm or 3.4 m

$(F_u^+)_{\text{FIF2-TBFD}}$ : Calibrated peak strength of the diagonal strut  $\approx 1.25 \times 80$  kN

$(KX)_{\text{FIF2-TBFD}}$ : Calibrated stiffness of the diagonal strut  $\approx 15000$  kN/m

1.25 is the peak strength calibration coefficient as shown in Figure 5.26.



Wayne Stewart Degrading Stiffness model data for Ruaumoko2D

!	N	MTYPE LABEL															
	5	SPRING STRUT															
!	12A BASIC SECTION PROPERTIES																
!	ITYPE	IHYST	ILOS	IDAMG	KX	KY	GJ	WGT	RF	RT	PSX	PSY	PSZ	THETA	ITRUSS	IOP	
	1	9	0	0	15000	0	0	0	-0.09	0	0	0	0	0	0	0	
!	12C YIELD SURFACE																
!	FX+	FX-	FY+	FY-	MZ+	MZ-											
	100	-70	0	0	0	0											
!	FU	FI	PTRI	PUNL	GAP+	GAP-	BETA	ALPHA	LOOP	1.25 x Diagonal Strength (80 kN)							
	100	0	0	2	0	0	1.04	0.2	1								

Figure 5.26. The numerical model of as built timber framed drywall FIF2-TBFD for Ruaumoko 2D

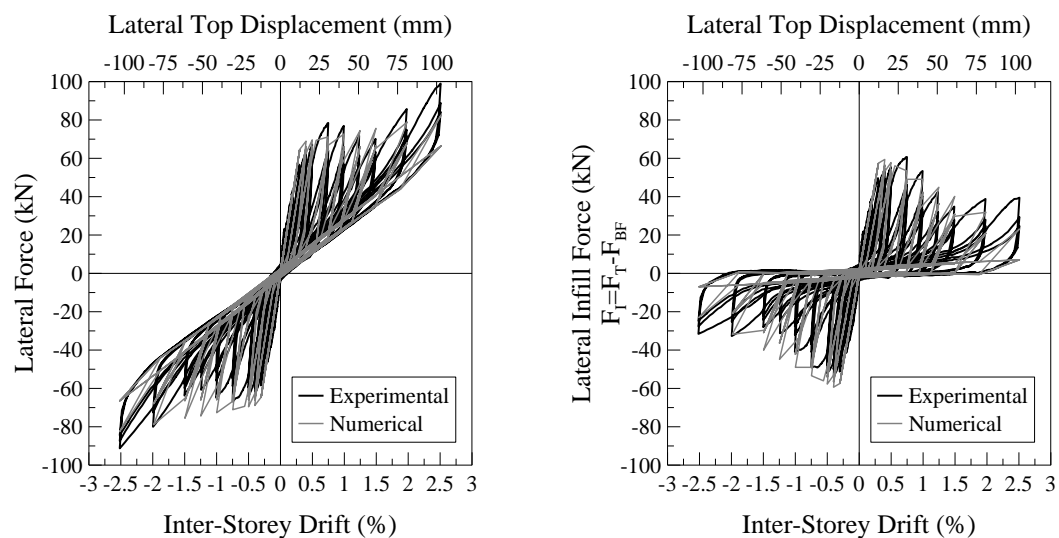


**Figure 5.27.** Hysteresis behaviour of the numerical model compared to the experimental result for as built timber framed drywall FIF2-TBFD

### 5.3 Observations, Energy Dissipation and Effective Stiffness Properties of the As Built Steel and Timber Framed Drywall Specimens

#### 5.3.1 Observations and Comparisons

One of the most important observations is that at very low drift levels, these as built walls suffer level of damage which would require repairing intervention, exceeding the designed serviceability limit state,. The as built steel framed specimen FIF1-STFD lost its serviceability at 0.3% drift and the as built timber framed specimen FIF2-TBFD lost it at 0.75% drift. According to the Table C1 in NZS1170.0 [55], plaster/gypsum walls (in plane) are expected to suffer lining damage/serviceability loss at mid-height deflection of  $Height / 300$ . In the tested specimens, the infill wall height was 2550 mm. Therefore, the resulting mid-height deflection is  $2550/300=8.5$  mm, which corresponds to  $8.5/1275 \times 100 \approx 0.667\%$  inter-storey drift level. These values are summarized in the total force envelope curves shown in Figure 5.28. It can be seen that the limit given by this equation does not provide a reliable serviceability drift limit for the steel framed drywall specimen FIF1-STFD. On the other hand, for the timber framed drywall specimen, FIF2-TBFD, it provides a conservative underestimation.

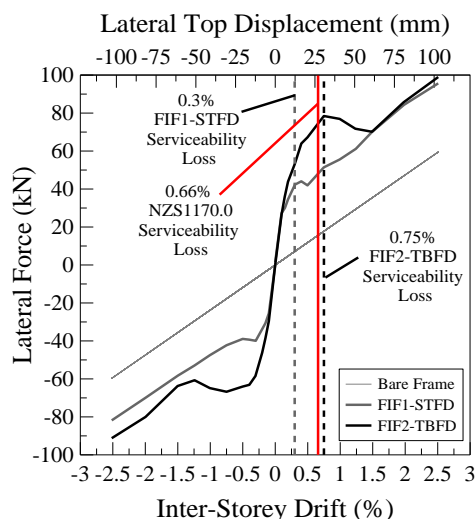


**Figure 5.28.** The envelope curves of the bare frame, as built steel framed drywall specimen FIF1-STFD and timber framed drywall specimen FIF2-TBFD



### 5.3.2 Energy Dissipation and Stiffness Degradation Properties

Because of the inevitable interaction between the infill wall and the structural frame, the drywalls also provided some level of energy dissipation. The equivalent viscous damping ( $\xi_{eq}$ ) of the tested specimens were calculated by using the standard area-based method suggested in literature (i.e. Chopra 2001 [56]):

$$\xi_{eq} = \frac{1}{4\pi} \frac{E_D}{E_{SO}} \quad (5.8)$$

where  $E_D$  : Energy dissipated at a cycle

$E_{SO}$  : Maximum strain energy at a cycle

The calculated values for  $\xi_{eq}$  and  $E_D$  were averaged at the applied drift amplitudes and plotted in Figure 5.29. As it can be seen, the steel framed and the timber framed drywall specimens have similar energy dissipation trends initially (0.1% - 0.3%) and at later cycles (1.5% - 2.5%). The difference is given by the different serviceability loss levels of the two specimens, 0.3% for steel and 0.75% for timber framed drywall

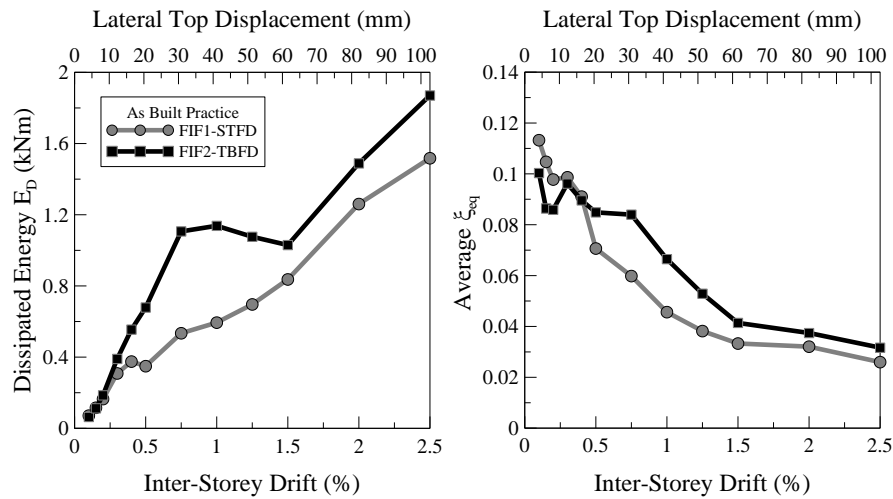


**Figure 5.29.** Average dissipated energy ( $E_D$ ) and average equivalent viscous damping ( $\xi_{eq}$ ) with respect to inter-storey drift for as built steel framed drywall specimen FIF1-STFD and as built timber framed drywall specimen FIF2-TBFD

The effective stiffness values were calculated using the points on the total lateral force ( $F_T$ ) and lateral infill force ( $F_I$ ) envelope curves of each specimen and the resulting

graph is shown in Figure 5.30. In the reported work, the effective stiffness of the bare frame is 0.55 kN/mm and due to the linear elastic behaviour of the setup, it remains approximately constant at each displacement stage. Depending on the bare frames with different stiffness, these curves may shift. In the reported study, the bare frame was a very flexible bare frame which was used to observe the wall behaviour and its interaction.

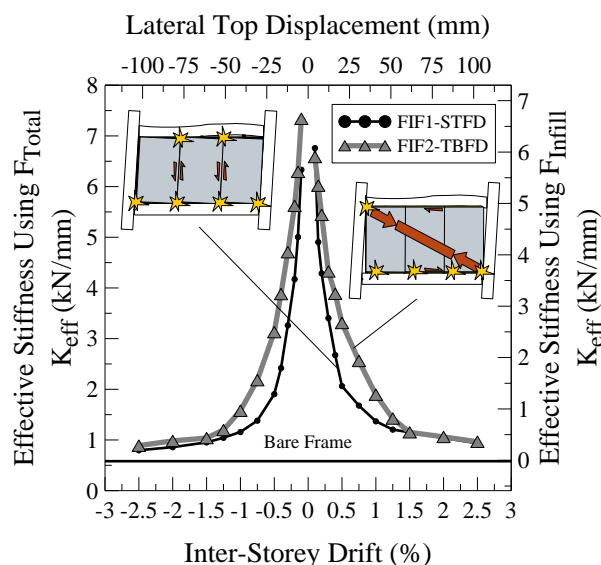


**Figure 5.30.** Stiffness degradation for as built steel framed drywall specimen FIF1-STFD and as built timber framed drywall specimen FIF2-TBFD with respect to the inter-storey drift, plotted using total lateral force (left axis) and using the lateral force exerted by the infill wall (right axis)

## 5.4 Conclusions

The existing (as built) construction practice is to completely fix the drywall system to the surrounding structural frame. This results in a non-negligible interaction between the drywall and the structural system. Until now, this interaction has generally been assumed to be relatively small and thus somehow negligible, but this is possibly based more on intuitive judgement than on empirical observation. In addition, the earthquakes have repeatedly shown that these walls suffer moderate-to-severe damage at very small drift levels, which has also been confirmed by the experiments reported herein.

Since the bare frame behaved elastically, the behaviour of the infill walls was extracted from the global force-deflection curves, which can analytically be described by Wayne

Stewart degrading stiffness hysteresis rule due to the similar pinching of the system. It was confirmed that the drywall systems adopted in the current practice for commercial buildings is susceptible to a level of damage which would require repairing interventions at low drift levels. The steel framed drywall lost serviceability condition at 0.3% inter-storey drift level with a ductile post-yield behaviour. On the other hand, the timber framed drywall lost serviceability at the higher drift level of 0.75% with a brittle behaviour.

The difference in the behaviour of the as built timber framed drywall specimen can be attributed to; i) the stiffer timber-to-timber connections, ii) the stiffer inner framing due to the horizontal timber elements in the framing and iii) the resulting shear failure of the lower anchors between the timber frame and lower RC beam, which agreed well with the achieved strength value in this specimen. As a result of this, it may be stated that as long as the linings and the timber frame are still intact to sustain the strut action, the strength of timber framed drywalls are governed by the dowel shear capacities given by the anchors. For existing and new buildings, depending on the relative stiffness between the drywall and the surrounding structural frame, this brittle behaviour may lead to structural issues to be addressed such as, in the extreme case scenario, soft storey mechanisms [10]. The assumption that these light infill walls does not affect the structural response may, in general terms, need to be revisited. On the other hand, for the as built steel framed drywall specimen, the rotation of the steel studs at the single-screw track connections imposed significant movement to the lining interfaces prior to damaging the boundary anchors. Therefore, their behaviour was ductile compared to that observed in the timber framed drywalls.

The above mentioned difference also showed that in the table C1 of AS/NZS 1170.0:2002 Plaster/Gypsum walls (in-plane) [55], the generalized serviceability limit state criterion might need to be revisited. The criterion in the Standard assumes the serviceability limit state is reached for a mid-height deflection of height/300. Although the test setup was more flexible than a typical multi-storey frame, this formula overestimated the limit state for the as built steel framed drywall specimen, the common drywall partition type in the commercial construction. For the as built steel framed drywalls, this criterion may need to be modified. On the other hand, the

existing criterion gave a reasonably accurate result for the timber framed drywalls. Therefore, it may be more realistic to give limit states for these two different types of drywalls under two different categories. This may require further testing and numerical study in order to strengthen the conclusions.

The tests once again showed that these non-structural walls are extremely susceptible to drift and suffer significant damage at very low drift levels (0.3%-0.75%). Considering that the costs associated with the loss of non-structural components are much higher than the structural components, it is very important to develop technological solutions to minimize the seismic damage to non-structural walls.

### 5.5 References

- [10] G. Magenes and S. Pampanin, "Seismic Response of Gravity-Load Design Frames with Masonry Infills," in 13th World Conference on Earthquake Engineering, Vancouver, B.C., Canada, 2004.
- [51] A. J. Carr, "Ruaumoko 2D-Computer Program for Inelastic Time History Analysis of Structures," ed. Christchurch, New Zealand: University of Canterbury, 2013.
- [53] NZS3404.1, "Steel Structures Standard," vol. 3404, ed. New Zealand Standard: Standards New Zealand, 1997.
- [54] RedHead, "Large Diameter Tapcon Anchors (LDT): Specifications," ed.
- [55] AS/NZS1170.0, "Part 0: General Principles," in Structural Design Actions vol. 1170, ed: Australian/New Zealand Standard, 2002.
- [56] A. K. Chopra, Dynamics of Structures: Theory and Applications to Earthquake Engineering, 2nd Edition ed. New Jersey: Prentice Hall, 2001.

# CHAPTER 6

## LOW DAMAGE DRYWALL TESTS

*Each problem that I solved became a rule, which served afterwards to solve other problems*

.

*Rene Descartes*



## 6 LOW DAMAGE DRYWALL TESTS

### 6.1 Low Damage Steel Framed Drywall: MIF1-STFD

#### 6.1.1 Development and Construction

After studying the behaviour of the as built drywall practice, it was observed that the horizontal displacement demand imposed at the lower and upper boundaries of the infill panel zone was significantly high as shown by the related potentiometer readings in the previous chapter. The fasteners used to fix the gypsum linings to the steel framing started to loosen even from the initial cycles, damaging the gypsum lining (Figure 6.1). Also, the screws used to fix the steel studs to the steel tracks remained in place, but they caused stud rotation as drift amplitudes were increased. This further imposed damage to lining-to-lining interfaces since the vertical steel studs were free to rotate about these screws.



**Figure 6.1.** Damage at the fasteners observed at as built steel framed drywall FIF1-STFD

Therefore, considering these observations and the given damage mechanism for as built steel framed drywall specimen FIF1-STFD, modifications to the existing practice were required. The inherent vulnerability of the as built system had to be eliminated without introducing additional cost or complicated details. The developed system had to be easily applied by the contractors with the readily available materials on site. The modifications developed and designed for this specimen are summarized and explained in Figure 6.2.

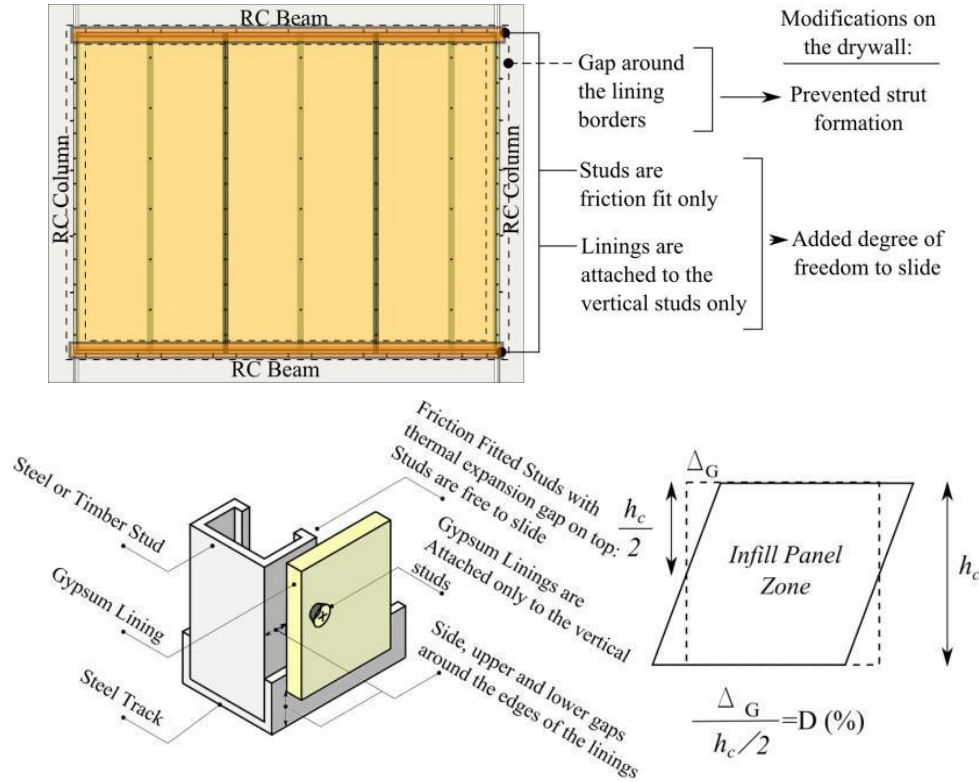


**Figure 6.2.** Modifications to the as built steel framed drywall practice

In order to accommodate any desired inter-storey drift, the required gap at the left and right lining borders,  $\Delta_G$ , can be calculated as given below:

$$\Delta_G = D \cdot \frac{h_c}{2} \cdot \frac{1}{100} \quad (6.1)$$

Where  $D$ : Design inter-storey drift limit in % after which damage is acceptable  
 $h_c$ : Infill wall clear height (2550 mm for the test specimen)

For this specimen,  $D=1.5\%$  drift was chosen. Using the equation above, the side gaps necessary to accommodate 1.5% inter-storey drift were calculated to be 20 mm (40 mm gap in total). In order to see whether the necessary gaps can work effectively when distributed to the adjacent internal lining joints, two 15 mm gaps were provided at the external edges of the linings A and C, near RC columns. Two 5 mm gaps were provided in the interior lining-to-lining interfaces, i.e. interface of the linings A-B and linings B-C. Also, in order to show different connection typologies, half of the connections were made fire rated and the other half was non-fire rated. Fire rating was achieved by using strips of gypsum boards to prevent exposing of the steel frame. The linings were only fixed to the vertical studs so that the wall was left free to slide in the



steel tracks with increasing inter-storey drift levels. In Figure 6.3, the resulting details of the specimen are shown. As can be seen in these details, the total gap of 40 mm is shared between the four connections, two of which are 15 mm (shared by the external connections) and the remaining 10 mm is shared by the two inner connections as 5 mm gaps.

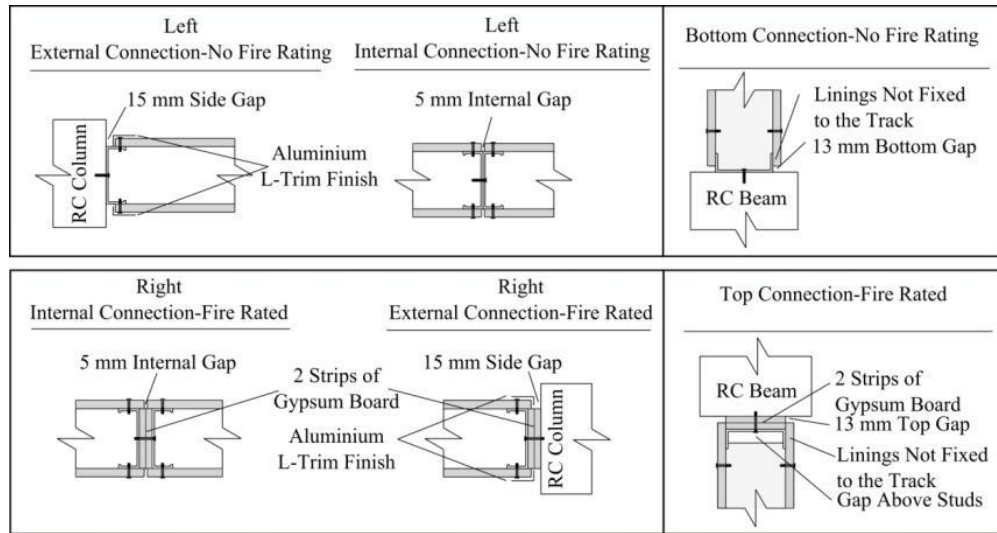


**Figure 6.3.** Connection details used in low damage steel framed drywall specimen MIF1-STFD

Construction was carried out using the same type of steel tracks, studs and anchors as the steel framed drywall specimen FIF1-STFD. The studs were combined in order to obtain the special H-studs required between the linings (Figure 6.4). It should be noted that the studs were cut so that some gap was left above the studs to allow for thermal expansion and vertical isolation from the structure (As shown in top connection detail in Figure 6.3).

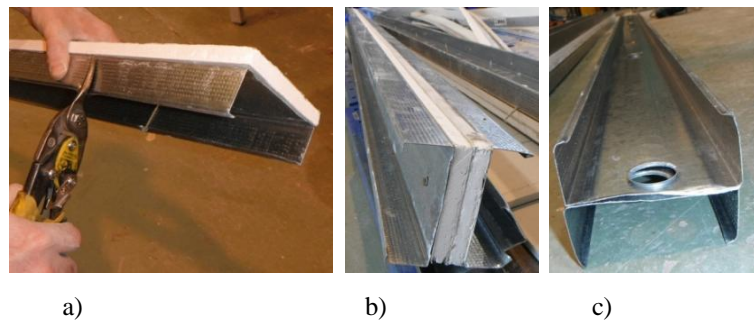


**Figure 6.4.** a) Formation of the special H-studs used in low damage steel framed drywall, b) Completed fire rated H- stud to be used at the fire-rated internal connection, c) Completed non fire rated H-stud to be used at the non-fire-rated internal connection

Similar to FIF1-STFD, the construction of the low damage steel framed drywall MIF1-STFD started by fixing the fire rated top, right and non-fire bottom, left border elements (Step 1 in Figure 6.5). Then, the prepared studs were friction fitted between the top and bottom tracks (Step 2 in Figure 6.5). Finally, the gypsum linings were cut according to the required gap dimensions and fixed only to the vertical studs. The procedure is summarized in Figure 6.5. Close ups of the connections of the specimen are shown in Figure 6.6.

Construction video: <http://youtu.be/FXShuxRWPdg>

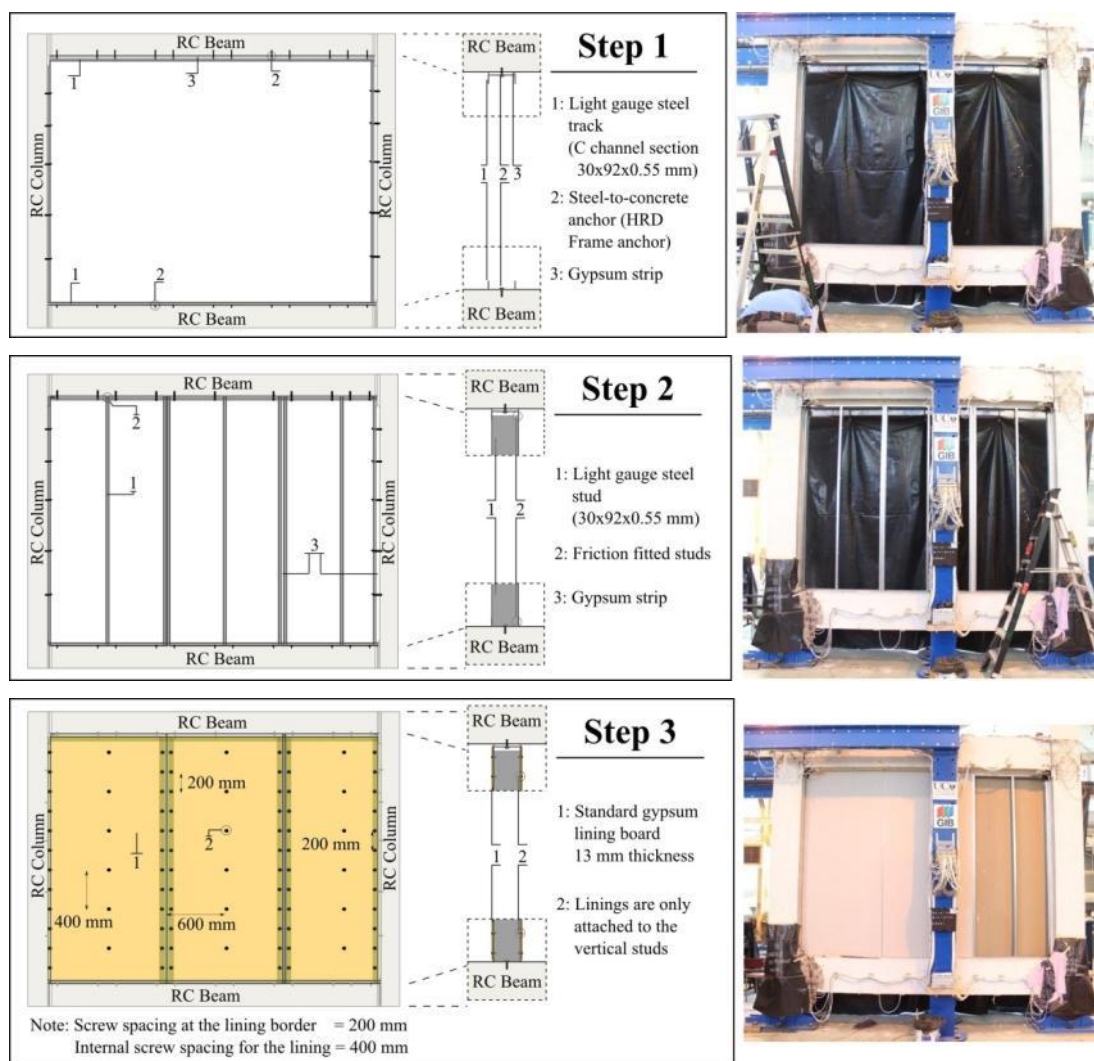


**Figure 6.5.** Construction sequence of low damage steel framed drywall specimen MIF1-STFD, for details refer to Figure 6.3

### 6.1.2 Finishing of the Drywall

Since the drywall had no flushed connection between linings (all had gaps in between), no paper tape application was applied at internal lining edges. The drywall screws

were simply flushed by using gypsum plaster and the gaps between the linings did not require any finishing since the lining edges provided a good finish here (Figure 6.6g). For the edges of the linings at the external gaps, aluminium L-trims were used to finish the rough edges left from the cutting of the linings (Figure 6.3 and Figure 6.7)

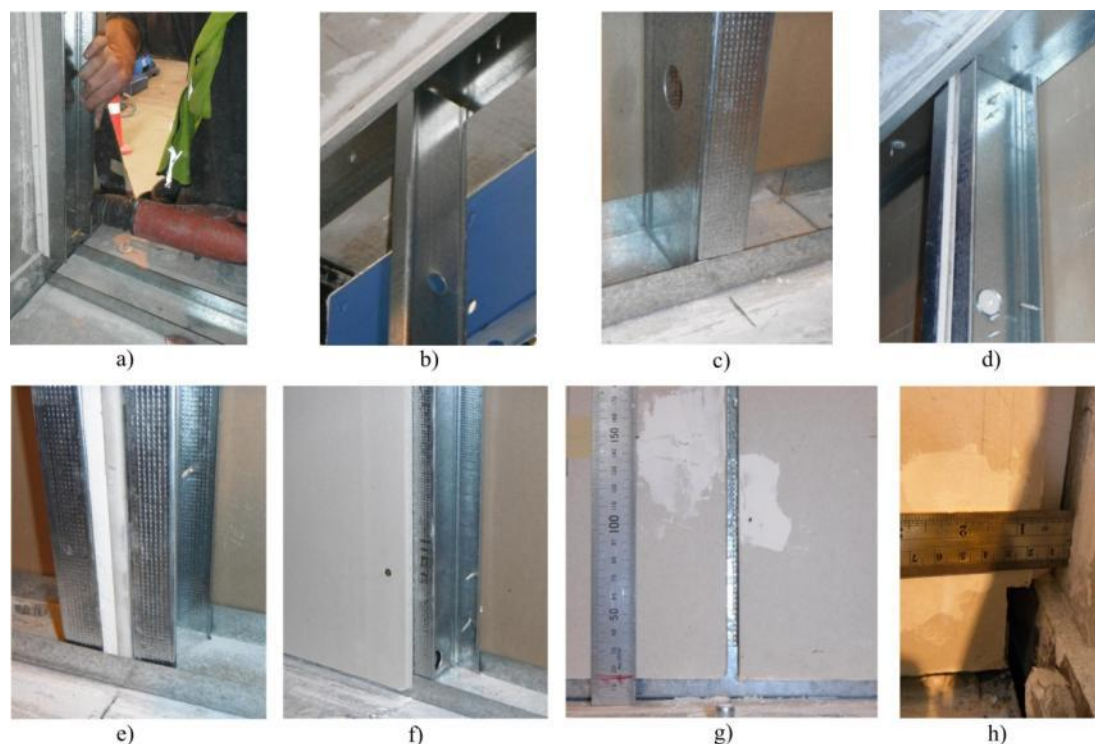
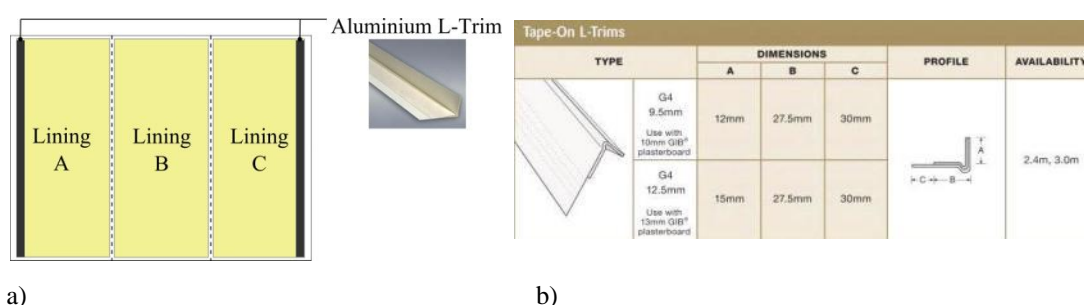


**Figure 6.6.** Close ups of the connections of low damage steel framed drywall specimen MIF1-STFD: a) External fire rated connection, b-c) Friction fitted stud, d-e) Fire rated H-stud, f) Linings connected to non-fire rated H-stud, g-h) Internal and external gaps



a)

b)

**Figure 6.7.** a) Finishing scheme, b) Aluminium L-trim specification, used at the edge of the external gypsum linings (GIB-[www.gib.co.nz](http://www.gib.co.nz))

### 6.1.3 Instrumentation

With the significant lateral displacement demand imposed to the infill panel zone known, the instrumentation of this specimen was modified in order to monitor the

deformations occurring at the provided gaps. Potentiometers h5, h9, h13, h8, h12 and h16 were placed at the external gaps in order to measure the lateral deformation of these gaps relative to the RC columns (Left of lining A and right of lining C). The potentiometers h6, h10, h14, h7, h11 and h15 were placed in order to measure the deformation of internal gaps relative to the adjacent linings (Left and right of lining B). The modified instrumentation scheme is shown in Figure 6.8. The measurement range of all the potentiometers was  $\pm 10$  to  $\pm 15$  mm.

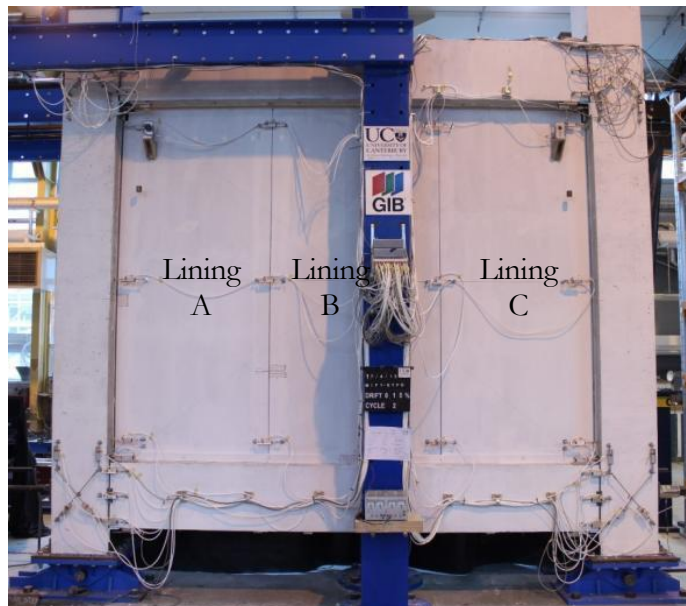
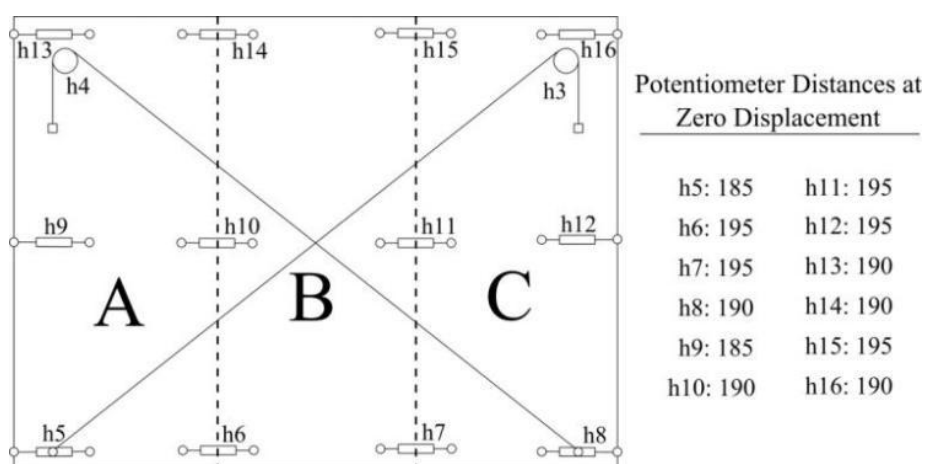


**Figure 6.8.** Instrumentation of the low damage steel framed drywall specimen MIF1-STFD



### 6.1.4 Test Results

#### 6.1.4.1 Damage Observations

No damage was observed until 1.0% drift level. At 1.0% drift, minor plaster cracking occurred at L-trim finish of lining C. Following this, at 1.25% drift, similar damage occurred at the L-trim finish of the lining A. However, this damage was very minor and caused by the closing of the side gaps on top and bottom, which were two 15mm gaps corresponding to 1.25% drift. At 1.5% drift, the internal gaps between the adjacent linings closed as designed and no further damage was observed. At 2.0% drift, existing plaster damage at L-trims progressed further and damage initiation at a few lining fasteners occurred since all the gaps were closed, which was expected since the design of the gaps were made for 1.5% drift level. Finally at 2.5% drift, not much additional damage occurred except for the progress of L-trim cracks. In overall, the drywall did not suffer any severe damage, performing very well until very high drift levels. The only problem observed was anchor pull out of the external studs on the RC columns at 2.0% drift level. However, this problem was later solved in the low damage timber framed drywall specimen MIF2-TBFD. The damage is summarized in the damage map given in Figure 6.9. The photographic report of the status of the specimen at the end of the test is shown in Figure 6.10.

Video of the test: <http://youtu.be/Qw5eRRnWbvY>

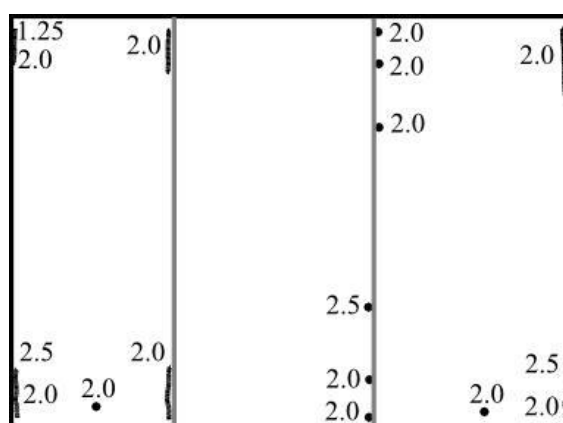


**Figure 6.9.** Drift based damage at the end of test of low damage steel framed drywall MIF1-STFD

#### 6.1.4.2 Behaviour Explanation

As shown in the damage observations, the ability of the low damage drywall to adaptively deform according the inter-storey drifts significantly prevented the damage. The behaviour mechanism of the low damage steel framed drywall specimen MIF1-

STFD is visually explained in Figure 6.11. Most of the plaster damage occurred after all of the provided gaps were closed in the system. Closing of the gaps initiated the rocking of the linings. Therefore, the cracks at L-trims occurred after 1.5% drift level. The obtained hysteresis curve and the measurements taken are shown in Figure 6.12.

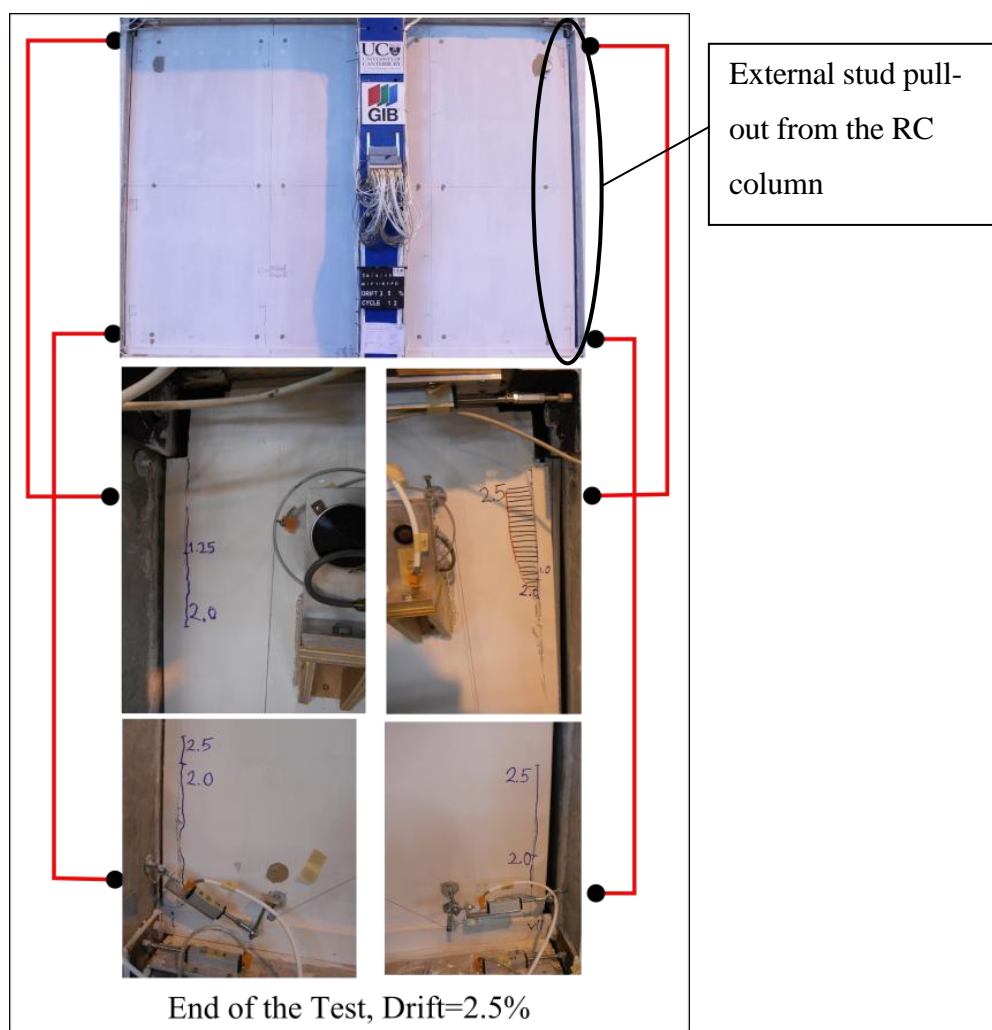


**Figure 6.10.** Damage at the end of the test of low damage steel framed drywall specimen MIF1-STFD

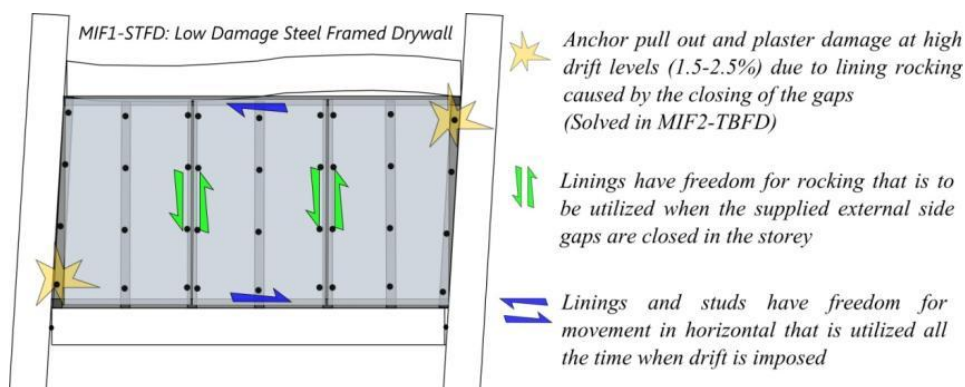


**Figure 6.11.** Behaviour of low damage steel framed drywall specimen MIF1-STFD

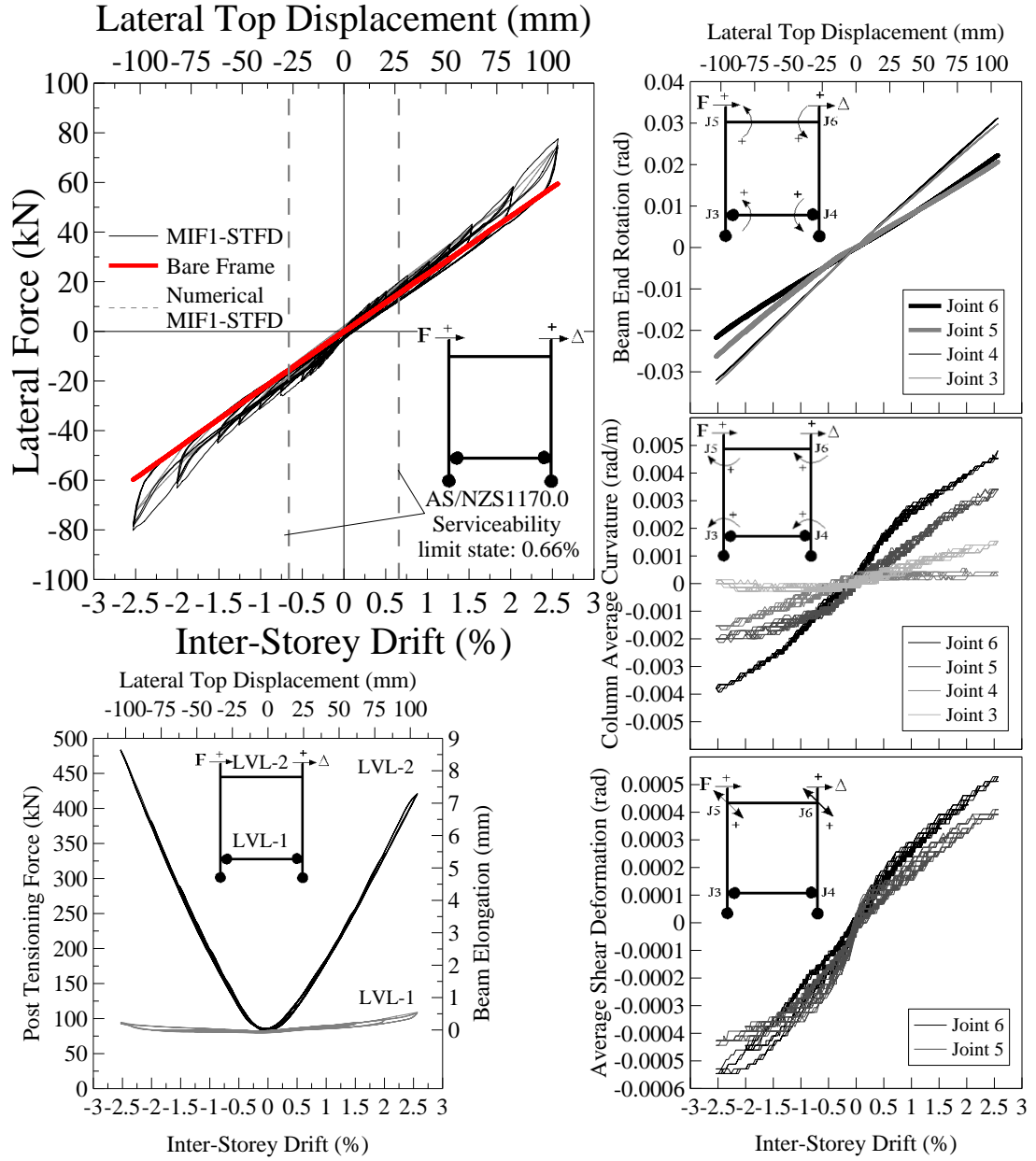


**Figure 6.12.** Test results for the low damage steel framed drywall specimen MIF1-STFD

The potentiometer measurements recorded during the test also confirmed the behaviour of the low damage drywall system. When the external potentiometers h5, h8 and h13, h16 at the lower and upper levels were inspected (Figure 6.13), it was seen that the  $15 \pm 1.5$  mm of external gap closed at about 1.00 to 1.25% drift level, which was approximately calculated as:

$$D = \frac{2}{h_c} \cdot \Delta_G \cdot 100 = \frac{2}{2550} \cdot 15 \cdot 100 \cong 1.2\%$$

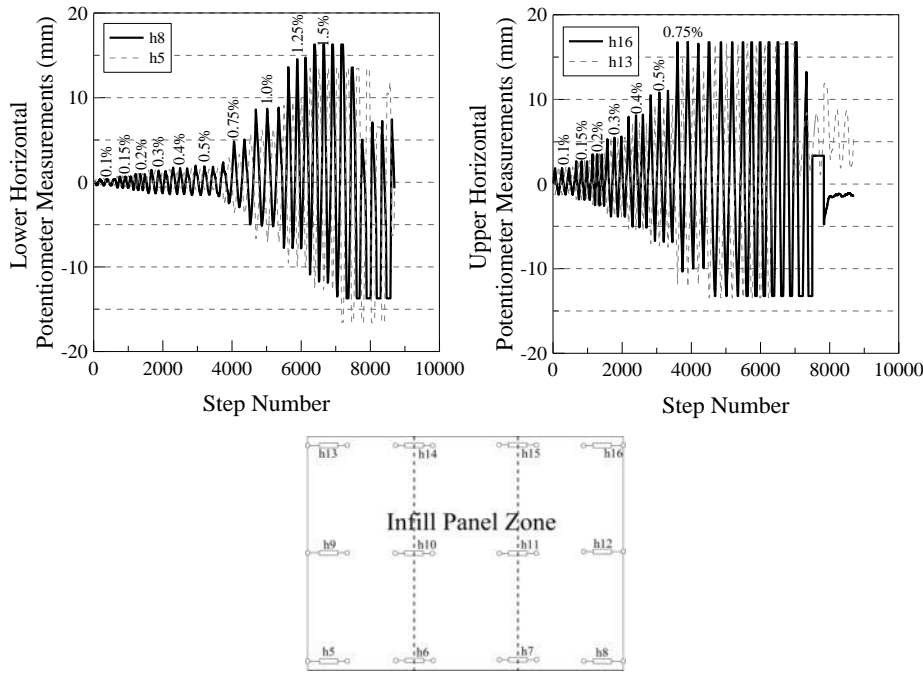


**Figure 6.13.** Lower and upper potentiometer readings at the external gaps and the locations of the potentiometers for low damage steel framed drywall specimen MIF1-STFD

Similarly, when the internal potentiometers h6, h7 and h14, h15 at the lower and upper levels were inspected,  $5 \pm 1.5$  mm of internal gap closed at about 1.50 to 2.00% (Figure 6.14), which was the approximate drift value at which the 5mm gap closed theoretically:

$$D = \frac{2}{h_c} \cdot \Delta_G \cdot 100 = \frac{2}{2550} \cdot (15 + 5) \cdot 100 = 1.57\%$$

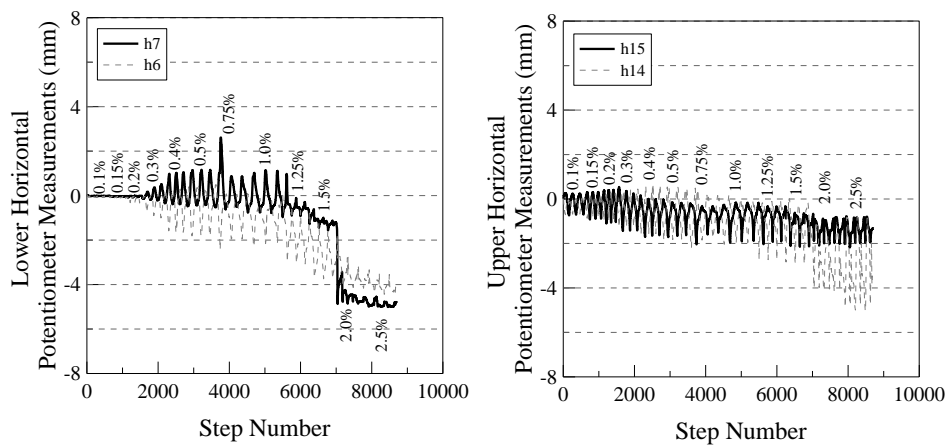


**Figure 6.14.** Lower and upper potentiometer readings at the internal gaps for low damage steel framed drywall MIF1-STFD (for potentiometer locations, refer to Figure 6.13)



When the potentiometer readings were inspected in overall, the drift values at which the external and internal gaps closed approximately matched the theoretical values (1.25% for exterior gaps, 1.5% for interior gaps). However, due to the pull out of the RC anchor observed at the external studs (Figure 6.10 and Figure 6.19) and the sliding ability of the wall, there were minor residual displacements over the gaps. When the specimen was brought back to zero displacement, the gaps were 5mm for the external and 3mm for the internal (Figure 6.15). Except for the RC anchor pull out, this was an expected and tolerable result. The RC anchor pull out problem was later addressed and solved in the low damage timber framed drywall specimen MIF2-TBFD.

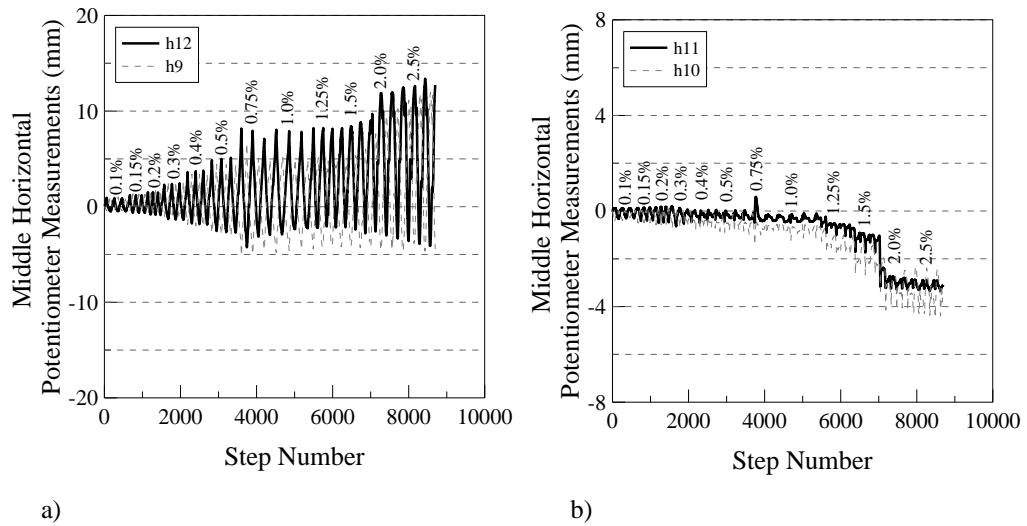


**Figure 6.15.** Potentiometer measurements taken at the gaps (MIF1-STFD, for locations refer to Figure 6.13): a) Exterior gaps, b) Interior gaps

In order to obtain the hysteresis behaviour of the infill content, the bare frame hysteresis was subtracted from the total hysteresis, shown in Figure 6.16a. Then the result was projected into the diagonal direction for use in modelling applications, shown in Figure 6.16b. As it can be seen from these figures, the contribution of infill panel zone content was minimized due to the significantly reduced interaction with the structural system, which prevented any significant damage to the low damage steel framed drywall specimen MIF1-STFD.

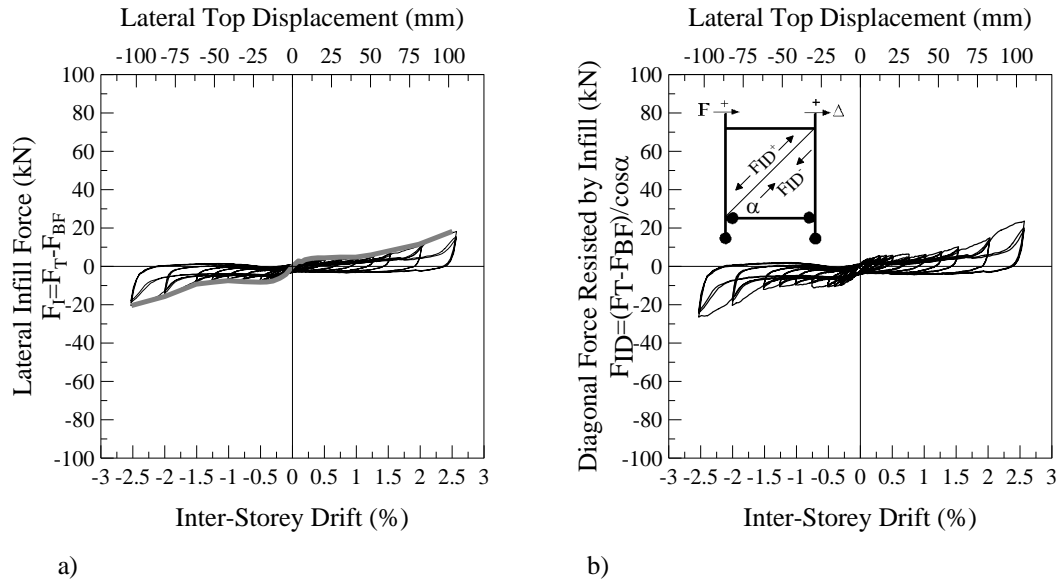
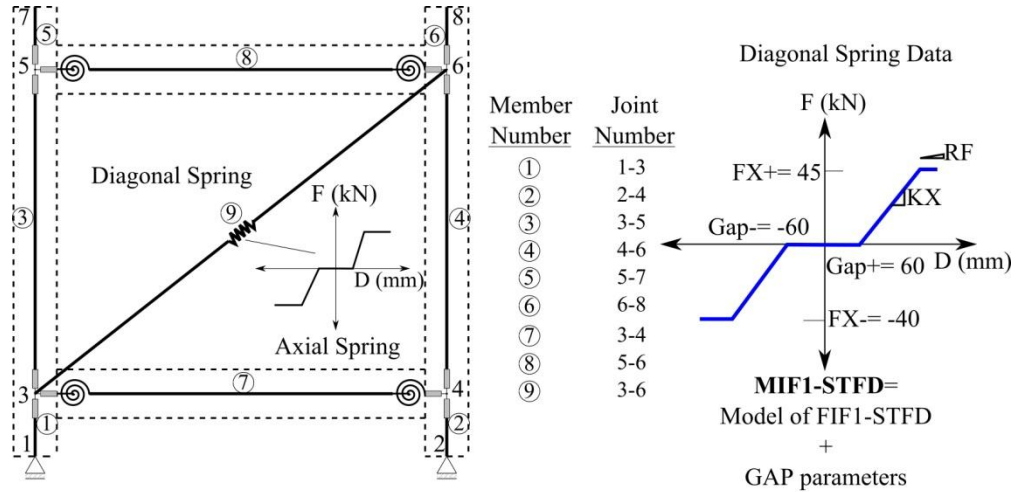


**Figure 6.16.** Low damage steel framed drywall MIF1-STFD: a) Lateral force exerted on the infill panel zone obtained by subtracting the bare frame from the total, b) Diagonal force exerted on the infill panel, projection of a) in diagonal direction

### 6.1.5 Numerical Model Calibration

The existing numerical model for as built steel framed drywall (FIF1-STFD) was modified by introducing the gap parameter in the Wayne Stewart degrading stiffness model (Figure 6.17). The provided total horizontal gap of  $40 \pm 5$  mm was projected into the diagonal direction with the cosine of the angle between the diagonal and the horizontal, which is  $(40 \pm 5) / \cos(41.42^\circ) \approx 60$  mm. An assumption of 5 mm error interval was made to account for the errors occurring in the construction stage. As shown in Figure 6.18, the model fits the experimental data with minimal calibration. This is a practical result considering that the same model can represent both the as built and the low damage specimens with the inclusion of a gap parameter. In addition, due to the significantly reduced interaction between the structural frame system and the non-structural drywall (infill), the low damage non-structural drywall can be neglected in the modelling for the seismic design of multi-storey buildings.



**Wayne Stewart Degrading Stiffness model with Gap data for Ruaumoko2D**

```

! N MTYPE LABEL
5 SPRING STRUT

! 12A BASIC SECTION PROPERTIES
! ITYPE IHYST ILOS IDAMG KX KY GJ WGT RF RT PSX PSY PSZ THETA ITRUSS IOP
1 9 0 0 15000 0 0 0 0.001 0 0 0 0 0 0 0

! 12C YIELD SURFACE
! FX+ FX- FY+ FY- MZ+ MZ-
45 -40 0 0 0 0

! FU FI PTRI PUNL GAP+ GAP- BETA ALPHA LOOP
45 0 0 2 0.06 -0.06 1.04 0.2 1
  
```

**Figure 6.17.** The numerical model of the low damage steel framed drywall specimen MIF1-STFD for Ruaumoko 2D

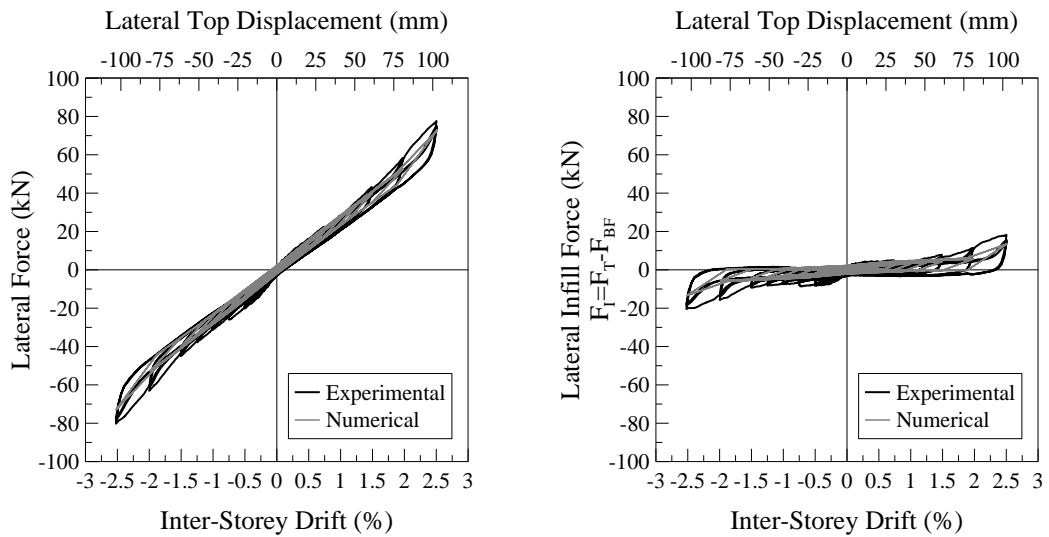


**Figure 6.18.** Hysteresis behaviour of the numerical model compared to the experimental result for low damage steel framed drywall specimen MIF1-STFD

## 6.2 Low Damage Timber Framed Drywall: MIF2-TBFD

### 6.2.1 Development and Construction

Following the good performance of the low damage steel framed drywall specimen MIF1-STFD, the same solution was adapted for its timber frame counterpart. However, the low damage solution for the steel system had to be modified to address the minor issue of the anchor pull out at the external stud on the RC column (Figure 6.19).

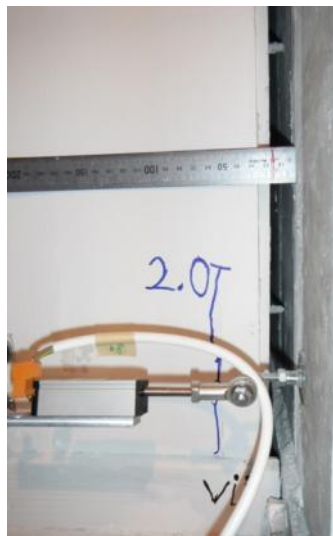


**Figure 6.19.** Anchor pull out of the external stud in low damage steel framed drywall specimen MIF1-STFD

The pull out issue was solved by adding two studs near the side edges of the drywall and the gypsum linings were fastened to those studs, which are friction fit to allow sliding between steel tracks on top and bottom RC beams. The studs on the RC columns were still used, but with no attachment to the gypsum linings, such that they only behaved as shear keys for out of plane. The reason for connecting the linings only to the vertical studs between the steel tracks was to allow the wall to slide between the upper and lower tracks. Moreover, for a better architectural finish, the required total gap of 40mm was only distributed to the exterior sides of the drywall. Therefore, this specimen had a flushed surface with two 20 mm side gaps at the edges of the gypsum linings. All of the modifications made are summarized in Figure 6.20 and resulting details are shown in Figure 6.21.

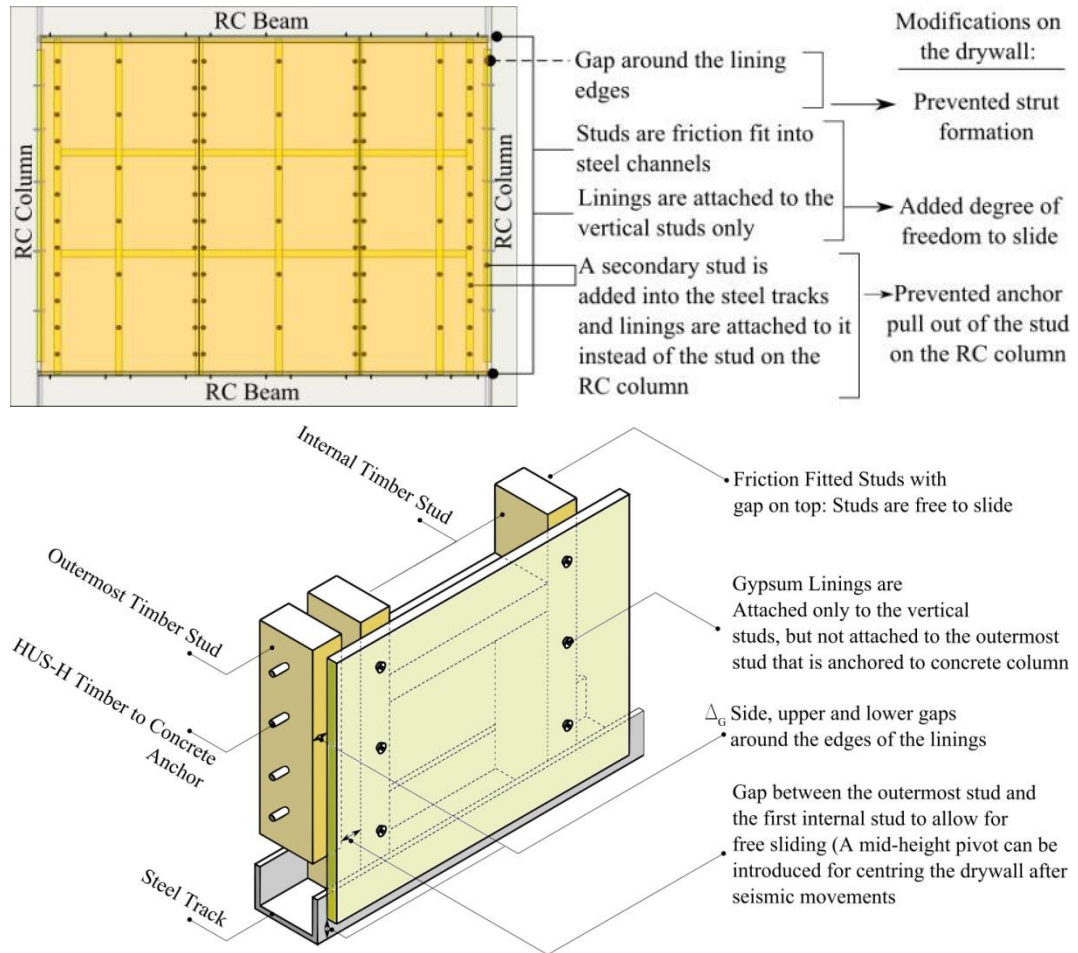


**Figure 6.20.** For low damage timber framed drywall; Modifications to the as built timber framed drywall to achieve a low damage solution for timber framed drywall (Modifications were made considering also the behaviour of the low damage steel framed drywall MIF1-STFD)

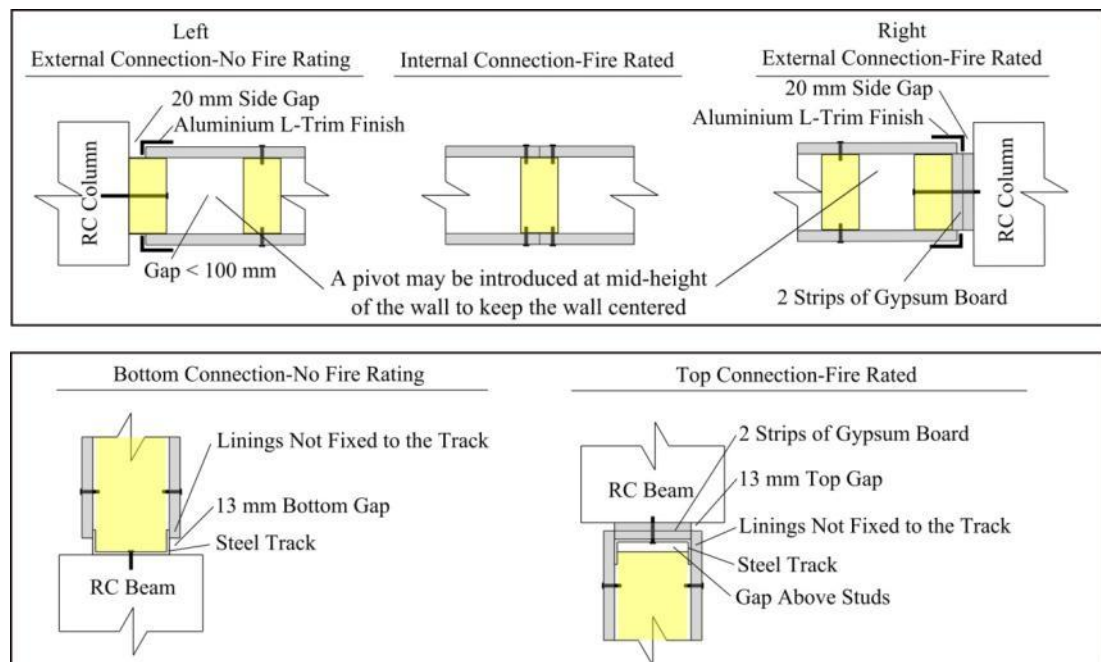


**Figure 6.21.** Connection details used in low damage timber framed drywall specimen MIF2-TBFD

For the construction, first, the fire rated top and non-fire rated bottom steel tracks were installed on the RC beams (Step 1 in Figure 6.22). In the second step, the timber studs were friction fitted between the steel tracks, horizontal elements were pre-installed on the studs for ease of construction (Step 2 in Figure 6.22). Lastly, the linings, which are cut to size considering the gaps at the edges, were installed on the formed timber framing system (Step 3 in Figure 6.22). Sample photos of the used elements and the connection types are shown in Figure 6.23 as close up views.

Construction video: <http://youtu.be/NlxsYaKRdvw>

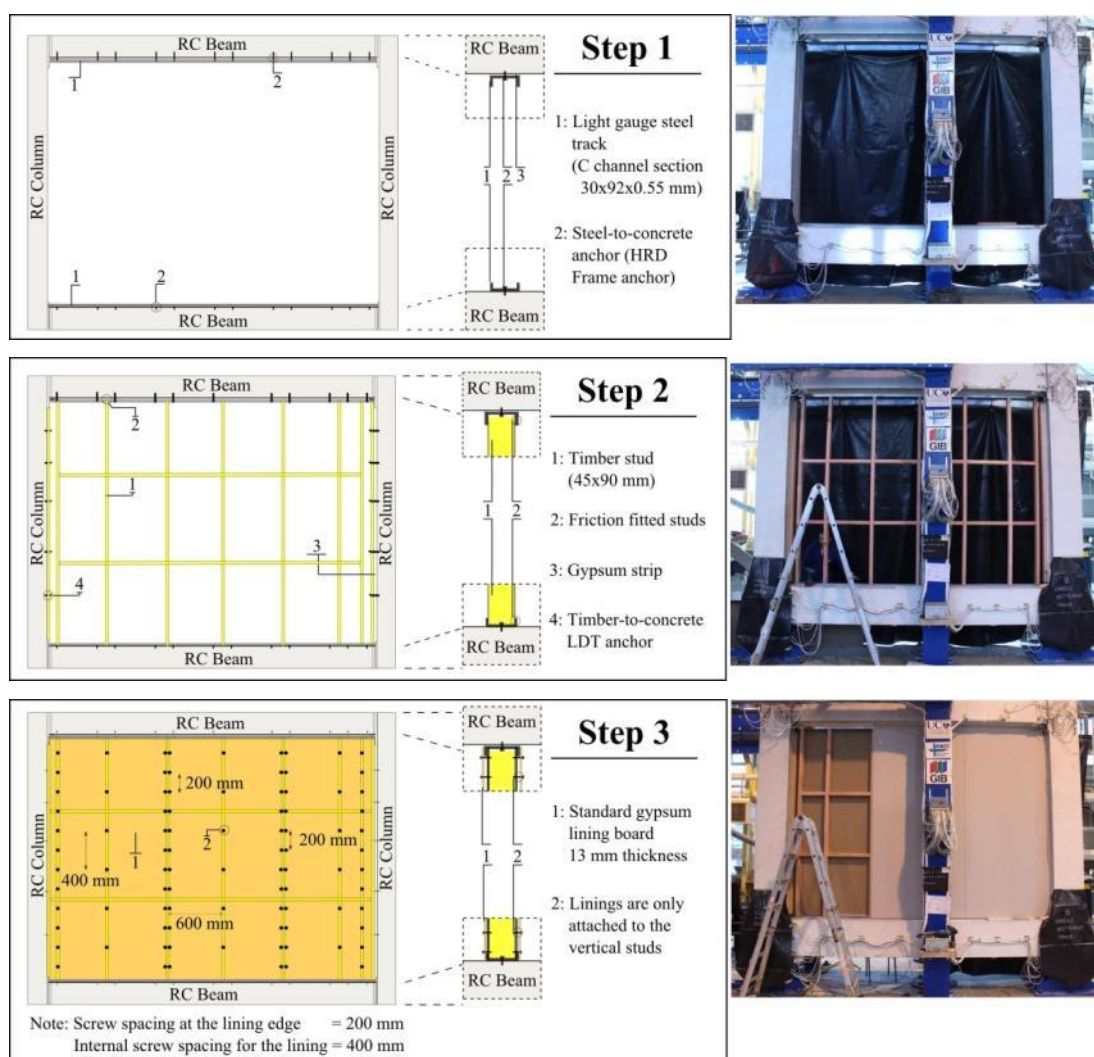


**Figure 6.22.** Construction sequence of the low damage timber framed drywall specimen MIF2-TBFD (for details refer to Figure 6.21)



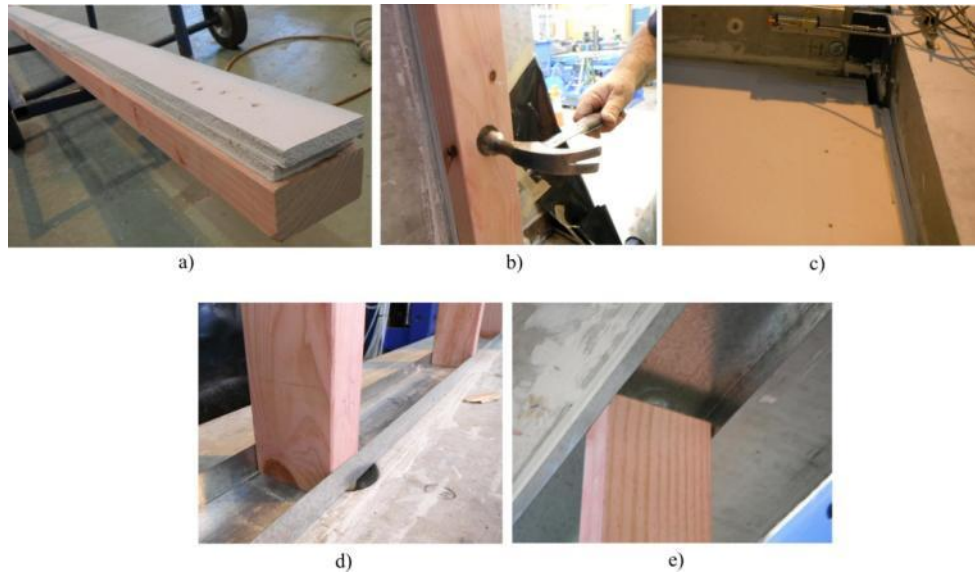


**Figure 6.23.** Low damage timber framed drywall specimen MIF2-TBFD: a-b) Fire rated external stud and installation, c) Gypsum lining is not fastened to the fire rated stud on RC column, d-e) Friction fitted studs into the steel channels

### 6.2.2 Finishing of the Drywall

The finishing of the linings was carried out by paper tape application on the lining interfaces, the same as the finishing of as built steel and timber framed drywall specimens FIF1-STFD and FIF2-TBFD. Similar to the low damage steel framed drywall specimen MIF1-STFD, at the exterior edges of the linings (Linings A and C), aluminium L-trims were applied to cover the rough edges caused by cutting the linings. The overall scheme of the finishing applied is summarized in Figure 6.24.

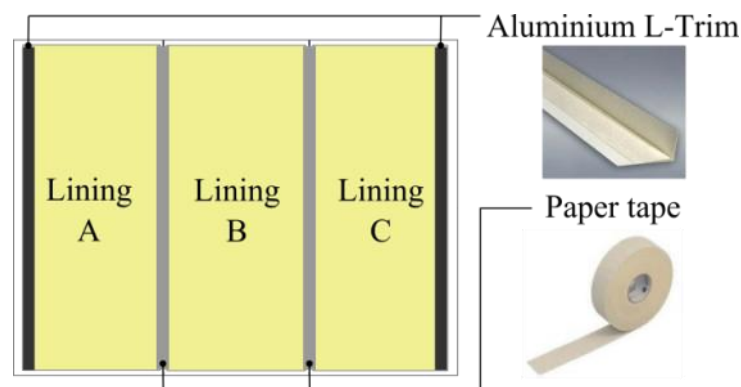


**Figure 6.24.** Finishing scheme of the low damage timber framed drywall specimen MIF2-TBFD

### 6.2.3 Instrumentation

The same instrumentation scheme given in 6.1.3 was used for this specimen as well. The only behavioural difference expected in this specimen was the potentiometer readings taken at the lining-to-lining interfaces. In the low damage steel framed drywall specimen MIF1-STFD, these connections had 5mm gaps among the linings. However, in the low damage timber framed drywall specimen MIF2-TBFD, all the required floor gap was provided at the edges of the linings with a completely flushed drywall surface at the internal lining connections. Therefore, the expected deformations at these locations were very minor compared to their steel framed counterpart.

### 6.2.4 Test Results

#### 6.2.4.1 Damage Observations

In this specimen, the low damage detailing used in the previous test was improved. The gaps placed at the sides of the gypsum linings closed, as per design, at around 1.5% drift level. No damage was observed until 2.0% drift level. Starting at 2.0% drift level, the only damage occurred at L-trim plaster finish together with damage initiation at a few gypsum lining fasteners. As a result of the adopted detailing, there was no pull-out of the side studs (Figure 6.26) and the system remained as it was built with no loss in strength and negligibly low damage. Overall, the drywall remained intact and serviceable. The damage map of the specimen is shown in Figure 6.25 and the damage photos taken at the end of the test are shown in Figure 6.26.

Video of the test: <http://youtu.be/KXYVw5iyzho>

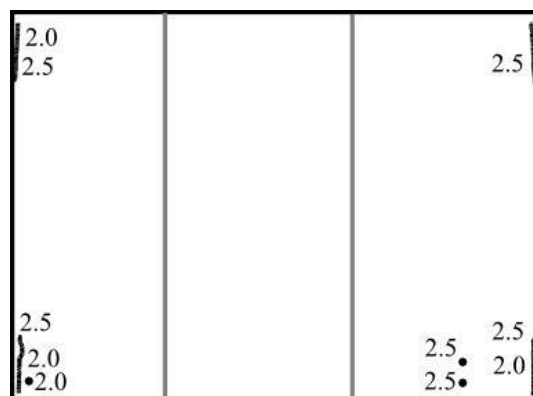


**Figure 6.25.** Damage map at the end of the test for low damage timber framed drywall specimen MIF2-TBFD



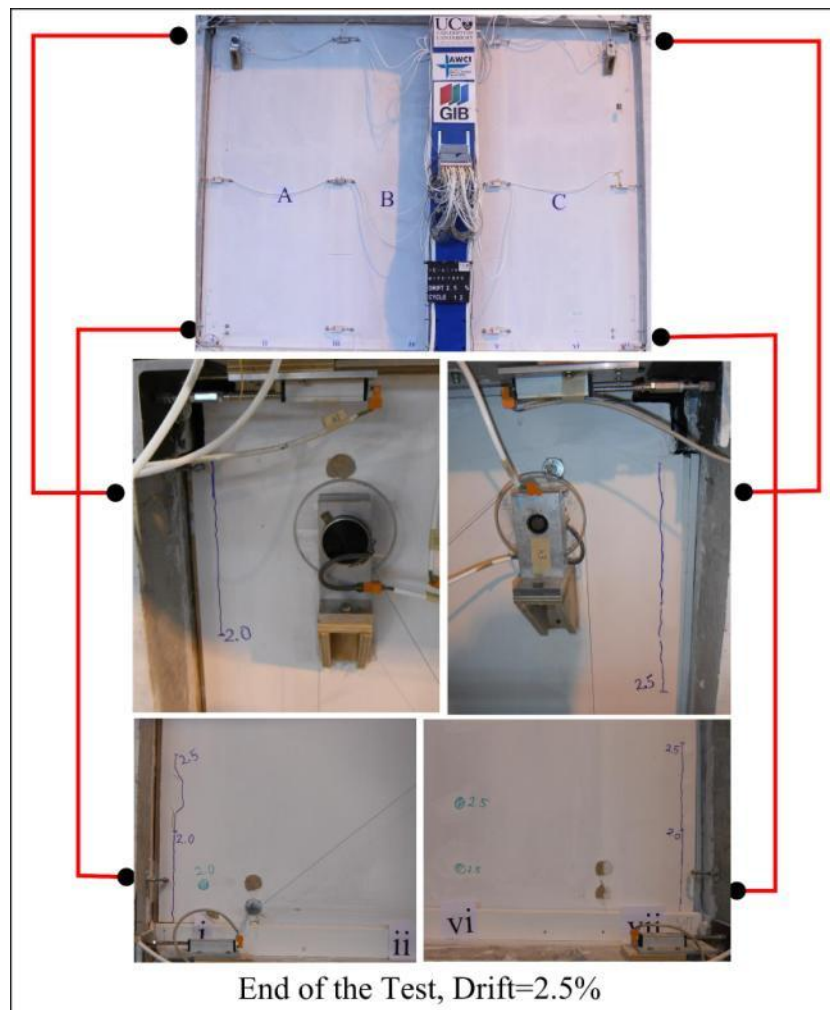


**Figure 6.26.** Damage photos at the end of the test (MIF2-TBFD)

#### 6.2.4.2 Behaviour Explanation

The experiment also confirmed the mechanism of the drywall system. The drywall slid in the provided steel channels at the infill panel zone. Instead of fixing the linings to the end studs on the RC columns, they were fixed to the added alternative end studs placed between the top and bottom steel channels close to RC columns. Therefore, the anchor pull out observed in MIF1-STFD did not reoccur. An additional improvement (optional) could be the addition of pivot points at mid-height of the wall between the alternative end stud and the end stud on the RC column, which would introduce some level of self centring to the drywall system. The behaviour mechanism of the low damage timber framed drywall is summarized in Figure 6.27. The hysteresis curve and the bare frame measurements are shown in Figure 6.28.

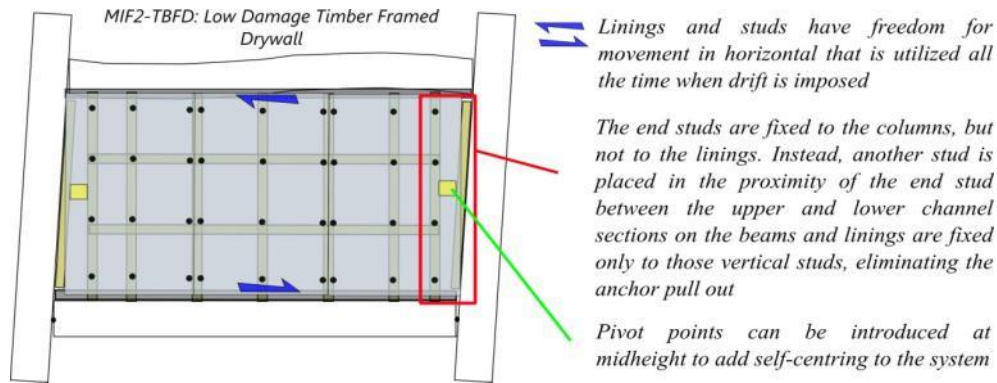


**Figure 6.27.** Behaviour mechanism for the low damage timber framed drywall specimen MIF2-TBFD

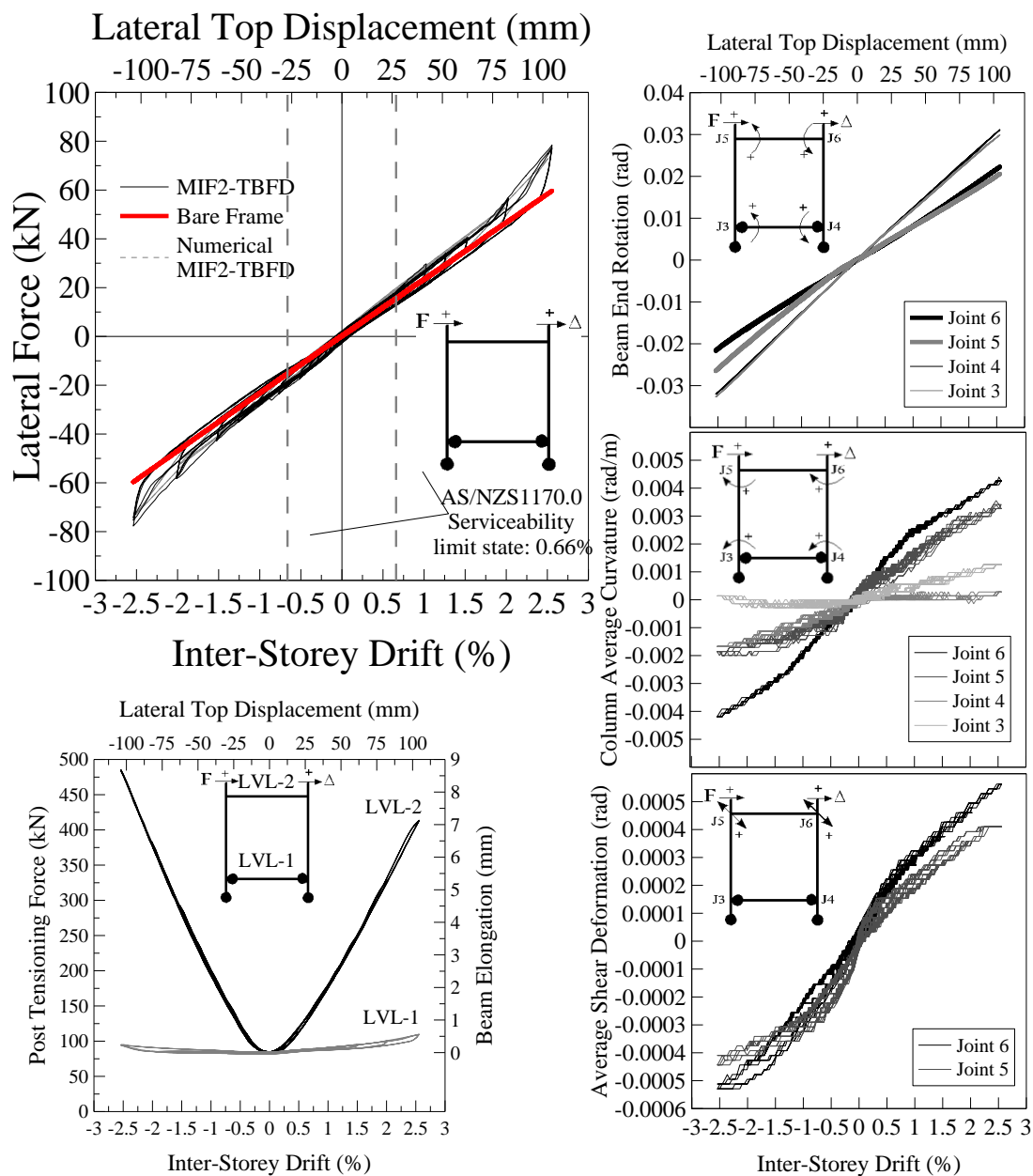


**Figure 6.28.** Test results for the low damage timber framed drywall specimen MIF2-TBFD

Potentiometers h5, h8 and h13, h16 show the displacement of the provided external gaps at lower and upper levels of the drywall (Figure 6.29). Inspecting the potentiometers h6, h7 and h14, h15 (lower and upper level at interior lining interfaces), it can be seen that no displacement was imposed on these lining joints until the end of the test (Figure 6.30). The only displacement demand imposed on the infill panel zone occurred at the external gaps (Figure 6.29). Moreover, the potentiometer readings taken at the mid height of the exterior gaps confirmed the sliding action of the whole drywall without forcing the internal lining joints (Figure 6.31). The maximum displacement that could be measured was  $\pm 15$  mm due to the capacity of the potentiometers and the provided gaps were closed during the test at about 1.5% drift level (Figure 6.29).

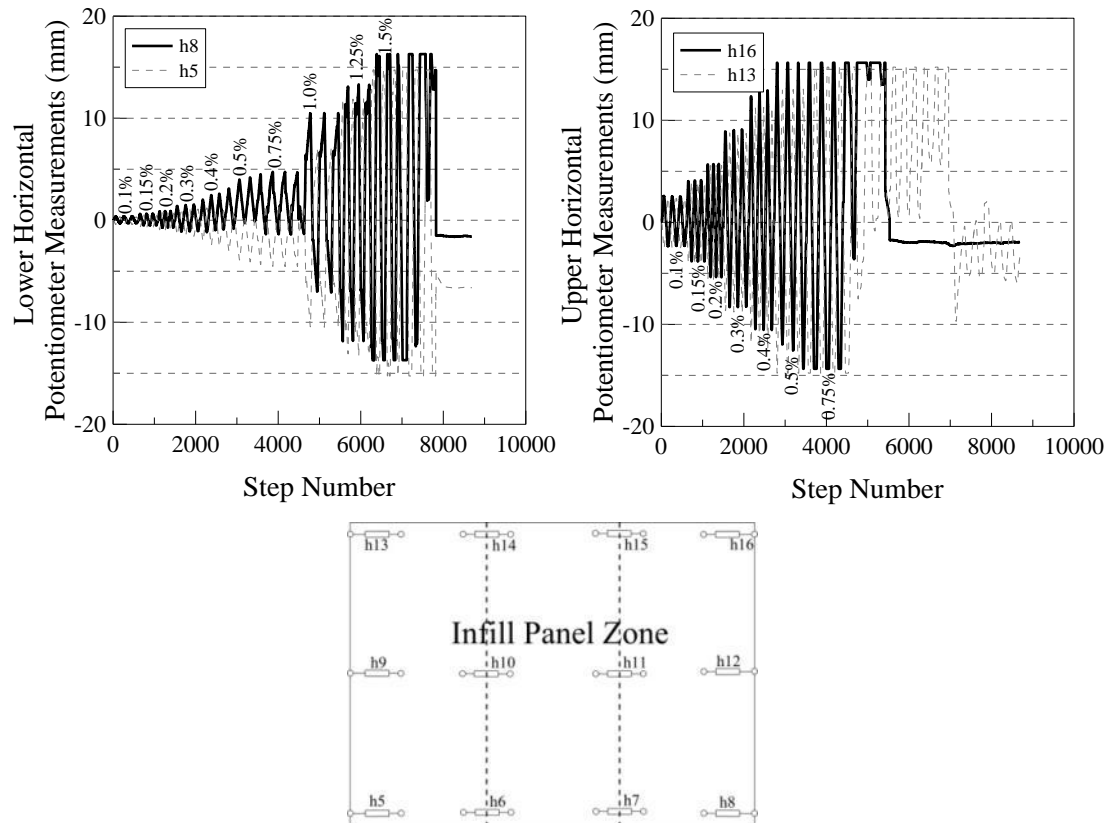


**Figure 6.29.** Lower and upper potentiometer readings at the external gaps and the locations of the potentiometers (MIF2-TBFD)

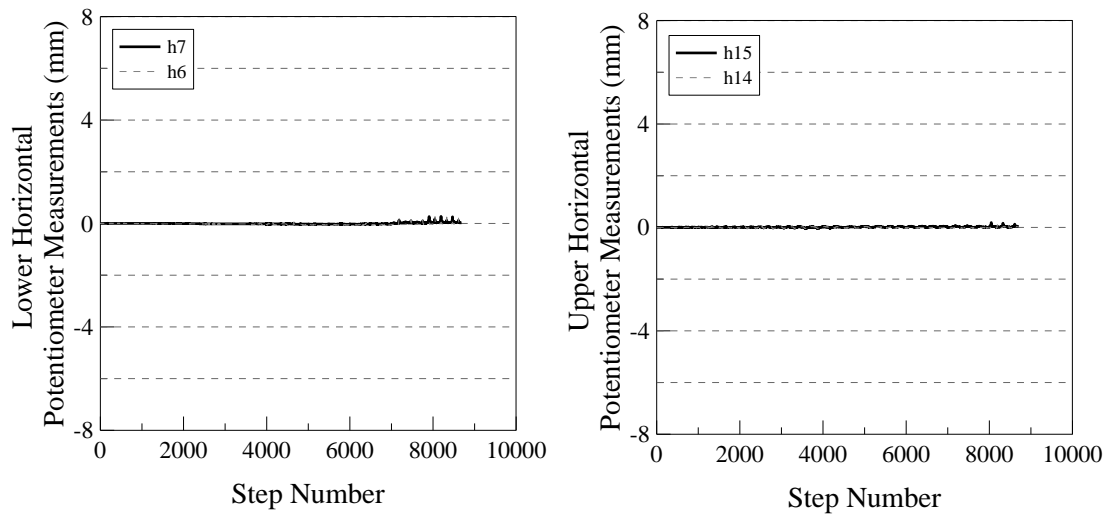


**Figure 6.30.** Lower and upper potentiometer readings at the internal lining joints (MIF2-TBFD, for potentiometer locations, refer to Figure 6.29)

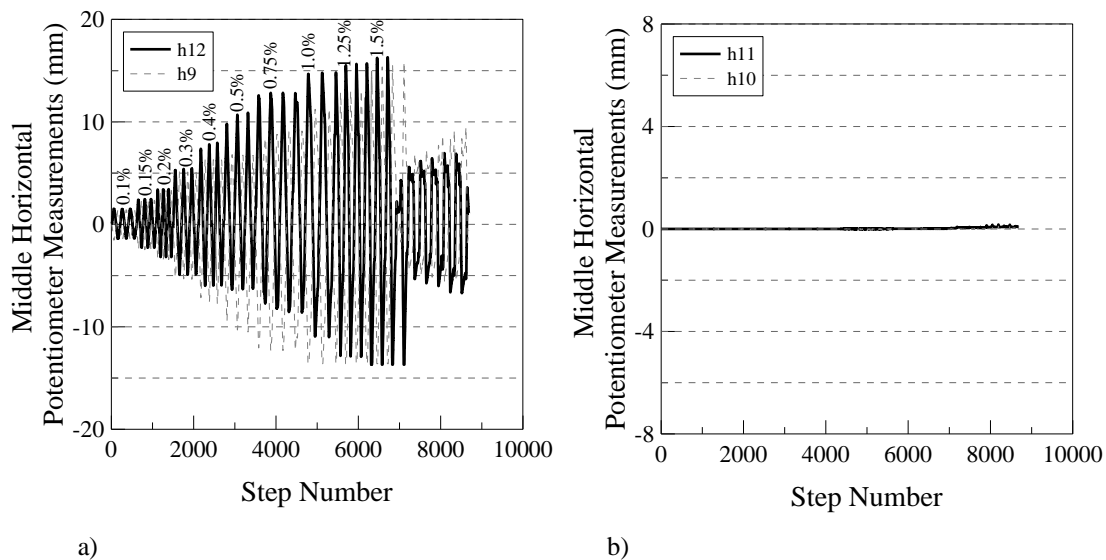


**Figure 6.31.** Potentiometer measurements taken at the mid height of the wall for the low damage timber framed drywall specimen MIF2-TBFD: a) Exterior gaps, b) Interior gaps (For locations refer to Figure 6.29)

In order to obtain the hysteresis behaviour of the infill itself, the bare frame hysteresis was subtracted from the total hysteresis, as shown in Figure 6.32a. Then the result was projected into the diagonal direction for use in modelling applications, shown in Figure 6.32b. It should be noted that these results were the same as the low damage steel framed drywall specimen MIF1-STFD. The contribution of infill panel zone content was minimized due to the further reduced interaction with the structural system. Damage to the non-structural wall was prevented except for the very minor L-trim plaster damage that occurred at 2.0% drift level.

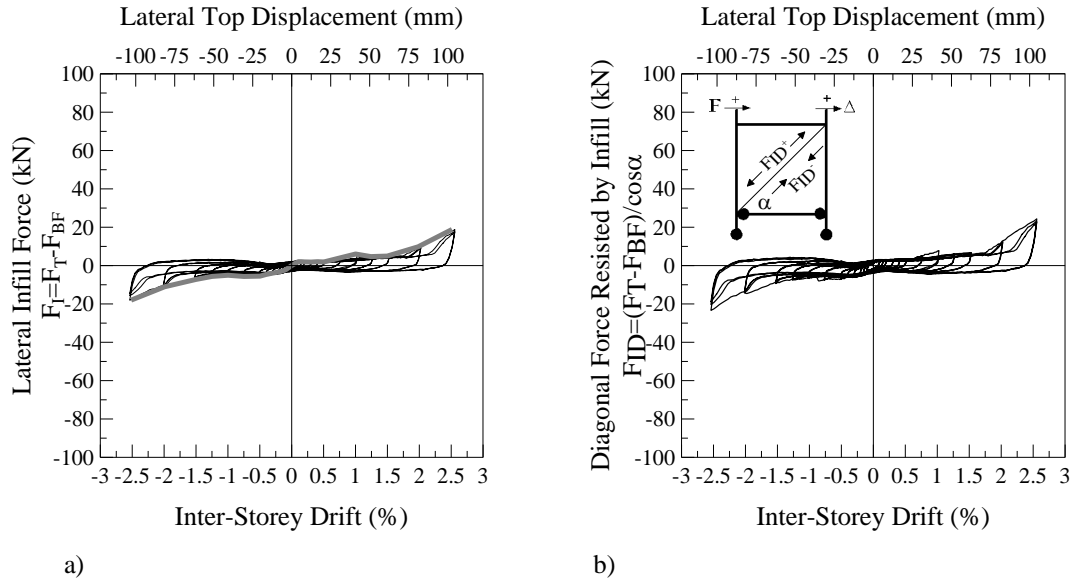
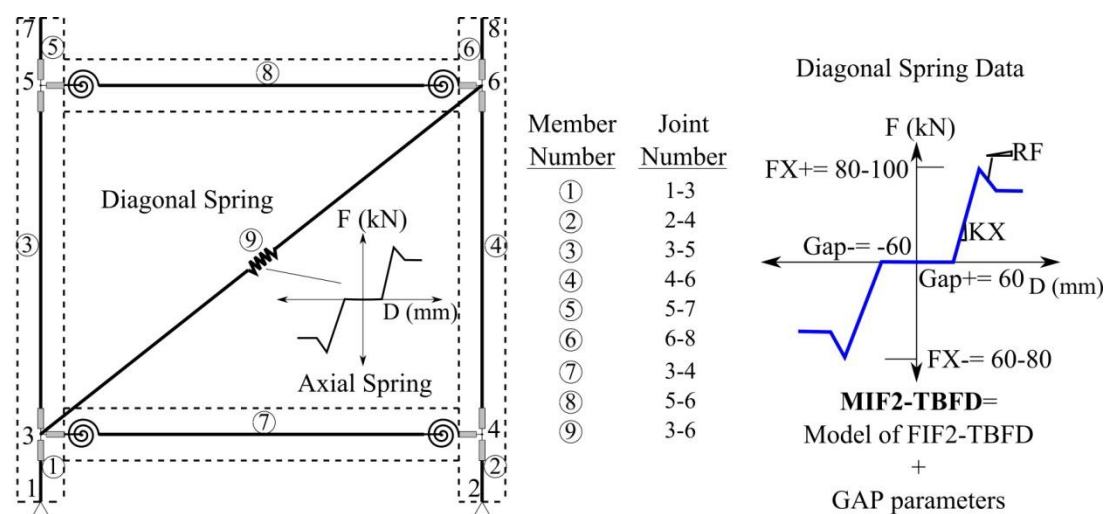


**Figure 6.32.** Low damage timber framed drywall MIF2-TBFD: a) Lateral force exerted on the infill panel zone obtained by subtracting the bare frame from the total, b) Diagonal force exerted on the infill panel, projection of a) in diagonal dir. (MIF2-TBFD)

### 6.2.5 Numerical Model Calibration

Similar to 6.1.5, the existing numerical model for as built timber framed drywall specimen FIF2-TBFD was modified by introducing the gap feature of the Wayne Stewart degrading stiffness model (Gap+, Gap- in Figure 6.33). The provided total horizontal gap of  $40 \pm 5$  mm was projected into the diagonal direction with the cosine of the angle between the diagonal and the horizontal, which is  $(40 \pm 5) / \cos(41.42^\circ) \approx 60$  mm. The model fit the experimental data without needing to calibrate further as it was the case for the low damage steel framed drywall specimen MIF1-STFD. The comparison of the numerical and the experimental hysteresis is shown in Figure 6.34.



Wayne Stewart Degrading Stiffness model with Gap data for Ruaumoko2D

```

! N MTYPE LABEL
5 SPRING STRUT

! 12A BASIC SECTION PROPERTIES
! ITYPE IHYST ILOS IDAMG KX KY GJ WGT RF RT PSX PSY PSZ THETA ITRUSS IOP
1 9 0 0 15000 0 0 0 -0.09 0 0 0 0 0 0 0 0

! 12C YIELD SURFACE
! FX+ FX- FY+ FY- MZ+ MZ-
100 -70 0 0 0 0

! FU FI PTRI PUNL GAP+ GAP- BETA ALPHA LOOP
100 0 0 2 0.06 -0.06 1.04 0.2 1

```

Figure 6.33. The numerical model of the low damage timber framed drywall specimen MIF2-TBFD for Ruaumoko 2D

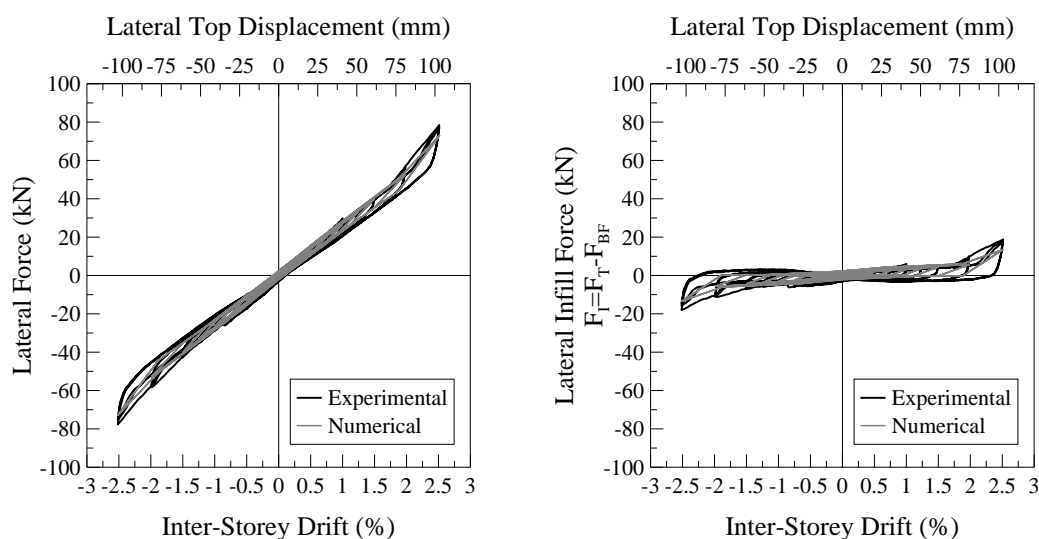
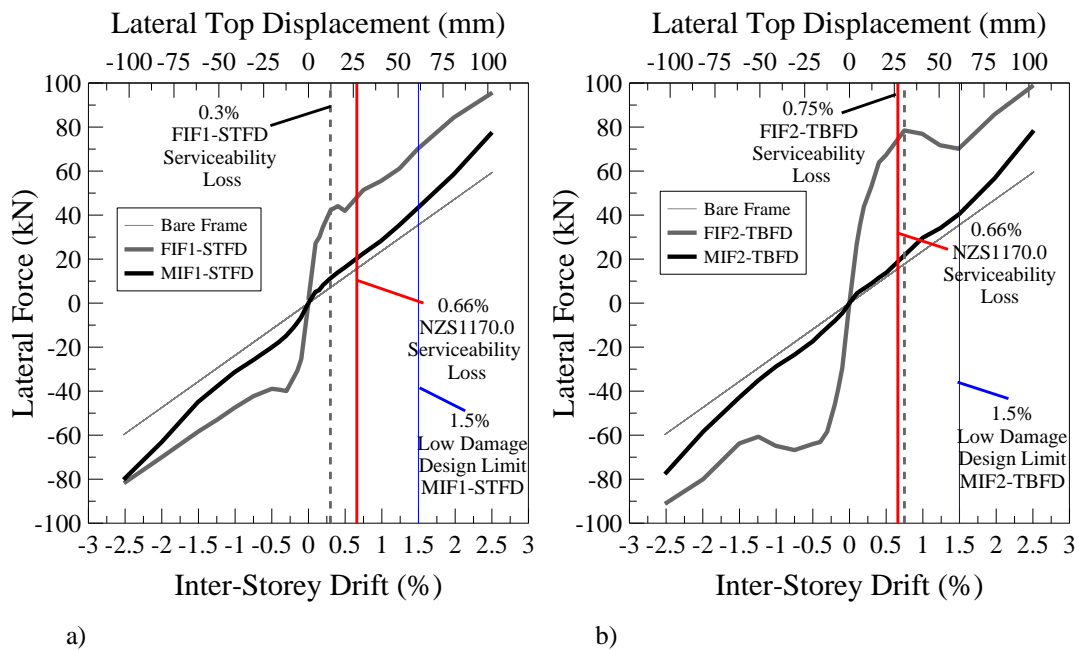


Figure 6.34. The hysteresis behaviour of the numerical model compared to the experimental result for the low damage timber framed drywall specimen MIF2-TBFD

### 6.3 Observations, Energy Dissipation and Effective Stiffness Properties of the Low Damage Steel and Timber Framed Drywalls

#### 6.3.1 Observations and Comparisons

The experiments showed that the as built drywall solutions can easily be modified and turned into low damage solutions. In the as built specimens, the serviceability loss occurred at 0.3% drift level for the steel framed and 0.75% drift level for the timber framed drywalls. The New Zealand code NZS1170.0 [55] estimated a serviceability loss drift level of about 0.66% for drywalls in general. On the other hand, the serviceability loss did not occur at all in low damage solutions, remaining operational even at high drift levels (2.5%).



**Figure 6.35.** Comparison of the as built and low damage drywall specimen global force-displacement envelopes: a) As built steel framed drywall specimen FIF1-STFD and low damage steel framed drywall specimen MIF1-STFD, b) As built timber framed drywall specimen FIF2-TBFD and low damage timber framed drywall specimen MIF2-TBFD

When the results were compared to the as built specimens, it was seen that both of the low damage solutions behaved similarly to the bare frame until 1.5% design drift limit of the low damage solutions (Figure 6.35). From this point onwards, due to the closing of the gaps, the low damage solutions started to take force.

### 6.3.2 Energy Dissipation and Stiffness Degradation Properties

The equivalent viscous damping values ( $\xi_{eq}$ ) of the tested specimens was calculated as mentioned previously. The resulting averaged energy dissipation ( $E_D$ ) and equivalent viscous damping values ( $\xi_{eq}$ ) are shown in Figure 6.36. When compared to the as built specimens, the dissipated energy was much less for the low damage solutions due to the reduced interaction of the structural and the non-structural system. The reduced interaction was also observed when the effective stiffness curves were compared. In Figure 6.37, the low damage solutions show very close effective stiffness values to the bare frame.

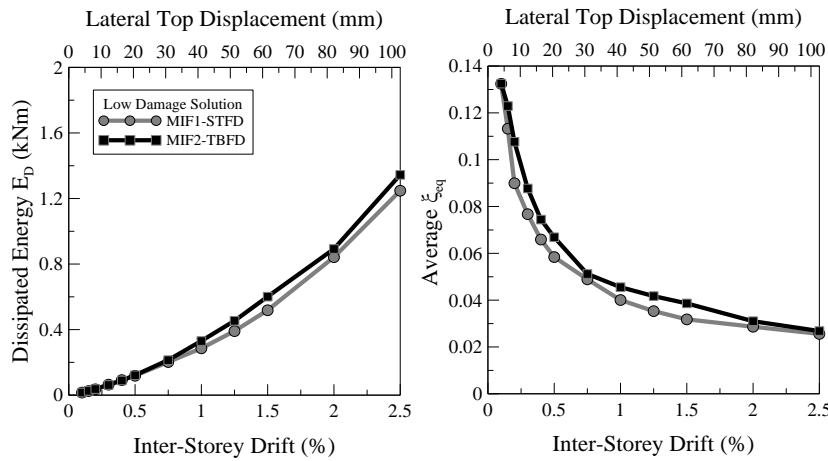


**Figure 6.36.** Average dissipated energy ( $E_D$ ) and average equivalent viscous damping ( $\xi_{eq}$ ) with respect to inter-storey drift for low damage steel MIF1-STFD specimen and timber framed drywall MIF2-TBFD specimen

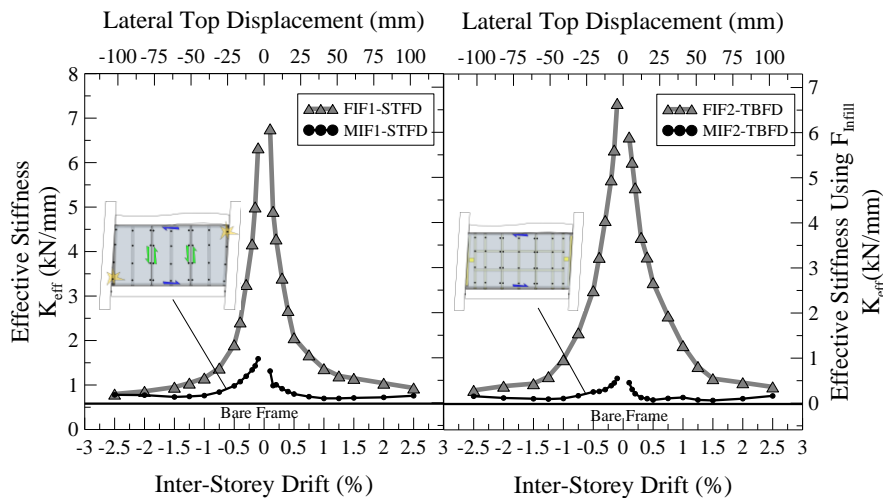


**Figure 6.37.** Stiffness degradation comparisons of as built and low damage solutions for steel framed (FIF1-STFD, MIF1-STFD) and timber framed drywalls (FIF2-TBFD, MIF2-TBFD), plotted using total lateral force (left axis) and the lateral force exerted by the infill wall (right axis)



## 6.4 Joint Details of the Generalized Low Damage Non-Structural Drywall

### Solution

Considering the tested specimens, the following details can be summarized in order to design a low damage steel or timber framed drywall (Figure 6.38). The necessary exterior gaps for the edge of the linings can be calculated by:

$$\Delta_G = D \cdot \frac{h_c}{2} \cdot \frac{1}{100}$$

Where  $D$  : Design inter-storey drift level in % after which damage is acceptable

$h_c$  : Clear height of the non-structural wall

The detailing can be done as shown in Figure 6.38. In this figure, the first two figures depict a scenario where the non-structural drywall is bounded by either structural members (RC columns, beams, or floor slabs). The third Figure depicts a plan view scenario where the non-structural drywall is bounded by another drywall.

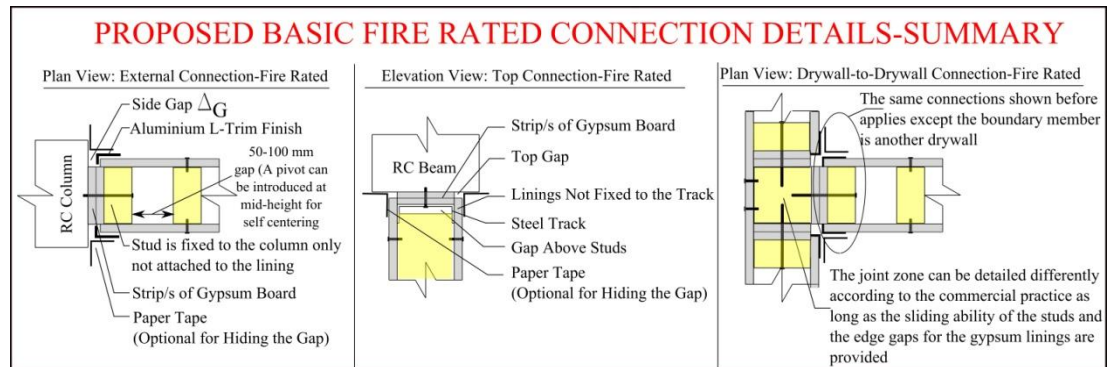


**Figure 6.38.** Proposed low damage non-structural drywall connection details

## 6.5 Conclusions

It has been shown that low damage solutions for steel and timber framed non-structural drywalls can easily be achieved. The developed low damage solutions were designed to eliminate the interaction until 1.5% drift level, which was the side gap closing drift for the gypsum linings. However, specimens remained un-damaged until 2.0% drift

level. From 2.0% onwards, the only damage observed was very minor cracking at aluminium L-trim finishes of the linings.

These solutions were achieved with no extra cost, material or labour. They can easily be adopted in real life applications by the contractors. The design can simply be carried out by the engineer.

The low damage drywall computer models can directly be modified from the as built models just with the introduction of the gap feature of the Wayne Stewart degrading stiffness hysteresis rule.

In most real life applications of low damage solutions, modelling the low damage drywall system (light) would not be required since their interaction with the structural system is negligibly small. Therefore, it is relatively safe to conclude that the low damage solutions isolated the non-structural wall from the structural system effectively and their effect on the global response can safely be neglected in order to simplify the design and/or analysis of buildings.

Due to the effective isolation of the non-structural walls, both low damage steel and timber framed drywalls showed the same force displacement response, which was very close to the response of the bare frame (Figure 6.35). Therefore, the low damage systems yielded the same behaviour independent of the underlying drywall framing.

## **6.6 References**

- [55] AS/NZS1170.0, "Part 0: General Principles," in Structural Design Actions vol. 1170, ed: Australian/New Zealand Standard, 2002.

# CHAPTER 7

## AS BUILT UNREINFORCED CLAY BRICK INFILL WALL TEST

*Anybody who has been seriously engaged in scientific work of any kind realizes that over the entrance to the gates of the temple of science are written the words: 'Ye must have faith.'*

*Max Planck*



## 7 AS BUILT UNREINFORCED CLAY BRICK INFILL WALL TEST

### 7.1 As Built Unreinforced Clay Brick Infill Wall: FIF3-UCBI

#### 7.1.1 Construction

Unreinforced clay brick infill walls have been obsolete for a long time as non-structural infill walls for buildings in New Zealand. Nevertheless, it is still a very common practice around the world (i.e. Mediterranean countries, South America, India etc.). Most of the buildings with unreinforced clay brick infill walls in New Zealand are of pre 60s. St. Elmo Courts was the oldest RC building in Christchurch (1930s), but was demolished due to the extensive damage suffered after 22 February 2011 earthquake in Christchurch (Figure 7.1). The type of unreinforced clay brick infill wall used in that specific building was cavity wall, which is a double skinned wall. The same wall type was also observed in other structures around the Christchurch Central Business District (CBD) during the building assessments. As a result of lack of current practice, these old examples were used for the construction of the test specimen. For the construction of the specimen, the specifications contained in the unreinforced masonry wall construction standard NZS 4210 (“Masonry Construction in Materials and Workmanship”) was followed and complied [57].

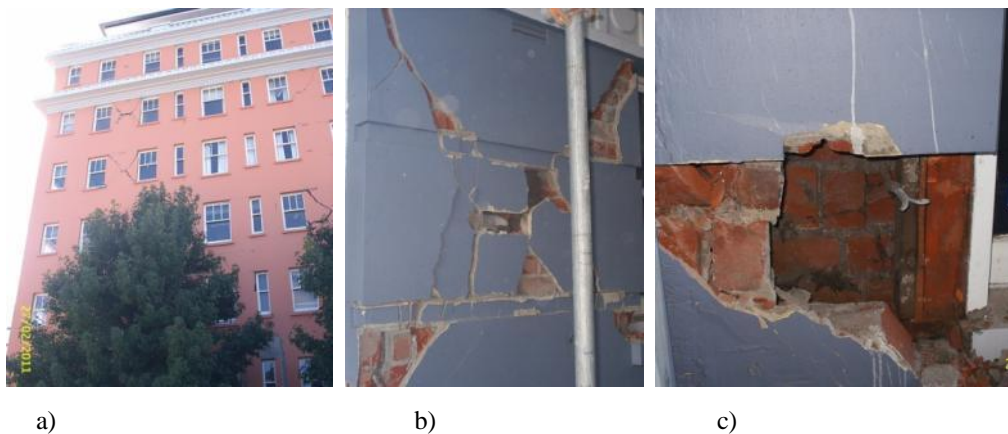


**Figure 7.1.** a) Damage photos from St. Elmo Courts building after 22 February 2011 Christchurch earthquake, b) Diagonal cracking at ground level, c) The revealed wall tie used in the unreinforced clay brick cavity wall (double skinned wall)

In the construction of the infill wall, standard clay bricks of 70 mm width, 75 mm height and 220 mm length were used. This was the same clay brick type used in St. Elmo Courts as well as for the construction of the masonry veneers in most of the residential houses in New Zealand (Figure 7.2).



**Figure 7.2.** Used clay brick type (70×75×220 mm), Portland cement and fine sand

The binding mortar was composed of Portland cement and fine sand mixed 1 to 4 weight ratios accordingly (Figure 7.2). The water content was arranged according to the workability of the mix by the contractor. In the construction of the infill wall, no specification was given to the contractor with the intent to respect the real life construction practice for brick work as much as possible.

The bricks were laid from the lower corners of the infill panel zone to meet at the mid-span of the RC beam, i.e. four courses at a time. Steel ties were placed between the two skins of the wall at every fourth course of clay bricks laid in vertical. The steel ties were placed 600 mm apart from each other horizontally. The average thickness of the mortar layers was about 10 mm. Including the 10 mm cavity in between the two skins, the total thickness of the infill wall was 150 mm (Figure 7.3).

Construction video: <http://youtu.be/4xRWa77iZfE>



**Figure 7.3.** The construction of the double skinned unreinforced clay brick infill wall, as built unreinforced clay brick infill wall FIF3-UCBI

### 7.1.2 Finishing of the Wall

For finishing, only a thin coat of white paint was applied on the wall for ease of crack visibility. As in overseas practice, a mortar based plaster layer could be made both inside and outside of the wall. Since this could affect the results of the tests, this option was not chosen. Moreover, in New Zealand, these types of walls were usually built without any external plaster in the past due to its architectural appeal. The completed state of the infill wall is shown in Figure 7.4.



**Figure 7.4.** Completed unreinforced clay brick infill wall before the white paint was applied FIF3-UCBI

7.1.3 Instrumentation

The specimen was instrumented to observe the deformations caused by the cracking at mortar layers. The cracking pattern of the infill wall at failure cannot exactly be predicted due to the high number of failure planes that can occur along the mortar joints. Therefore, the potentiometers were installed at locations where there is a high likelihood of cracking. Horizontal potentiometers were installed to measure the deformations caused by the vertical cracking and vertical potentiometers were installed to measure the possible deformations that might occur in vertical due to uplift (Figure 7.5). The potentiometers were mostly installed to understand the behaviour of the unreinforced clay brick infill panel so that a low damage solution could be developed.

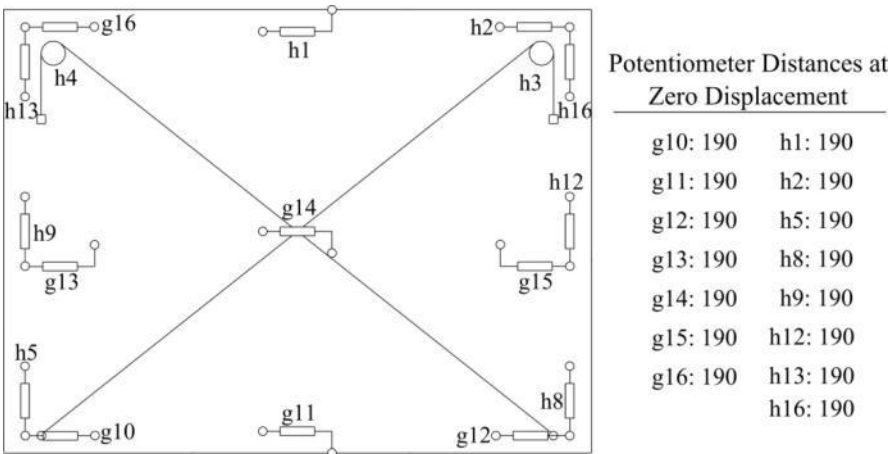


Figure 7.5. Instrumentation of the as built unreinforced clay brick infill wall specimen FIF3-UCBI

7.1.4 Test Results

7.1.4.1 Damage Observations

The same displacement protocol used in the previous tests was applied to the specimen. In the first drift level of 0.1%, boundary cracks occurred between the infill wall and the RC frame. Until 0.2% drift, minor but many vertical cracks formed at vertical mortar joints. In the negative cycle of 0.2% drift (pulling cycle), a diagonal crack formed stretching from the lower left corner to the upper right corner of the infill



wall. The width of the diagonal crack at this level of drift was 0.35-0.8 mm near the lower left corner and 1.5-2.5 mm at the middle of the infill panel zone. In the positive 0.3% drift level (pushing cycle), another diagonal crack formed stretching from lower right corner to upper left corner of the infill wall panel. The width of this crack was 0.4-0.5 mm near the corners of the specimen and 1.5 mm at the middle of the infill panel zone. Then, in the negative cycle of 0.3% drift, additional diagonal cracks formed in parallel to the previous one, stretching from lower left to upper right corner of the infill wall. It was mainly from 0.3% drift level onwards that sliding cracks started to form at different levels of the infill wall. In some cases, these sliding cracks were forming in combination with additional diagonal cracks. However, the formation of the sliding cracks only continued till 1.25% drift level. From 1.25% drift level till 2.5% drift, short but many vertical cracks formed at vertical mortar joints. At 2.0% and 2.5% drift level, the corner crushing occurred at the lower and upper corners accordingly. At 2.5% drift level, the test was finalized.

The progress of damage on the unreinforced clay brick infill wall panel is summarized in the damage map sequence shown in Figure 7.6. In the same Figure, all of the damage progress till the end of the test is combined and showed as end of the test damage map.

Video of the test: <http://youtu.be/804H7uckzgE>

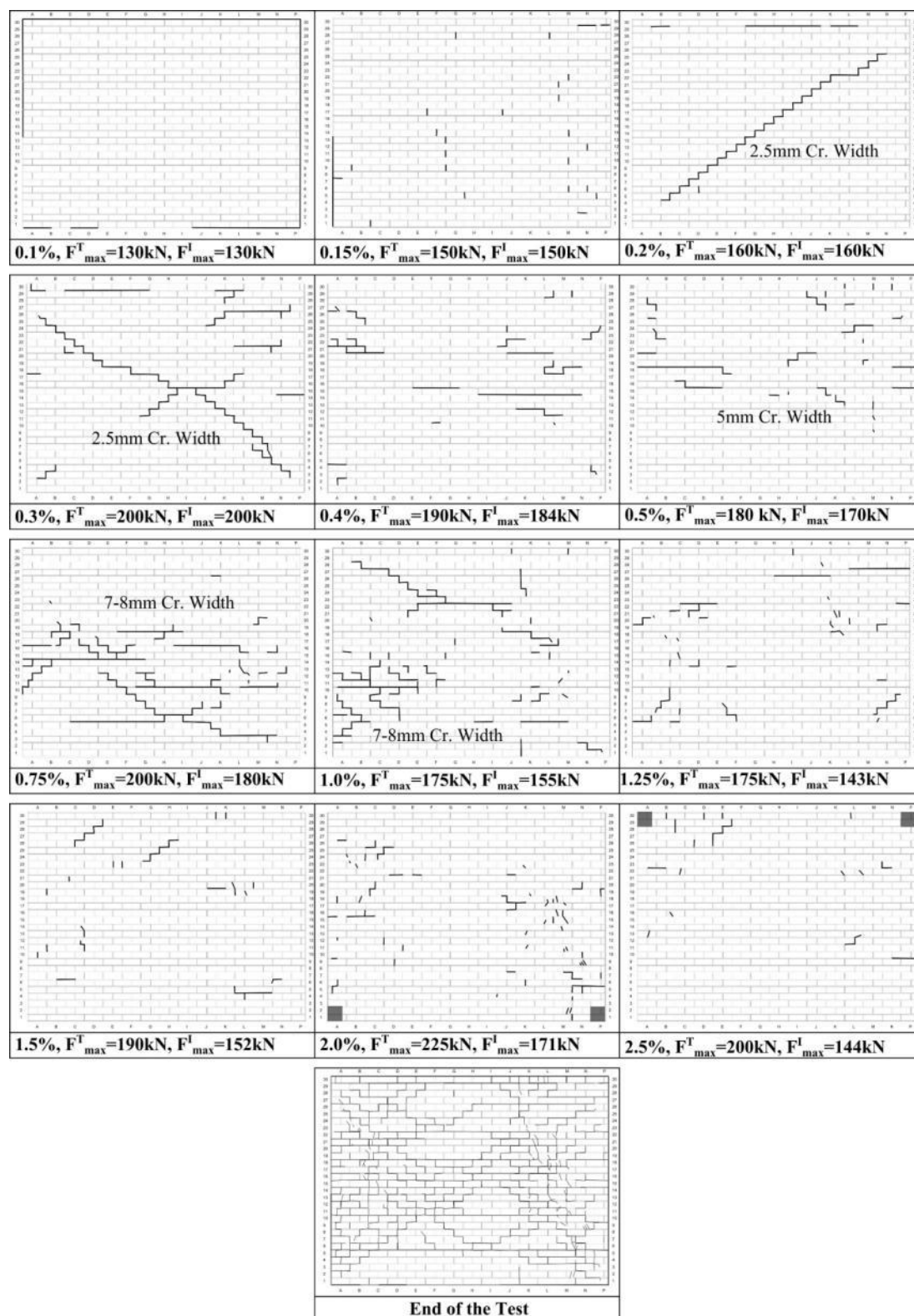


**Figure 7.6.** Damage progress of the as built clay brick infill wall specimen FIF3-UCBI

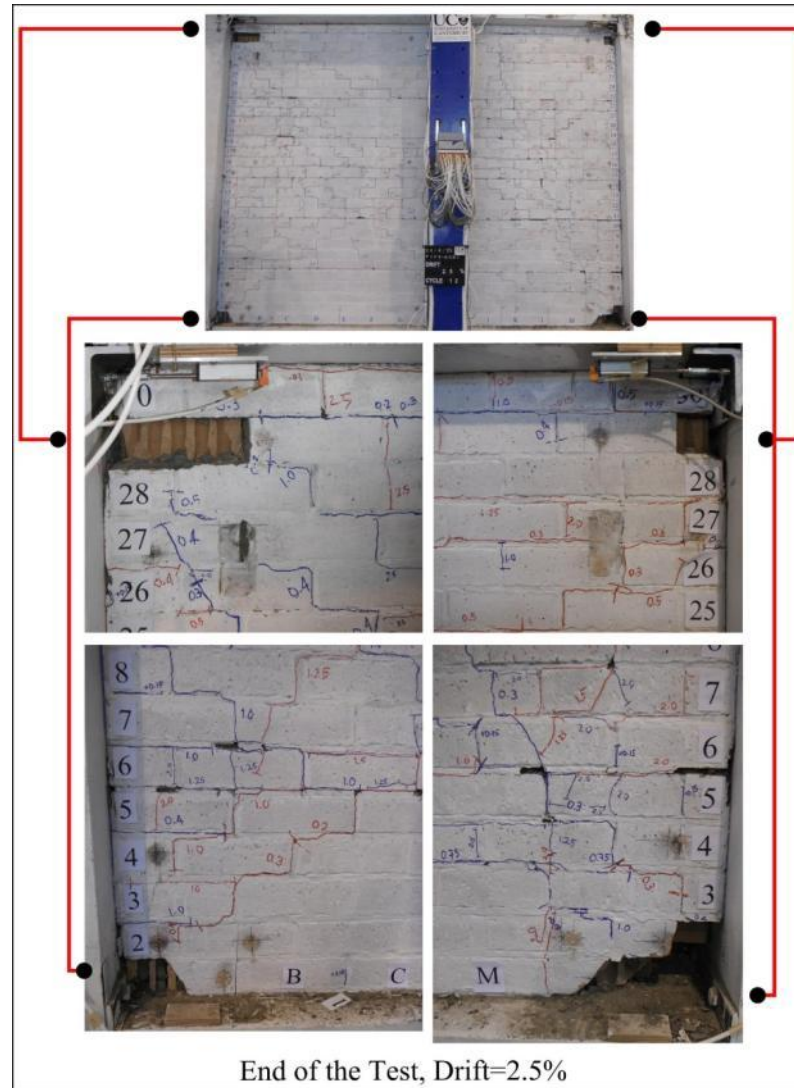


**Figure 7.7.** Damage photos at the end of the as built unreinforced clay brick infill wall test FIF3-UCBI

#### 7.1.4.2 Behaviour Explanation

Considering the observations taken, the infill wall reached its diagonal cracking capacity at 0.2 and 0.3% inter-storey drift levels. It should be noted that there were also horizontal sliding cracks at the upper part of the infill wall that occurred with the diagonal cracks simultaneously (0.2 and 0.3% drifts in Figure 7.6). After the formation of the diagonal cracks, the infill wall basically used up its diagonal load bearing capacity as shown in Figure 7.11b, which was around 250 kN and was also approximately estimated by the equations in 4.4.1 reported by Bertoldi et.al. [49]. From this drift level onwards, the infill wall redistributed the exerted displacements to different horizontal mortar joints, causing more sliding cracks. In some cases, these sliding cracks were forming in combination with diagonal cracks. This was most likely

due to the infill wall's behavioural attempt to find the weakest planes of failure that can be utilized as compression struts to resist the imposed displacements. However, this redistribution via sliding cracks only continued till the end of 1.25% drift. Since the infill wall used all its resistance capacity given by the diagonal and sliding cracks at mortar layers, the only remaining resistance was given by the strut action forming due to extreme displacements (2.0 and 2.5% drift levels). Due to these high displacements, crushing at the clay bricks in the corners of the infill panel zone occurred at 2.0 and 2.5% inter-storey drifts.

The most important outcome in these observations was that unreinforced clay brick infill walls may show a number of failure modes triggered by the increasing displacement demands in a structure. A structure that experiences only 0.3% drift may only exhibit diagonal cracking. However, another structure that experiences 1.0% drift level, the cracking mode may seem like sliding cracks. Similarly, a structure experiencing 2.0% drift may further develop corner crushing. In this particular case, these failures were not exactly different and exclusive failure modes, but rather incremental members of a chain of consecutive failures starting with the weakest one, i.e. diagonal cracking.

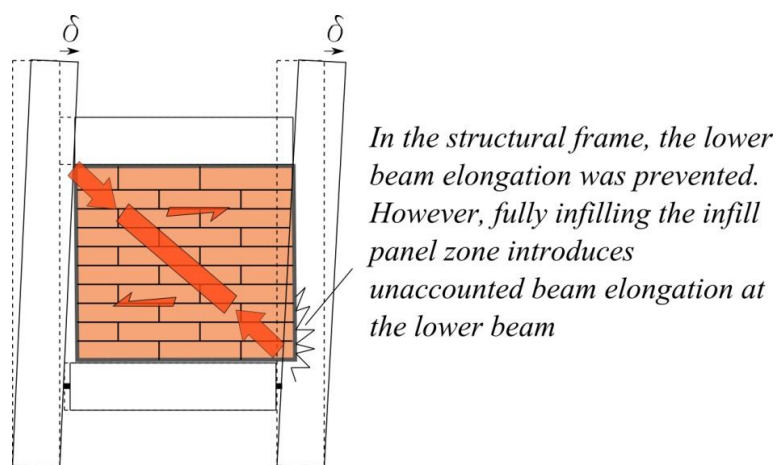


**Figure 7.8.** Damage mechanism for as built unreinforced clay brick infill wall specimen FIF3-UCBI

The specially designed test setup used in this test revealed another important observation. In the bare frame, the beam elongation was prevented at the lower RC beam level. The only beam elongation was given by the upper RC beam in order to enable the re-centring effect of the post tensioning. However, when the infill panel zone was fully infilled, as in this specimen FIF3-UCBI, the infill panel zone introduced

an unaccounted beam elongation at the lower beam level, possibly affecting the upper beam also. This phenomenon is explained in Figure 7.8. Therefore, it was deduced that any low damage solution existing for the structural frames require similar low damage solutions in its non-structural components if stiff (heavy) partitions are adopted. Considering the PRESSS system [46], using fully infilled heavy non-structural walls may affect the post-tensioning values when deformations are imposed on the structure, which may introduce complications in the behaviour of the PRESSS or similar low damage structural solutions. As stated in NZS4230 (2004) [4], this complication should either be taken into consideration during the design, or sufficient separation should be provided between the non-structural wall and the structural frame. The effect of the fully infilled panel zone on the beam elongation and the resulting post tensioning values can be clearly seen in Figure 7.9b. The global hysteresis curve of the specimen is also shown in Figure 7.9a. The exerted lateral and diagonal force by the infill panel zone is shown in Figure 7.11.

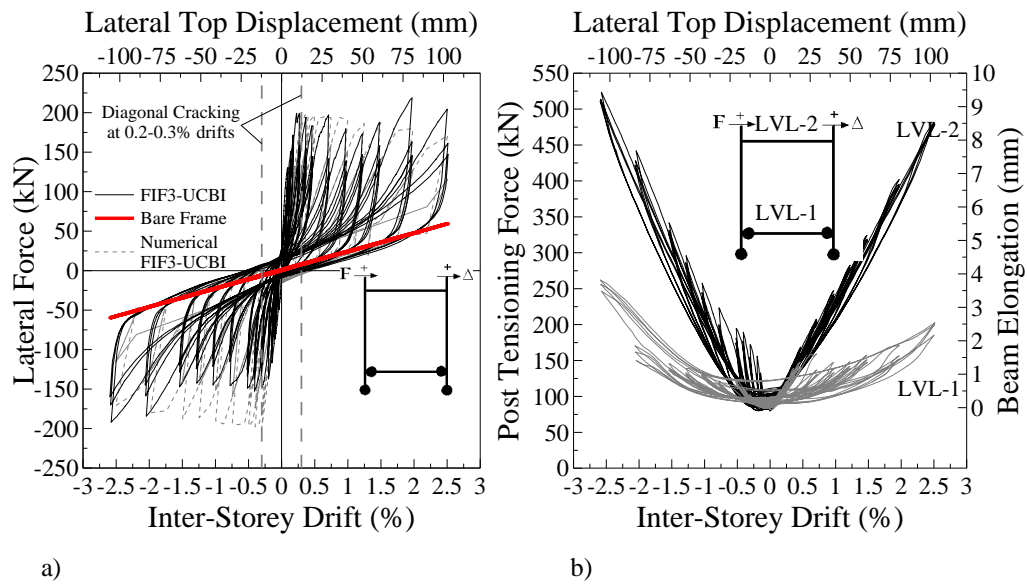


**Figure 7.9.** Test results for as built unreinforced clay brick infill wall specimen FIF3-UCBI: a) Global force vs. inter-storey drift hysteresis, b) Post tensioning and beam elongation vs. inter-storey drift

Considering the potentiometer measurements, except for the potentiometers g11, h1 (Lateral deformation of infill panel relative to the RC frame) and g13, g14, g15 (Sliding at the middle mortar joint), the other measurements were negligibly small. The displacements measured at these potentiometers are reported in Figure 7.10. In this figure, inspecting g13, g14 and g15, it can be clearly seen that the sliding crack



measurements started after 0.2% and 0.3% inter-storey drift levels, which confirmed the damage progress shown in Figure 7.6 and the redistributive behaviour mechanism explained earlier.

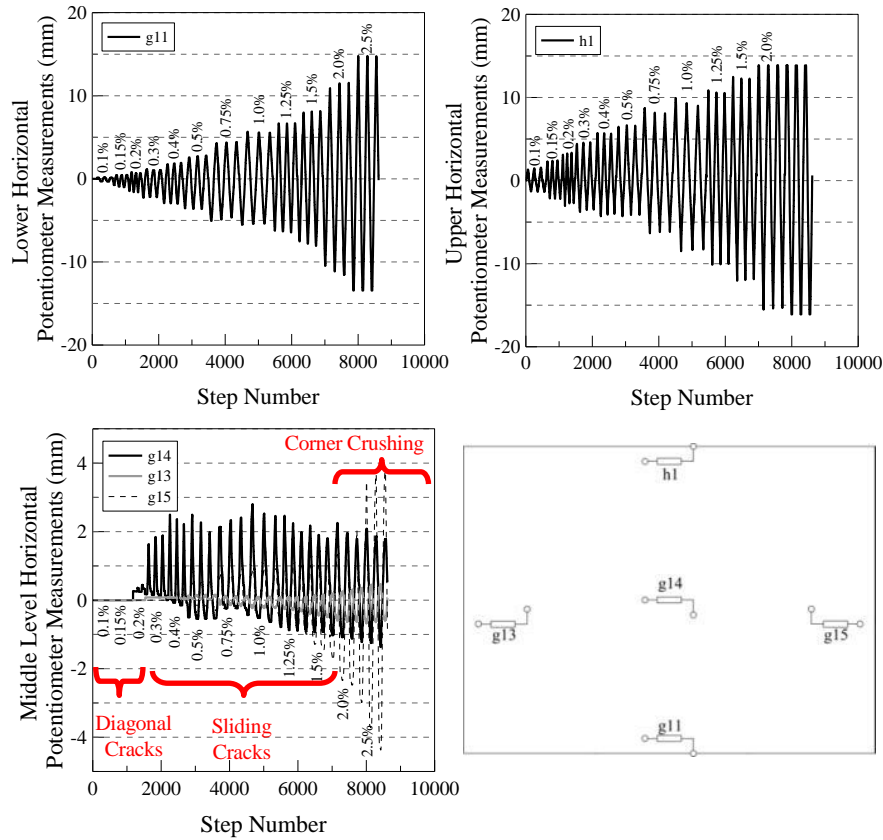


**Figure 7.10.** The potentiometer readings taken during the testing of the as built unreinforced clay brick infill wall specimen FIF3-UCBI (Potentiometer locations has also been given above)

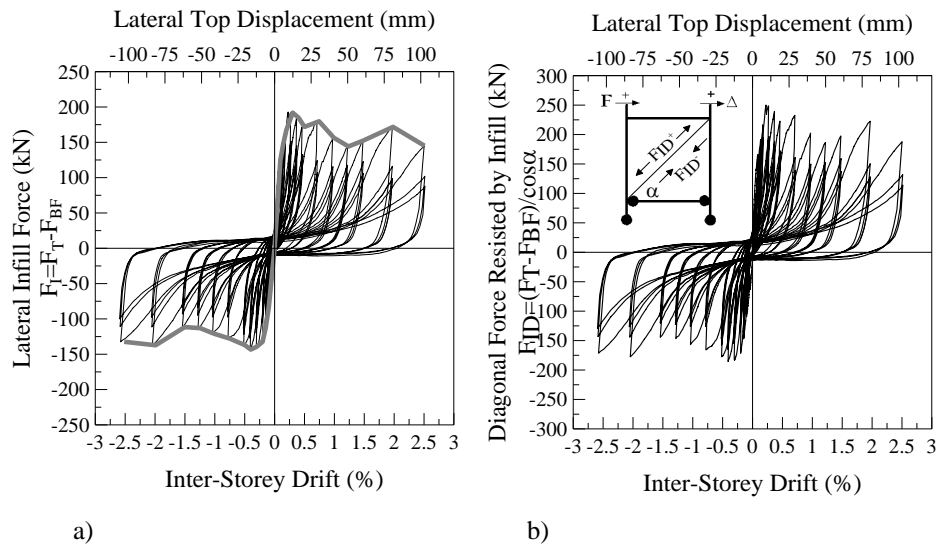


**Figure 7.11.** As built unreinforced clay brick infill wall specimen FIF3-UCBI: a) Lateral force exerted on the infill panel zone obtained by subtracting the bare frame from the total, b) Diagonal force exerted on the infill panel zone, projection of a) in diagonal dir.

### 7.1.5 Numerical Model Calibration

The unreinforced clay brick infill was modelled simply using a single strut, acting both in tension and in compression, as in previous specimens. As mentioned previously, one can model the infill wall as two compression-only (no tension) struts in order to see the effect of infill wall on the columns and beams. For simplicity in calibrating the numerical model with the experimental results, the use of a single strut was adequate and provided a very close result to that of the experiment. Wayne Stewart degrading stiffness showed to simulate the behaviour of the infill panel very closely to the experimental observation. Using the given unique test setup, it was possible to purely extract the behaviour of the clay brick infill wall from the global response (Figure 7.11), which may not be easily achieved in other types of test setups with conventional RC frames due to the frame non-linearity. This property of the test setup eliminated the behaviour contribution given by the structural frame and made it possible to choose the most suitable hysteresis model for the infill panel.

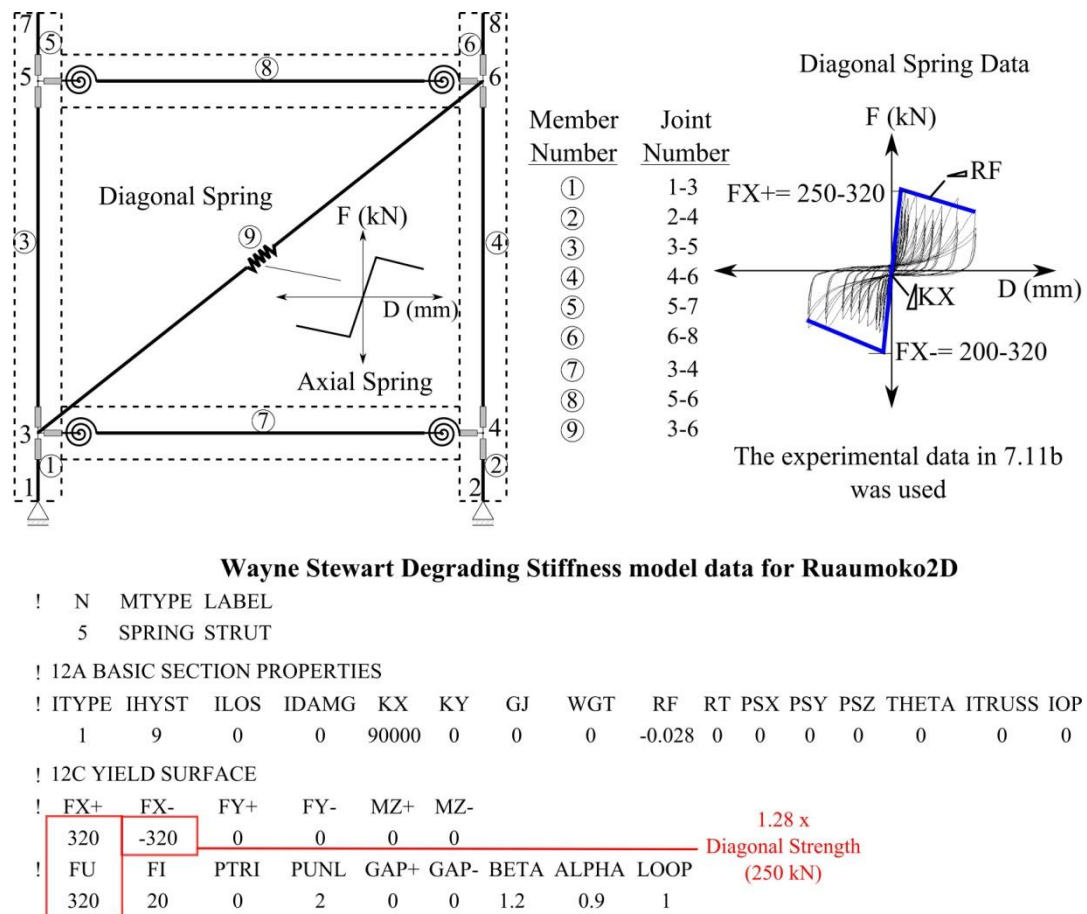


**Figure 7.12.** The numerical model of as built unreinforced clay brick infill wall for Ruaumoko 2D (fully infilled in the infill panel zone)

Using the experimental results in Figure 7.11b, the strut model was calibrated to match the experimental results. The parameters used for the numerical model are shown in Figure 7.12. As shown in Figure 7.13, the numerical model closely matched the experimental result. The asymmetric behaviour of the experimental result was partly due to the single sided point of application of the loading on the test setup and the damage to the specimen in the previous half cycle affecting the following cycle.

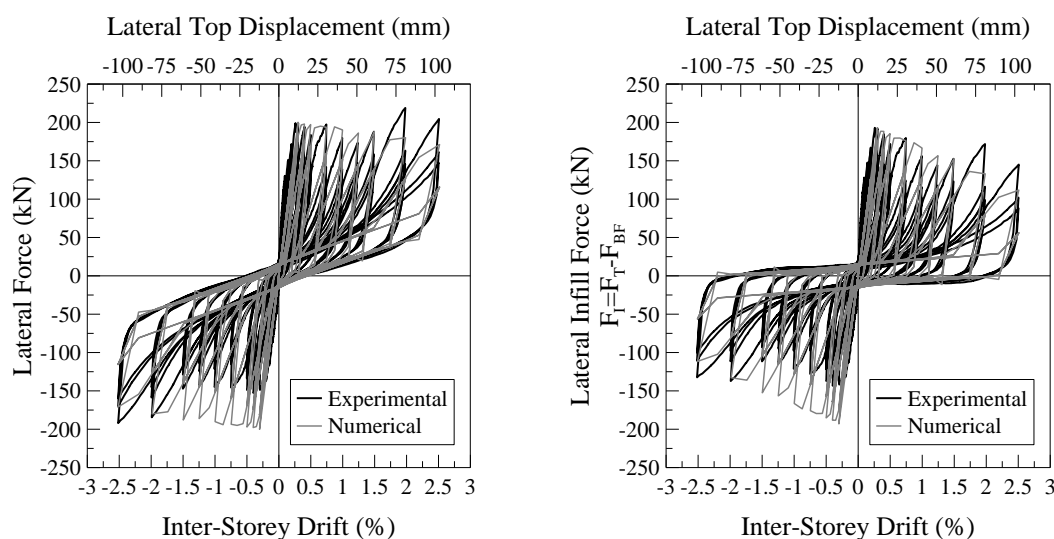


**Figure 7.13.** Hysteresis behaviour of the numerical model compared to the experimental result for as built unreinforced clay brick infill wall specimen FIF3-UCBI

## 7.2 Observations, Energy Dissipation and Effective Stiffness Properties of the As Built Unreinforced Clay Brick Infill Wall

### 7.2.1 Observations and Comparisons

Although unreinforced clay brick infill wall construction is not allowed for new buildings in New Zealand, there is a suggested serviceability limit state criterion given for masonry walls (in plane) in NZS1170.0 [55]. This criterion is defined as the top deflection of  $Height / 600$ . For the unreinforced clay brick infill wall specimen, this value was  $2550/600=4.25\text{mm}$ , which was equivalent to  $4.25/2550 \times 100 \approx 0.2\%$  drift. According to the standard, at this limit, noticeable cracking on the wall was expected. Although, this limit state criterion was meant for masonry walls, it also yielded a reasonable approximation for unreinforced clay brick infill wall specimen (Figure 7.14).



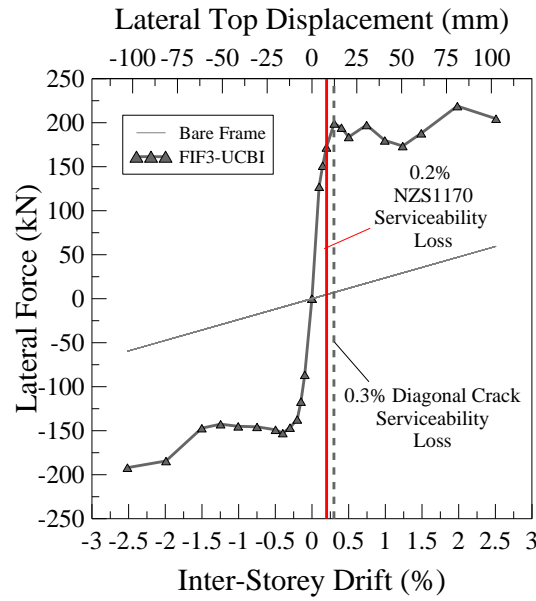


**Figure 7.14.** The envelope curves of the bare frame and as built unreinforced clay brick infill wall specimen FIF3-UCBI

### 7.2.2 Energy Dissipation and Stiffness Degradation Properties

The resulting averaged energy dissipation ( $E_D$ ) and equivalent viscous damping values ( $\xi_{eq}$ ) were calculated and are shown in Figure 7.15. Unlike the drywall specimens, the as built unreinforced clay brick infill wall specimen showed a rather constant averaged equivalent viscous damping value,  $\xi_{eq}=0.08$ , independent of the different inter-storey drift levels. The calculations were carried out over the global hysteresis curves. However, the dissipation can be assumed to be given only by the non-structural infill wall due to the linear elastic behaviour of the bare frame (i.e. negligible dissipation given by the bare frame  $E_D \approx 0$ ). Also, the range of average energy dissipated in the specimen was about five times higher than the as built drywalls. The difference in energy dissipation may be attributed to the high number of possible failure planes that can be utilized by the clay brick infill wall when compared to the drywall solutions. As for the stiffness degradation properties, this specimen had values four times higher than those for the drywall specimen, which was expected. The effective stiffness with respect to the applied inter-storey drift levels is shown in Figure 7.16.

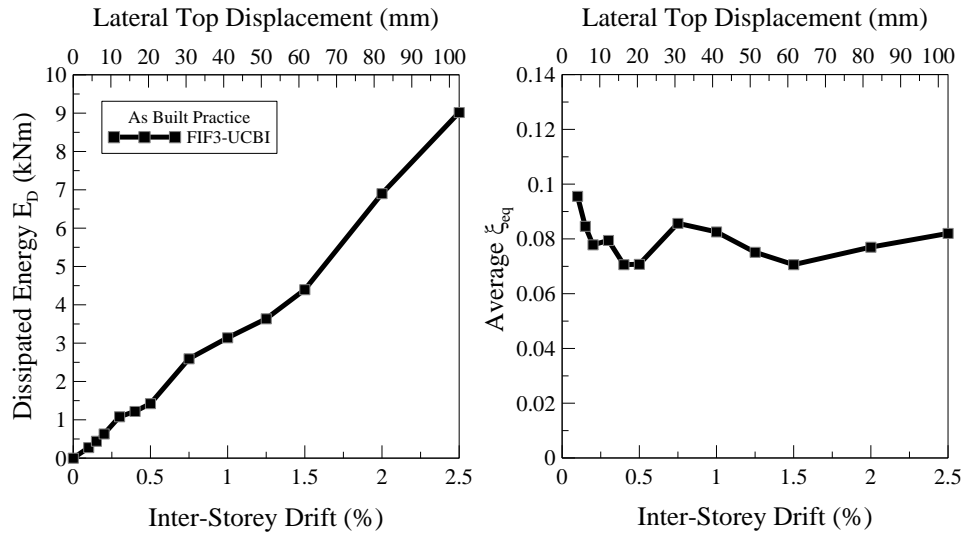


**Figure 7.15.** Average viscous damping and average dissipated energy with respect to inter-storey drift for as built unreinforced clay brick infill wall specimen FIF3-UCBI

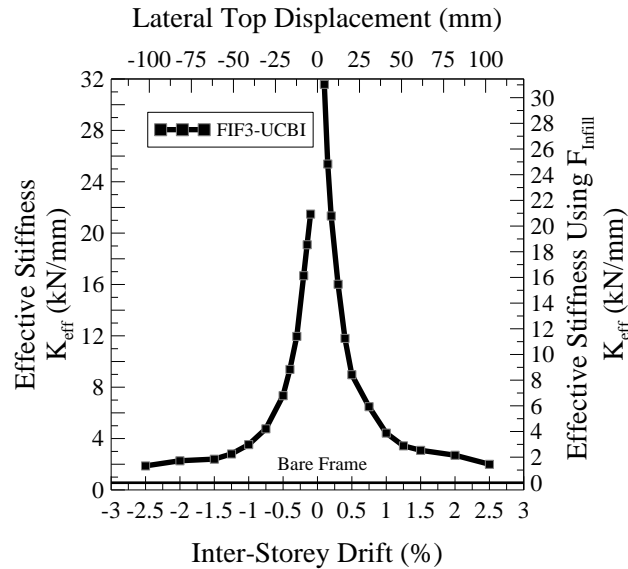


**Figure 7.16.** Stiffness degradation with respect to the inter-storey drift, plotted using total lateral force (left axis) and using the lateral force exerted by the infill wall (right axis) for as built unreinforced clay brick infill wall specimen FIF3-UCBI

### 7.3 Conclusions

Unreinforced clay brick infill walls were shown to have a very low drift level, 0.2-0.3%, at which they lose their capacity and serviceability. The behaviour was rather brittle since the infill wall cannot sustain its strength with increasing displacements, which partly conflicts with the overall earthquake resistant seismic design philosophy where structures are expected to behave in a ductile manner. As built practice of unreinforced clay brick infill walls can in fact change the global response, resulting in

possibly deficient and brittle earthquake responses. Even new structural designs could be affected from such a modification, which confirmed the necessity of reduced interaction with the structural system and the resulting low damage solutions for such heavy masonry infill walls.

The major failure type of the unreinforced clay brick infill wall specimen was diagonal cracking. However, considering the observations made during the test, it could be concluded that diagonal cracking did not occur itself. It was observed that the behaviour was rather similar to the concept of a progressive redistribution starting with the mortar layers. Since the main action on the infill panel zone was via the diagonal struts, initially the cracks were very close to the diagonals. However, after using this capacity, the additional demand acting on the infill panel zone was redistributed to other horizontal mortar joints and caused sliding cracks after 0.3% drift level. In certain cases, the sliding cracks formed in combination with diagonal cracks. Formation of sliding cracks were not only limited to the mid-height of the wall, but they formed at different heights at different drift levels. Only after the utilization of all the possible horizontal and diagonal mortar joints, widespread cracking in the clay bricks themselves was observed (instead of the mortar cracks), which were the last redistributive elements. This continued until 1.5% drift level. At 2.0 and 2.5% drift levels, the clay bricks at the corners of the infill panel zone crushed. This behaviour is graphically summarized in Figure 7.17.

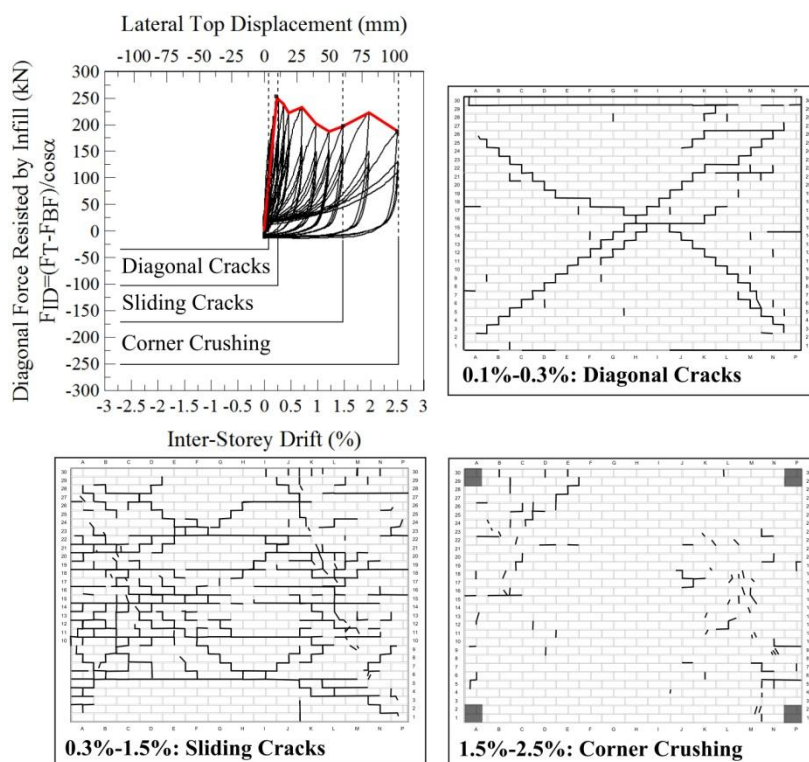


**Figure 7.17.** Summary of the unreinforced clay brick infill wall specimen FIF3-UCBI behaviour

It was also concluded that when infill panel zone was fully infilled with as built unreinforced clay brick wall, the infill wall contributed to the beam elongation occurring in the structural frame. In the utilized test setup, the beam elongation at the lower level was prevented by using pivots at the ends of the beam. Unlike the other specimens, the clay brick infill was strong and stiff enough to induce beam elongation at the lower level beam. According to this result, the behaviour of the structures can be further complicated by this aspect of the as built clay brick or any other type of relatively strong infill walls. It can also be stated that low damage solutions for non-structural vertical elements, capable of reducing the interaction between the main structure and the non-structural infill walls, are important new features to be considered for all types of structures including low damage systems (i.e. PRESSS [46]). For example, this unaccounted effect on the beam elongation may alter the behaviour of the post tensioning tendons and thus the re-centring mechanism of PRESSS structures.

Considering the limit state criteria given in NZS1170.0, the criterion given for masonry walls deforming under in-plane load was shown to give a realistic in-plane

serviceability loss drift value for unreinforced clay brick infill walls. This value was confirmed by the observed experimental serviceability loss drift level.

As a final remark, the test of the as built clay brick infill wall specimen helped further understand the behaviour of this wall type when fully infilled within a structural frame. It is based on this understanding that a low damage seismic solution could be developed for unreinforced clay brick infill walls, which has been developed and will be discussed in the next chapter.

#### **7.4 References**

- [4] NZS4230, "Design of Reinforced Concrete Masonry Structures," vol. 4230, ed: New Zealand Standard, 2004.
- [46] S. Pampanin, A. Palermo, and D. Marriott, PRESSS Design Handbook: NZ Concrete Society Inc., 2010.
- [49] S. H. Bertoldi, L. D. Decanini, and C. Gavarini, "Telai Tamponati Soggetti ad Azione Sismica, un Modello Semplificato: Confronto Sperimentale e Numerico (in Italian), ," presented at the Atti Del 6 Convegno Nazionale ANIDIS, 1993.
- [55] AS/NZS1170.0, "Part 0: General Principles," in Structural Design Actions vol. 1170, ed: Australian/New Zealand Standard, 2002.
- [57] NZS4210:2001, "Masonry Construction," in Materials and Workmanship vol. 4210, ed: New Zealand Standard, 2001.



# CHAPTER 8

## LOW DAMAGE UNREINFORCED CLAY BRICK INFILL WALL TEST

*A scientific truth does not triumph by convincing its opponents and making them see the light, but rather because its opponents eventually die and a new generation grows up that is familiar with it.*

*Max Planck*





## 8 LOW DAMAGE UNREINFORCED CLAY BRICK INFILL WALL TESTS

### 8.1 Low Damage Unreinforced Clay Brick Infill Wall: MIF5-UCBI

#### 8.1.1 Development and Design

As shown in the previous chapter, unreinforced clay brick infill walls behave in a rather brittle manner in structures. This brittle behaviour is usually due to the brittle properties of the clay bricks and the used mortar. Hence, this wall type, as it currently is, has not well suited in a seismic design philosophy since 1960s, which is based on ductile design. If used as infill walls in ductile structures, heavy masonry bricks or blocks may change the response from a ductile behaviour to a brittle one, which is not desired for seismic performance (Sudden loss of strength at infilled frames in Figure 8.1). Their design and interaction with the surrounding structural system have been a complicated research topic with no unified results since 1960s (i.e. [58], [59], [60]).

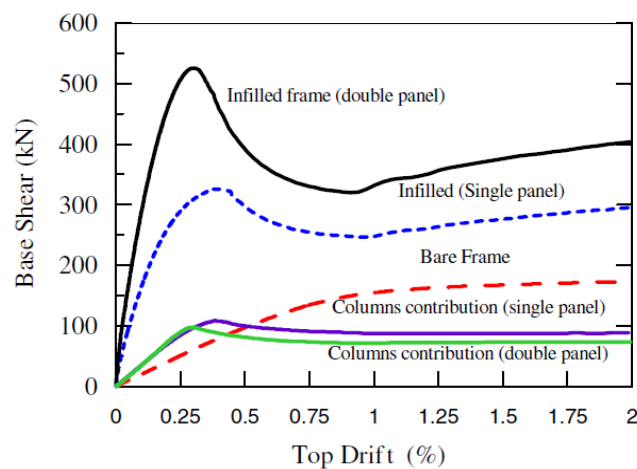


**Figure 8.1.** Comparison of base shear vs. drift for bare frames and clay brick infilled frames by Magenes and Pampanin [10]

To address this problem regarding unreinforced clay brick infills, there have been suggestions made in codes. NZS4230:2004 [4] suggests to either reinforce these infill walls with reinforcing steel and to make them an integral part of the structural system or to isolate them from the structure, without mentioning the modelling aspect of the integral solution. However, due to their brittle properties, clay bricks are not well suited to be engineered in the context of integrating them with the structural system.

As per the development of innovative low damage solutions for clay brick infills, only very few researches are available in literature [19, 20] and [21], as summarized previously in Chapter 3. The solution developed herein was typically and fundamentally inspired from the old construction practice of armature cross walls and recent rocking structural systems [46, 61]. As summarized by Langenbach [37], sub-framing masonry walls was a very old practice of construction especially in old structures in Turkey. After 1999 Duzce earthquake in Turkey, there were houses of this type without significant damage (Figure 8.2).



**Figure 8.2.** Armature cross walled structure at epicentre after the Duzce 1999 earthquake in Turkey from Langenbach [37]

Therefore, initially the behaviour of armature cross walls was investigated by the author with the aim to develop a modernized low damage solution for unreinforced masonry infill walls.

Referring to the equations of Bertoldi et. al. [49] for the capacity calculations of unreinforced clay brick infill walls, given in Section 4.4.1, certain parameters were studied, i.e. wall thickness, mortar strength, axial load on the wall. It was found that the strength of any given unreinforced clay brick infill wall was affected more by its geometry, i.e. thickness, and axial load rather than the material properties of the infill wall. As an example, using two different values of mortar strength for two different infill wall thicknesses, it was found that the change in strength given by the increase in mortar strength was negligible. On the other hand, just a fraction of change in

geometry, i.e. 20 mm increase in wall thickness, yielded much higher strength values, as graphically shown in Figure 8.3. As can be seen, the strength values shown in both figures are almost the same for very different mortar strength values while the strength is much higher for the 20 mm thicker wall.

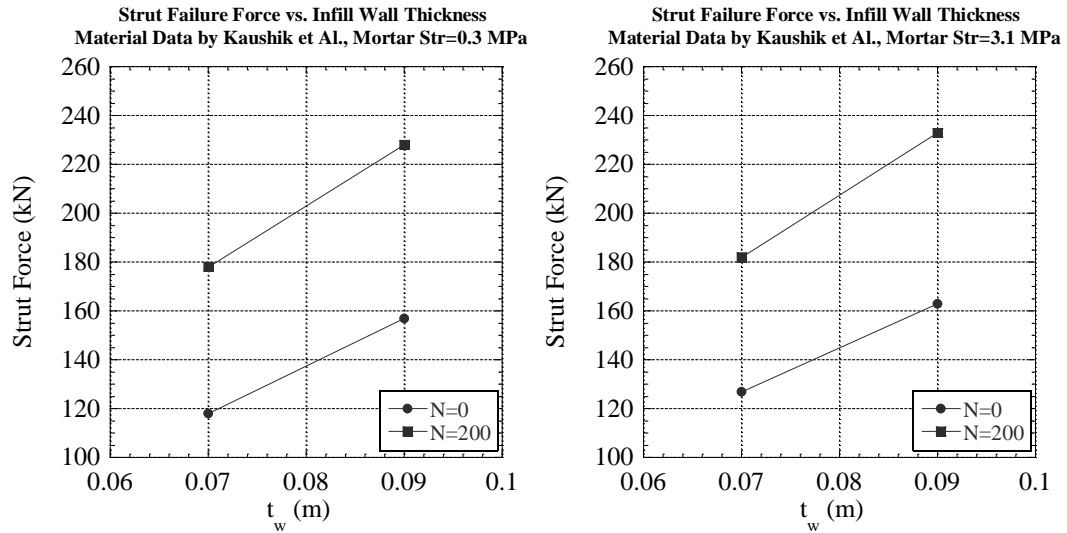


**Figure 8.3.** Change of governing failure modes of clay brick infills relative to change in thickness  $t_w=70$  to  $90\text{mm}$  and change in mortar strength  $0.3$  to  $3.1\text{ MPa}$  (The material data has been taken from Kaushik et. al. [50] and N stands for the vertical axial load on the clay brick infill wall in kN)

Using this observation, it can be assumed that the behaviour of unreinforced clay brick infill walls is largely affected by their geometry and the boundary conditions with the beams, as axial load is transferred from the beams. A low damage solution that does not depend on the material properties but rather depends on the geometry can make the design and construction of such walls much easier for the engineers. Based on this observation, the sub-framing idea of armature cross walls may be effectively working since it also modifies the geometry of the wall itself. This idea was adapted for use with unreinforced clay brick infill walls by subdividing the infill panel zone into 3 or more by using vertical joints between each infill panel. The structural vertical joints in structural walls was theoretically studied by Cholewick [62] as well as reported by Glogau for the notes on partition wall isolation systems/requirements [63]. Therefore, the low damage system shown in Figure 8.4 was developed. The system consists of a light gauge steel sub-framing with three individual cantilever infill panel zones separated by isolation gaps. For sub-framing, commercially available light gauge steel channel sections of  $50\times 75\times 0.75\text{ mm}$  were chosen. The available sizes are shown in

Figure 8.5. In order to ensure the sub-framing to carry out of plane weight of the unreinforced clay bricks, the capacity of the provided studs and the RC anchors at the borders had to be checked. These checks are summarized in Figure 8.6 and Figure 8.7.

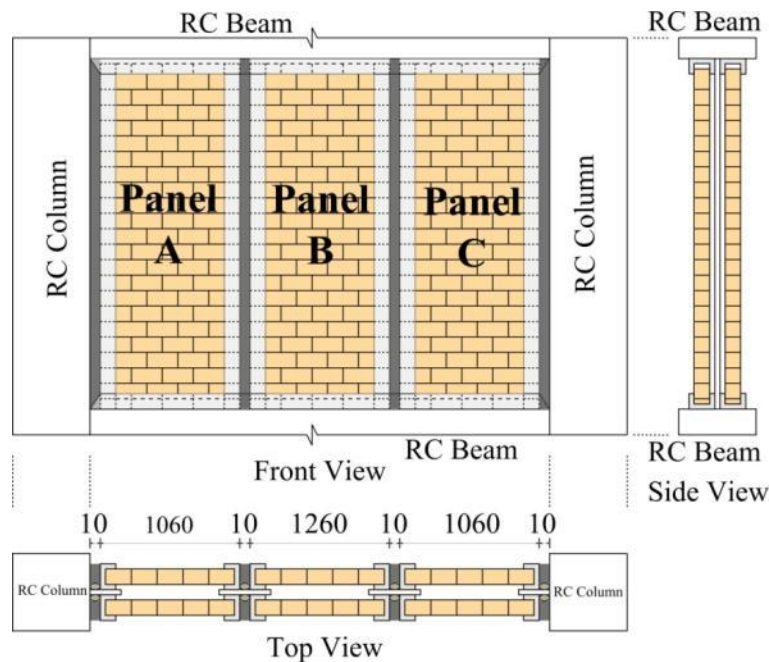


**Figure 8.4.** Developed low damage solution for unreinforced clay brick infill wall specimen MIF5-UCBI with four 10 mm width isolation gaps between the individual infill panels

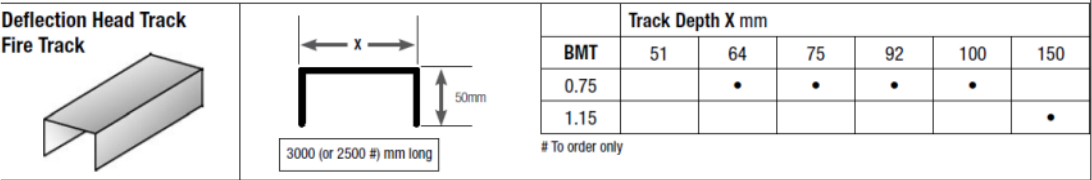


**Figure 8.5.** Used light gauge steel channel section by USG [64] (50×75×0.75 mm was chosen)

Dividing the infill panel zone into individual cantilever macro elements prevents the formation of a brittle diagonal strut mechanism, i.e. squat walls. The imposed deformations on the structure are resisted by the rocking action of each of the cantilever infill wall panels, ductile flexural behaviour. In this system, the addition of a secondary sub-framing and polyurethane joint sealant in the vertical joints between the wall panels increases the out-of-plane stability and confinement of the infill panel zone. Moreover, these vertical joints with the provided elastic structural sealant prevent stress concentrations occurring due to different contact lengths between the infill wall the structural system, unlike the as built option. This system was tested and proved to work effectively as reported further in this chapter.

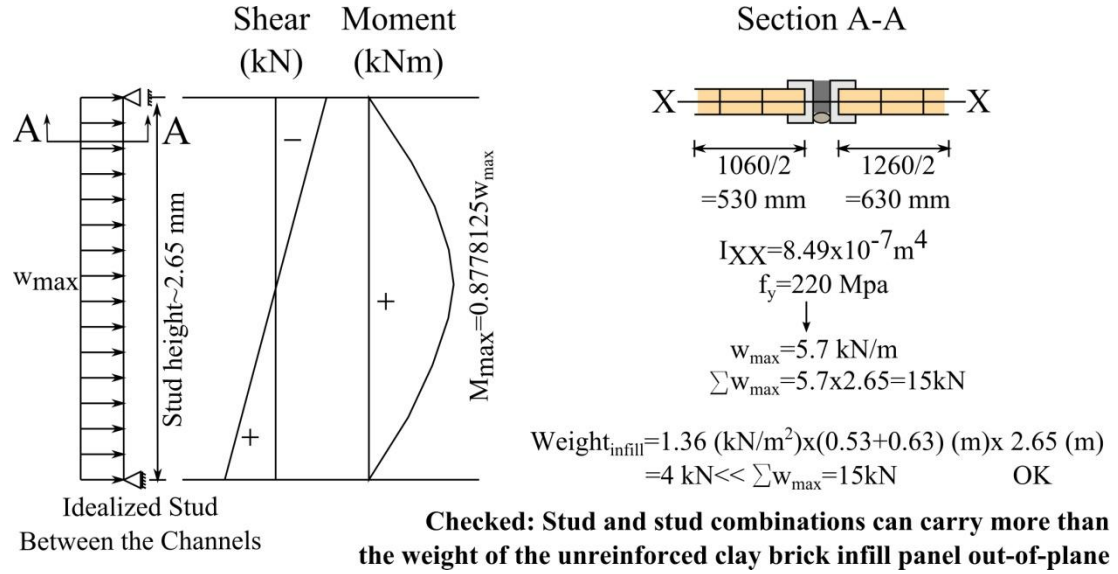


**Figure 8.6.** Capacity check for the stud members between the top and bottom steel channels (Calculations were carried out for a single skin of the infill wall)

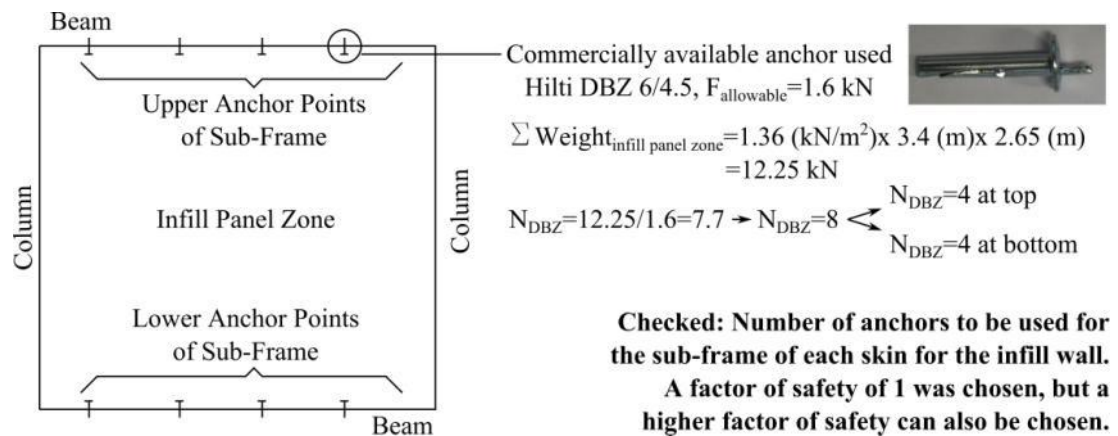


**Figure 8.7.** Capacity check for the RC anchors at top and bottom steel channels (Calculations were carried out for a single skin of the infill wall and it has been assumed that the whole weight of the infill panel zone will be carried by the constructed steel sub-frame)

After the capacity of the designed sub-frame was checked and confirmed, the details were finalized. Using this sub-framing, the infill panel zone was divided into three panels. Each of these panels was separated from the adjacent member by a 10 mm gap, summing up to 40 mm in total. The 40 mm total isolation gap corresponded to an allowable drift limit of 1.5%, the same as the low damage drywall specimens (MIF1-STFD and MIF2-TBFD). At each of these gaps, a strip of gypsum board was placed in between the two skins of the infill wall for additional fire rating. Then, these gaps were reduced by placing polyethylene foam, which also helps for thermal insulation. As the final step for preparing the gap for structural/seismic actions, the gap was filled with

fire rated polyurethane joint sealant, fire rated Sikaflex construction AP (Figure 8.9). The resulting details are shown in Figure 8.8.

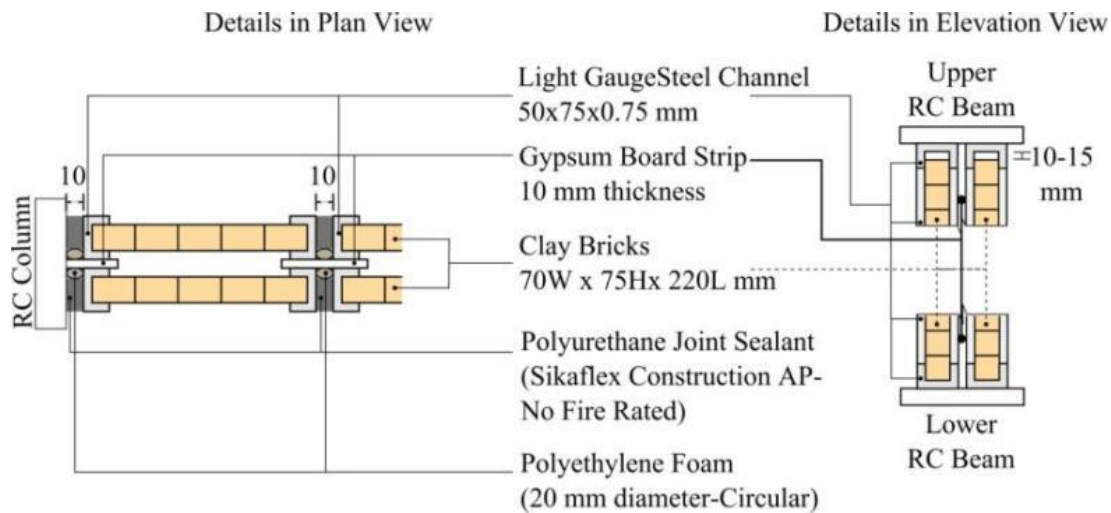


**Figure 8.8.** Details of the low damage solution for double skinned unreinforced clay brick infill wall specimen MIF5-UCBI



**Figure 8.9.** Polyurethane joint sealant application (Fire rated Sikaflex construction AP)

### 8.1.2 Construction

In general, the construction consisted of only two steps. First, the light gauge steel sub-frame was constructed by following the developed details. Then, the clay brick wall was constructed inside the sub-frame. Clay bricks were laid the same way as FIF3-UCBI, with wall ties at every fourth course in vertical and 600 mm apart in horizontal. However, no mortar was used at the bottom and top of the infill panel zone to allow sliding. Instead of a single infill panel, the wall was constructed as three separate cantilever panels as shown in Figure 8.10. Seven days after the infill wall was finished, the gaps were filled with polyethylene foam and polyurethane joint sealant.



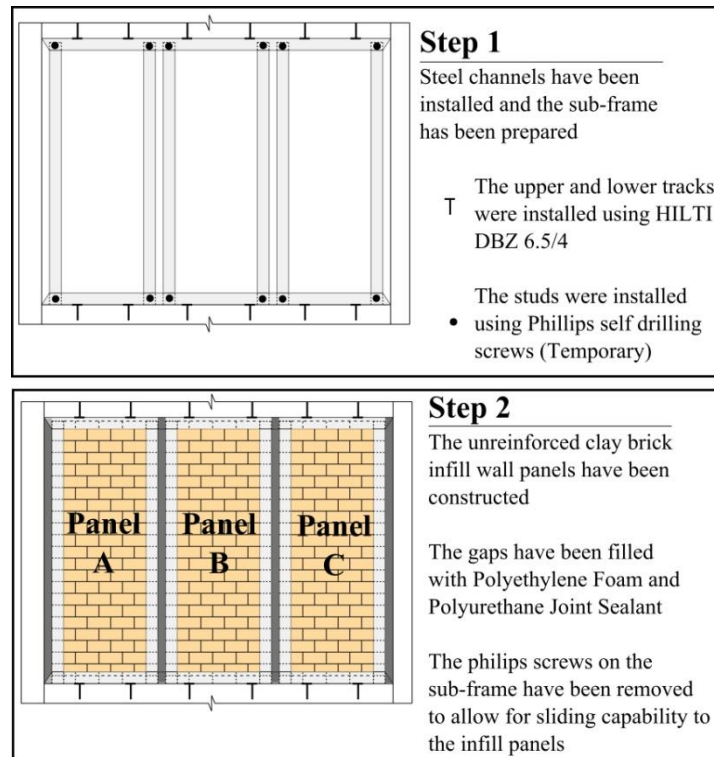


**Figure 8.10.** Construction process of the low damage unreinforced clay brick infill wall specimen MIF5-UCBI

Once the joint sealant set within two weeks' time, the infill wall was completely integrated with the structural frame due to these flexible joints. The Phillips-head self drilling screws were then removed from the sub-frame, adding sliding capability to the infill wall. The photos from the various stages during the construction are shown in Figure 8.11 and Figure 8.12. The finishing was carried out in the same way as the as built specimen with a thin coat of white paint to allow for crack visibility.



**Figure 8.11.** Low damage unreinforced clay brick infill wall specimen MIF5-UCBI: a) Connection of stud to the top track, b) The lower right corner of the infill panel zone after the construction started, c) General view during the construction



**Figure 8.12.** Low damage unreinforced clay brick infill wall specimen MIF5-UCBI: a) Polyethylene foam installation, b-c) External and internal joints after the polyurethane joint sealant application, d) General view after the construction was finished

8.1.3 Instrumentation

The specimen was instrumented in order to measure the same displacements as FIF3-UCBI. In addition to those, potentiometers h10 and h11 were installed to measure the vertical displacements between Panel A-B and Panel B-C. The potentiometers h6, h7 and h14, h15 were installed to measure the uplift at the lower and upper levels of the Panel B, which is the centre panel. The instrumentation scheme and the specimen before the test are shown in Figure 8.13.

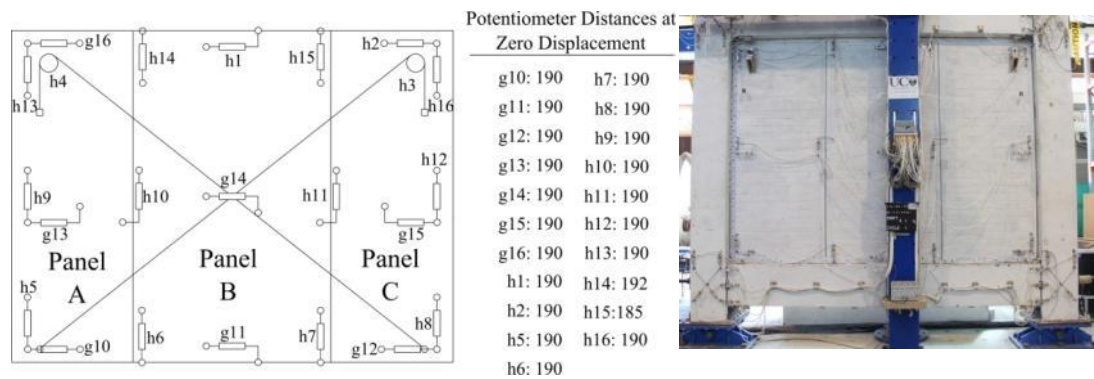


**Figure 8.13.** Instrumentation of the low damage unreinforced clay brick infill wall specimen MIF5-UCBI



### 8.1.4 Test Results

#### 8.1.4.1 Damage Observations

The displacement protocol was applied to the specimen as in the other tests. The specimen did not show any significant damage until the end of the test at 2.5% drift. At 0.75% drift, one minor horizontal mortar crack at the top right corner of the Panel C was observed. Then at 1.5% drift, two other minor mortar cracks were observed at the bottom left and top right corners of the Panel A. 1.5% drift was the drift limit until which the interaction with the structural system was minimized. After this, the individual infill wall panels engaged with the structural system. Following this, another horizontal crack and minor toe crushing occurred at the top right corner of the Panel C, which was caused by the rocking of the panels and the interaction with the structural system. Similar horizontal cracks formed at the top left corner of the Panel A at 2.5% drift level. Overall, the infill wall did not suffer any serious in-plane damage and it did not lose its out of plane capacity, which was due to the in-plane integrity of the clay brick infill wall and the integrity of the sub-frame system. The damage progress and the end of the test photos of the specimen are shown in Figure 8.14 and Figure 8.15.

Video of the test: <http://youtu.be/1h97J9YgFSI>

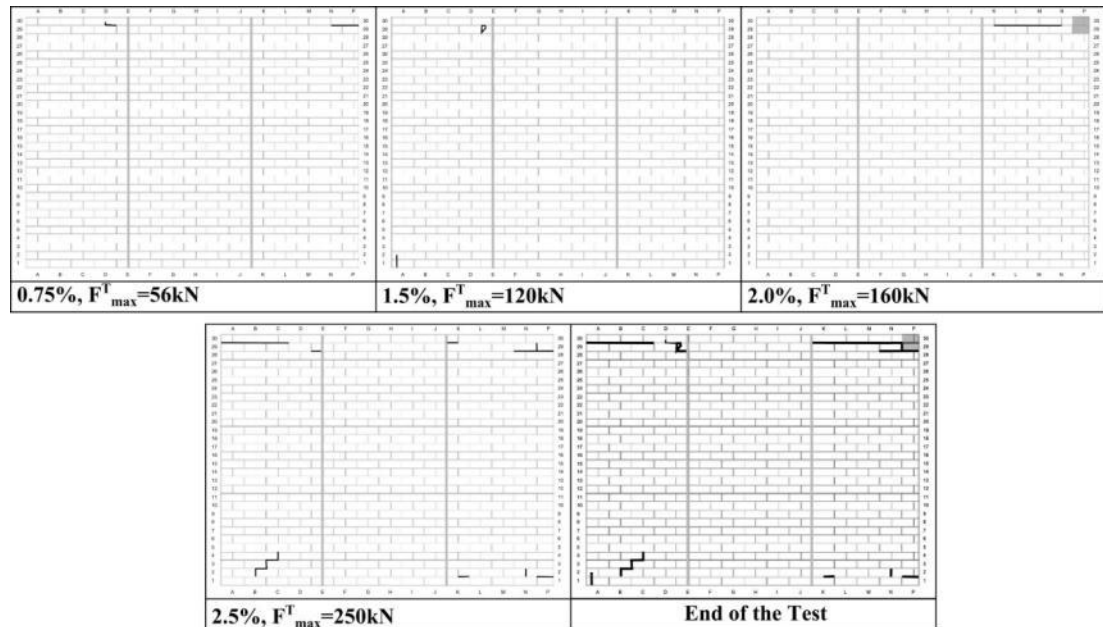


**Figure 8.14.** Damage progress of the low damage unreinforced clay brick infill wall specimen MIF5-UCBI

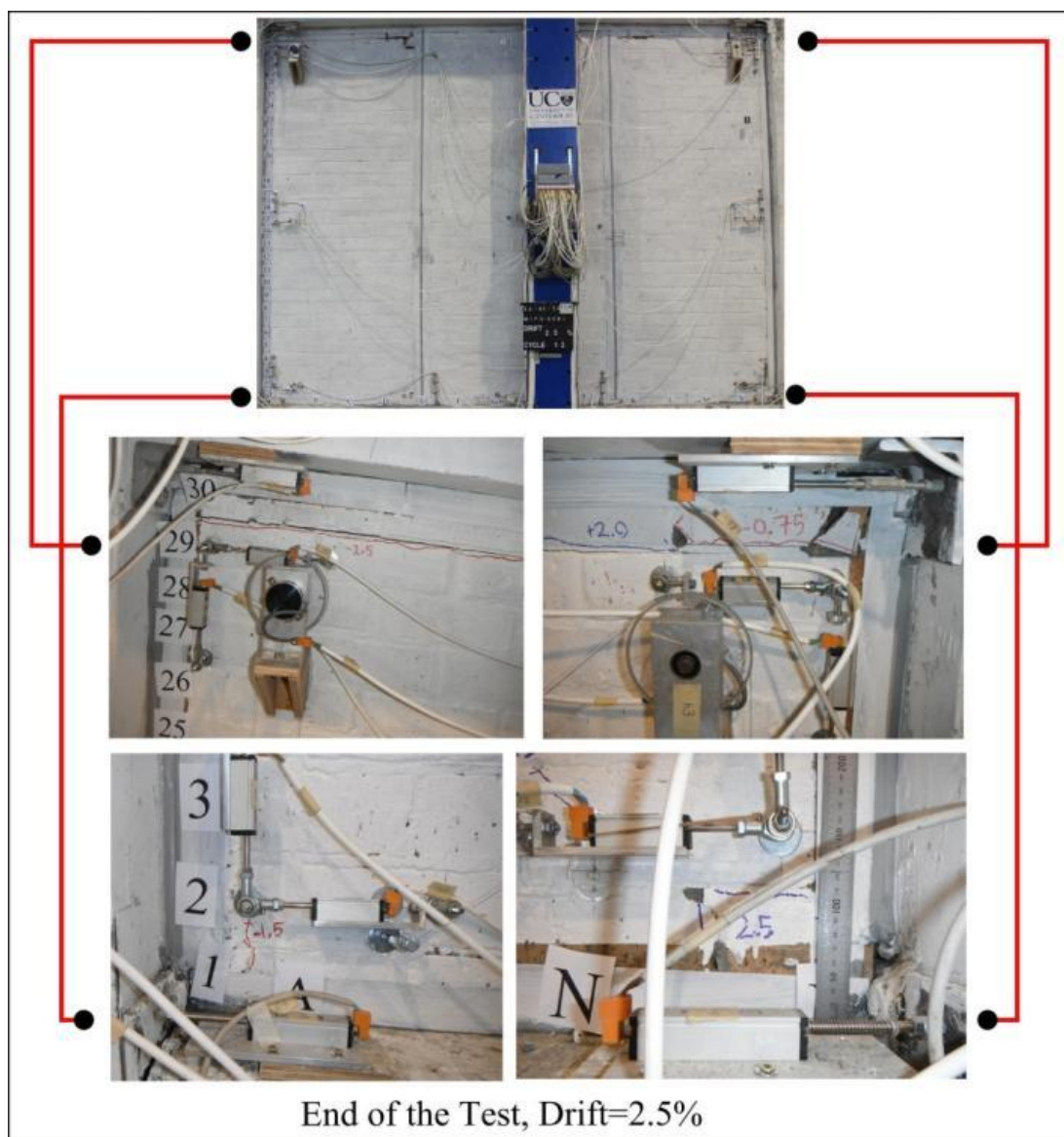


**Figure 8.15.** Damage photos of low damage unreinforced clay brick infill wall specimen MIF5-UCBI at the end of the test

#### 8.1.4.2 Behaviour Explanation

The adopted details worked effectively and prevented the formation of in-plane damage. As a result, the solutions preserved the out-of-plane capacity, which was dependent on the in-plane strength of the infill wall and the condition of the sub-frame. The system worked as it was intended; the infill wall panel had degree of freedom to slide, and the polyurethane joint sealant acted as a bumper for sliding. In addition, the infill panels were able to rock as sliding action reached its limit, which started when the compressibility of the polyurethane reached its limit. At the end of the test very low and minor damage was observed at the specimen. Also, polyurethane joint sealant proved its strong bonding capabilities within the given low damage concept (Figure

8.16b). At the end of the test, the joint sealant was intact and functional. The behaviour of the specimen is schematically summarized in Figure 8.16a.

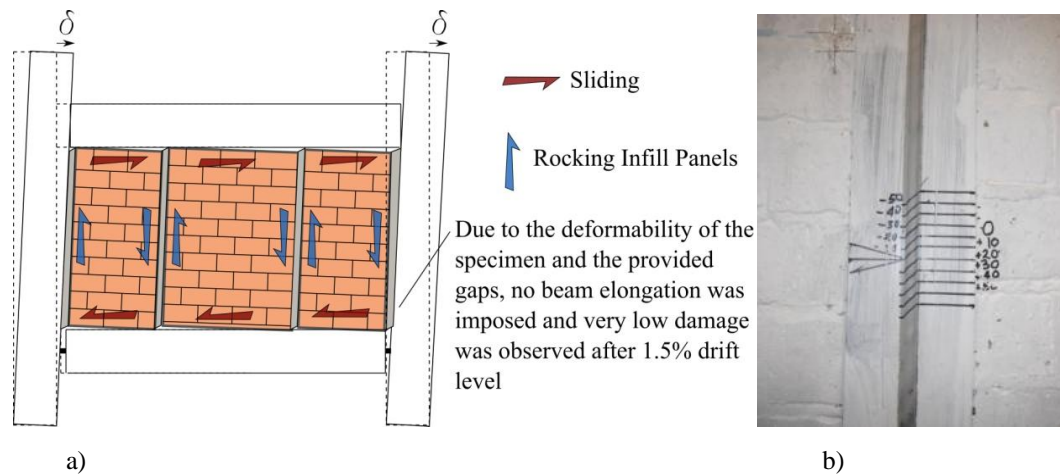


**Figure 8.16.** a) Behaviour of the low damage unreinforced clay brick infill wall specimen MIF5-UCBI, b) The deformation of polyurethane joint sealant at +2.5% drift level

Structurally, the effect of these flexible gaps was observed in the resulting global hysteresis curve, shown in Figure 8.17a. As design suggested, the interaction of the infill panel zone with the structural system was minimized until the design drift limit of 1.5%, theoretical gap closing drift. After this drift, the infill panel zone started to interact with the structural system. However, even the highest drift limit of 2.5% could not cause a serious damage to the developed low damage infill solution. The infill remained intact and serviceable both structurally and architecturally. The beam elongation was also prevented until the gap closing drift level (1.5%), reducing the effect of the infill panel to the beam elongation effects and thus to the level of post tensioning (Figure 8.17b). In Figure 8.18, the lateral force exerted by the infill panel zone and its projection into diagonal direction are shown for numerical modelling purposes.

When the potentiometer readings of h6, h7 and h14, h15 were inspected, the uplift occurring at lower and upper part of the Panel B could easily be observed, which shows the rocking observed in the panels. This can also be seen when h10 and h11 were checked, showing the relative vertical deformation occurring between the panels (Figure 8.19). In addition to rocking at panels, the infill panel zone also showed some sliding behaviour as intended by the design (Figure 8.19d).

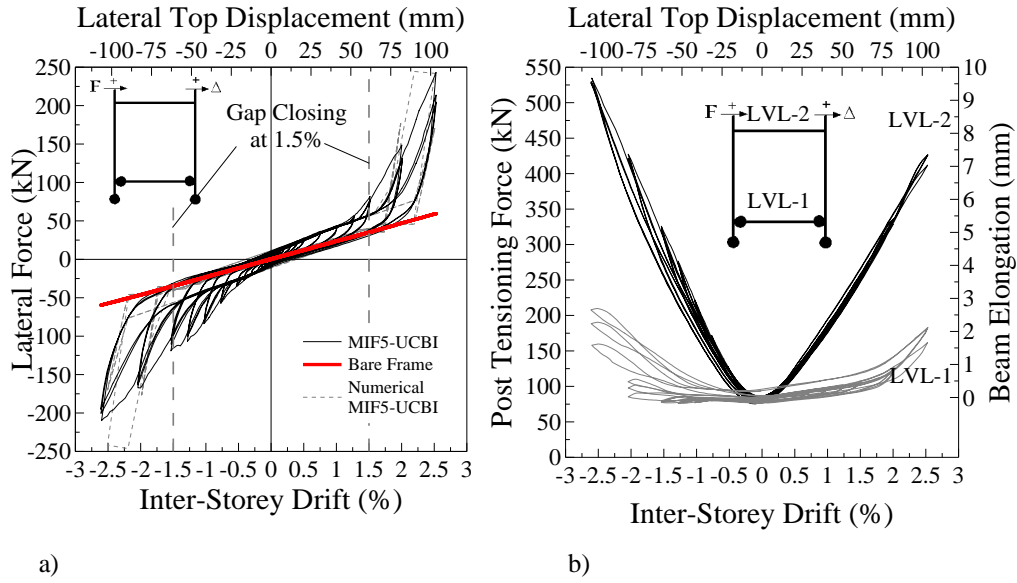


**Figure 8.17.** Test results for low damage unreinforced clay brick infill wall specimen MIF5-UCBI: a) Global force vs. inter-storey drift hysteresis, b) Post tensioning and beam elongation vs. inter-storey drift.

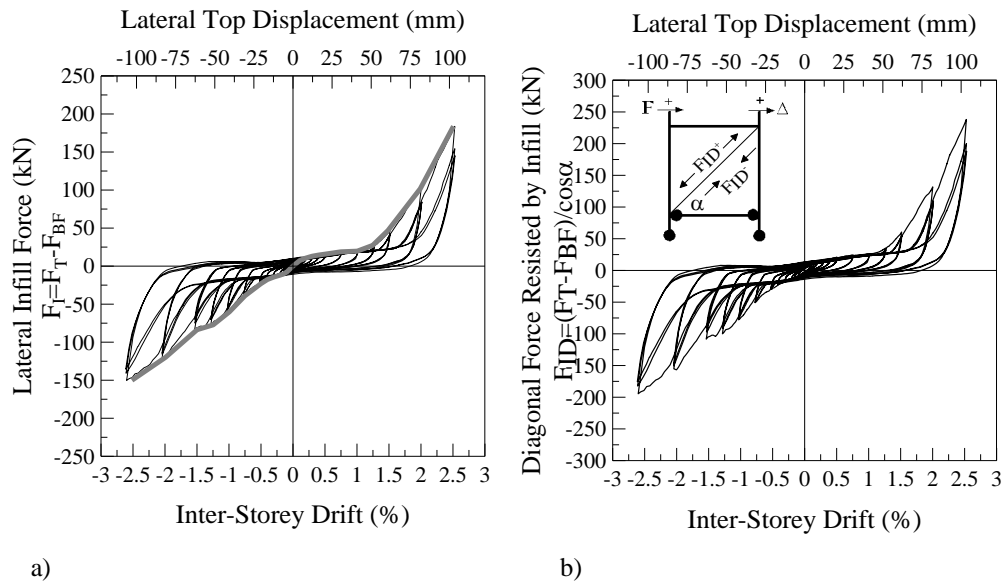


**Figure 8.18.** a) Lateral force exerted on the infill panel zone obtained by subtracting the bare frame from the total, b) Diagonal force exerted on the infill panel zone, projection of a) in diagonal dir.

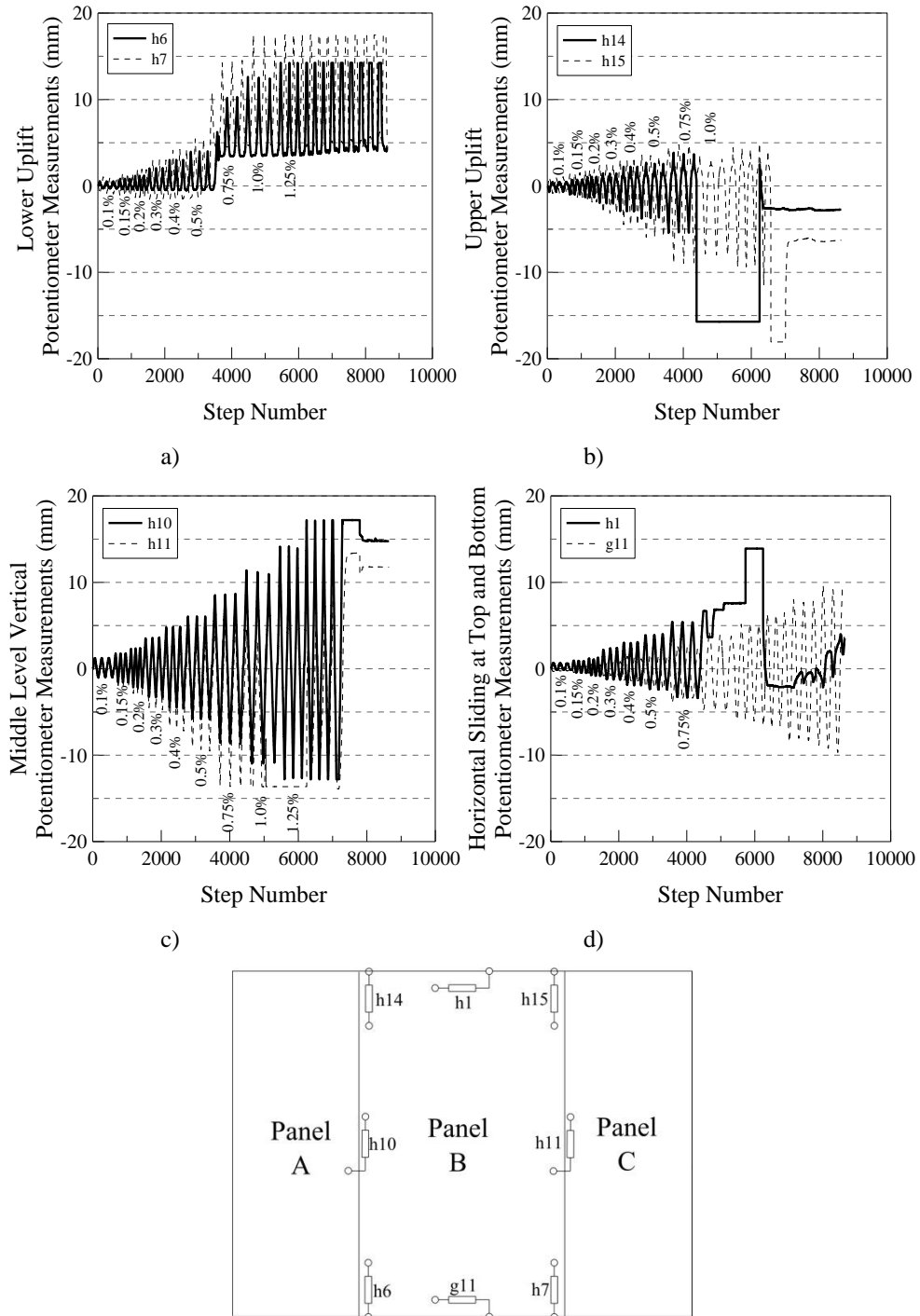


**Figure 8.19.** Potentiometer readings taken at the shown locations: a-b) Uplift at bottom and top, c) Relative vertical deformation between the Panel A and B, the Panel B and C, d) Sliding at top and bottom of the infill wall

### 8.1.5 Numerical Model Calibration

The model used for FIF3-UCBI was modified with the introduction of the gap parameter in Wayne Stewart degrading stiffness hysteresis rule. As in the low damage drywall solutions, the provided total gap of 40mm was projected into diagonal

direction. The required gap in the diagonal was approximately 50 mm when 40 mm was projected. Unlike the low damage drywall solutions, the gap was filled with the polyurethane joint sealant. This sealant had an elastic behaviour and very strong bond properties with the structural materials. Due to the presence of this elastic material in the gaps, the provided gap of 40 mm could not freely act. Therefore, the gap parameter was reduced and calibrated to match the experimental result. Calibration showed that 0.85 times the provided diagonal gap length (52 mm) matched the experimental and theoretical gap opening at 1.5%. Also, the analytical diagonal strut strength value multiplied by 1.28 resulted in a good match to the experimental hysteresis. The parameters of the calibrated model are given in Figure 8.20 and the comparison of the numerical and the experimental results are shown in Figure 8.21.

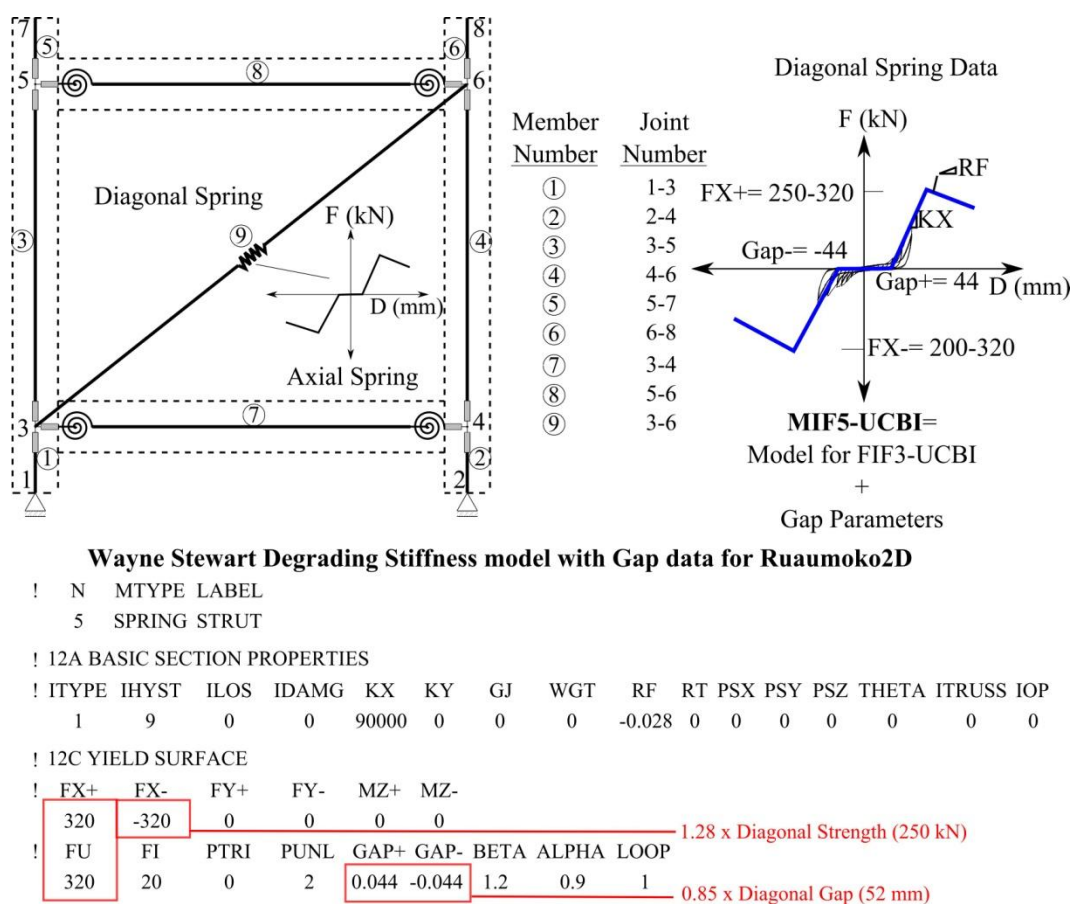


**Figure 8.20.** The numerical model of low damage unreinforced clay brick infill wall specimen MIF4-UCBI for Ruaumoko 2D (Strut model with a  $\pm$ gap to account for the vertical isolation joints)



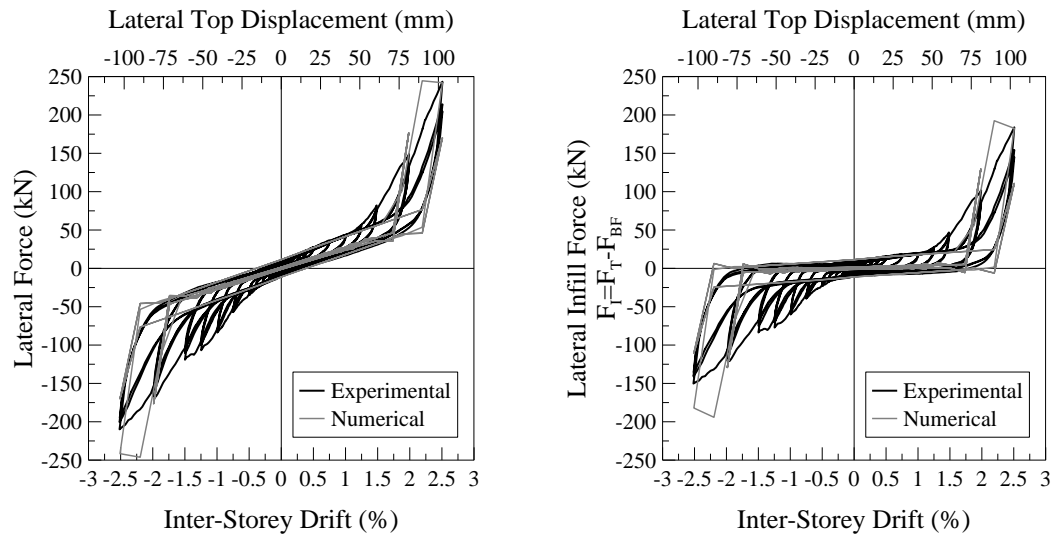


**Figure 8.21.** Hysteresis behaviour of the numerical model compared to the experimental result for low damage unreinforced clay brick infill wall specimen MIF5-UCBI

## 8.2 Observations, Energy Dissipation and Effective Stiffness Properties of the Low Damage Unreinforced Clay Brick Infill Wall

### 8.2.1 Observations and Comparisons

The experiments showed that as built clay brick infill walls can easily be turned into a low damage seismic infill wall type. The developed low damage solution remained serviceable even at the highest drift of 2.5% with very minor cracks. The low damage solution minimized the interaction with the structural frame, resulting in behaviour close to the bare frame until the design drift limit of 1.5%. After 1.5%, the infill wall interacted with the structure due to the activated strut action. This aspect of the developed low damage solution suggests that the system is an effective low damage non-structural wall solution. After the design drift level, it turns into an additional structural component in the system, a back up element. Accordingly, it can be stated that the system can well be an alternative dissipative solution to be utilized/activated when the inter-storey drift level in the structure exceeds the design drift level. The performance of the low damage solution is compared to the as built specimen and shown in Figure 8.22. Also, this solution does not apply only to unreinforced clay bricks, but to any kind of panels that can be installed as non-structural walls with enough strength and dissipative properties to be utilized as structural elements also (i.e. timber panels, steel plate shear walls, reinforced concrete panels, etc.)

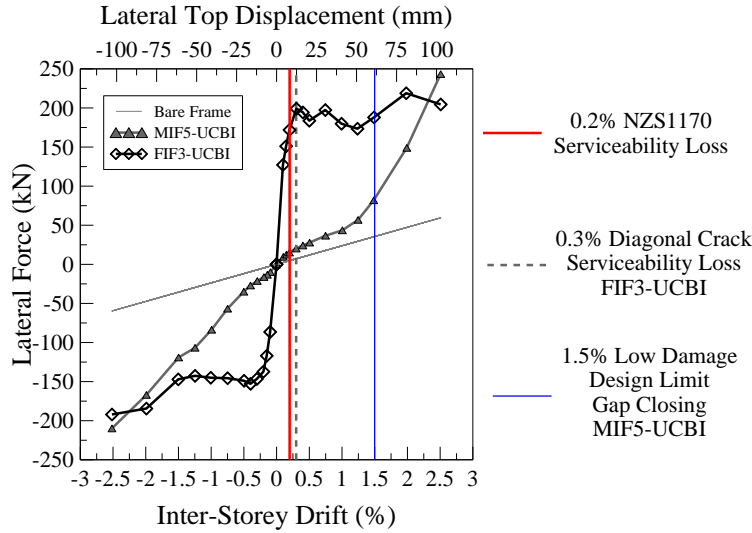


**Figure 8.22.** The envelope curves of the bare frame, as built and low damage unreinforced clay brick infill wall specimens (FIF3-UCBI and MIF5-UCBI) along with the key drift values

The efficiency of the low damage solution can also be shown by using the axial strut strain ( $\varepsilon_w$ ) in relation to the drift ( $\delta$ ) and aspect ratio ( $L/H$ ) of the infill panel zone using equation 8.1 shown below suggested by Magenes and Pampanin [10]. Low damage design drift directly adds up in the given equation so that it causes an increased drift capacity for each level of strain. This modification given by the low damage solution is shown in equation 8.2. The graphical comparison of these two equations, using a low damage design drift of 1.5%, summarizes the effect of the low damage solution compared to the as built option in Figure 8.23.

$$\delta = \frac{L}{H} - \sqrt{(1 - \varepsilon_w)^2 \cdot \left(1 + \left(\frac{L}{H}\right)^2\right) - 1} \quad (8.1)$$

$$\delta_{low} = D + \frac{L}{H} - \sqrt{(1 - \varepsilon_w)^2 \cdot \left(1 + \left(\frac{L}{H}\right)^2\right) - 1} \quad (8.2)$$



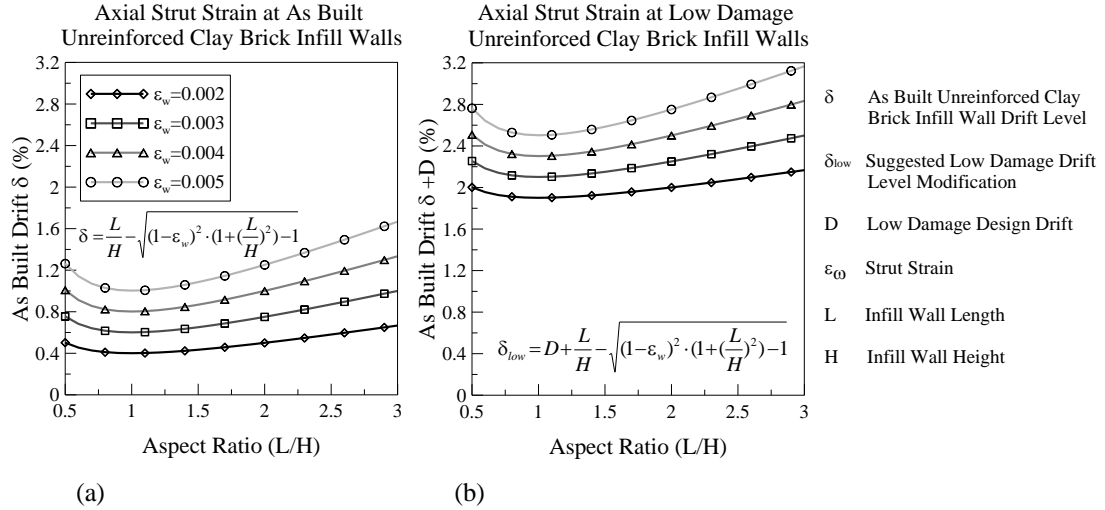


**Figure 8.23.** Axial diagonal strut strains with respect to aspect ratio of the infill panel zone and imposed drift levels given by Magenes and Pampanin [10] and the modification to incorporate the gap system in the low damage infill wall solution ( $D=1.5\%$  in the shown case above): a) As built clay brick infill walls, b) Low damage solution

For the tested specimens, the aspect ratio ( $L/H$ ) was 1.33, which corresponded to a diagonal strut strain of 0.002 at 0.4% drift level (Figure 8.23a). Incorporating the low damage solution increased this drift limit to approximately 2.0% (0.4%+1.5% design drift=1.9%) for the same strain of 0.002. These results also confirmed the experimental observations since the damage to the infill wall started only after 2.0% drift level while the interaction was minimized until 1.5% drift level.

### 8.2.2 Energy Dissipation and Stiffness Degradation Properties

When compared to as built specimen FIF3-UCBI, the use of the elastic polyurethane joint sealant and sub-framing the infill panel zone into three separate panels introduced a 12 to 25% higher equivalent viscous damping in the system until engaging with the structure at 1.5% design drift limit (Figure 8.24b). After 1.5% drift (i.e. activation of diagonal strut), the equivalent viscous damping dropped significantly. However, due to the reduced interaction and damage, the dissipated energy was approximately 50% less than in the as built specimen (Figure 8.24a).

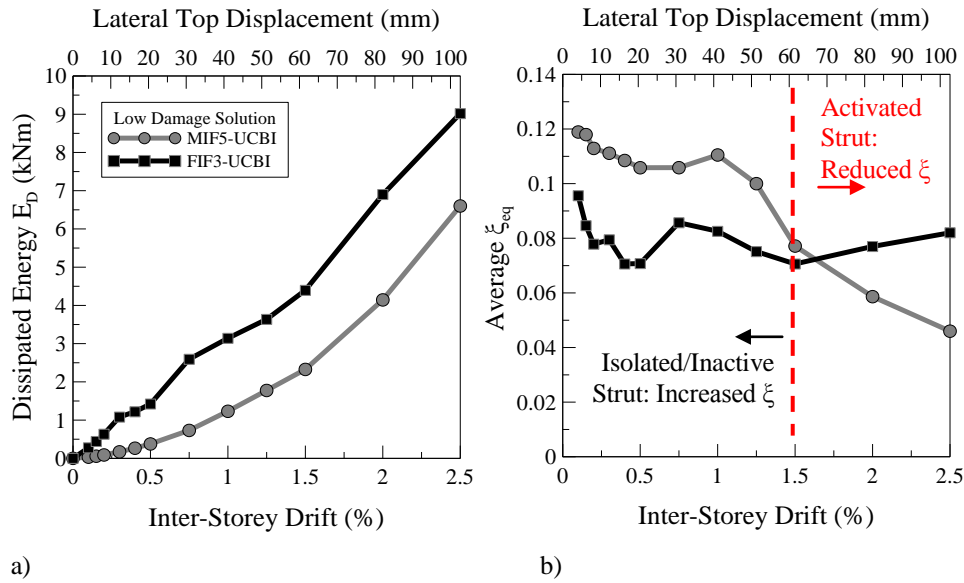


**Figure 8.24.** The low damage unreinforced clay brick infill wall compared to as built (MIF5-UCBI and FIF3-UCBI): a) Average dissipated energy vs. the inter-storey drift, b) Average equivalent viscous damping

The significantly reduced interaction with the structural system is also evident when the stiffness degradation properties are inspected. As it can be seen in Figure 8.25, the effective stiffness values are very close to the bare frame and significantly lower than the as built unreinforced clay brick infill wall specimen (FIF3-UCBI).

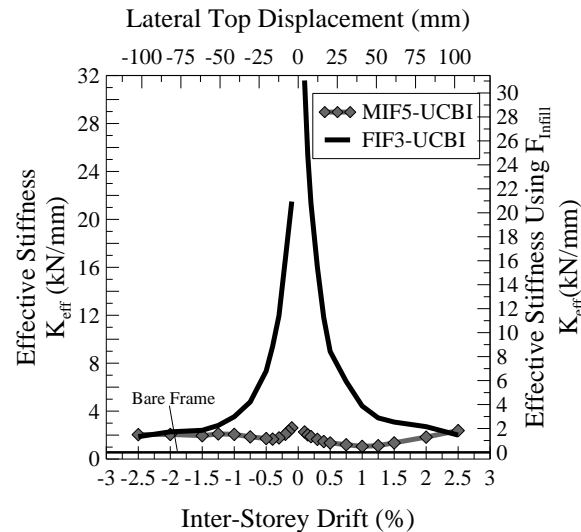


**Figure 8.25.** Stiffness degradation vs. inter-storey drift compared to as built specimen, plotted using the total lateral force (left axis) and using the lateral force exerted by the infill wall (right axis),

### 8.3 Conclusions

The old practice of armature cross walls and the concept of rocking systems were adapted to be used in modern structures in order to obtain a low damage solution for unreinforced clay brick infill walls. The low damage solution concept was developed by dividing the infill panel zone into three using light gauge steel sub-framing. The three panels were separated by 10 mm vertical gaps from each other and from the RC columns. These gaps were filled with polyurethane joint sealant, a very elastic structural joint sealant. The achieved low damage system was, in principle, a rocking infill wall system, which can further be studied for added external dissipaters to the infill wall system (Figure 8.26).

To see how the system works: <http://youtu.be/1h97J9YgFSI>

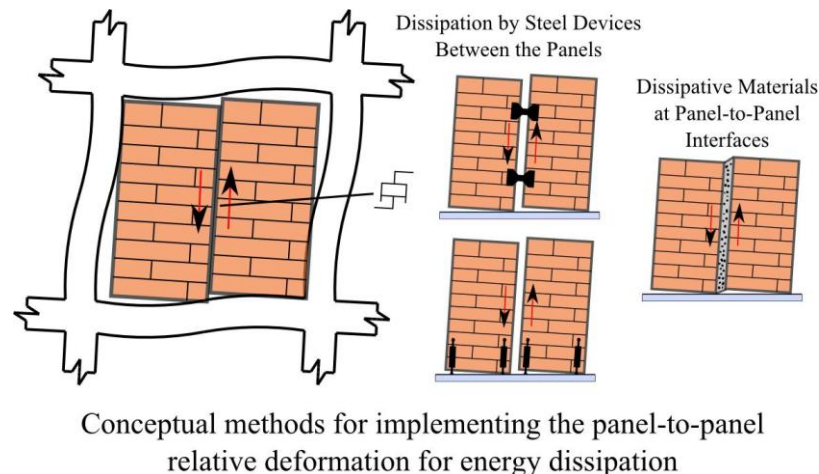


**Figure 8.26.** Conceptual added external dissipation options for the suggested low damage solution for unreinforced clay brick infill wall panels (instead of clay bricks, CLT panels can also be used as infill walls)

The low damage system proved its effectiveness and remained serviceable even at high drift levels (2-2.5% drift) imposed during the test. Until the design drift limit of 1.5%, the low damage system's behaviour was very close to the bare frame, which meant the interaction between the structural frame and the non-structural wall was minimized. After the design drift (gap closing), the low damage infill wall started to take forces by the activation of a strut action. This observation had another implication in addition to the low damage property of the system. The low damage non-structural wall solution worked as a low damage system until the design drift limit was reached and the gaps were fully closed. After the design drift level, the system acted as a structural component. Therefore, they may behave as backup or secondary seismic resisting

structural elements that activate as a structure experiences extreme drifts provided that they do not develop brittle local or global mechanisms. Other than clay bricks, this solution can also be applicable to other types of materials that can be used as structural infill panels by selecting appropriate materials for this purpose (i.e. timber walls, steel plate shear walls, RC panels, etc.).

As it was observed in as built unreinforced clay brick infill wall specimen FIF3-UCBI, the as built infill panel imposed beam elongation at the lower beam level due to the interaction with the structural system though this elongation was prevented in the bare frame. With the developed low damage solution, the interaction with the structural system was minimized until 1.5% drift level and the beam elongation given by the infill panel was also minimized. However, after 1.5% drift, the low damage infill wall interacted with the structural system and had the same level of beam elongation as the as built specimen at 2.0 and 2.5% drift levels.

For energy dissipation, the polyurethane joint sealant introduced 12-25% higher equivalent viscous damping, but 50% less hysteretic energy dissipation when compared to the as built option. Until 1.0% drift level, the low damage solution gave approximately 12% to 10% equivalent viscous damping (whereas this number was approximately 8% for as built option)

#### **8.4 References**

- [4] NZS4230, "Design of Reinforced Concrete Masonry Structures," vol. 4230, ed: New Zealand Standard, 2004.
- [10] G. Magenes and S. Pampanin, "Seismic Response of Gravity-Load Design Frames with Masonry Infills," in 13th World Conference on Earthquake Engineering, Vancouver, B.C., Canada, 2004.
- [19] M. Aliaari and A. M. Memari, "Experimental Evaluation of a Sacrificial Seismic Fuse Device for Masonry Infill Walls," *Journal of Architectural Engineering*, vol. 13, pp. 111-125, June 2007.
- [20] M. Aliaari and A. M. Memari, "Analysis of Masonry Infilled Steel Frames with Seismic Isolator Subframes," *Engineering Structures*, vol. 27, pp. 487-500, 2005.

- [21] M. Mohammadi and V. Akrami, "An Engineered Infilled Frame: Behavior and Calibration," *Journal of Constructional Steel Research*, vol. 66, pp. 842-849, 2010.
- [37] R. Langenbach, "Learning from the Past to Protect the Future: Armature Crosswalls," *Engineering Structures*, vol. 30, pp. 2096-2100, 2008.
- [46] S. Pampanin, A. Palermo, and D. Marriott, *PRESSS Design Handbook: NZ Concrete Society Inc.*, 2010.
- [49] S. H. Bertoldi, L. D. Decanini, and C. Gavarini, "Telai Tamponati Soggetti ad Azione Sismica, un Modello Semplificato: Confronto Sperimentale e Numerico (in Italian),", presented at the *Atti Del 6 Convegno Nazionale ANIDIS*, 1993.
- [50] H. B. Kaushik, D. C. Rai, and S. K. Jain, "Stress-Strain Characteristics of Clay Brick Masonry under Uniaxial Compression," *Journal of Materials in Civil Engineering*, vol. 19, pp. 728-739, September 1, 2007.
- [58] B. S. Smith, "Methods for Predicting the Lateral Stiffness and Strength of Multi-Storey Infilled Frames," *Build. Sci.*, vol. 2, pp. 247-257, 1967.
- [59] T. C. Liauw, "An Approximate Method of Analysis for Infilled Frames With or Without Opening," *Build. Sci.*, vol. 7, pp. 233-238, 1972.
- [60] T. C. Liauw, "Stress Analysis for Panel of Infilled Frames," *Build. Sci.*, vol. 8, pp. 105-112, 1973.
- [61] M. J. N. Priestley, S. Sritharan, J. R. Conley, and S. Pampanin, "Preliminary Results and Conclusions from the PRESSS Five-Story Precast Concrete Test Building," *PCI Journal*, vol. 44, November-December 1999.
- [62] A. Cholewick, "Loadbearing Capacity and Deformability of Vertical Joints in Structural Walls of Large Panel Buildings," *Build. Sci.*, vol. 6, pp. 163-184, 1971.
- [63] O. A. Glogau, "Separation of Non-Structural Components in Buildings," presented at the *South Pacific Conference on Earthquake Engineering*, Wellington, 1975.
- [64] USG, "Steel Stud and Track System Height Tables," ed, 2008.



# CHAPTER 9

## NUMERICAL CASE STUDIES

*What is a scientist after all? It is a curious man looking through a keyhole, the keyhole  
of nature, trying to know what's going on.*

*Jacques Yves Cousteau*





## 9 NUMERICAL CASE STUDIES

The seismic performance of the as built non-structural walls and the performance of the developed low damage solutions were numerically studied using a typical multi storey building for New Zealand. The aim was to confirm the global benefits arising from the implementation of the proposed and tested low damage solutions. The models of the infill walls, calibrated using the experimental results, were implemented in a 10 storey bare frame model. Then, 16 ground motion accelerations were used to carry out time-history analyses in order to observe the resulting inter-storey drift levels.

### 9.1 Case Study Building: 10 Storey NZS 3101 Compliant Redbook Building

The selected building was a case study RC frame building designed according to the guidelines given in NZS 3101 [65]. The design and the detailing of this example building are reported in details in the ‘Redbook’ by Bull, D. [66]. Due to the well defined design and ease of modelling, this building was chosen to be a good representative of the buildings resulting from the application of the New Zealand Reinforced Concrete Design Code (NZS3101). Section sizes, plan and elevation view of the building are shown in Table 9.1 and in Figure 9.1. For the analyses, the finite element dynamic structural analysis software Ruaumoko 2D was used.

**Table 9.1.** Section sizes of the modelled building

Section	Area	$0.6I_g$	$A \times I_g$ (x)	$B \times I_g$ (y)	Comment
900×460	0.414	0.0168	-	-	Exterior Column (x)
900×460	0.414	0.0044	-	-	Exterior Column (y)
900×400	0.360	-	( <b>A=0.4</b> ), 0.0097	( <b>B=0.4</b> ), 0.0019	Exterior Beam
750×530	0.431	-	( <b>A=0.35</b> ), 0.0078	( <b>B=0.35</b> ), 0.0033	Interior Beam

For modelling, a lumped plasticity approach was implemented in Ruaumoko 2D. Structural elements were modelled elastically with concentrated plasticity at member ends where Takeda hysteresis rule was assigned for beams and columns. As per the diagonal struts for non-structural walls, the calibrated Wayne Stewart degrading stiffness models were added to all the bays and the floors of the bare frame model. The weight contribution given by the non-structural drywalls was neglected since these are

very light elements compared to the weight of the structural elements. The additional weight given by the unreinforced clay bricks were considered in the building model. The building model was assumed to have fixed base supports with no soil structure interaction and the damping was typically assumed as 5%. The RC frame section details and their behaviour are shown in Figure 9.2 and Figure 9.3. More details about this building can be found in [66]. For reference, the Ruaumoko2D model of the building with as built steel framed drywalls is given in the Appendix H. The strut data can be replaced by any of the other given models to obtain the other building models adopted in the study reported herein.

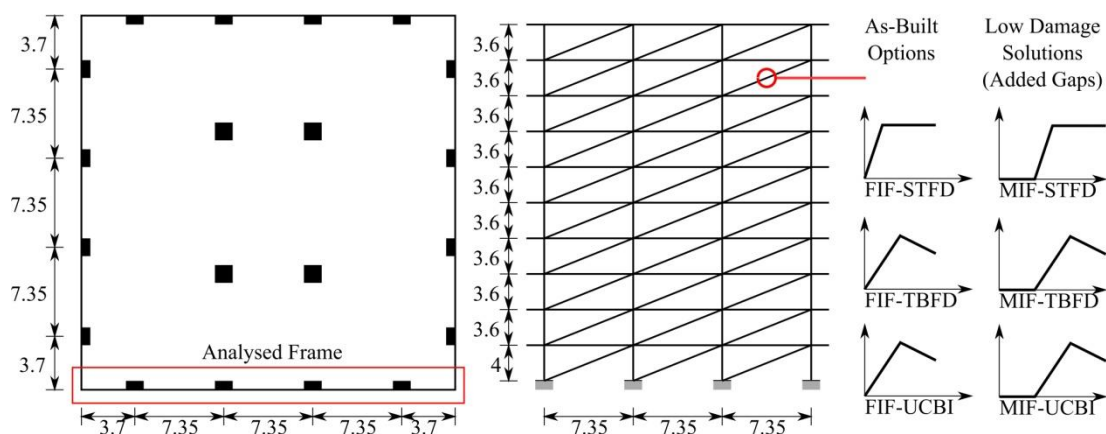


**Figure 9.1.** The plan and elevation view of the modelled exterior bare frame

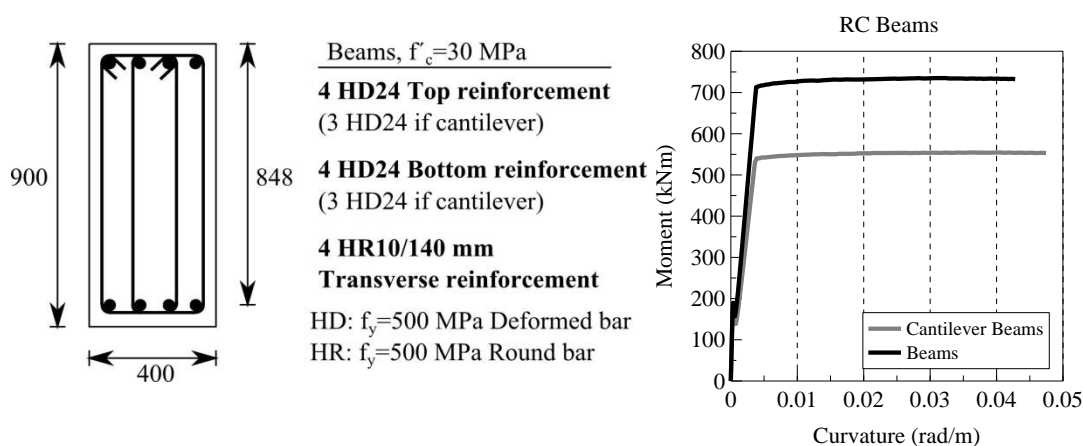


**Figure 9.2.** The details and the moment curvature of the RC beams from Bull and Brunsdon [66]

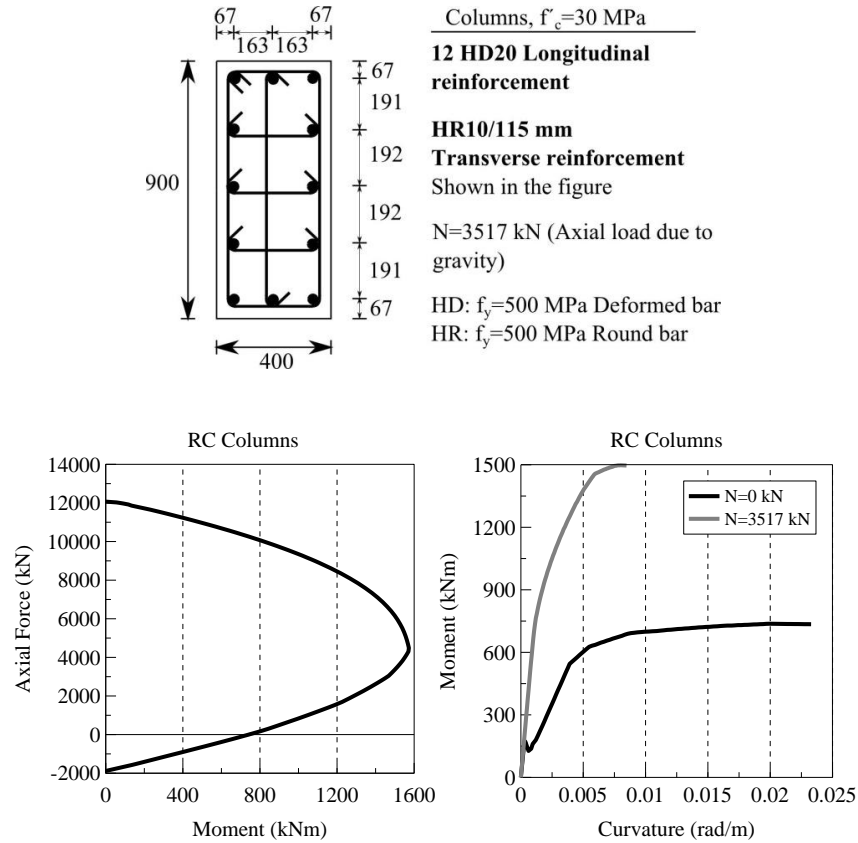


**Figure 9.3.** The details, the axial force-moment interaction and moment curvature diagrams of the RC columns from Bull and Brunsdon [66]

## 9.2 Applied Earthquakes

Recently, Christchurch has been struck by an unusual sequence of earthquake events starting with 4<sup>th</sup> of September 2010. The total number of earthquakes above the magnitude 3.0, 4.0, 5.0 and 6.0 were reported as 4423, 958, 82, 9 respectively (EQC/GNS [34]) with the most intensive and devastating one being February 22, 2011 ( $M_w$  6.3, depth 5 km). One of the most common observations was that during the sequence of strong aftershocks ( $M_w$  5+), many if not most of the modern buildings suffered moderate to extensive damage to the non-structural walls that needed repeatedly extensive repair or complete replacement. Among these earthquakes, two were outstanding considering their destructive intensity and the resulting levels of imposed drifts on the buildings. These two earthquakes were the 4<sup>th</sup> September 2010 (main shock) and the 22<sup>nd</sup> February 2011 (aftershock) earthquakes in Darfield and Christchurch respectively. The aftermath of these series of earthquakes was well reported by the Royal Commission of Canterbury Earthquakes in 2012 and by the New Zealand Society for Earthquake Engineering (NZSEE) in two special issues of the

bulletin [35, 36, 67]. Due to their relevance, 8 ground motion records taken during these two earthquakes were primarily chosen for the analyses. In order to investigate the seismic response of the structure under different type of earthquake ground motions, 8 additional records were chosen, which were compatible with the acceleration and displacement response spectrum suggested by the NZS1170.5 guidelines. It should be noted that these ground motions were selected such that they follow approximately the acceleration response spectrum for NZ. The purpose of the analyses was to show the performance of the developed low damage solutions when compared to the as built and the bare frame options by comparing the resulting maximum inter-storey drift profiles.

The adopted ground motion records are listed in Table 9.2. The ground motions of the given earthquakes, NZS1170.5: 2004 acceleration and displacement response spectrum [68] are summarized in Figure 9.4 (i.e. compatible with 1/500 year spectrum) and in Figure 9.5 (i.e. compatible with 1/2500 year spectrum). For the NZS1170.5 acceleration and displacement response spectrum, soil type D and the post earthquake seismicity of  $Z=0.3$  was adopted. The ground motion data for Christchurch earthquakes (EQ1-EQ8) was obtained from Canterbury Earthquakes and Ground Motion Prediction Data given by Bradley [69] and the remaining earthquake data (EQ9-EQ16) was obtained from PEER Ground motion database [70].

**Table 9.2.** List of the earthquakes

#	Earthquake	Station	Notation	PGA (g)	$M_w$
EQ1	Darfield 2010	Christchurch Cathedral College	EQ1-DAR-CCCC-1	0.23	7.1
EQ2	Darfield 2010	Christchurch Hospital	EQ2-DAR-CHHC-2	0.15	7.1
EQ3	Darfield 2010	Christchurch Resthaven	EQ3-DAR-REHS-1	0.25	7.1
EQ4	Darfield 2010	Christchurch Botanic Gardens	EQ4-DAR-CBGS-1	0.15	7.1
EQ5	Christchurch 2011	Christchurch Cathedral College	EQ5-LYT-CCCC-1	0.5	6.3
EQ6	Christchurch 2011	Christchurch Hospital	EQ6-LYT-CHHC-2	0.38	6.3
EQ7	Christchurch 2011	Christchurch Resthaven	EQ7-LYT-REHS-1	0.71	6.3
EQ8	Christchurch 2011	Christchurch Botanic Gardens	EQ8-LYT-CBGS-1	0.57	6.3
EQ9	Imperial Valley 1979	El Centro Array	EQ9-IMPV-ECA	0.53	6.5
EQ10	Northridge 1994	LA Dam	EQ10-NTHR-LD	0.42	6.7
EQ11	Erzincan, Turkey 1992	Erzincan	EQ11-ERZTR-E	0.49	6.7
EQ12	Chi-Chi, Taiwan 1999	TCU076	EQ12-CCTW-TCU076	0.3	7.6
EQ13	Tabas, Iran 1978	Tabas	EQ13-TIR-T	0.81	7.3
EQ14	Loma Prieta 1989	LGPC	EQ14-LP-LGPC	0.94	6.9
EQ15	Northridge 1994	Rinaldi Receiving	EQ15-NTHR-RR	0.87	6.7
EQ16	Kobe, Japan 1995	Takatori	EQ16-KBJP-T	0.6	6.9

**PGA:** Peak ground acceleration  
 **$M_w$ :** Richter magnitude

These 16 earthquake records were used for the analyses of 7 models namely: Bare frame, frame infilled with as built steel/timber framed drywalls, frame infilled with as built unreinforced clay brick infill wall, and the low damage versions of these infill wall types. A total of 112 time history analyses were carried out.

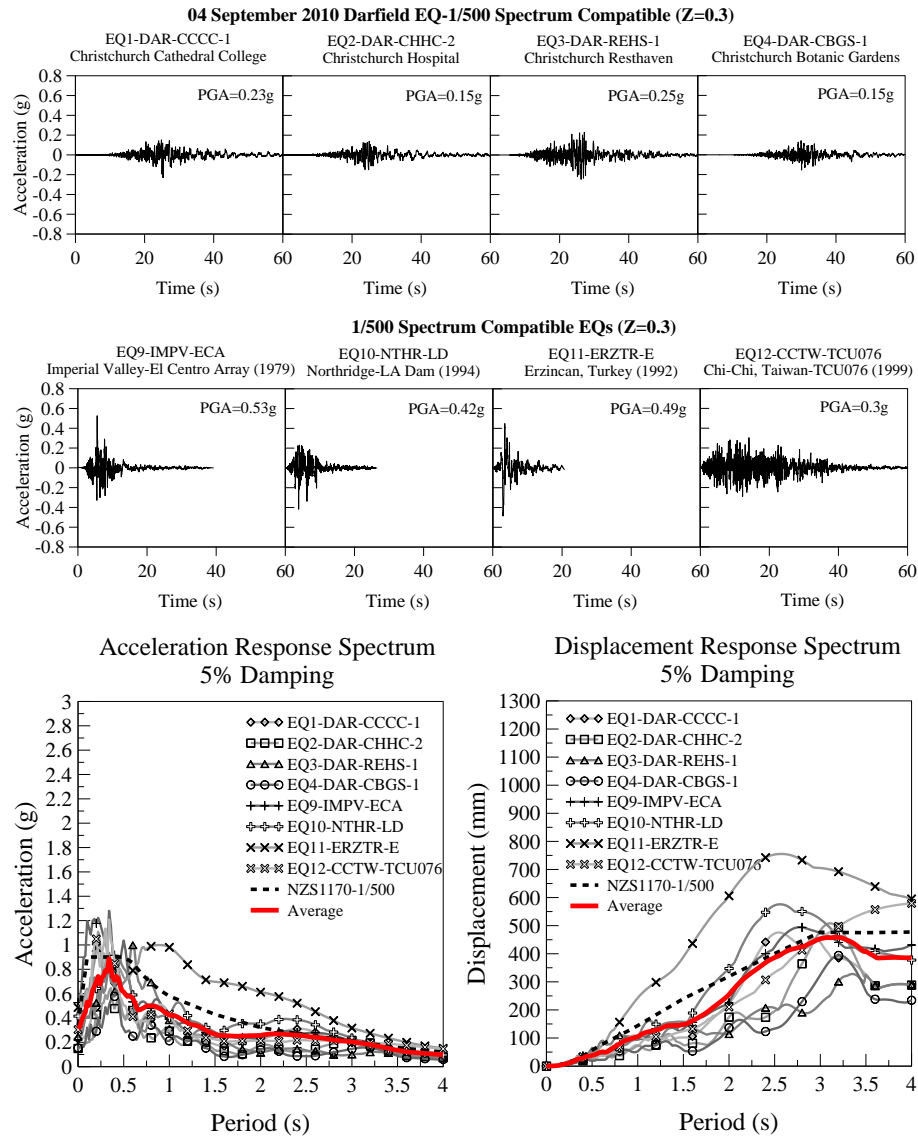


**Figure 9.4.** Recorded ground acceleration data, acceleration and displacement response spectrum for EQ1, EQ2, EQ3, EQ4 and EQ9, EQ10, EQ11, EQ12 (set compatible with 500 year return period spectrum)

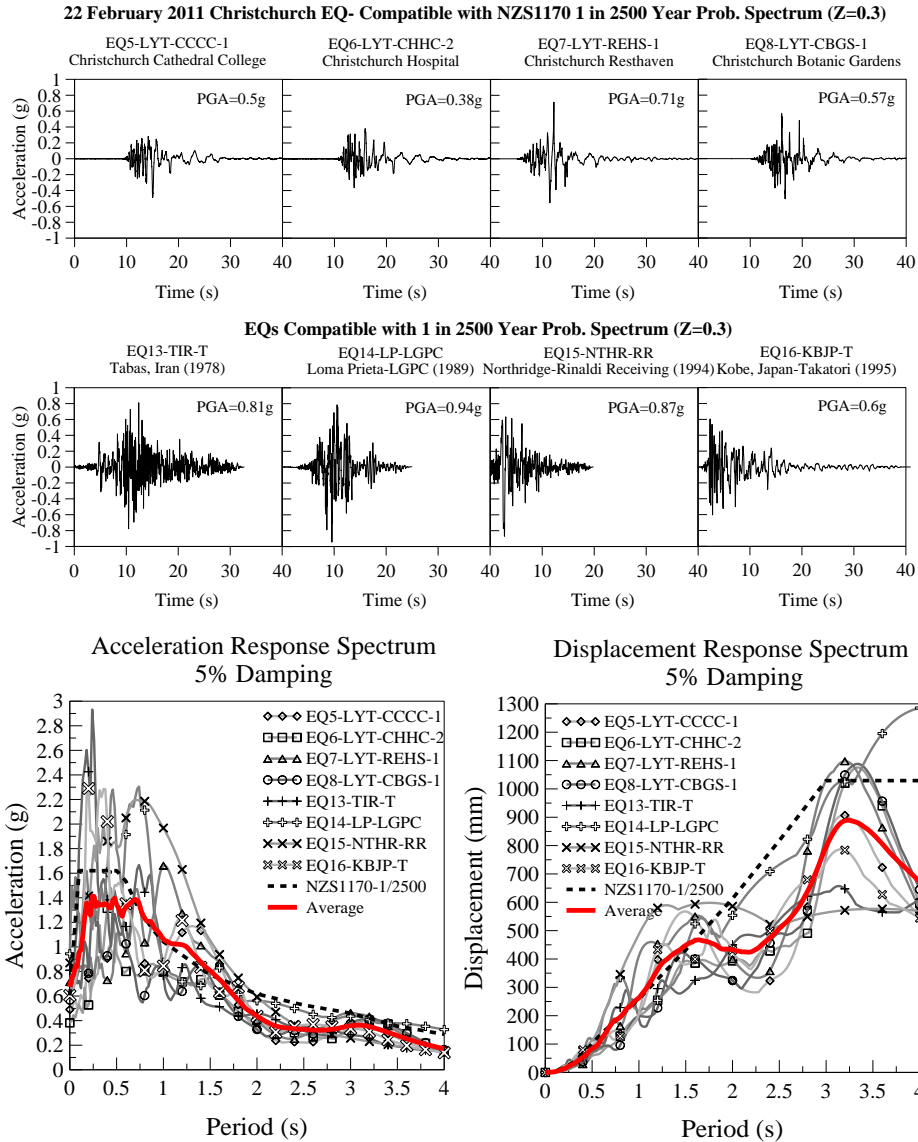


**Figure 9.5.** Recorded ground acceleration data, acceleration and displacement response spectrum for EQ5, EQ6, EQ7, EQ8 and EQ13, EQ14, EQ15, EQ16 (set compatible with 2500 year return period spectrum)

### 9.3 Results for As Built and Low Damage Drywalls

Using the calibrated models for as built and low damage steel/timber framed drywalls (Described by STFD and TBFD), diagonal struts were assigned to all the bays and the floors in the building. The weight contribution was neglected since these are very light elements compared to the weight of the structural elements. Then the given ground motion accelerations were applied to the structure. The results are summarized in Figure 9.6 for EQ1-EQ4, EQ9-EQ12 (500 year-NZ spectrum compatible set) and in Figure 9.7 for EQ5-EQ8, EQ13-EQ16 (2500 year-NZ spectrum compatible set).

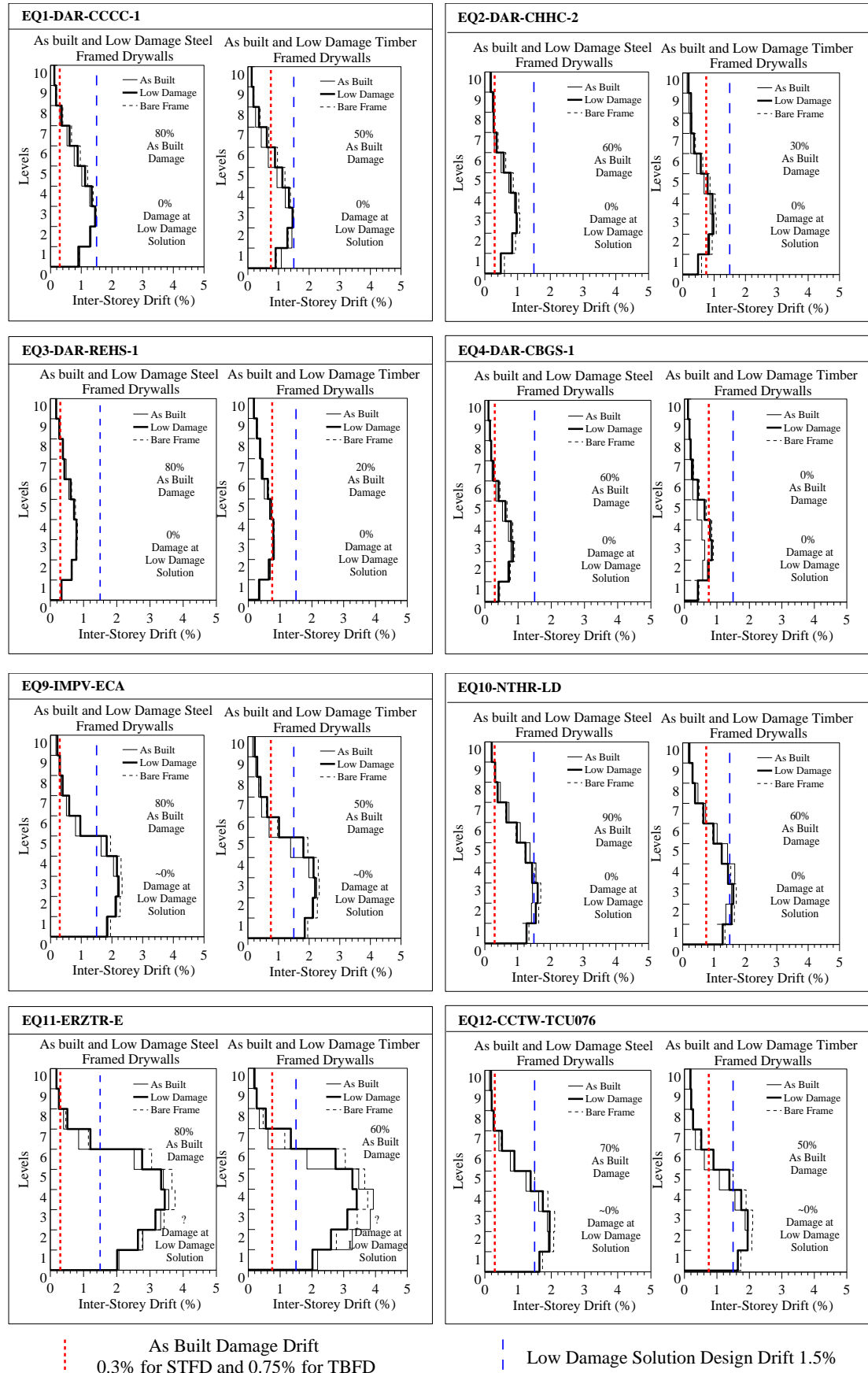


**Figure 9.6.** Comparison of as built and low damage drywall solutions using EQ1-EQ4 and EQ9-EQ12 (Set compatible with 500 year response spectrum)

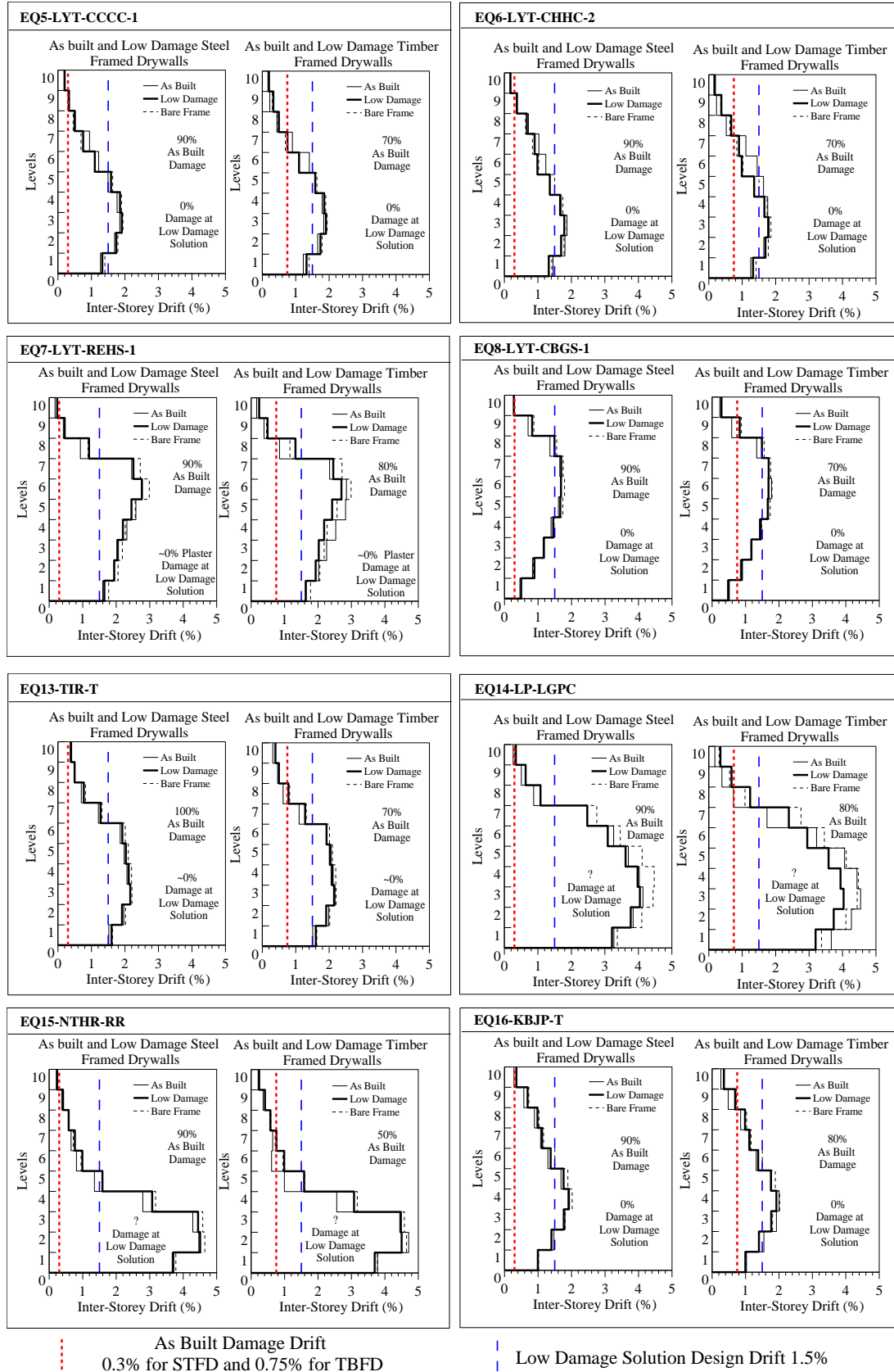


**Figure 9.7.** Comparison of as built and low damage drywall solutions using EQ5, EQ6, EQ7, EQ8 and EQ13, EQ14, EQ15, EQ16 (Set compatible with 2500 year spectrum)



From the results of Figure 9.6 and Figure 9.7, it can be concluded that both the as built and the low damage drywalls do not affect the resulting inter-storey drift profiles of the structure significantly, except for the as built timber framed drywall, which contributes slightly to reduce the inter-storey drifts. A slight change in the natural period of vibration of the structure was also observed in the results of the analyses. The bare frame and the frame infilled with the low damage solutions had a natural period of 1.95s. On the other hand, the as built steel and timber framed drywall infills resulted in a period of 1.74s (10% less than the bare frame).

Considering the extent of overall damage, it can be seen that the damage ratio of the as built steel framed drywalls were in the range of 60 to 100 percent. In other words, the number of floors where the inter-storey drift exceeded the damage drift was between 6 to 10 storeys. For the as built timber framed drywalls, these numbers were ranging from 0 to 80 percent. Compared to those, as expected, the low damage solutions performed very well with negligible damage during these earthquakes (Table 9.3). However, since there were no experimental observations about the damage state of low damage solutions after 2.5%, the damage estimations for higher drift levels is unknown (especially if higher than 3.0%). For those high drift levels, it was assumed that the L-trim plaster cracks progressed with no significant damage to linings. The statistical distribution of these results is summarized in Figure 9.8 using the given mean ( $\mu$ ) and standard deviation ( $\sigma$ ) values in Table 9.3.

**Table 9.3.** Summary for the percentage of the damage to non-structural walls in the model building

Earthquakes	As Built STFD	As Built TBFD	Low Damage	Low Damage
	T=1.74s Drift > 0.3%	T=1.74s Drift > 0.75%	STFD T=1.95s	TBFD T=1.95s
EQ1-EQ4(1/500)	60-80%	0-50%	0%	0%
EQ5-EQ8(1/2500)	90%	70-80%	~0%	~0%
EQ9-EQ12(1/500)	70-90%	50-60%	~0%	~0%
EQ13-EQ16(1/2500)	90-100%	50-80%	~0%	~0%
$\mu$ and $\sigma$ for 1/500yr	$\mu=75\%$ , $\sigma=10\%$	$\mu=40\%$ , $\sigma=20\%$	0%	0%
$\mu$ and $\sigma$ for 1/2500yr	$\mu=91.25\%$ , $\sigma=3.3\%$	$\mu=71.25\%$ , $\sigma=9.3\%$	0%	0%

Note: The damage percentage was calculated by dividing the number of floors exceeding the damage drift to the total number of floors

STFD : Steel Framed Drywall,

TBFD : Timber Framed Drywall,

~0 : Stands for Minor Damage (i.e. plaster cracks)

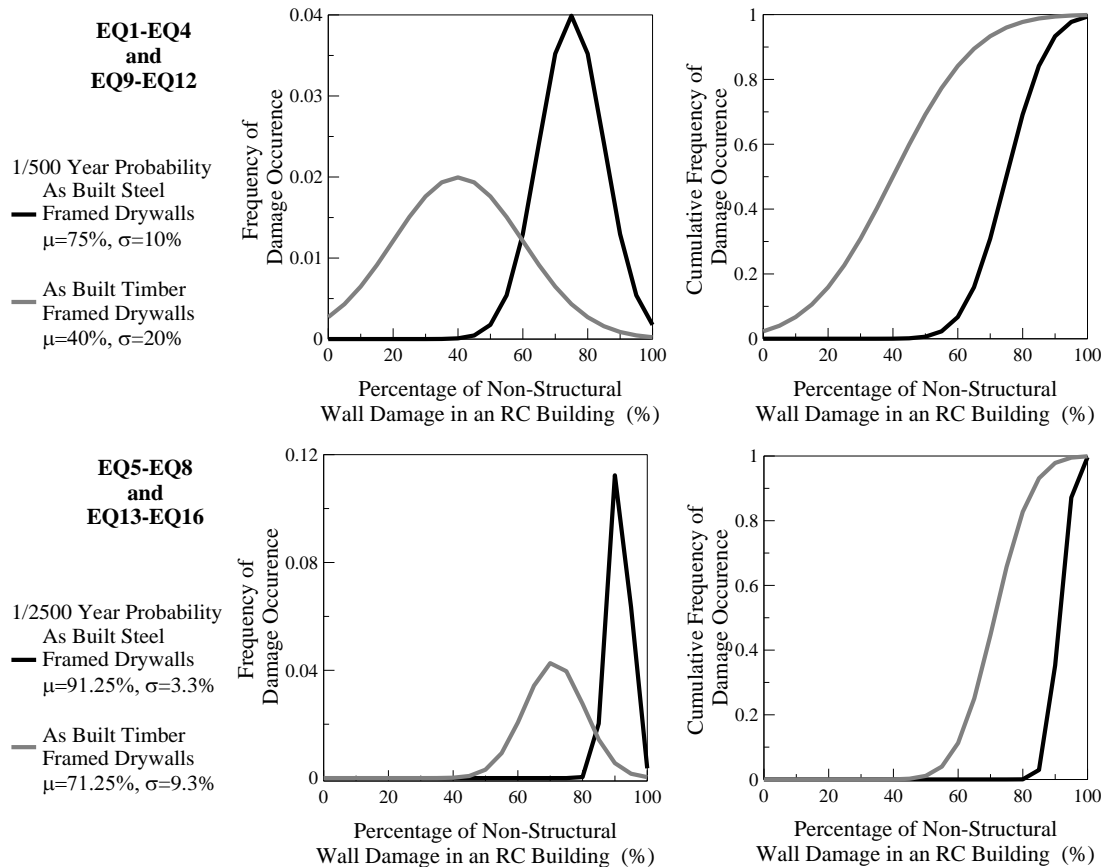


**Figure 9.8.** Distribution of the damage percentage for as built steel and timber framed drywalls for 1/500 year and 1/2500 year events

When EQ5-EQ8 and EQ13-EQ16 were applied on the structure, the damage to both the as built steel and timber framed drywalls was very high, which was expected due to the extreme intensity. The steel framed experienced 90% damage without any exception. The timber framed drywalls experienced damage ranging from 60 to 80%. On the other hand, again, the low damage solutions would provide superior seismic performance by very minor damage such as plaster cracks, which were observed in the experimental campaign after 2.0% drift. The low damage solutions caused no impairment to the serviceability of the drywalls when the global behaviour of the model building was inspected. It also confirmed the global benefits of using such walls in reducing the damage/costs associated with the failure/serviceability loss of these components.

#### 9.4 Results for As Built and Low Damage Unreinforced Clay Brick Infill Walls

Using the calibrated models for as built and low damage unreinforced clay brick infill walls (Described by UCBI), diagonal struts were assigned to all the bays and the floors in the building. The weight contribution given by the unreinforced clay brick infills was added to the existing building model. Then the given ground motion accelerations were applied on the structure. The resulting inter-storey drift profiles are summarized in Figure 9.9 and Figure 9.10.

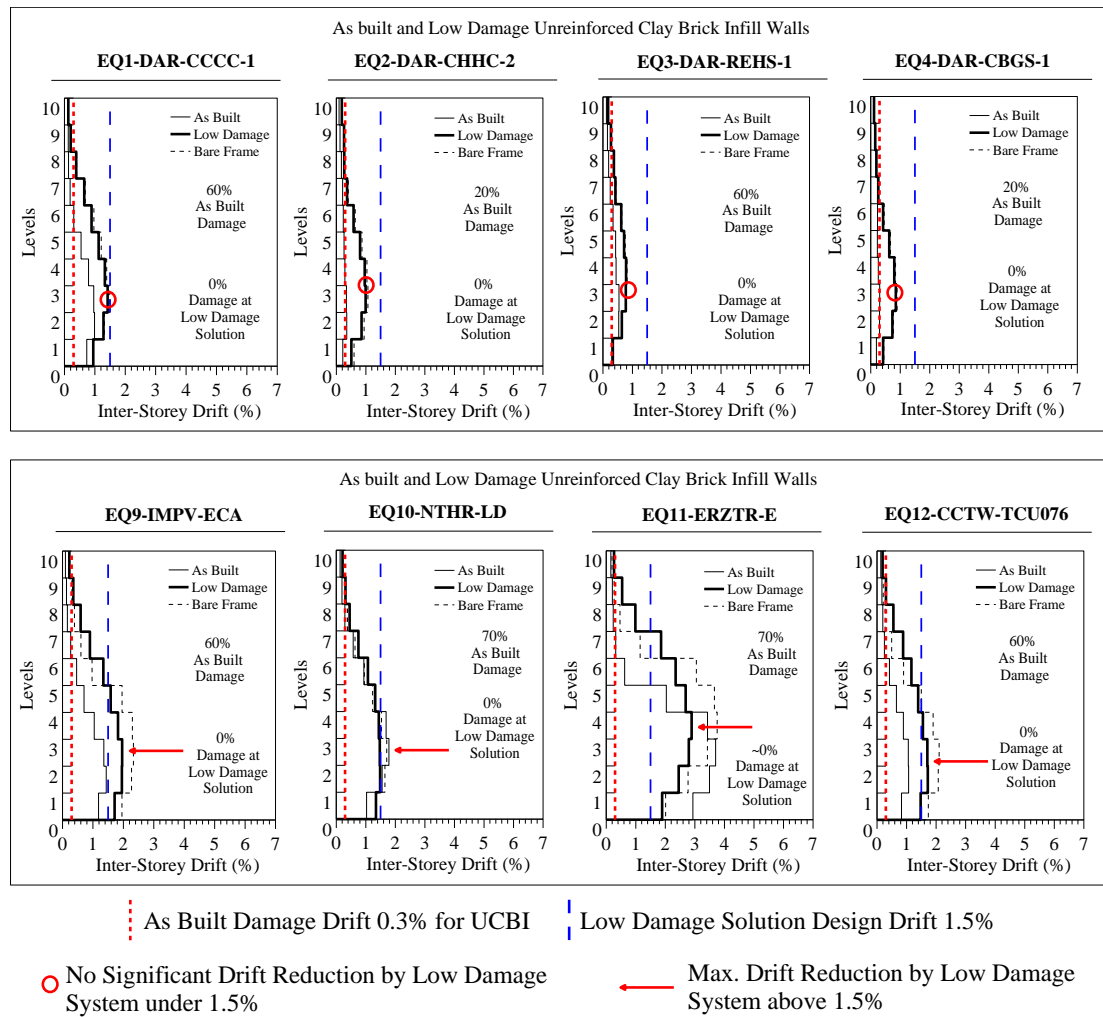


**Figure 9.9.** Inter-storey drift profile comparisons using EQ1-EQ4 and EQ9-EQ12, Soft storey mechanism at as-built and bare frame in EQ11 (Set compatible with 500 year spectrum)

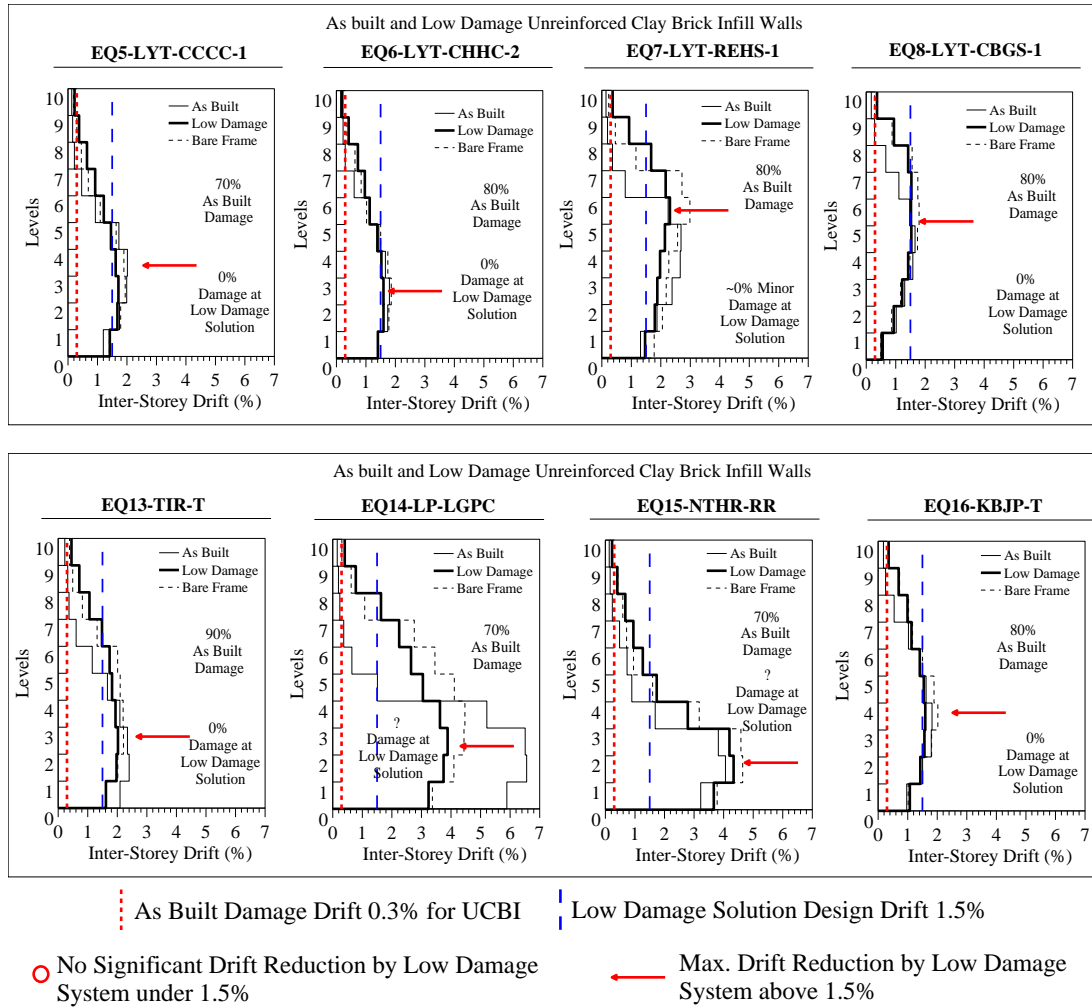


**Figure 9.10.** Inter-storey drift comparisons using EQ5-EQ8 and EQ13-EQ16, Soft storey mechanism at as built and bare frame in EQ7, EQ14 and EQ15 (Set compatible with 2500 year spectrum)

Although the EQ1-EQ8 were not as destructive as EQ9-EQ16, the damage to the unreinforced clay brick infill walls were significant due to the inherent vulnerabilities of the as built infill wall system and their low drift capacity ( $\sim 0.3\%$ ). The extent of damage to the as built clay brick infills were in the range of 20-60% for EQ1-EQ4 and 60-70% for EQ9-EQ12. In these events, the low damage solutions performed well and remained almost undamaged. For EQ1-EQ4, the low damage solution resulted in very similar inter-storey drift profiles to the bare frame due to the effectiveness of isolation/low damage system until 1.5% drift (The infill panel does not engage with the structural system until design drift). When the other earthquakes are inspected (EQ5-EQ8 and EQ13-EQ16), it can be observed that the as built infill walls suffered much higher damage rates due to the much higher ground accelerations caused by these ground motions. The extent of damage to the as built clay brick infilled structure was in the range of 70-90%. The low damage clay brick infill wall solution again showed

approximately 0% damage for most cases. However, due to the lack of experimental evidences on the level of damage for drift levels higher than 2.5%, an exact damage percentage could not be given for these walls at extreme inter-storey drift levels and they have been identified with a question mark in the given inter-storey drift profiles. The overall damage summary is shown in Table 9.4. The statistical distribution of these results is summarized in Figure 9.8 using the given mean ( $\mu$ ) and standard deviation ( $\sigma$ ) values in Table 9.4.

**Table 9.4.** Summary of the percentage of the damage to non-structural walls in the model building

Earthquake	As Built UCBI, T=1.28s	Low Damage UCBI, T=1.96s
	Drift > 0.3%	
EQ1-EQ4	20-60%	0%
EQ5-EQ8	70-80%	~0%
EQ9-EQ12	60-70%	~0%
EQ13-EQ16	70-90%	~0%-?
$\mu$ and $\sigma$ for 1/500yr	$\mu=52.5\%$ , $\sigma=19.2\%$	-
$\mu$ and $\sigma$ for 1/2500yr	$\mu=77.5\%$ , $\sigma=6.61\%$	-

UCBI : Unreinforced Clay Brick Infill Wall

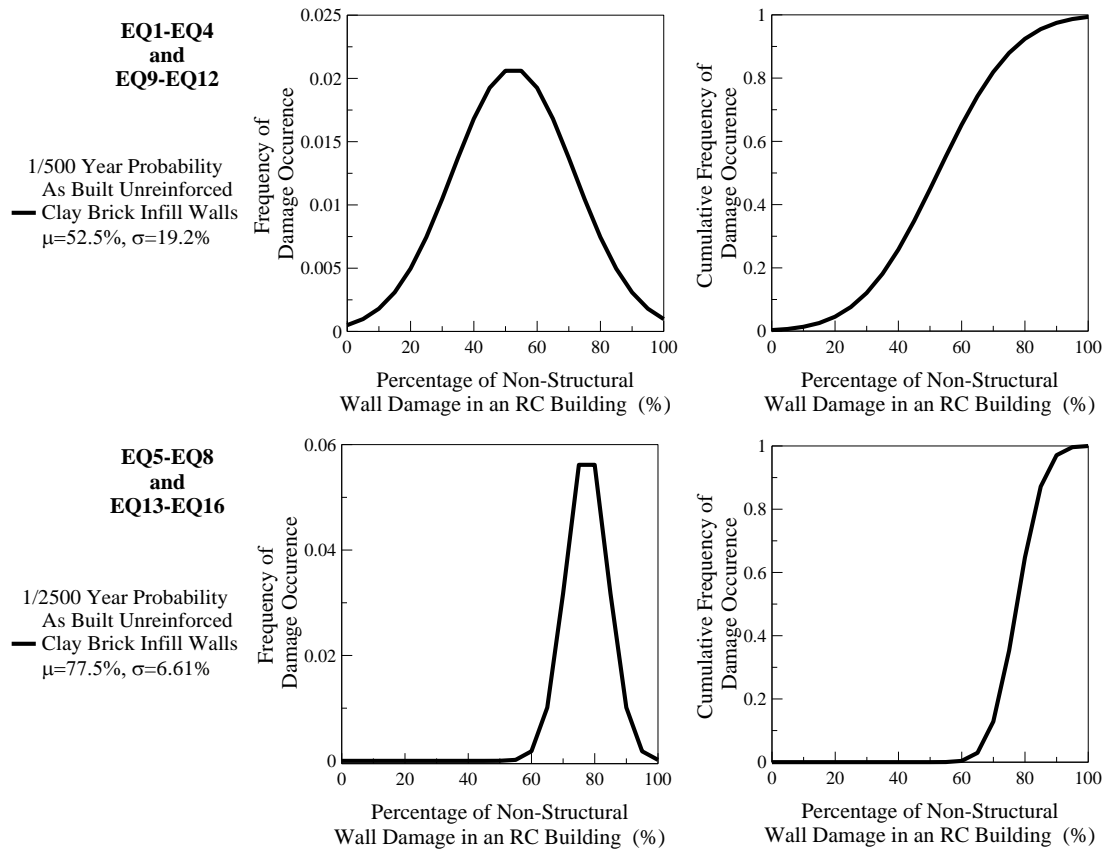


**Figure 9.11.** Distribution of the damage percentage for as built unreinforced clay brick infill walls for 1/500 year and 1/2500 year events

If the inter-storey drift profiles in Figure 9.9 and Figure 9.10 are studied, the effect of the low damage solution on the global response is evident. For earthquakes that impose inter-storey drift levels less than the design drift level (1.5%), the low damage solution provides full isolation between the infill panel zone and the structural system. This results in the same drift profiles for the bare frame and the low damage solution (i.e. EQ1-EQ4 in Figure 9.9). In the same earthquakes, although the as-built clay brick infills reduce the global drift profiles, they suffer in-plane damage, impairing their serviceability even if the building survives the event. The low damage non-structural unreinforced clay brick infill wall solution engages the structural system after the structure exceeds the design drift level, turning into a back up structural element. The reserved in-plane capacity is utilized from this drift level onwards, causing an adaptive bracing system that activates only at the required floor levels where the inter-storey drift level is higher than the design drift level, reducing the inter-storey drift level. For other floors with inter-storey drift levels smaller than 1.5%, they behave as bare frame.

Overall, this structural modification on the global behaviour results in more uniform inter-storey drift profiles. In some cases, this can prevent the formation of a soft-storey mechanism that develops in the as built option or the bare frame. The prevention of the soft-storey mechanism can clearly be observed in the inter-storey drift profiles under EQ11 in Figure 9.9 and EQ7, EQ14 in Figure 9.10. These analyses confirmed the global performance of the low damage solutions in both preventing infill wall damage and improving the global seismic performance. The inter-storey drift profiles shown in Figure 9.6, Figure 9.7 and Figure 9.9, Figure 9.10 are numerically summarized in Table 9.5 for EQ1-EQ8 and in Table 9.6 for EQ9-EQ16.

**Table 9.5.** Numerical summary of the inter-storey drift profiles for EQ1-EQ8

Inter-Storey Drifts	EQ1-DAR-CCCC-1								EQ2-DAR-CHHC-2								EQ3-DAR-RHS-1								EQ4-DAR-CBGS-1							
	FIF		MIF		TFBD		UBFI		FIF		MIF		TFBD		UBFI		FIF		MIF		TFBD		UBFI		FIF		MIF		TFBD		UBFI	
	BF	STFD	STFD	STFD	TFBD	TFBD	UBFI	UBFI	BF	STFD	STFD	STFD	TFBD	TFBD	UBFI	UBFI	BF	STFD	STFD	STFD	TFBD	TFBD	UBFI	UBFI	BF	STFD	STFD	STFD	TFBD	TFBD	UBFI	UBFI
LVL1	0.926	0.9518	0.9054	1.09	0.9054	0.7319	0.9475	0.5992	0.5149	0.4893	0.4666	0.4893	0.2192	0.5094	0.5094	0.3401	0.3365	0.3368	0.3607	0.3368	0.2999	0.3349	0.3349	0.4467	0.3906	0.4142	0.3104	0.4142	0.1916	0.4192		
LVL2	1.315	1.318	1.29	1.438	1.29	0.989	1.284	0.9403	0.838	0.8371	0.7986	0.8371	0.3528	0.8555	0.8555	0.6542	0.6462	0.6445	0.6894	0.6445	0.536	0.6404	0.6404	0.7695	0.6917	0.7278	0.5617	0.7278	0.2995	0.7343		
LVL3	1.489	1.435	1.438	1.481	1.458	0.9628	1.42	1.07	0.9582	0.977	0.9312	0.977	0.3411	0.9931	0.9931	0.7986	0.7843	0.7812	0.8193	0.7812	0.5439	0.7757	0.7757	0.8934	0.7882	0.8444	0.6242	0.8444	0.3034	0.8521		
LVL4	1.39	1.278	1.343	1.223	1.343	0.7911	1.33	1.037	0.9064	0.9482	0.8718	0.9482	0.2877	0.963	0.963	0.818	0.7795	0.7875	0.7885	0.7875	0.4454	0.7844	0.7844	0.8431	0.7111	0.79	0.5381	0.79	0.255	0.7987		
LVL5	1.21	1.017	1.126	0.9507	1.126	0.5452	1.125	0.8704	0.7332	0.7921	0.6803	0.7921	0.2259	0.8041	0.8041	0.7579	0.6971	0.7165	0.6654	0.7165	0.4295	0.7177	0.7177	0.6706	0.5298	0.6205	0.3921	0.6205	0.2248	0.6288		
LVL6	0.968	0.7704	0.8847	0.6659	0.8847	0.3046	0.8923	0.6407	0.4972	0.5767	0.444	0.5767	0.234	0.584	0.584	0.6406	0.5548	0.6133	0.6133	0.3434	0.6202	0.6202	0.457	0.3324	0.4131	0.2554	0.4131	0.2294	0.4187			
LVL7	0.685	0.5362	0.6198	0.4359	0.6198	0.1838	0.6515	0.4053	0.2888	0.3611	0.2573	0.3611	0.213	0.3639	0.3639	0.4409	0.4763	0.4241	0.4717	0.4241	0.2463	0.4229	0.4229	0.2812	0.2168	0.2553	0.2109	0.2553	0.2267	0.2581		
LVL8	0.401	0.3057	0.3626	0.2499	0.3626	0.1328	0.3856	0.2785	0.2551	0.2741	0.2352	0.2741	0.1698	0.2686	0.2686	0.3844	0.3948	0.3768	0.351	0.3768	0.1924	0.3715	0.3715	0.1958	0.1843	0.1924	0.1834	0.1924	0.186	0.1932		
LVL9	0.195	0.1599	0.1809	0.1769	0.1809	0.1244	0.2048	0.2696	0.2316	0.2653	0.1955	0.2653	0.1238	0.2619	0.2619	0.2778	0.2535	0.2725	0.2458	0.2725	0.1517	0.2736	0.2736	0.1565	0.15	0.1559	0.1533	0.1559	0.133	0.1538		
LVL10	0.125	0.121	0.125	0.1367	0.125	0.1041	0.1268	0.1896	0.1595	0.1871	0.1398	0.1871	0.0914	0.1859	0.1859	0.1784	0.1674	0.1767	0.1673	0.1767	0.1165	0.1757	0.1757	0.1129	0.1045	0.1104	0.1131	0.1104	0.1008	0.1129		
Damage (%)	-	80	0	50	0	60	0	-	60	0	30	0	20	0	0	-	80	0	20	0	60	0	0	-	60	0	0	0	0	20	0	
μ (%)	Mean and Standard Deviation Considering EQ1-EQ4 and EQ9-EQ12																EQ8-LYT-CBGS-1															
σ (%)	Mean and Standard Deviation Considering EQ1-EQ4 and EQ9-EQ12																EQ8-LYT-CBGS-1															
Inter-Storey Drifts	EQ5-LYT-CCCC-1								EQ6-LYT-CHHC-2								EQ7-LYT-RHS-1								EQ8-LYT-CBGS-1							
	FIF		MIF		TFBD		UBFI		FIF		MIF		TFBD		UBFI		FIF		MIF		TFBD		UBFI		FIF		MIF		TFBD		UBFI	
	BF	STFD	STFD	STFD	TFBD	TFBD	UBFI	UBFI	BF	STFD	STFD	STFD	TFBD	TFBD	UBFI	UBFI	BF	STFD	STFD	STFD	TFBD	TFBD	UBFI	UBFI	BF	STFD	STFD	STFD	TFBD	TFBD	UBFI	UBFI
LVL1	1.402	1.268	1.324	1.225	1.324	1.198	1.419	1.416	1.453	1.325	1.255	1.325	1.426	1.407	1.407	1.776	1.599	1.646	1.621	1.637	1.312	1.468	1.468	0.8945	0.4576	0.4971	0.4607	0.4971	0.3861	0.5272		
LVL2	1.789	1.69	1.74	1.656	1.74	1.747	1.677	1.78	1.807	1.694	1.645	1.694	1.739	1.599	1.599	2.056	1.933	1.942	2.02	1.93	1.871	1.798	1.798	0.8645	0.834	0.8919	0.8432	0.8919	1.017	0.9339		
LVL3	1.941	1.847	1.907	1.84	1.907	1.992	1.711	1.861	1.869	1.789	1.761	1.789	1.797	1.597	1.597	2.184	2.067	2.035	2.258	2.023	2.382	1.833	1.833	1.166	1.152	1.177	1.164	1.177	1.305	1.221		
LVL4	1.897	1.765	1.853	1.791	1.853	2.014	1.618	1.745	1.692	1.664	1.762	1.664	1.661	1.526	1.526	2.273	2.318	2.201	2.529	2.184	2.658	1.977	1.977	1.482	1.388	1.455	1.415	1.455	1.581	1.424		
LVL5	1.635	1.493	1.585	1.57	1.585	1.726	1.459	1.502	1.356	1.357	1.637	1.357	1.438	1.391	1.391	2.57	2.587	2.456	2.824	2.423	2.685	2.141	2.141	1.739	1.609	1.665	1.687	1.665	1.655	1.532		
LVL6	1.094	1.216	1.101	1.407	1.101	0.928	1.214	1.025	1.237	0.9877	1.447	0.9877	1.118	1.13	1.13	2.988	2.779	2.765	2.851	2.702	2.248	2.31	2.31	1.793	1.691	1.687	1.776	1.687	1.474	1.519		
LVL7	0.689	0.9423	0.7529	0.8999	0.7529	0.4634	0.9231	0.8393	1.029	0.904	1.109	0.904	0.6011	0.9648	0.9648	2.719	2.462	2.514	2.347	2.456	0.794	2.167	2.167	1.752	1.649	1.692	1.69	1.692	1.108	1.354		
LVL8	0.455	0.5046	0.4966	0.4367	0.4966	0.2174	0.6452	0.6298	0.7169	0.6709	0.5214	0.6709	0.2259	0.7308	0.7308	1.159	0.9303	1.19	0.8484	1.327	0.3612	1.673	1.673	1.558	1.355	1.491	1.333	1.491	0.6636	1.422		
LVL9	0.301	0.3045	0.3303	0.2238	0.3303	0.1573	0.3769	0.3566	0.3767	0.3757	0.23	0.3757	0.2284	0.4167	0.4167	0.4592	0.4206	0.4645	0.3849	0.4921	0.1928	0.9259	0.9259	0.8777	0.7032	0.8257	0.5856	0.8257	0.2843	0.9415		
LVL10	0.187	0.1853	0.2007	0.1687	0.2007	0.1269	0.2239	0.1856	0.1665	0.1829	0.1505	0.1829	0.1434	0.1995	0.1995	0.2341	0.1749	0.2398	0.1635	0.2398	0.1419	0.367	0.367	0.286	0.2703	0.2804	0.2279	0.2804	0.1721	0.367		
Damage (%)	-	90	0	70	0	70	0	-	90	0	70	0	80	0	0	-	90	0	80	0	80	0	0	-	90	0	70	0	80	0	0	
μ (%)	Mean and Standard Deviation Considering EQ5-EQ8 and EQ13-EQ16																EQ9-LYT-CBGS-1															
σ (%)	Mean and Standard Deviation Considering EQ5-EQ8 and EQ13-EQ16																EQ9-LYT-CBGS-1															
Notation	EQ9-LYT-CCCC-1								EQ10-LYT-CHHC-2								EQ11-LYT-RHS-1								EQ12-LYT-CBGS-1							
	FIF		MIF		TFBD		UBFI		FIF		MIF		TFBD		UBFI		FIF		MIF		TFBD		UBFI		FIF		MIF		TFBD		UBFI	
	BF	STFD	STFD	STFD	TFBD	TFBD	UBFI	UBFI	BF	STFD	STFD	STFD	TFBD	TFBD	UBFI	UBFI	BF	STFD	STFD	STFD	TFBD	TFBD	UBFI	UBFI	BF	STFD	STFD	STFD	TFBD	TFBD	UBFI	UBFI
LVL1	0.926	0.9518	0.9054	1.09	0.9054	0.7319	0.9475	0.5992	0.5149	0.4893	0.4666	0.4893	0.2192	0.5094	0.5094	0.3401	0.3365	0.3368	0.3607	0.3368	0.2999	0.3349	0.3349	0.4467	0.3906	0.4142	0.3104	0.4142	0.1916	0.4192		
LVL2	1.315	1.318	1.29	1.438	1.29	0.989	1.284	0.9403	0.838	0.8371	0.7986	0.8371	0.3528	0.8555	0.8555	0.6542	0.6462	0.6445	0.6894	0.6445	0.536	0.6404	0.6404	0.7695	0.6917	0.7278	0.5617	0.7278	0.2995	0.7343		
LVL3	1.489	1.435	1.438	1.481	1.458	0.9628	1.42	1.07	0.9582	0.977	0.9312	0.977	0.3411	0.9931	0.9931	0.7986	0.7843	0.7812	0.8193	0.7812	0.5439	0.7757	0.7757	0.8934	0.7882	0.8444	0.6242	0.8444	0.3034	0.8521		
LVL4	1.39	1.278	1.343	1.223	1.343	0.7911	1.33	1.037	0.9064	0.9482	0.8718	0.9482	0.2877	0.963	0.963	0.818	0.7795	0.7875	0.7885	0.7875	0.4454	0.7844	0.7844	0.8431	0.7111	0.79	0.5381	0.79	0.255	0.7987		
LVL5	1.21	1.017	1.126	0.9507	1.126	0.5452	1.125	0.8704	0.7332	0.7921	0.6803	0.7921	0.2259	0.8041	0.8041	0.7579	0.6971	0.7165	0.6654	0.7165	0.4295	0.7177	0.7177	0.6706	0.5298	0.6205	0.3921	0.6205	0.2248	0.6288		
LVL6	0.968	0.7704	0.8847	0.6659	0.8847	0.3046	0.8923	0.6407	0.4972	0.5767	0.444	0.5767	0.234	0.584	0.584	0.6406	0.5548	0.6133	0.6133	0.3434	0.6202	0.6202	0.457	0.3324	0.4131	0.2554	0.4131	0.2294	0.4187			
LVL7	0.685	0.5362	0.6198	0.4359	0.6198	0.1838	0.6515	0.4053	0.2888	0.3611	0.2573	0.3611	0.213	0.3639	0.3639	0.4409	0.4763	0.4241	0.4717	0.4241	0.2463	0.4229	0.4229	0.2812	0.2168	0.2553	0.2109	0.2553	0.2267	0.2581		
LVL8	0.401	0.3057	0.3626	0.2499	0.3626	0.1328	0.3856	0.2785	0.2551	0.2741	0.2352	0.2741	0.1698	0.2686	0.2686	0.3844	0.3948	0.3768	0.351	0.3768	0.1924	0.3715	0.3715	0.1958	0.1843	0.1924	0.1834	0.1924	0.186	0.1932		
LVL9	0.195	0.1599	0.1809	0.1769	0.1809	0.1244	0.2048	0.2696	0.2316	0.2653	0.1955	0.2653	0.1238	0.2619	0.2619	0.2778	0.2535	0.2725	0.2458	0.2725	0.1517	0.2736	0.2736	0.1565	0.15	0.1559	0.1533	0.1559	0.133	0.1538		
LVL10	0.125	0.121	0.125	0.1367	0.125	0.1041	0.1268	0.1896	0.1595	0.1871	0.1398	0.1871	0.0914	0.1859	0.1859	0.1784	0.1674	0.1767	0.1673	0.1767	0.1165	0.1757	0.1757	0.1129	0.1045	0.1104	0.1131	0.1104	0.1008	0.1129		
Damage (%)	-	80	0	50	0	60	0	-	60	0	30	0	20	0	0	-	80	0	20	0	60	0	0	-	60	0	0	0	0	20	0	
μ (%)	Mean and Standard Deviation Considering EQ5-EQ8 and EQ13-EQ16																EQ9-LYT-CBGS-1															
σ (%)	Mean and Standard Deviation Considering EQ5-EQ8 and EQ13-EQ16																EQ9-LYT-CBGS-1															
Notation	EQ13-LYT-CCCC-1								EQ14-LYT-CHHC-2								EQ15-LYT-RHS-1								EQ16-LYT-CBGS-1							
	FIF		MIF		TFBD		UBFI		FIF		MIF		TFBD																			



**Table 9.6.** Numerical summary of the inter-storey drift profiles for EQ9-EQ16

Inter-Storey Drifts	EQ9-IMPV-ECA										EQ10-NTHR-LD										EQ11-ERZIRE										EQ12-CCTW-TCU076																																																																																																																																																																																																																																																																																																																																																																																																																																																																																																																																																																																																																																																																																																																																																																																																														
	FIF					STFD					FIF					STFD					FIF					STFD					FIF					STFD					FIF					STFD																																																																																																																																																																																																																																																																																																																																																																																																																																																																																																																																																																																																																																																																																																																																																																																															
	BF	STFD	STFD	STFD	STFD	BF	STFD	STFD	STFD	STFD	BF	STFD	STFD	STFD	STFD	BF	STFD	STFD	STFD	STFD	BF	STFD	STFD	STFD	STFD	BF	STFD	STFD	STFD	STFD	BF	STFD	STFD	STFD	STFD																																																																																																																																																																																																																																																																																																																																																																																																																																																																																																																																																																																																																																																																																																																																																																																																										
LVL1	1.954	1.817	1.851	1.841	1.856	1.183	1.712	1.348	1.146	1.274	1.094	1.274	1.026	1.344	2.011	2.066	2.012	2.178	2.017	2.932	2.932	1.893	1.893	1.62	1.645	1.674	1.645	1.645	0.8267	1.477	1.737	1.737	1.737	1.737	1.737	1.737	1.737	1.737	1.737	1.737	1.737	1.737	1.737	1.737	1.737	1.737	1.737	1.737	1.737	1.737	1.737	1.737	1.737	1.737	1.737	1.737	1.737	1.737	1.737	1.737	1.737	1.737	1.737	1.737	1.737	1.737	1.737	1.737	1.737	1.737	1.737	1.737	1.737	1.737	1.737	1.737	1.737	1.737	1.737	1.737	1.737	1.737	1.737	1.737	1.737	1.737	1.737	1.737	1.737	1.737	1.737	1.737	1.737	1.737	1.737	1.737	1.737	1.737	1.737	1.737	1.737	1.737	1.737	1.737	1.737	1.737	1.737	1.737	1.737	1.737	1.737	1.737	1.737	1.737	1.737	1.737	1.737	1.737	1.737	1.737	1.737	1.737	1.737	1.737	1.737	1.737	1.737	1.737	1.737	1.737	1.737	1.737	1.737	1.737	1.737	1.737	1.737	1.737	1.737	1.737	1.737	1.737	1.737	1.737	1.737	1.737	1.737	1.737	1.737	1.737	1.737	1.737	1.737	1.737	1.737	1.737	1.737	1.737	1.737	1.737	1.737	1.737	1.737	1.737	1.737	1.737	1.737	1.737	1.737	1.737	1.737	1.737	1.737	1.737	1.737	1.737	1.737	1.737	1.737	1.737	1.737	1.737	1.737	1.737	1.737	1.737	1.737	1.737	1.737	1.737	1.737	1.737	1.737	1.737	1.737	1.737	1.737	1.737	1.737	1.737	1.737	1.737	1.737	1.737	1.737	1.737	1.737	1.737	1.737	1.737	1.737	1.737	1.737	1.737	1.737	1.737	1.737	1.737	1.737	1.737	1.737	1.737	1.737	1.737	1.737	1.737	1.737	1.737	1.737	1.737	1.737	1.737	1.737	1.737	1.737	1.737	1.737	1.737	1.737	1.737	1.737	1.737	1.737	1.737	1.737	1.737	1.737	1.737	1.737	1.737	1.737	1.737	1.737	1.737	1.737	1.737	1.737	1.737	1.737	1.737	1.737	1.737	1.737	1.737	1.737	1.737	1.737	1.737	1.737	1.737	1.737	1.737	1.737	1.737	1.737	1.737	1.737	1.737	1.737	1.737	1.737	1.737	1.737	1.737	1.737	1.737	1.737	1.737	1.737	1.737	1.737	1.737	1.737	1.737	1.737	1.737	1.737	1.737	1.737	1.737	1.737	1.737	1.737	1.737	1.737	1.737	1.737	1.737	1.737	1.737	1.737	1.737	1.737	1.737	1.737	1.737	1.737	1.737	1.737	1.737	1.737	1.737	1.737	1.737	1.737	1.737	1.737	1.737	1.737	1.737	1.737	1.737	1.737	1.737	1.737	1.737	1.737	1.737	1.737	1.737	1.737	1.737	1.737	1.737	1.737	1.737	1.737	1.737	1.737	1.737	1.737	1.737	1.737	1.737	1.737	1.737	1.737	1.737	1.737	1.737	1.737	1.737	1.737	1.737	1.737	1.737	1.737	1.737	1.737	1.737	1.737	1.737	1.737	1.737	1.737	1.737	1.737	1.737	1.737	1.737	1.737	1.737	1.737	1.737	1.737	1.737	1.737	1.737	1.737	1.737	1.737	1.737	1.737	1.737	1.737	1.737	1.737	1.737	1.737	1.737	1.737	1.737	1.737	1.737	1.737	1.737	1.737	1.737	1.737	1.737	1.737	1.737	1.737	1.737	1.737	1.737	1.737	1.737	1.737	1.737	1.737	1.737	1.737	1.737	1.737	1.737	1.737	1.737	1.737	1.737	1.737	1.737	1.737	1.737	1.737	1.737	1.737	1.737	1.737	1.737	1.737	1.737	1.737	1.737	1.737	1.737	1.737	1.737	1.737	1.737	1.737	1.737	1.737	1.737	1.737	1.737	1.737	1.737	1.737	1.737	1.737	1.737	1.737	1.737	1.737	1.737	1.737	1.737	1.737	1.737	1.737	1.737	1.737	1.737	1.737	1.737	1.737	1.737	1.737	1.737	1.737	1.737	1.737	1.737	1.737	1.737	1.737	1.737	1.737	1.737	1.737	1.737	1.737	1.737	1.737	1.737	1.737	1.737	1.737	1.737	1.737	1.737	1.737	1.737	1.737	1.737	1.737	1.737	1.737	1.737	1.737	1.737	1.737	1.737	1.737	1.737	1.737	1.737	1.737	1.737	1.737	1.737	1.737	1.737	1.737	1.737	1.737	1.737	1.737	1.737	1.737	1.737	1.737	1.737	1.737	1.737	1.737	1.737	1.737	1.737	1.737	1.737	1.737	1.737	1.737	1.737	1.737	1.737	1.737	1.737	1.737	1.737	1.737	1.737	1.737	1.737	1.737	1.737	1.737	1.737	1.737	1.737	1.737	1.737	1.737	1.737	1.737	1.737	1.737	1.737	1.737	1.737	1.737	1.737	1.737	1.737	1.737	1.737	1.737	1.737	1.737	1.737	1.737	1.737	1.737	1.737	1.737	1.737	1.737	1.737	1.737	1.737	1.737	1.737	1.737	1.737	1.737	1.737	1.737	1.737	1.737	1.737	1.737	1.737	1.737	1.737	1.737	1.737	1.737	1.737	1.737	1.737	1.737	1.737	1.737	1.737	1.737	1.737	1.737	1.737	1.737	1.737	1.737	1.737	1.737	1.737	1.737	1.737	1.737	1.737	1.737	1.737	1.737	1.737	1.737	1.737	1.737	1.737	1.737	1.737	1.737	1.737	1.737	1.737	1.737	1.737	1.737	1.737	1.737	1.737	1.737	1.737	1.737	1.737	1.737	1.737	1.737	1.737	1.737	1.737	1.737	1.737	1.737	1.737	1.737	1.737	1.737	1.737	1.737	1.737	1.737	1.737	1.737	1.737	1.737	1.737	1.737	1.737	1.737	1.737	1.737	1.737	1.737	1.737	1.737	1.737	1.737	1.737	1.737	1.737	1.737	1.737	1.737	1.737	1.737	1.737	1.737	1.737	1.737	1.737	1.737	1.737	1.737	1.737	1.737	1.737	1.737	1.737	1.737	1.737	1.737	1.737	1.737	1.737	1.737	1.737	1.737	1.737	1.737	1.737	1.737	1.737	1.737	1.737	1.737	1.737	1.737	1.737	1.737	1.737	1.737	1.737	1.737	1.737	1.737	1.737	1.737	1.737	1.737	1.737	1.737	1.737	1.737	1.737	1.737	1.737	1.737	1.737	1.737	1.737	1.737	1.737	1.737	1.737	1.737	1.737	1.737	1.737	1.737	1.737	1.737	1.737	1.737	1.737	1.737	1.737	1.737	1.737	1.737	1.737	1.737	1.737	1.737	1.737	1.737	1.737	1.737	1.737	1.737	1.737	1.737	1.737	1.737	1.737	1.737	1.737	1.737	1.737	1.737	1.737	1.737	1.737	1.737	1.737	1.737	1.737	1.737	1.737	1.737	1.737	1.737	1.737	1.737	1.737	1.737	1.737	1.737	1.737	1.737	1.737	1.737	1.737	1.737



## 9.5 Conclusions

The numerical case study analyses on a typical NZ reinforced concrete building model, once again, confirmed the significant vulnerability possessed by the as built non-structural walls even for minor or moderate intensity earthquakes. Although the September earthquake (Darfield 2010) was not a very destructive earthquake, it caused widespread non-structural wall damage and the same observation was made by the results of the given numerical case study.

The developed low damage solutions proved to be very effective isolation systems between the non-structural walls and the structural system below the design drift limit. When the structure deforms such that it exceeds this limit, such as the 22<sup>nd</sup> February 2011 earthquake, these low damage non-structural elements interact with the structure. For non-structural drywalls, this interaction results in negligible effect on the global behaviour of the structure due to their low strength and stiffness properties. On the other hand, for the stronger and stiffer low damage unreinforced clay brick infill wall system, the reserved in-plane strength and the stiffness of the infill wall content turns the non-structural wall into a back up structural element activating after the design drift limit (1.5%) is exceeded. This behaviour results in more uniform inter-storey drift profiles when compared to both bare frame structures and the structure with as built infill wall content. This can easily be observed when the comparison is made between the behaviour of the building models.

Soft storey mechanisms inherent in the as built and the bare frame options may be prevented by the low damage unreinforced clay brick infill wall solution in certain cases. In the light of the analyses carried out, the captured soft storey mechanisms are summarized in Figure 9.12. In the shown figure, the soft storey mechanisms are between floors 6 and 7 for EQ7, floors 4-5 and 5-6 for EQ11, floors 4 and 5 for EQ14, and floors 3 and 4 for EQ15. These mechanisms occurred either at bare frame or at as built options. In all of the cases, the low damage solution caused a more uniform drift profile, preventing the soft storey mechanisms. Although the low damage solution promises superior low damage and seismic structural performance, an earthquake that can impose very high drift levels, such as 4-6%, the low damage solution may still fail in-plane and cause a soft storey. Considering the expected drift limit for a good seismic

performance is about 2.5-3%, it can be stated that the low damage solution performs exceptionally in all of the considered cases with favourable seismic performances.

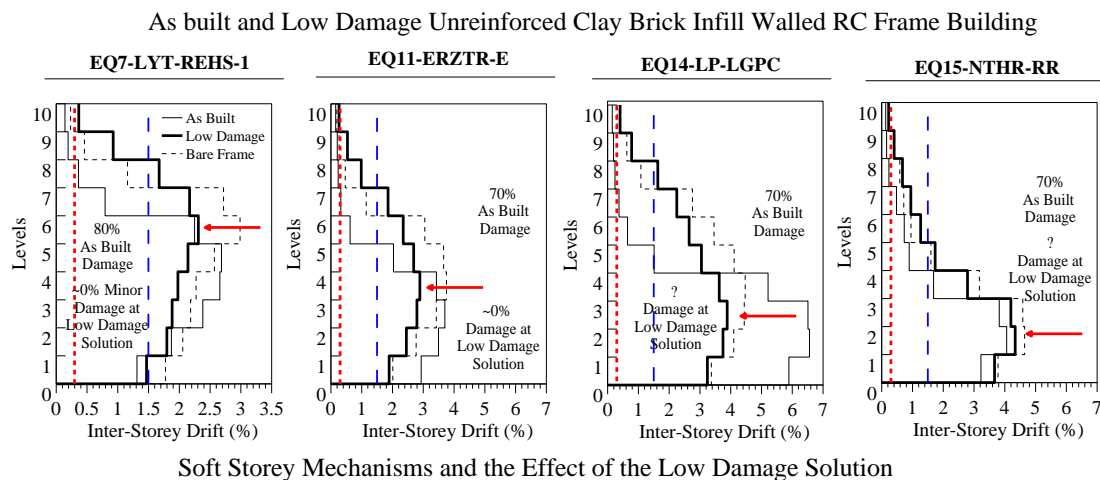


**Figure 9.12.** Inter-storey drift profiles for the RC frame with the bare frame, as built and low damage options using EQ7, EQ11, EQ14 and EQ15 (which cause soft storey mechanisms for either bare frame or the as built option especially in EQ14: as built soft storey mechanism prevented and drifts were pulled from about 6.5% to 4% by the low damage solution)

## 9.6 References

- [34] EQC/GNS. (2012). GeoNet-Geological Hazard Information for New Zealand.
- [35] "Darfield Earthquake Special Issue," Bulletin of the New Zealand Society for Earthquake Engineering, vol. 43, December 2010.
- [36] "Christchurch Earthquake Special Issue," Bulletin of the New Zealand Society for Earthquake Engineering, vol. 44, December 2011.
- [65] NZS3101.1, "Part 1: The Design of Concrete Structures," in Concrete Structures Standard vol. 3101, ed: New Zealand Standard, 2006.
- [66] D. K. Bull and D. Brunson, "Examples of concrete structural design to New Zealand Standard 3101 (Red Book)," NZCS: Cement & Concrete Association of New Zealand, Wellington, New Zealand 2008.

- [67] C. E. R. Commission, "Final Report, Volume 1: Seismicity, Soils and the Seismic Design of Buildings, Volume 2: The Performance of Christchurch CBD Buildings, Volume 3: Low Damage Building Technologies," 2012.
- [68] NZS1170.5, "Part 5: Earthquake Actions-New Zealand," in Structural Design Actions vol. 1170, ed: New Zealand Standard, 2004.
- [69] B. A. Bradley. (2013). <https://sites.google.com/site/brendonabradley/home>.
- [70] PEER. (2013). Ground Motion Database. Available: [http://peer.berkeley.edu/peer\\_ground\\_motion\\_database](http://peer.berkeley.edu/peer_ground_motion_database)



# CHAPTER 10

## GENERAL DESIGN RECOMMENDATIONS, CONCLUSIVE REMARKS and SUGGESTIONS for FUTURE STUDIES

*Man is an artifact designed for space travel. He is not designed to remain in his present biologic state any more than a tadpole is designed to remain a tadpole.*

*William S. Burroughs*



## 10 GENERAL DESIGN RECOMMENDATIONS, CONCLUSIVE REMARKS AND SUGGESTIONS FOR FUTURE STUDIES

### *10.1 General Design Recommendations for the Low Damage Non-Structural Wall Solutions*

In this section, the behaviour of the developed low damage solutions is summarized and general design recommendations are given for each of the low damage solutions; namely drywalls and unreinforced clay brick infill walls.

The low damage drywall solutions can be achieved by friction fitting the studs between the light gauge top and bottom steel tracks. As a result, the internal framing system (steel or timber frame) can slide laterally in between the tracks. The gypsum linings should be attached only to these vertical studs so that the completed system can slide without any constrain given by the surrounding structural components (i.e. the wall is integral in itself and non-integral with the surrounding structure). When the gypsum linings are attached to the framing, the linings should be sized and cut according to the required gaps around the edges of the linings. The summary of the design and construction details for low damage drywalls is shown in Figure 10.1.

Similar to the low damage drywalls, low damage capability of the unreinforced clay brick infill walls can be achieved by giving the infill panel the ability to deform. This can be achieved by dividing the infill panel zone into individual cantilever panels using a light gauge steel secondary framing system. The secondary framing system should be constructed in a way that it should let the individual infill panels behave as rocking cantilever walls with gaps of an equal width between the individual panels and the surrounding structure. In this method, the constructed secondary framing system should have adequate strength and anchorage to carry the out-of-plane weight of the infill panels completely. Moreover, the gaps should be completely filled with a fire rated construction sealant, which integrates the individual cantilever panels into one large deformable infill panel. The summary of this low damage solution is shown in Figure 10.2.

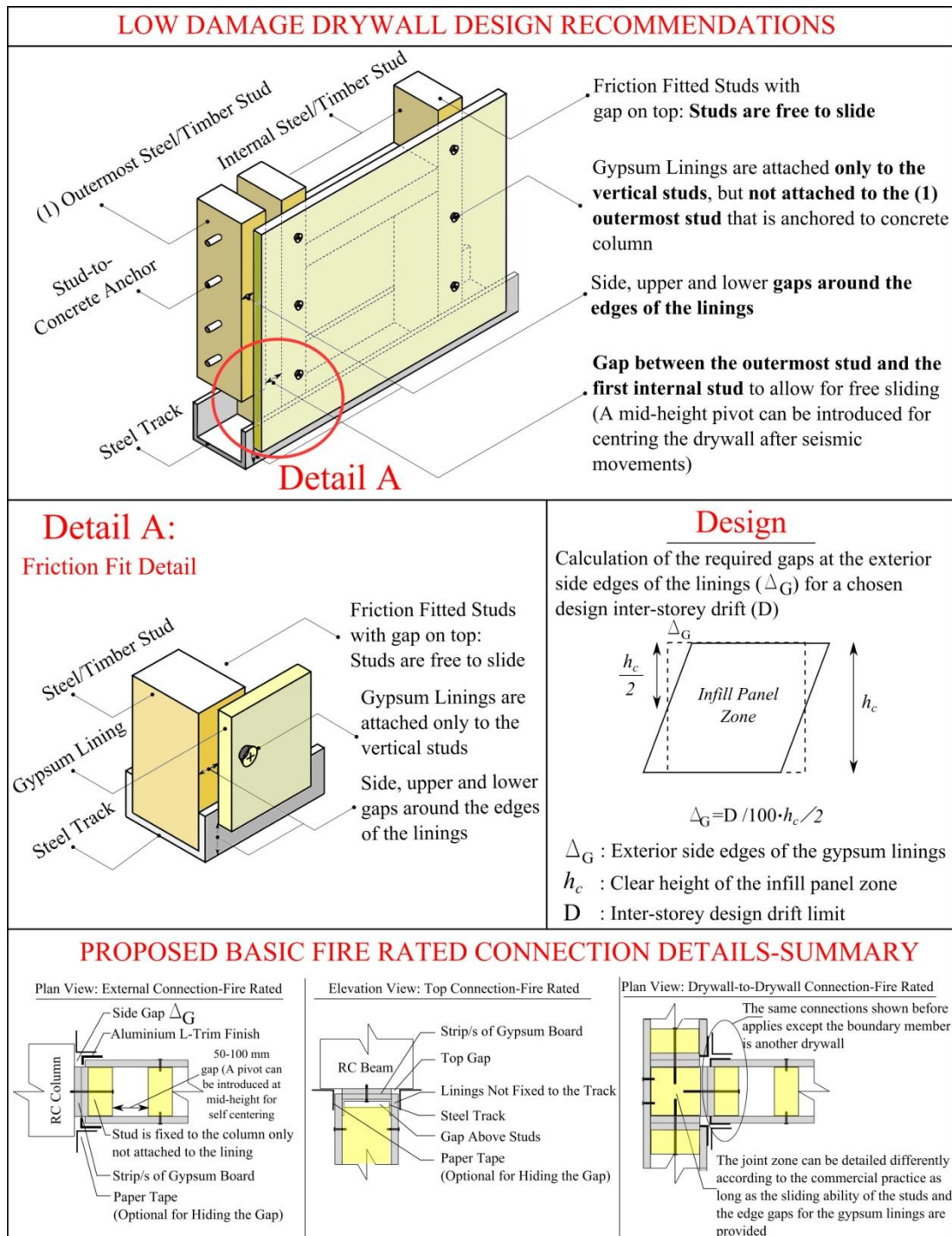
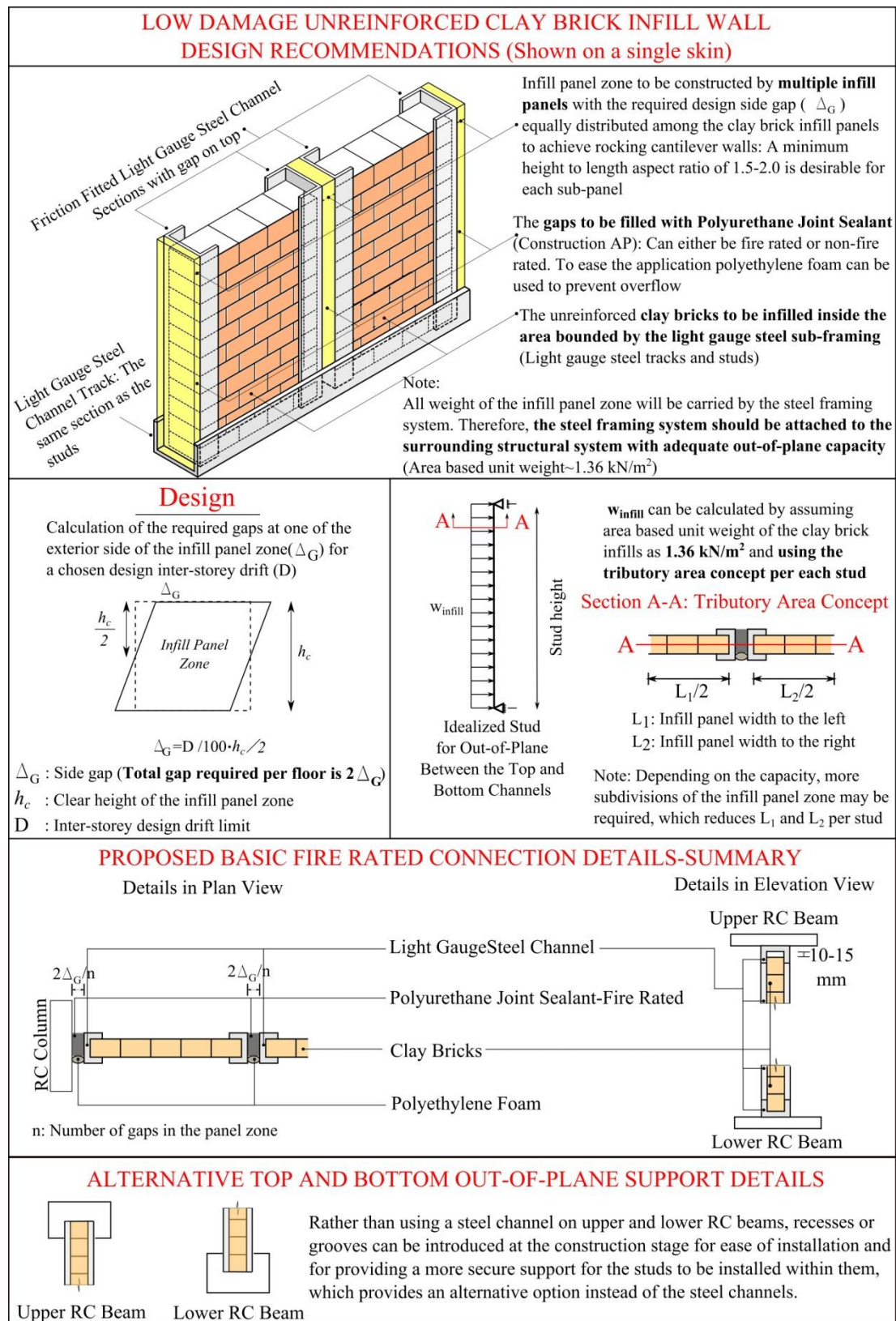


Figure 10.1. Design recommendations for low damage drywalls (either steel or timber framed)





**Figure 10.2.** Design recommendations for low damage unreinforced clay brick infill walls

## **10.2 Conclusive Remarks**

### **10.2.1 Steel and Timber Framed Drywalls: As Built Practice and Low Damage Solutions**

It was confirmed that the drywall systems adopted in current practice for commercial buildings are susceptible to a level of damage which would require repairing interventions even at very low inter-storey drift levels. The as built steel framed drywall lost serviceability 0.3% inter-storey drift level with a ductile post-yield behaviour. On the other hand, the timber framed drywall lost serviceability at a higher drift level of 0.75% with a brittle behaviour.

Due to the different damage mechanisms associated with the as built steel and timber framed drywalls; the generalized serviceability limit state criterion in table C1 of AS/NZS 1170.0:2002-Plaster/Gypsum walls (in-plane) might need to be revisited. The criterion in the Standard states the serviceability limit is reached when the mid-height deflection exceeds height/300. Although the test setup adopted for this research was more flexible than a typical multi-storey frame, this formula appears to overestimate the serviceability limit state for the steel framed drywalls (i.e. the common drywall partition type in the commercial construction). On the other hand, the existing criterion gave a reasonably accurate result for the timber framed drywalls. Therefore, it may be more realistic to give limit states for these two different types of drywalls under two different categories. For steel framed drywalls, this criterion may need to be modified in the standard, which may require further testing and numerical study in order to strengthen the conclusions.

It was shown that low damage solutions for steel and timber framed non-structural drywalls can be achieved by simple modifications to the as built practice (i.e. existing practice). The low damage solutions were designed to eliminate the interaction until 1.5% drift level, which was the theoretical side gap closing drift for the gypsum linings on the drywall framing. Overall, the low damage specimens remained undamaged until 1.5% drift level. From 1.5% onwards, the only damage observed was very minor cracking at exterior aluminium L-trim finishes of the linings. These solutions were achieved with no extra cost, material or labour. They can easily be adopted in real life

applications by the contractors. Moreover, their design can simply be carried out by the engineers and the architects.

In most real life applications of low damage solutions, modelling the low damage drywall system would not be required since their interaction with the structural system is negligible. Therefore, it is safe to conclude that the low damage solutions isolate the non-structural wall from the structural system effectively. Their effect on the global response can be neglected in order to simplify the analysis of buildings, which was also confirmed in the numerical case study building.

### ***10.2.2 Unreinforced Clay Brick Infill Walls: As Built Practice and Low Damage Solution***

It was shown that the as built unreinforced clay brick infill walls have a very low drift level at which they lose their capacity and serviceability (0.2%-0.3%). The associated behaviour is rather brittle since the infill wall cannot sustain its strength with increasing displacements, which conflicts with ductile seismic design philosophy. In certain cases, they may even affect the global response in a brittle manner and cause soft-storey mechanisms. Even a new ductile structural design can be affected by their brittle response and interaction with the structure.

The failure type of the as built unreinforced clay brick infill wall specimen was classified as diagonal cracking. It was also observed that the complete behaviour was rather similar to the concept of a progressive redistribution starting with the mortar layers. Since the main action on the infill panel zone was via the diagonal struts, initially the cracks were very mainly diagonal. After using this capacity, the additional demand acting on the infill panel zone was redistributed to horizontal mortar joints and caused sliding cracks after 0.3% drift level, which was proven by the related potentiometer measurements in FIF3-UCBI (i.e. the potentiometers g13, g14, g15). In certain cases, the sliding cracks formed in combination with diagonal cracks. Formation of sliding cracks were not only limited to the mid-height of the wall, but they formed at different heights at different drift levels. Only after the formation of all the possible horizontal and diagonal cracks at mortar joints, widespread cracking in the

clay bricks themselves was observed (i.e. instead of the mortar cracks), which are the last redistribution elements. This continued until 1.5% drift level. At 2.0 and 2.5% drift levels, the clay bricks at the corners of the infill panel zone were crushed.

It was also observed that when the infill panel zone was fully infilled with clay bricks, the infill wall contributes to the beam elongation occurring in the structural frame. In the adopted test setup, the beam elongation at the lower level was prevented by using pivots at the ends of the lower beam. Unlike the drywall specimens, the as built clay brick infill wall was strong and stiff enough to affect the structural response, inducing beam elongation at the lower beam. This observation suggests that low damage solutions are important for all types of structures including low damage structural systems with rocking/dissipating connections. This unaccounted effect on the beam elongation may alter the behaviour of the post tensioning tendons and thus the re-centring mechanism of PRESSS structures.

Considering the limit state criteria given in NZS1170.0, the criterion given for masonry walls deforming under in-plane load was shown to give realistic in-plane drift values for *unreinforced clay brick infill walls*. The code suggested a serviceability drift limit of 0.2% for a masonry wall of the same geometrical dimensions as the unreinforced clay brick infill wall specimen FIF3-UCBI. In addition, for unreinforced clay brick infill wall specimen, the serviceability loss occurred in the range of 0.2-0.3% drift level.

The old practice of armature cross walls and the concept of rocking structures were adapted to develop low damage unreinforced clay brick infill walls. The low damage solution concept was developed by dividing the infill panel zone into three individual cantilever panels using a light gauge steel sub-frame. The three panels were separated by 10 mm vertical gaps from each other and from the RC columns. These gaps were filled with polyurethane joint sealant, an elastic structural joint sealant. In principle, the achieved low damage system was a rocking multi-panel infill wall system, which was supported for out-of-plane by a secondary sub-frame made of light gauge steel sections. The low damage system proved its seismic performance and remained serviceable even at high drift levels (2-2.5% drift). Until the design drift limit of 1.5%,

the low damage system behaviour was very close to the bare frame, which meant the interaction between the structural frame and the non-structural wall was minimized. After the design drift (gap closing), the low damage infill wall started to take forces by activation of the diagonal strut. This observation showed another implication in addition to the low damage property of the system. The low damage non-structural wall solution works as a low damage system until the design drift limit. After the design drift level is exceeded, the system can act as a backup structural element and become a structural component. Therefore, they may behave as back up structural elements that are activated as the structure experiences high levels of drift. Moreover, other than clay bricks, this solution can also be adapted to other types of suitable materials with enough stiffness and strength (i.e. timber walls, steel plate shear walls, RC panels, etc.).

The beam elongation imposed by the as built unreinforced clay brick infill wall was also prevented by the developed low damage solution until the chosen design drift limit (1.5%). After this level of drift, the low damage infill wall interacted with the structural system and affected the beam elongation of the structural system.

### ***10.2.3 Observations from the Numerical Case Study Building***

The numerical case study analyses on a typical NZ reinforced concrete building model, once again, confirmed the significant vulnerability possessed by the as built non-structural walls using the given 16 earthquake events. The percentages of overall damage to the non-structural walls were in the range of 20-60% for EQ1-EQ4, 70-80% for EQ5-EQ8, 60-70% for EQ9-EQ12 and 70-90% for EQ13-EQ16. These percentages were calculated by dividing the number of floors where the inter-storey drift exceeded the damage drift level to the total number of floors. The summary of the numerical observations on non-structural wall damage is shown in Table 10.1.

**Table 10.1.** Summary of the non-structural wall damage in the building resulting from the numerical analyses of the building

Non-Structural Wall		As Built	As Built	As Built
Damage in Case Study Building		Steel Framed	Timber Framed	Unreinforced Clay
(%)		Drywall	Drywall	Brick Infill Wall
EQ1-EQ4	$\mu$ (%)	75%	40%	52.5%
EQ9-EQ12	$\sigma$ (%)	10%	20%	19.2%
EQ5-EQ8	$\mu$ (%)	91.25%	71.25%	77.5%
EQ13-EQ16	$\sigma$ (%)	3.3%	9.3%	6.61%

$\mu$ : Mean of the damage percentage of the as built non-structural walls

$\sigma$ : Standard deviation of the damage percentage of the as built non-structural walls

The developed low damage solutions proved to be very effective isolation systems between the non-structural walls and the structural system until the design drift limit (1.5%). When the structure deformed such that it exceeded this limit, such as the results of 22<sup>nd</sup> February 2011 earthquake (EQ5-EQ8), these low damage non-structural elements started to interact with the structure. For non-structural drywalls, this interaction resulted in negligible effect on the global behaviour of the structure due to their low strength and stiffness properties. For stronger and stiffer unreinforced clay brick infills, the reserved in-plane strength and the stiffness of the infill wall turned the non-structural wall into a backup structural element. This backup element activated once the design drift limit was exceeded in stronger earthquakes (i.e. EQ5-EQ8 and EQ13-EQ16). This behaviour resulted in reduced and more uniform inter-storey drift profiles when compared to both bare frame structure and the structure with as built infill wall. In certain cases, it prevented the formation of soft storey mechanism that occurred in both bare frame and the frame with as built unreinforced clay brick infill walls

### 10.3 Recommendations for Future Studies

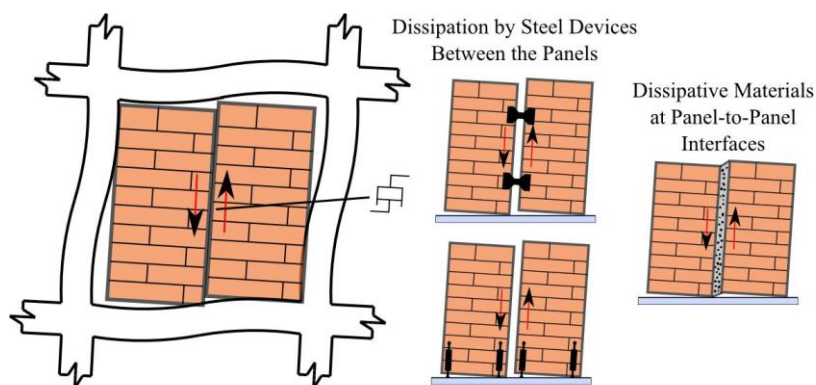
The low damage solutions for drywalls were developed considering the professional and practical recommendations given by Hans Gerlich, technical manager in Winstone Wallboards Ltd. (GIB), and Bruce Levey, local sales manager in Winstone Wallboards. The solutions have been planned to be included in the next updated construction guidelines of GIB and practitioners are being educated about these

solutions, which can be followed on their website (<http://gib.co.nz/systems/gib-fire-rated-systems/>). If these guidelines are published, within two years' time, non-structural drywalls for buildings will start incorporating these details due to the high seismicity of most of the country.

The developed low damage drywall solutions will also be tested in the near future as part of a two storey low damage frame (low damage frame + low damage non-structural elements) on the shake table at the University of Canterbury by other post-graduate research assistant, as part of the SAFER (Significant Advances in Earthquake Resistance), Concrete Technology Research Project funded by the Natural Hazard Research Platform (NHRP). The aim is to test the dynamic performance of these solutions during an earthquake. Moreover, one more recommendation for that study may be to install the drywall types such that they undergo out-of-plane deformations. Although, the solutions are expected to stay in-tact for out-of-plane, this may require experimental confirmation.

Considering the low damage unreinforced clay brick infill walls, the possibility of using them as backup structural elements that activate after a drift level should be studied further. They may be tested within a model structure using a shake table in order to confirm the results obtained herein. Moreover, if the performance of the system is confirmed and they are studied well, using clay bricks as infill walls can again be popular in NZ with introduced seismic performance advantages. However, the acoustic and thermal properties may still need to be studied and improved before real life applications. One way to address the acoustics issue can be to utilize a suitable material in between the two skins of clay brick infill wall panels that can act as such.

For low damage unreinforced clay brick infill walls, another recommendation, natural evolution of this thesis, is to apply the same concept as a retrofit solution on an as built unreinforced clay brick masonry specimen. The recommended study can investigate saw cutting (selective weakening) the infill panel zone into smaller panel zones, securing them for out-of-plane deformations and then studying the resulting structural performance.



Conceptual methods for implementing the panel-to-panel relative deformation for energy dissipation

**Figure 10.3.** Possible dissipation options for future studies

The same concept may be improved further by implementing the solution to different materials that can be used as non-structural infill walls such as timber walls infilled within a structural frame. Then, external dissipaters can be added to the infill walls (either at the base or at the interfaces of the infill panels) in order to study whether they are able to perform as well while adding dissipation to the structure (Figure 10.3). The dissipaters can be either steel dissipaters or other materials injected with the polyurethane joint sealant or dissipative rubber blocks. In principle, anything that can utilize the panel-to-panel relative deformation can be an alternative dissipation strategy for such walls, which may require further research.

For low damage system with clay brick infill walls, the structural beams can be produced with grooves such that the secondary framing system can be installed in these grooves in upper and lower beams. This provides an alternative solution for a more stable out-of-plane fixing of the low damage multi-panel cantilever infill wall system even when a different material is used other than clay bricks as shown in Figure 10.2.



## REFERENCES



**REFERENCES**

- [1] R. Villaverde, "Seismic Design of Secondary Structures: State of the Art," *Journal of Structural Engineering*, vol. 123, pp. 1011-1019, August 1997.
- [2] S. Taghavi and E. Miranda, "Response Assessment of Nonstructural Building Elements," Pacific Earthquake Engineering Research Center, September 2003.
- [3] NZS95, "New Zealand Standard of Model Building By-Law," vol. 95, ed: New Zealand Standard, 1935.
- [4] NZS4230, "Design of Reinforced Concrete Masonry Structures," vol. 4230, ed: New Zealand Standard, 2004.
- [5] NZSS595, "New Zealand Specification for Concrete Bricks and Blocks," vol. 595, ed: New Zealand Standard, 1952.
- [6] NZSS1900, "New Zealand Standard of Model Building Bylaw," vol. 1900, ed: New Zealand Standard, 1964.
- [7] I. L. Holmes, "Concrete Masonry Buildings in New Zealand," in *3rd World Conference on Earthquake Engineering*, Auckland, New Zealand, pp. 244-255, 1965.
- [8] NZS4230P, "Provisional New Zealand Standard-The Design of Masonry Structures," vol. 4230P, ed: New Zealand Standard, 1985.
- [9] GIB, "GIB Noise Control Systems-Specifications for Drywalls," ed, 2006.
- [10] G. Magenes and S. Pampanin, "Seismic Response of Gravity-Load Design Frames with Masonry Infills," in *13th World Conference on Earthquake Engineering*, Vancouver, B.C., Canada, 2004.
- [11] T. Paulay and M. J. N. Priestley, *Seismic Design of Reinforced Concrete and Masonry Buildings*: John Wiley and Sons, Inc., 1992.
- [12] S. Ozden, U. Akguzel, and T. Ozturan, "Seismic Strengthening of Infilled Reinforced Concrete Frames with Composite Materials," *ACI STRUCTURAL JOURNAL*, vol. 108, pp. 414-422, July-August 2011.
- [13] V. Bertero and S. Brokken, "Infills in Seismic Resistant Building," *Journal of Structural Engineering*, vol. 109, pp. 1337-1361, 06 June 1983.
- [14] M. Dolšek and P. Fajfar, "Soft Storey Effects in Uniformly Infilled Reinforced Concrete Frames," *Journal of Earthquake Engineering*, vol. 5, pp. 1-12, 2001.

- 
- [15] M. Dolšek and P. Fajfar, "The Effect of Masonry Infills on the Seismic Response of a Four-Storey Reinforced Concrete Frame-A Deterministic Assessment," *Engineering Structures*, vol. 30, pp. 1991-2001, 2008.
- [16] M. N. Fardis and T. B. Panagiotakos, "Seismic Design and Response of Bare and Masonry-Infilled Reinforced Concrete Buildings. Part 11: Infilled Structures," *Journal of Earthquake Engineering*, vol. 1, pp. 475-503, 1997.
- [17] M. Galli, "Evaluation of the Seismic Response of Existing R.C. Frame Buildings with Masonry Infills," Master Degree in Earthquake Engineering Master Thesis, European School of Advanced Studies in Reduction of Seismic Risk (ROSE School), ROSE School, Pavia, 2006.
- [18] S. Personeni, P. M.D., A. Palermo, and S. Pampanin, "Numerical Investigations on the Seismic Response of Masonry Infilled Steel Frames," presented at the The 14th World Conference on Earthquake Engineering, Beijing, China, 2008.
- [19] M. Aliaari and A. M. Memari, "Experimental Evaluation of a Sacrificial Seismic Fuse Device for Masonry Infill Walls," *Journal of Architectural Engineering*, vol. 13, pp. 111-125, June 2007.
- [20] M. Aliaari and A. M. Memari, "Analysis of Masonry Infilled Steel Frames with Seismic Isolator Subframes," *Engineering Structures*, vol. 27, pp. 487-500, 2005.
- [21] M. Mohammadi and V. Akrami, "An Engineered Infilled Frame: Behavior and Calibration," *Journal of Constructional Steel Research*, vol. 66, pp. 842-849, 2010.
- [22] S. A. Freeman, "Third Progress Report on Racking Tests of Wall Panels," University of California, Berkeley November, 1971.
- [23] S. S. Rihal, "Racking Tests of Non-Structural Building Partitions," California Polytechnic State University December 1980.
- [24] M. L. Wang, "Cladding Performance on a Full Scale Test Frame," *Earthquake Spectra*, vol. 3, pp. 119-172, 1987.
- [25] S. A. Adham, V. Avanesian, C. Hart, R. W. Anderson, J. Elmlinger, and J. Gregory, "Shear Wall Resistance of Lightgage Steel Stud Wall Systems," *Earthquake Spectra*, vol. 6, pp. 1-14, 1990.

- 
- [26] A. M. Kanvinde and G. G. Deierlein, "Analytical Models for the Seismic Performance of Gypsum Drywall Partitions," *Earthquake Spectra*, vol. 22, pp. 391-411, May 2006.
- [27] K. M. McMullin and D. S. Merrick, "Seismic Performance of Gypsum Walls- Experimental Test Program," 2001.
- [28] T. H. Lee, M. Kato, T. Matsumiya, K. Suita, and M. Nakashima, "Seismic Performance Evaluation of Non-Structural Components: Drywall Partitions," *Earthquake Engineering and Structural Dynamics*, 2006.
- [29] K. M. McMullin and D. S. Merrick, "Seismic Damage Thresholds for Gypsum Wallboard Partition Walls," *Journal of Architectural Engineering*, vol. 13, pp. 22-29, March 1, 2007.
- [30] A. Filiatrault, G. Mosqueda, R. Retamales, R. Davies, Y. Tian, and J. Fuchs, "Experimental Seismic Fragility of Steel Studded Gypsum Partition Walls and Fire Sprinkler Piping Subsystems," presented at the ASCE Structures Congress, Orlando, Florida, 2010.
- [31] J. I. Restrepo and A. F. Lang, "Study of Loading Protocols in Light-Gauge Stud Partition Walls," *Earthquake Spectra*, vol. 27, pp. 1169-1185, November 2011.
- [32] G. Araya-Letelier and E. Miranda, "Novel Sliding/Frictional Connections for Improved Seismic Performance of Gypsum Wallboard Partitions," in *15th World Conference on Earthquake Engineering*, Lisbon, Portugal, 2012.
- [33] M. R. Eatherton and J. F. Hajjar, "Residual Drifts of Self-Centring Systems Including Effects of Ambient Building Resistance," *Earthquake Spectra*, vol. 27, pp. 719-744, August 2011.
- [34] EQC/GNS. (2012). *GeoNet-Geological Hazard Information for New Zealand*.
- [35] "Darfield Earthquake Special Issue," *Bulletin of the New Zealand Society for Earthquake Engineering*, vol. 43, December 2010.
- [36] "Christchurch Earthquake Special Issue," *Bulletin of the New Zealand Society for Earthquake Engineering*, vol. 44, December 2011.
- [37] R. Langenbach, "Learning from the Past to Protect the Future: Armature Crosswalls," *Engineering Structures*, vol. 30, pp. 2096-2100, 2008.
- [38] IBC, "INTERNATIONAL BUILDING CODE," ed: International Code Council, 2009.

- [39] G. M. Calvi and D. Bolognini, "Seismic Response of Reinforced Concrete Frames Infilled with Weakly Reinforced Masonry Panels," *Journal of Earthquake Engineering*, vol. 5, pp. 153-185, 2001.
- [40] K. M. Mosalam, R. N. White, and P. Gergely, "Static Response of Infilled Frames Using Quasi-Static Experimentation," *Journal of Structural Engineering*, vol. 123, pp. 1462-1469, 1997.
- [41] S. Pujol and D. Fick, "The Test of a Full-Scale Three-Story RC Structure with Masonry Infill Walls," *Engineering Structures*, vol. 32, pp. 3112-3121, 2010.
- [42] A. A. Tasnimi and A. Modebkhah, "Investigation on the Behavior of Brick-Infilled Steel Frames with Openings, Experimental and Analytical Approaches," *Engineering Structures*, vol. 33, pp. 968-980, 2011.
- [43] M. M. Kose, "Parameters Affecting the Fundamental Period of RC Buildings with Infill Walls," *Engineering Structures*, vol. 31, pp. 93-102, 2009.
- [44] P. Ricci, G. M. Verderame, and G. Manfredi, "Analytical Investigation of Elastic Period of Infilled RC MRF Buildings," *Engineering Structures*, vol. 33, pp. 308-319, 2011.
- [45] B. H. Hashemi and M. Hassanzadeh, "Study of Semi-Rigid Steel Braced Building Damaged in the Bam Earthquake " *Journal of Constructional Steel Research*, vol. 64, pp. 704-721, 2008.
- [46] S. Pampanin, A. Palermo, and D. Marriott, *PRESSS Design Handbook*: NZ Concrete Society Inc., 2010.
- [47] Macalloy, "Macalloy 1030 Post Tensioning Kit, Internal Bonded or Unbonded Bar Post-Tensioning Kit Using High Tensile Plain Bar 25 to 40 mm and Ribbed Bar 25 to 50 mm in Accordance with European Technical Approval ETA-07/0046," EOTA, Kent/United Kingdom 08.10.2007.
- [48] ACI374.1-05, "Acceptance Criteria for Moment Frames Based on Structural Testing and Commentary," vol. 374.1-05, ed: American Concrete Institute, 2005.
- [49] S. H. Bertoldi, L. D. Decanini, and C. Gavarini, "Telai Tamponati Soggetti ad Azione Sismica, un Modello Semplificato: Confronto Sperimentale e Numerico (in Italian), ," presented at the Atti Del 6 Convegno Nazionale ANIDIS, 1993.

- [50] H. B. Kaushik, D. C. Rai, and S. K. Jain, "Stress-Strain Characteristics of Clay Brick Masonry under Uniaxial Compression," *Journal of Materials in Civil Engineering*, vol. 19, pp. 728-739, September 1, 2007.
- [51] A. J. Carr, "Ruaumoko 2D-Computer Program for Inelastic Time History Analysis of Structures," ed. Christchurch, New Zealand: University of Canterbury, 2013.
- [52] F. J. Crisafulli, "Seismic Behaviour of Reinforced Concrete Structures with Masonry Infills," PhD, Civil Engineering, University of Canterbury, Christchurch, 1997.
- [53] NZS3404.1, "Steel Structures Standard," vol. 3404, ed. New Zealand Standard: Standards New Zealand, 1997.
- [54] RedHead, "Large Diameter Tapcon Anchors (LDT): Specifications," ed.
- [55] AS/NZS1170.0, "Part 0: General Principles," in *Structural Design Actions* vol. 1170, ed. Australian/New Zealand Standard, 2002.
- [56] A. K. Chopra, *Dynamics of Structures: Theory and Applications to Earthquake Engineering*, 2nd Edition ed. New Jersey: Prentice Hall, 2001.
- [57] NZS4210:2001, "Masonry Construction," in *Materials and Workmanship* vol. 4210, ed. New Zealand Standard, 2001.
- [58] B. S. Smith, "Methods for Predicting the Lateral Stiffness and Strength of Multi-Storey Infilled Frames," *Build. Sci.*, vol. 2, pp. 247-257, 1967.
- [59] T. C. Liauw, "An Approximate Method of Analysis for Infilled Frames With or Without Opening," *Build. Sci.*, vol. 7, pp. 233-238, 1972.
- [60] T. C. Liauw, "Stress Analysis for Panel of Infilled Frames," *Build. Sci.*, vol. 8, pp. 105-112, 1973.
- [61] M. J. N. Priestley, S. Sritharan, J. R. Conley, and S. Pampanin, "Preliminary Results and Conclusions from the PRESSS Five-Story Precast Concrete Test Building," *PCI Journal*, vol. 44, November-December 1999.
- [62] A. Cholewick, "Loadbearing Capacity and Deformability of Vertical Joints in Structural Walls of Large Panel Buildings," *Build. Sci.*, vol. 6, pp. 163-184, 1971.
- [63] O. A. Glogau, "Separation of Non-Structural Components in Buildings," presented at the South Pacific Conference on Earthquake Engineering, Wellington, 1975.

- 
- [64] USG, "Steel Stud and Track System Height Tables," ed, 2008.
- [65] NZS3101.1, "Part 1: The Design of Concrete Structures," in *Concrete Structures Standard* vol. 3101, ed: New Zealand Standard, 2006.
- [66] D. K. Bull and D. Brunsdon, "Examples of concrete structural design to New Zealand Standard 3101 (Red Book)," NZCS: Cement & Concrete Association of New Zealand, Wellington, New Zealand, 2008.
- [67] C. E. R. Commission, "Final Report, Volume 1: Seismicity, Soils and the Seismic Design of Buildings, Volume 2: The Performance of Christchurch CBD Buildings, Volume 3: Low Damage Building Technologies," 2012.
- [68] NZS1170.5, "Part 5: Earthquake Actions-New Zealand," in *Structural Design Actions* vol. 1170, ed: New Zealand Standard, 2004.
- [69] B. A. Bradley. (2013). <https://sites.google.com/site/brendonabradley/home>.
- [70] PEER. (2013). *Ground Motion Database*. Available: [http://peer.berkeley.edu/peer\\_ground\\_motion\\_database](http://peer.berkeley.edu/peer_ground_motion_database)



# APPENDICES



## APPENDICES

### *A-Additional Photos for the Bare Frame*



a)

b)

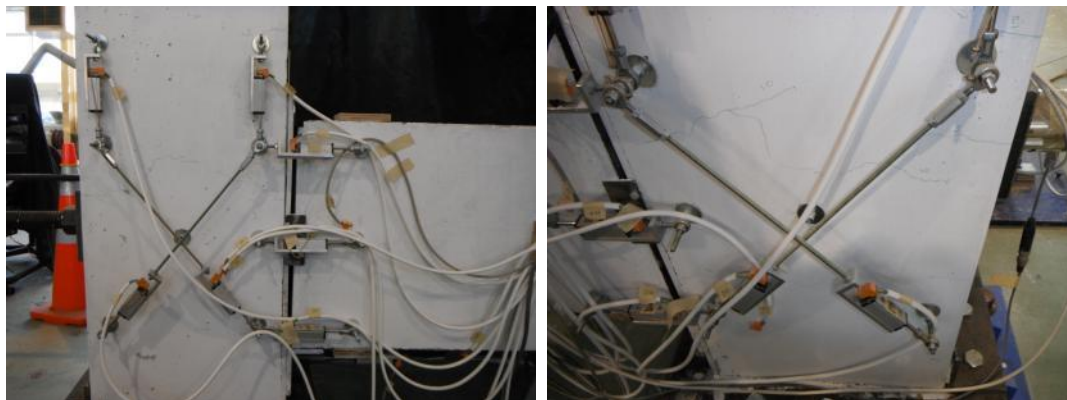
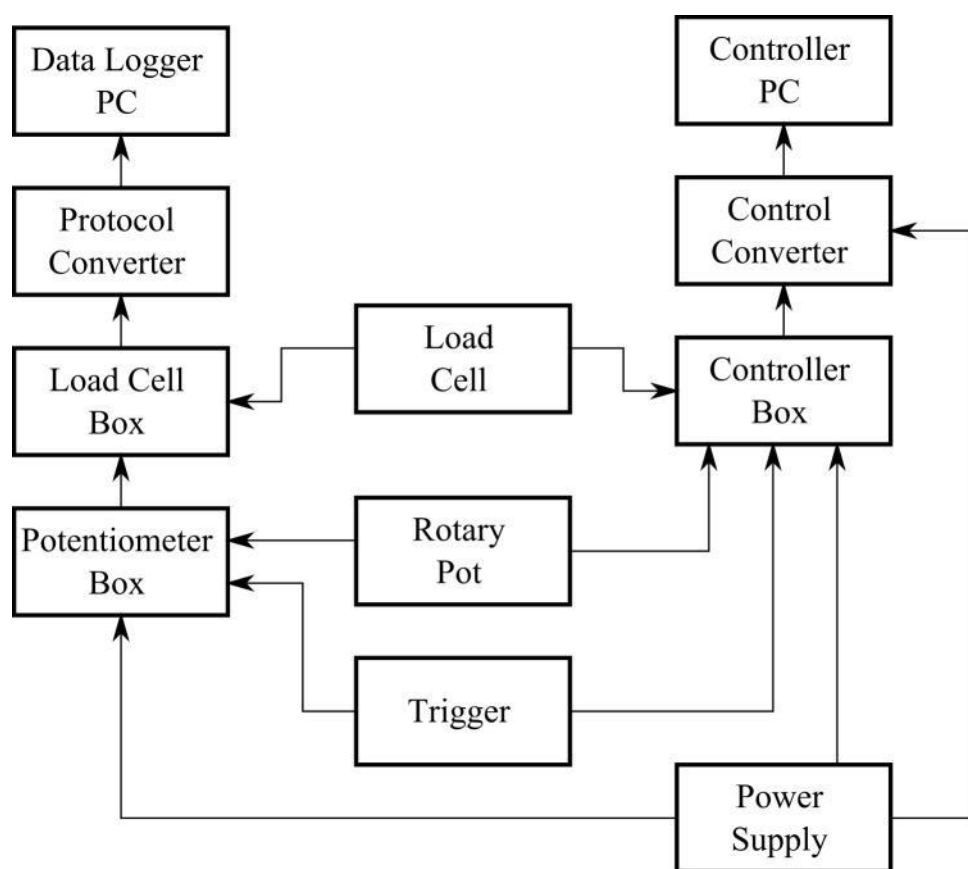
**Figure 0.1.** a) Reinforcing cage, b) Casting



a)

b)

**Figure 0.2.** a) Bare frame specimen BF, b) The reaction frame

**Figure 0.3.** Instrumentation layout at the joints**Figure 0.4.** Data collection and control system

***B-Additional Photos for the As Built Steel Framed Drywall Specimen FIF1-STFD***

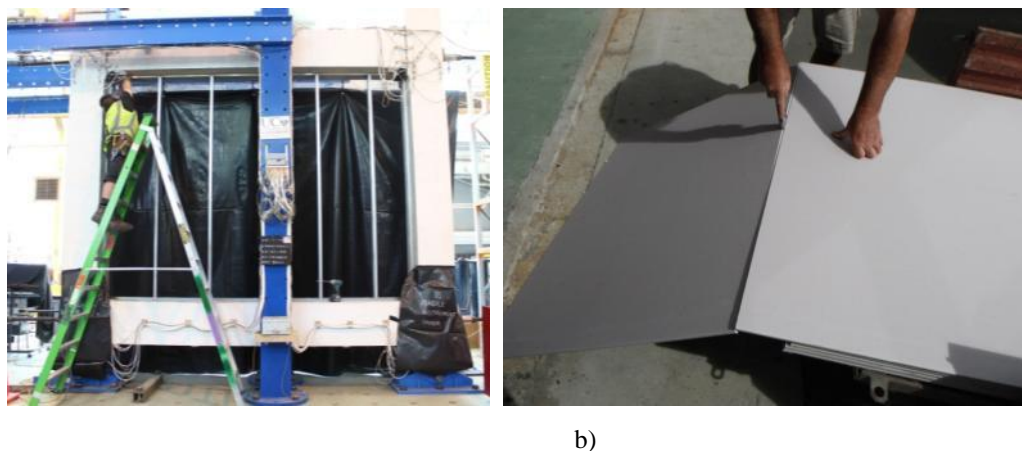


**Figure 0.5.** a) Steel stud installation, b) Cutting the gypsum lining

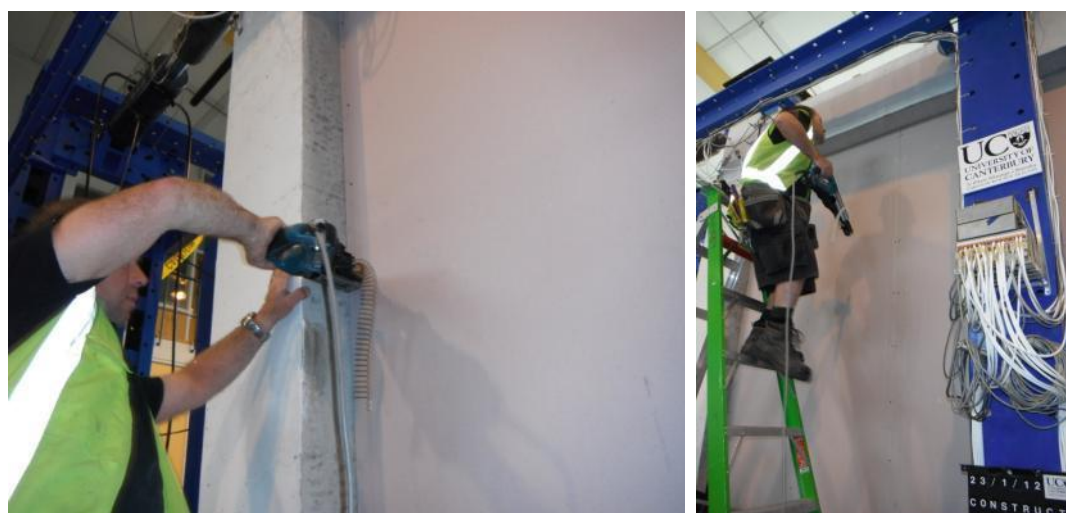


**Figure 0.6.** Gypsum lining installation

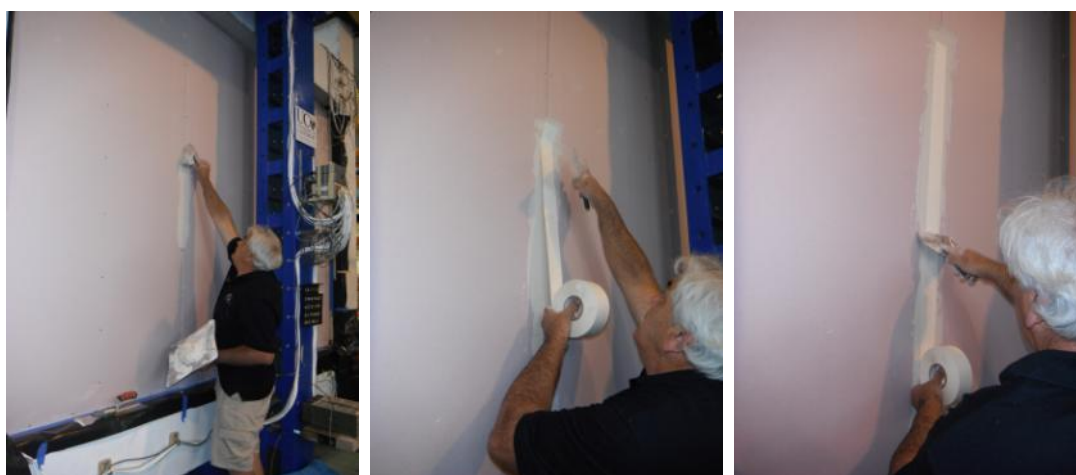
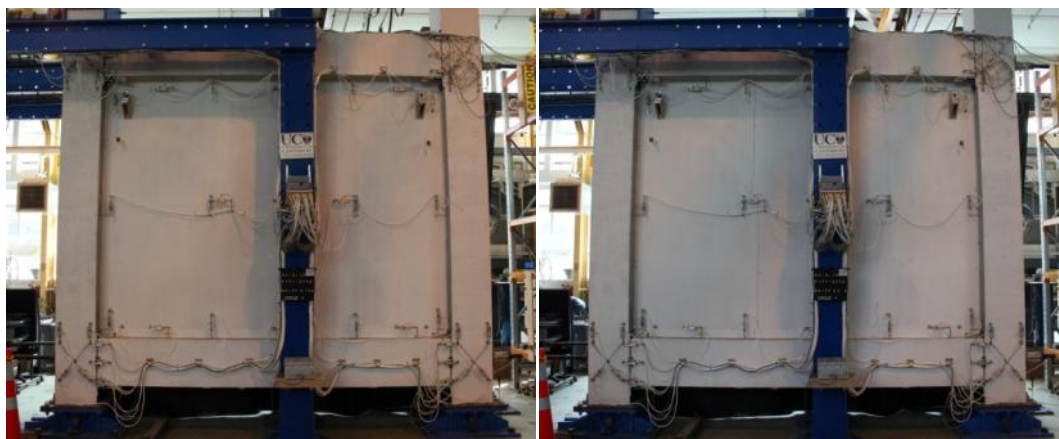


**Figure 0.7.** Paper tape application for the finishing of the gypsum lining interfaces





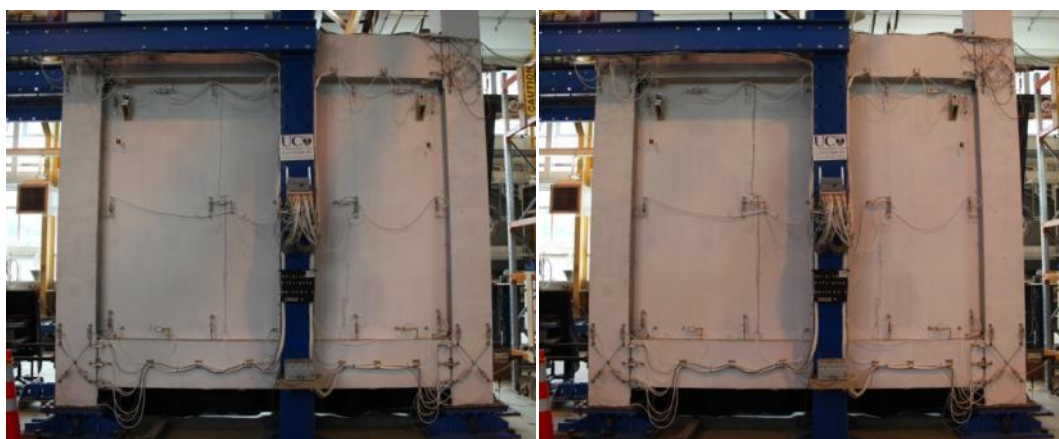
**Figure 0.8.** As built steel framed drywall specimen FIF1-STFD after the finishing



a) 0.1%

b) 0.2%

**Figure 0.9.** As built steel framed drywall specimen FIF1-STFD: a) 0.1% drift, b) 0.2% drift



a) 0.3%

b) 0.4%

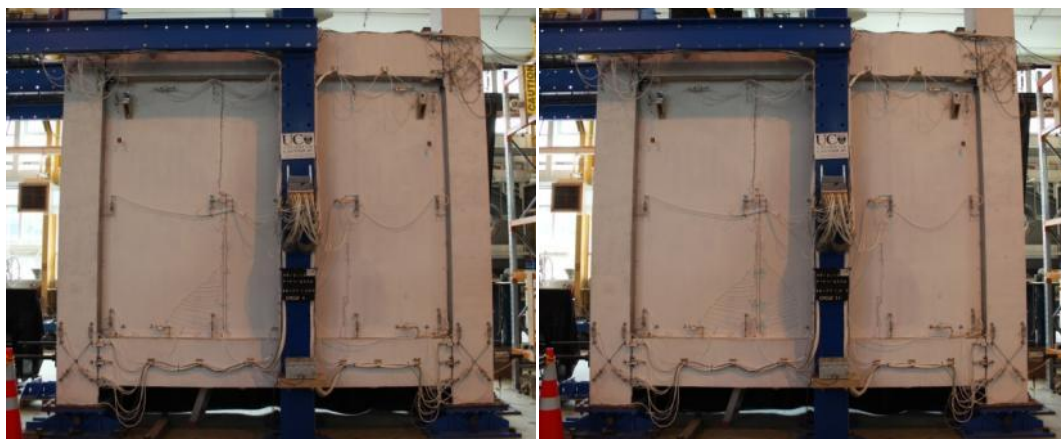
**Figure 0.10.** As built steel framed drywall specimen FIF1-STFD: a) 0.3% drift, b) 0.4% drift



a) 0.5%

b) 0.75% drift

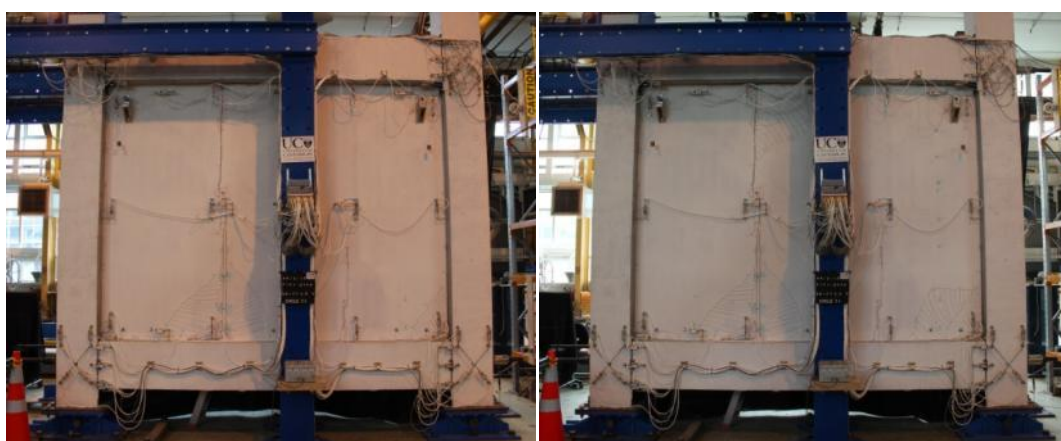
**Figure 0.11.** As built steel framed drywall specimen FIF1-STFD: a) 0.5% drift, b) 0.75% drift



a) 1.0%

b) 1.25% drift

**Figure 0.12.** As built steel framed drywall specimen FIF1-STFD: a) 1.0% drift, b) 1.25% drift



a) 1.5%

b) 2.0%

**Figure 0.13.** As built steel framed drywall specimen FIF1-STFD: a) 1.5% drift, b) 2.0% drift

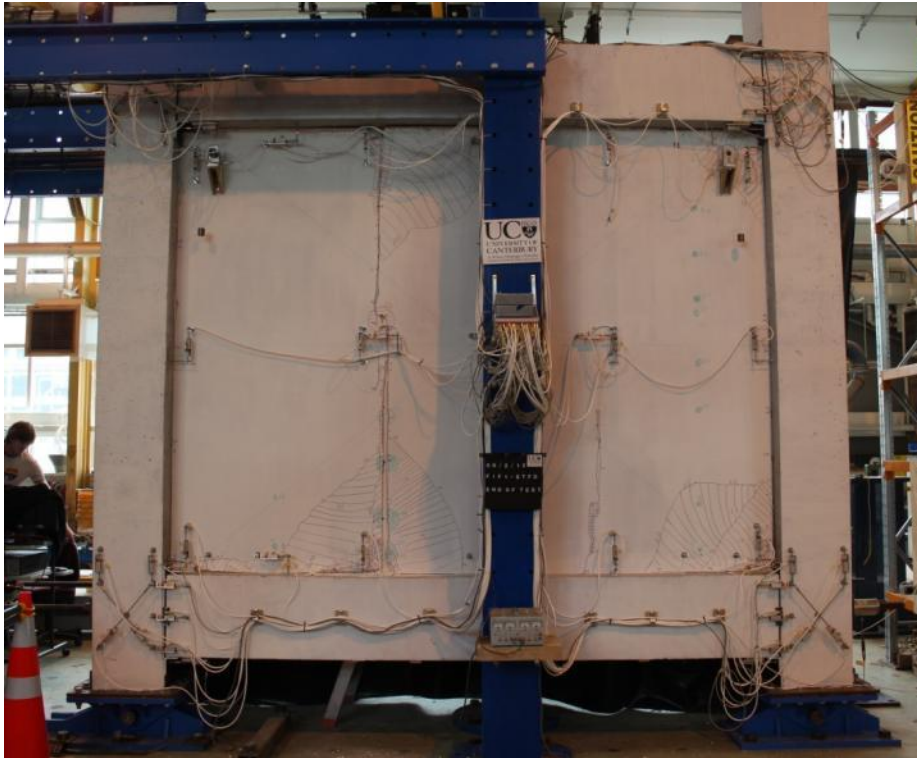


**Figure 0.14.** As built steel framed drywall specimen FIF1-STFD at 2.5% drift (end of the test)



***C-Additional Photos for the As Built Timber Framed Drywall Specimen  
FIF2-TBFD***



**Figure 0.15.** As built timber framed drywall specimen FIF2-TBFD: Installation of the timber elements

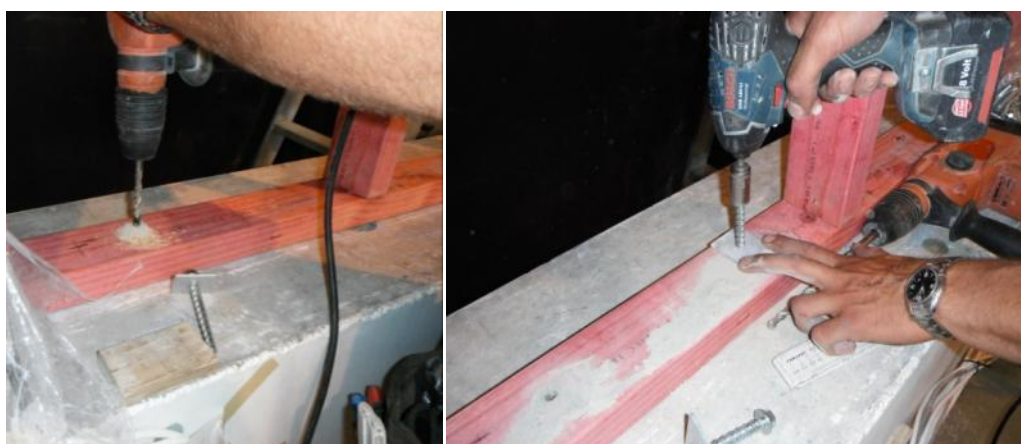
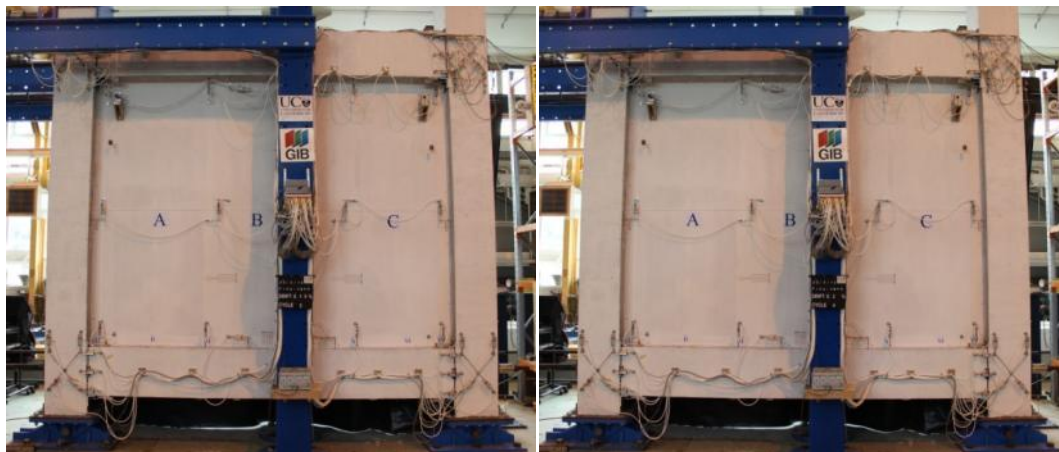


**Figure 0.16.** As built timber framed drywall specimen FIF2-TBFD: Installation of the timber-to-concrete anchors



**Figure 0.17.** As built timber framed drywall specimen FIF2-TBFD, Installation of the gypsum linings



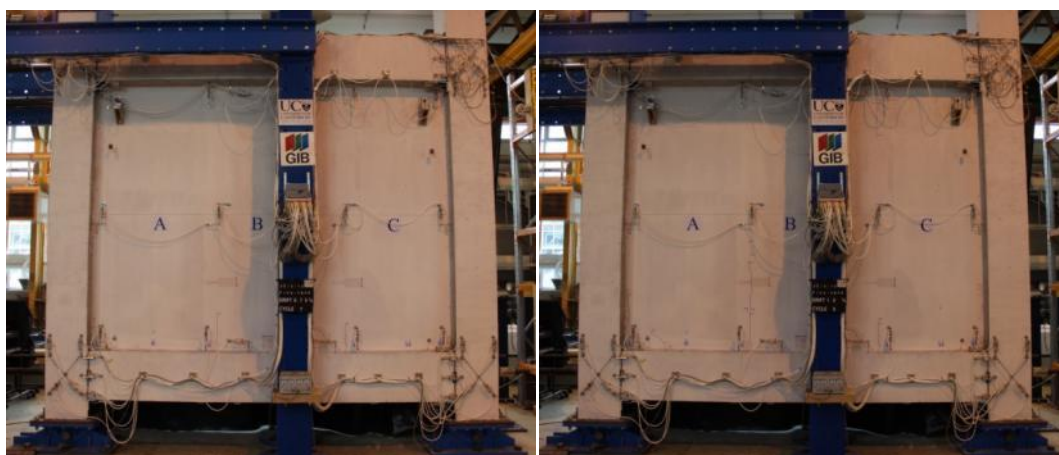
a) 0.1%

b) 0.2%

**Figure 0.18.** As built timber framed drywall specimen FIF2-TBFD: a) 0.1% drift, b) 0.2% drift

a) 0.3%

b) 0.4%

**Figure 0.19.** As built timber framed drywall specimen FIF2-TBFD: a) 0.3% drift, b) 0.4% drift

a) 0.5%

b) 0.75%

**Figure 0.20.** As built timber framed drywall specimen FIF2-TBFD: a) 0.5% drift, b) 0.75% drift

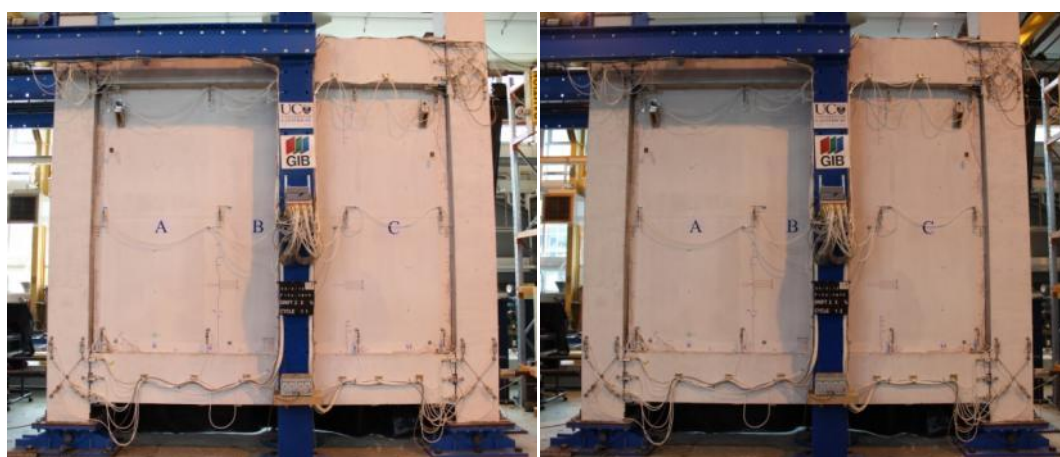




a) 1.0%

b) 1.25%

**Figure 0.21.** As built timber framed drywall specimen FIF2-TBFD: a) 1.0% drift, b) 1.25% drift



a) 1.5%

b) 2.0%

**Figure 0.22.** As built timber framed drywall specimen FIF2-TBFD: a) 1.5% drift, b) 2.0% drift



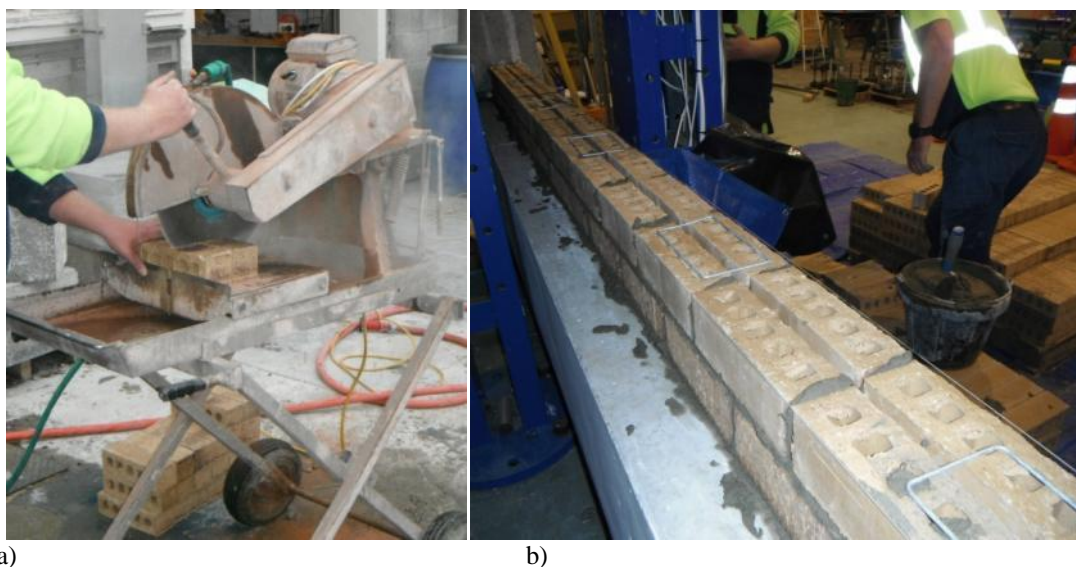
**Figure 0.23.** As built timber framed drywall specimen FIF2-TBFD at 2.5% drift (end of test)



***D-Additional Photos for the As Built Unreinforced Clay Brick Infill Wall  
Specimen FIF3-UCBI***



**Figure 0.24.** As built unreinforced clay brick infill wall specimen: Construction of the clay bricks



a)

b)

**Figure 0.25.** As built unreinforced clay brick infill wall specimen FIF3-UCBI: a) Saw cutting the clay bricks wherever required, b) Wall ties between the two skins of clay bricks



**Figure 0.26.** Four course laid clay bricks at the lower corners of the infill panel zone

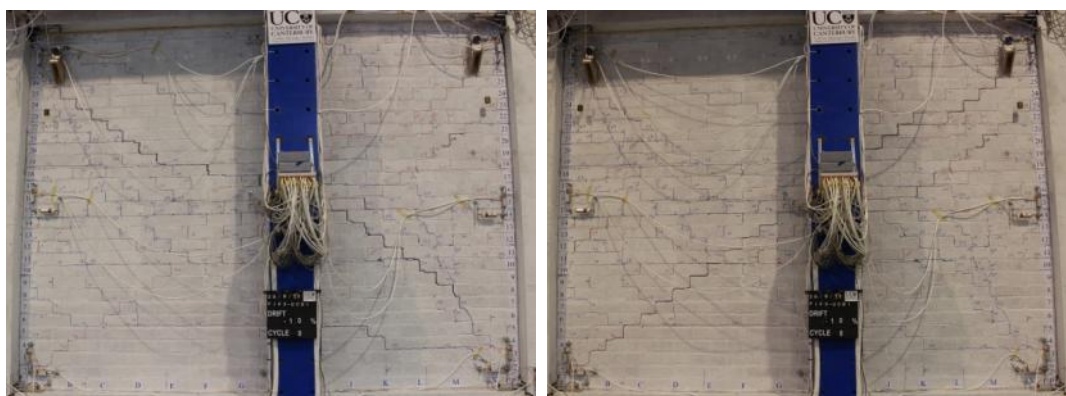




a) +0.75%

b) -0.75%

**Figure 0.27.** As built unreinforced clay brick infill wall specimen FIF3-UCBI: a) +0.75% drift (push), b) -0.75% drift (pull)



a) +1.0%

b) -1.0%

**Figure 0.28.** As built unreinforced clay brick infill wall specimen FIF3-UCBI: a) +1.0% drift (push), b) -1.0% drift (pull)



a) +1.25%

b) -1.25%

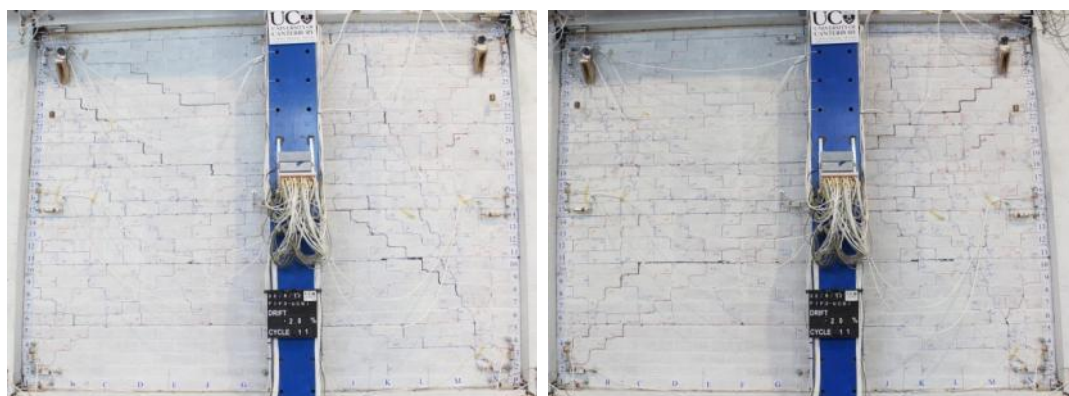
**Figure 0.29.** As built unreinforced clay brick infill wall specimen FIF3-UCBI: a) +1.25% drift (push), b) -1.25% drift (pull)



a) +1.5%

b) -1.5%

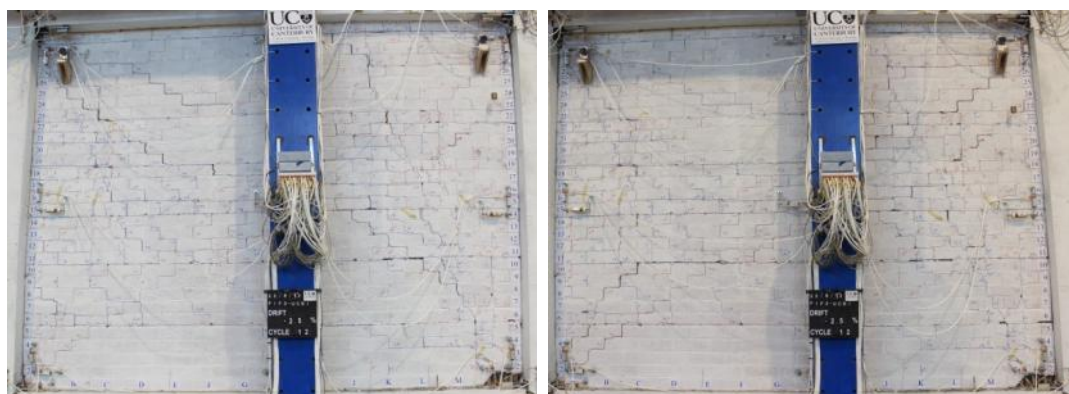
**Figure 0.30.** As built unreinforced clay brick infill wall specimen FIF3-UCBI: a) +1.5% drift (push), b) -1.5% drift (pull)



a) +2.0%

b) -2.0%

**Figure 0.31.** As built unreinforced clay brick infill wall specimen FIF3-UCBI: a) +2.0% drift (push), b) -2.0% drift (pull)



a) +2.5%

b) -2.5%

**Figure 0.32.** As built unreinforced clay brick infill wall specimen FIF3-UCBI: a) +2.5% drift (push), b) -2.5% drift (pull)





***E-Additional Photos for the Low Damage Steel Framed Drywall Specimen  
MIF1-STFD***

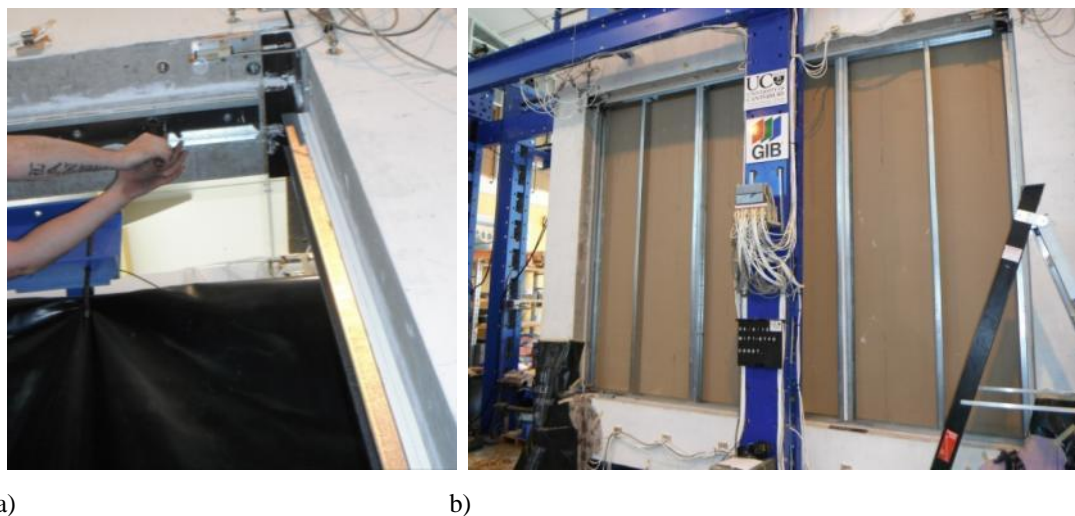


**Figure 0.33.** Low damage steel framed drywall specimen MIF1-STFD: a) Installation of the fire-rated exterior studs, b) Installation of the interior studs and the gypsum lining



**Figure 0.34.** Low damage steel framed drywall specimen MIF1-STFD: Friction fitted interior fire-rated stud



**Figure 0.35.** Low damage steel framed drywall specimen MIF1-STFD: Installation of the gypsum lining to the steel studs (no screw to the steel track)



a)

b)

**Figure 0.36.** Low damage steel framed drywall specimen MIF1-STFD: a) Exterior gap of 15 mm at the edge of the gypsum lining, b) Interior gap of 5 mm and bottom gap of 13 mm at the edges of the gypsum linings



**Figure 0.37.** Finished low damage steel framed drywall specimen MIF1-STFD

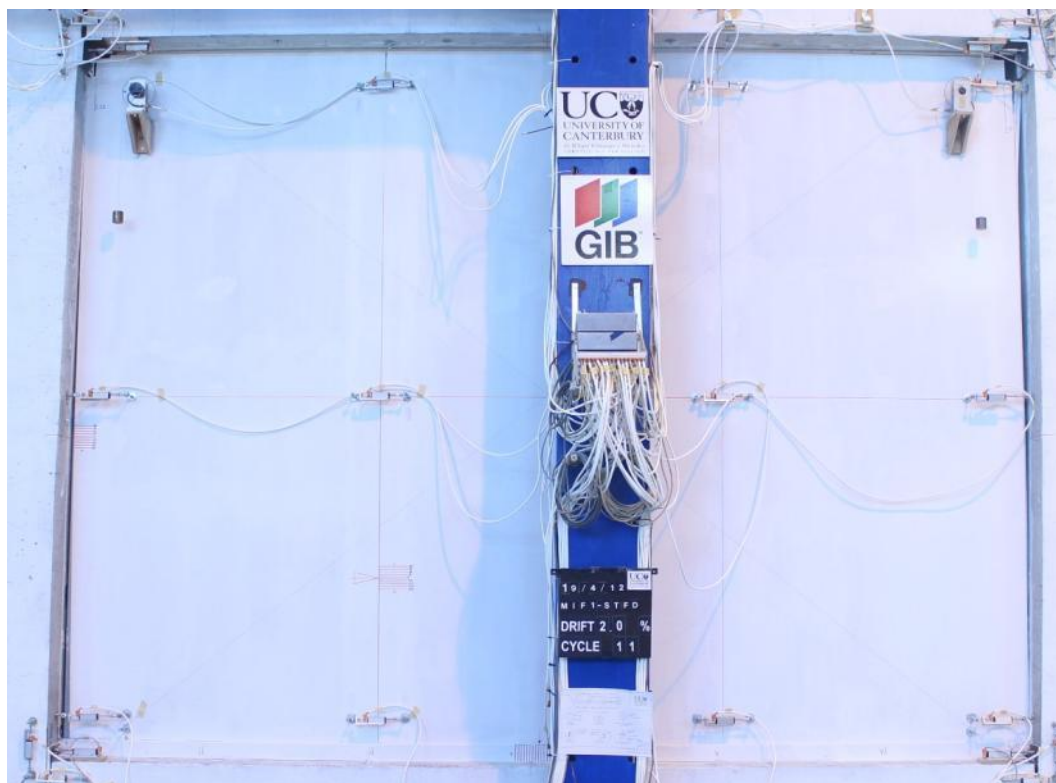


**Figure 0.38.** Low damage steel framed drywall specimen MIF1-STFD at +2.0% drift: Pull-out of the exterior studs of the drywall

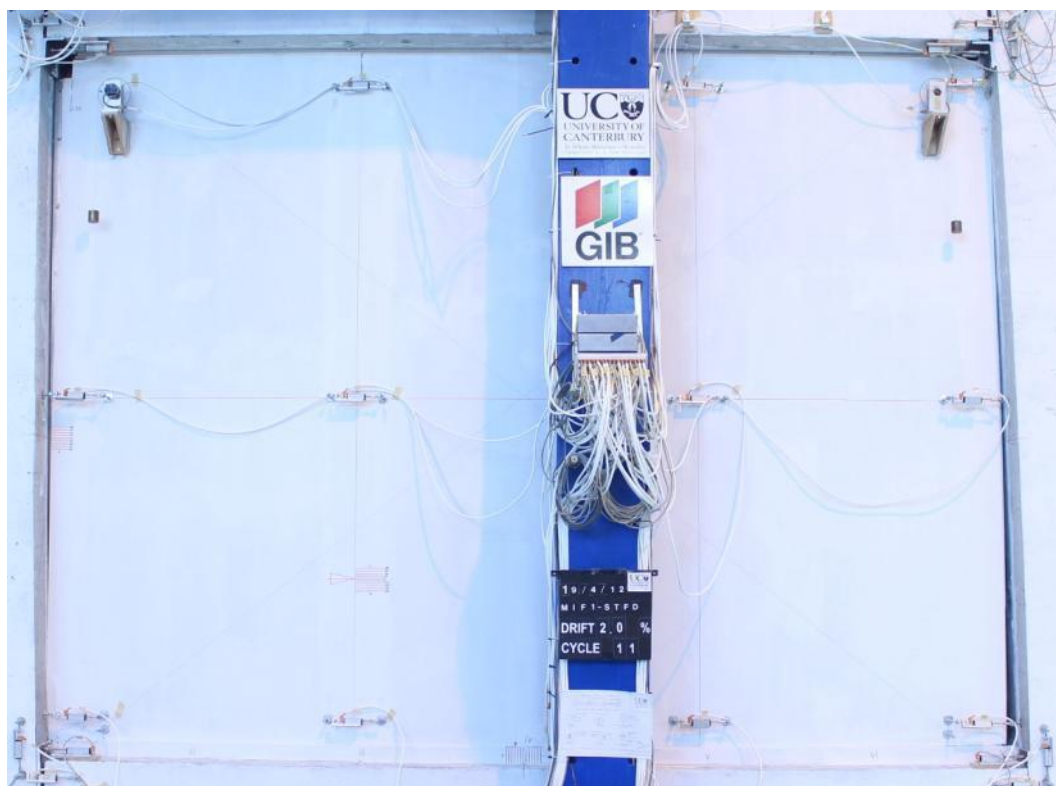


**Figure 0.39.** Low damage steel framed drywall specimen MIF1-STFD at -2.0% drift: Pull-out of the exterior studs of the drywall



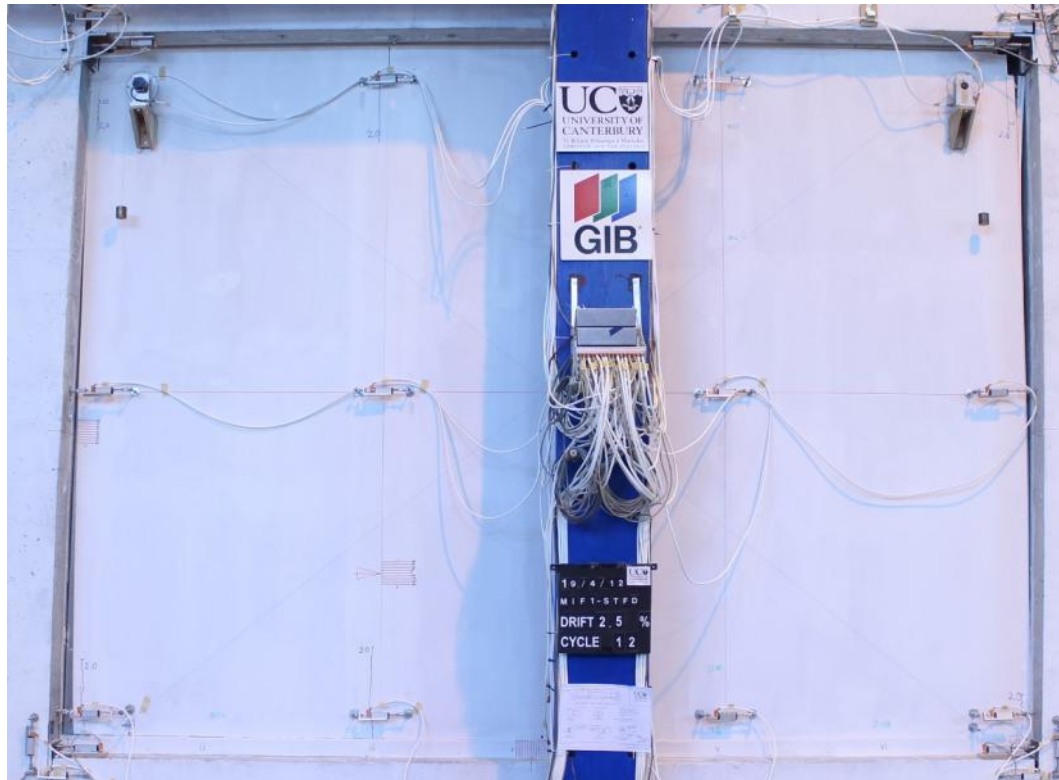


**Figure 0.40.** Low damage steel framed drywall specimen MIF1-STFD at +2.5% drift

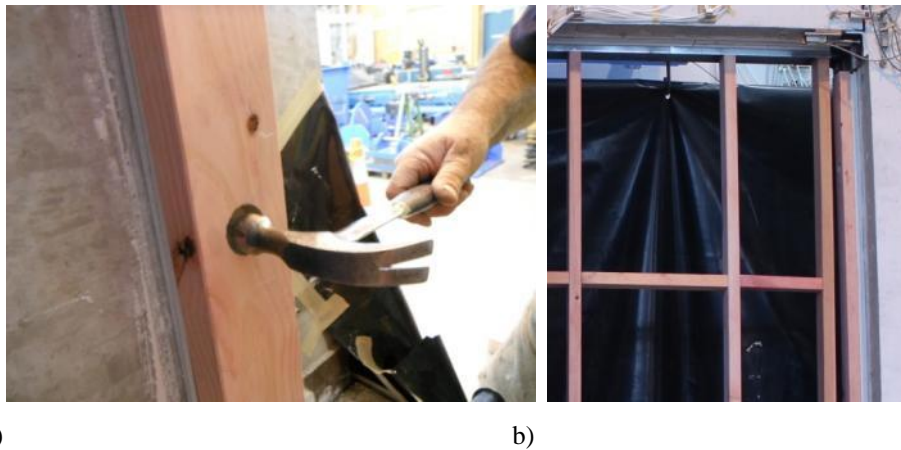


**Figure 0.41.** Low damage steel framed drywall specimen MIF1-STFD at -2.5% drift

***F-Additional Photos for the Low Damage Timber Framed Drywall Specimen***  
***MIF2-TBFD***



**Figure 0.42.** Low damage timber framed drywall specimen MIF2-TBFD: a) Construction of the timber frame within the steel tracks, b) Friction fitted timber studs into steel channels



a)

b)

**Figure 0.43.** Low damage timber framed drywall specimen MIF2-TBFD: a) Installation of the exterior fire-rated timber stud on the tight RC column (Fire rating given by the two strips of gypsum boards), b) Installed fire-rated steel track on top and fire-rated exterior stud on the right RC column



**Figure 0.44.** Low damage timber framed drywall specimen MIF2-TBFD about to be completed

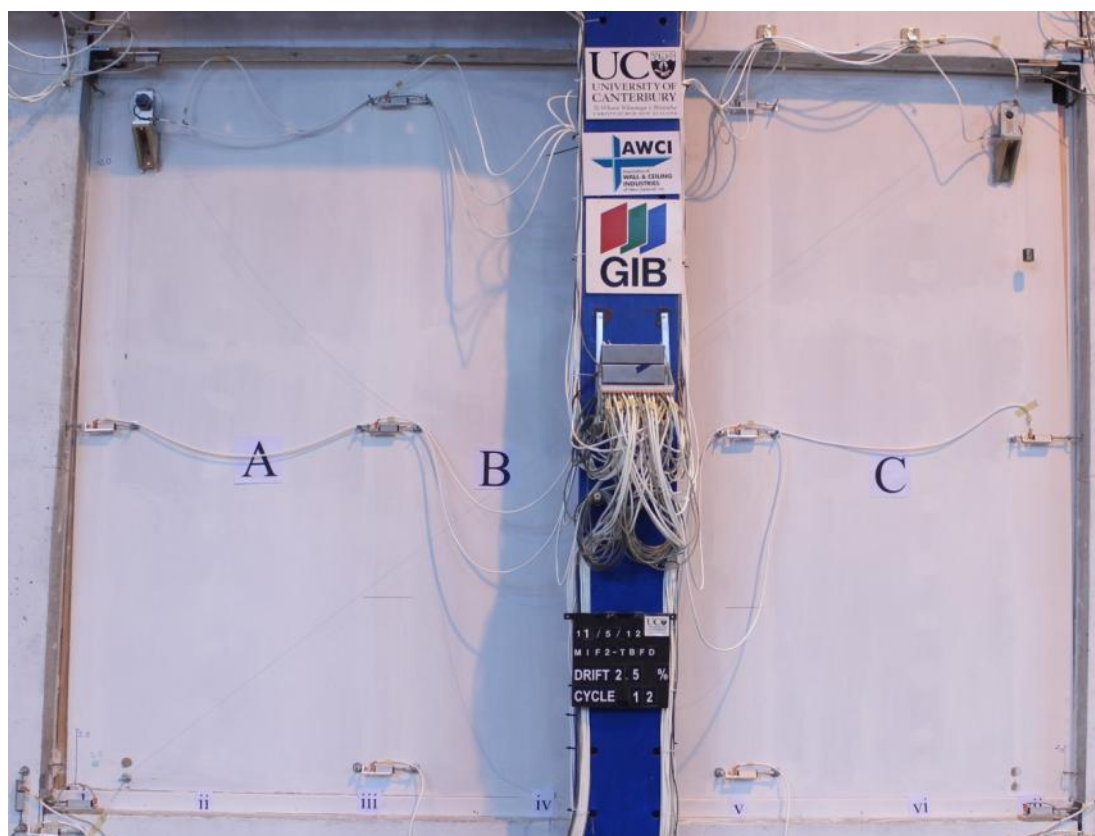


**Figure 0.45.** Low damage timber framed drywall specimen MIF2-TBFD at +2.5% drift (push)



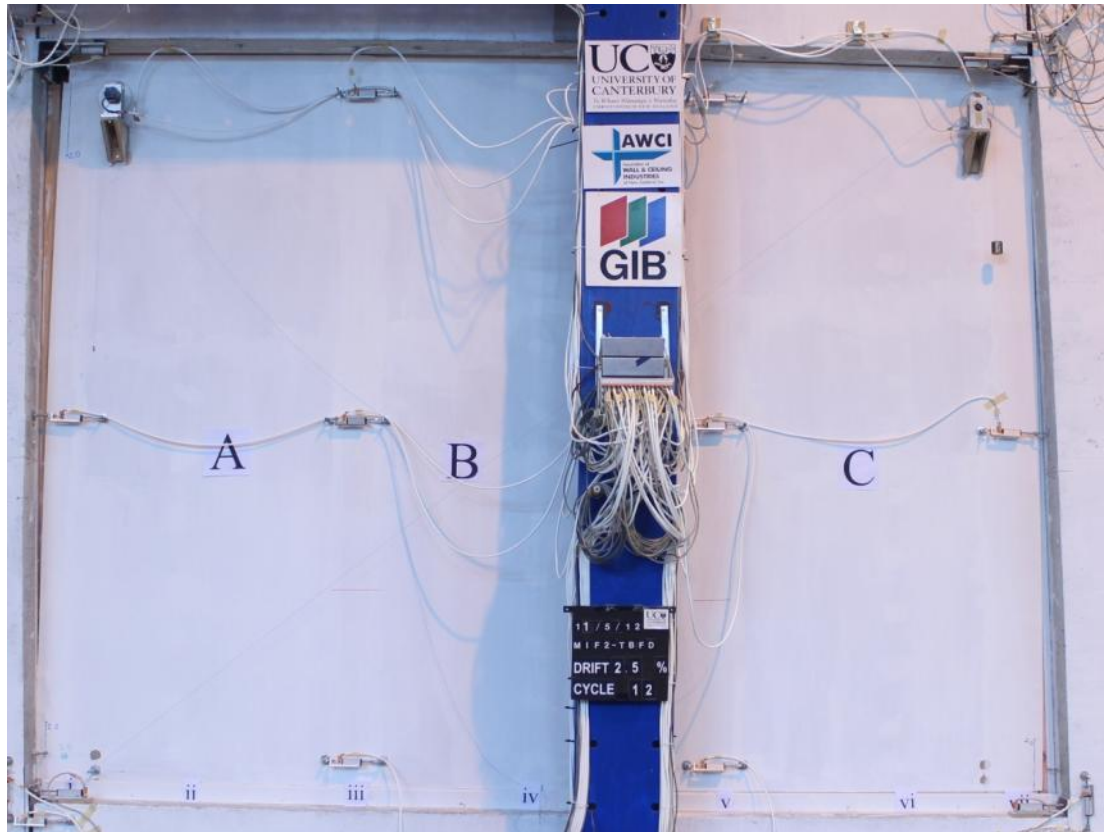


**Figure 0.46.** Low damage timber framed drywall specimen MIF2-TBFDat -2.5% drift (pull)





***G-Additional Photos for the Low Damage Unreinforced Clay Brick Infill  
Wall Specimen MIF5-UCBI***



**Figure 0.47.** Construction of the low damage unreinforced clay brick infill wall specimen MIF5-UCBI



a)



b)

**Figure 0.48.** Low damage unreinforced clay brick infill wall specimen MIF5-UCBI: a) The sub-frame system, b) The clay bricks infilled within the sub-frame



**Figure 0.49.** Low damage unreinforced clay brick infill wall specimen MIF5-UCBI: The installation of the polyethylene foam



**Figure 0.50.** Low damage unreinforced clay brick infill wall specimen MIF5-UCBI after the installation of the polyurethane structural joint sealant



**Figure 0.51.** Completed low damage unreinforced clay brick infill wall specimen MIF5-UCBI



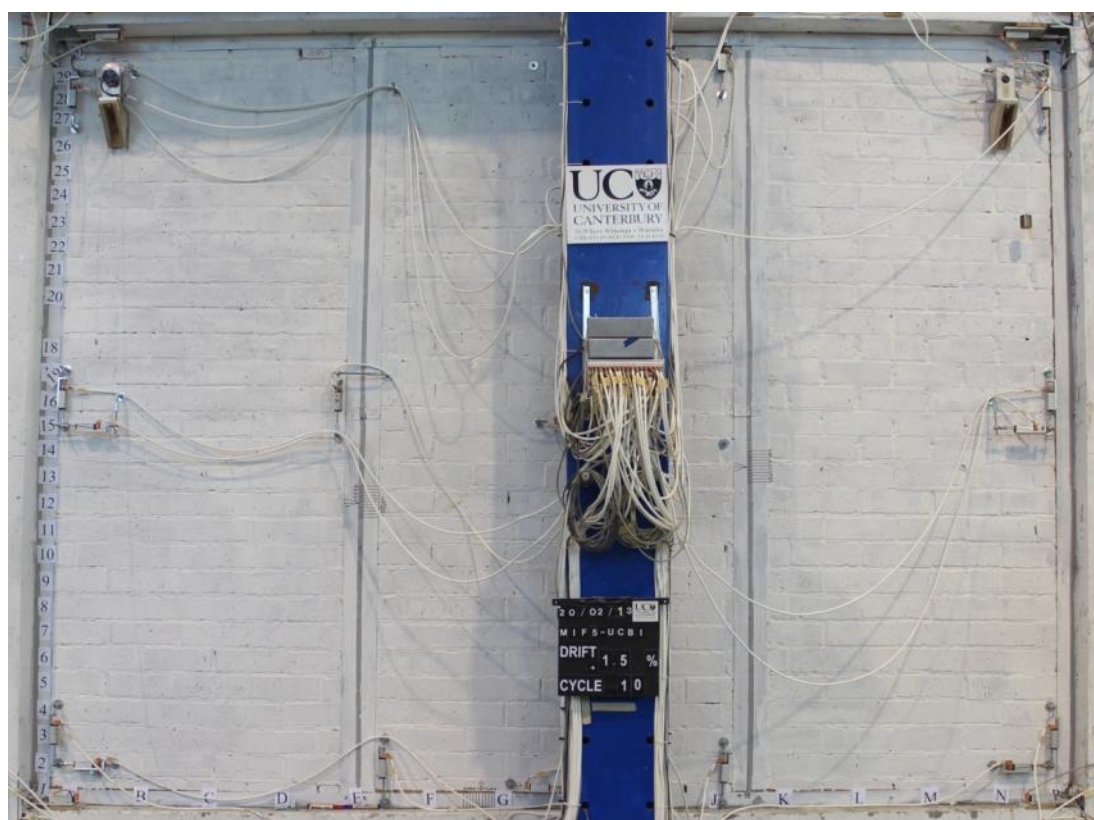


**Figure 0.52.** Low damage unreinforced clay brick infill wall specimen MIF5-UCBI at +1.5% drift

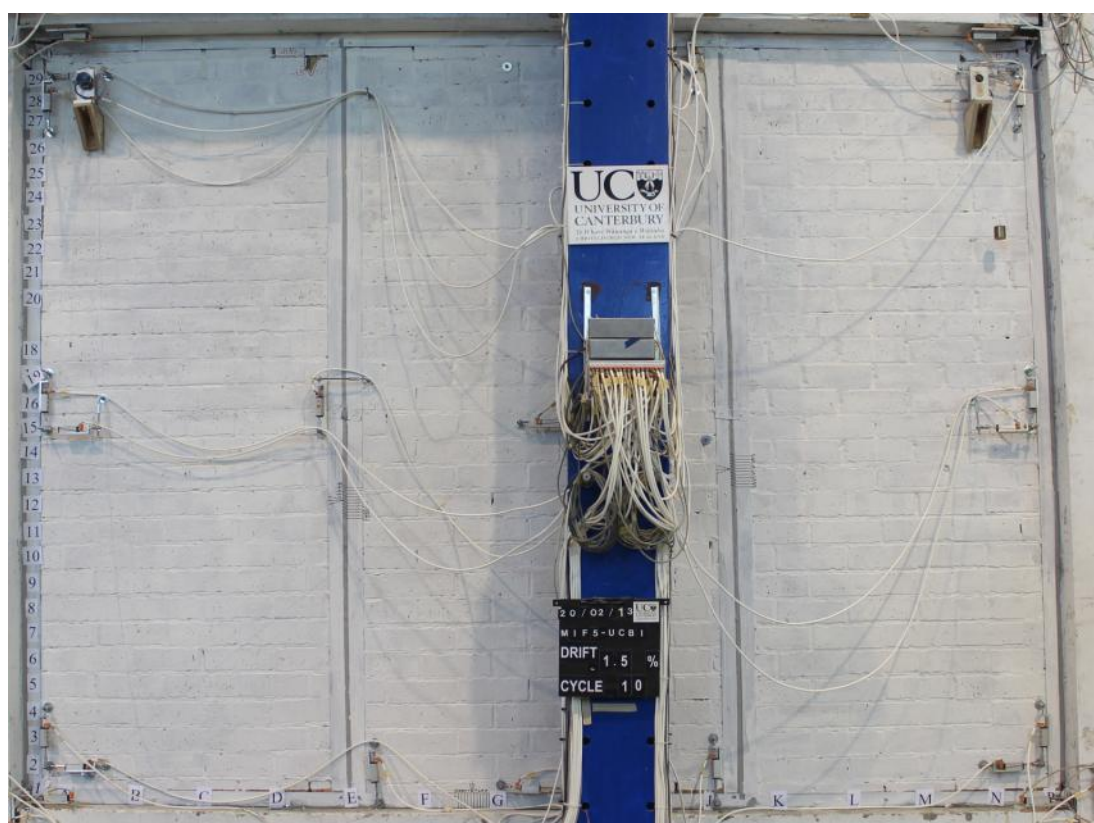


**Figure 0.53.** Low damage unreinforced clay brick infill wall specimen MIF5-UCBI at -1.5% drift

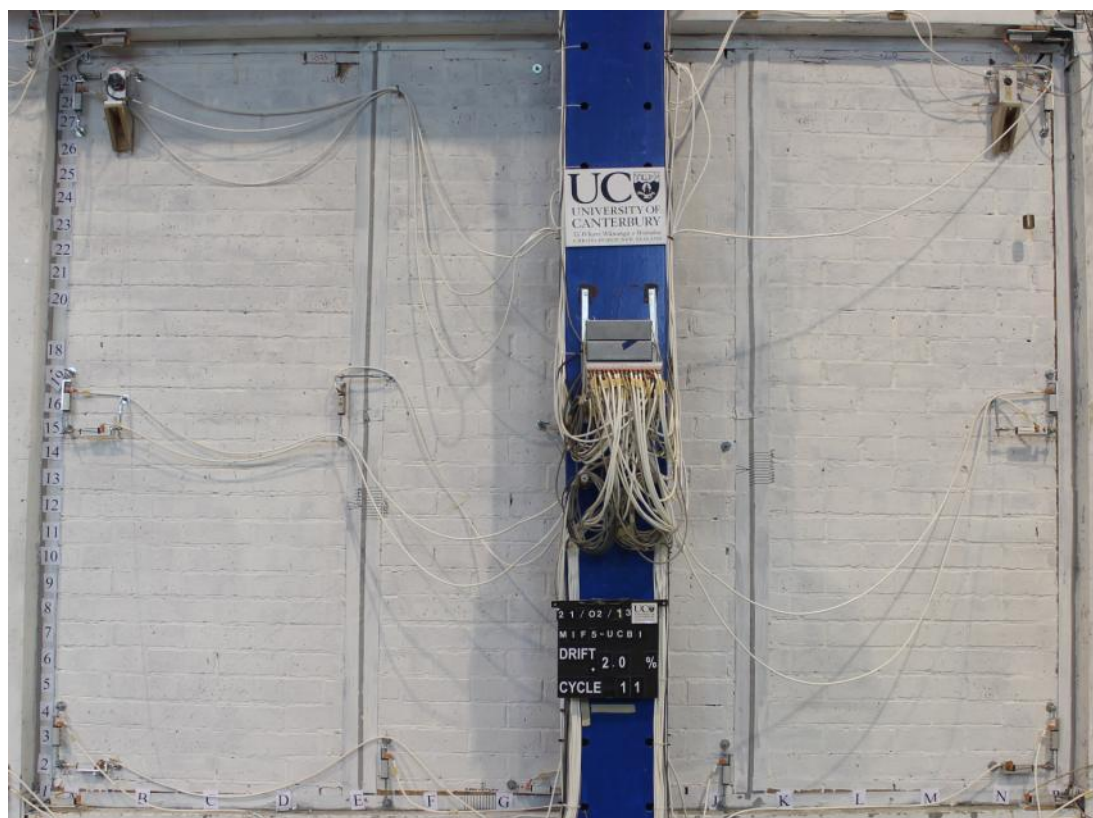


**Figure 0.54.** Low damage unreinforced clay brick infill wall specimen MIF5-UCBI at +2.0% drift

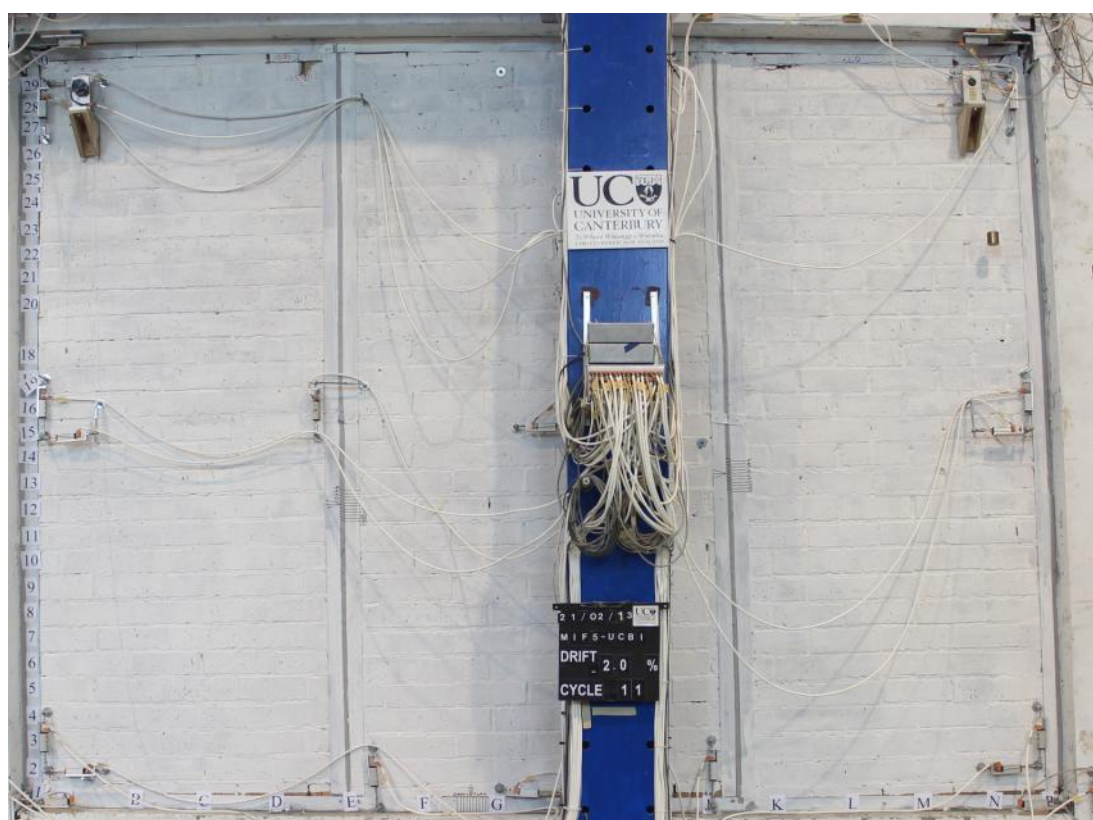


**Figure 0.55.** Low damage unreinforced clay brick infill wall specimen MIF5-UCBI at -2.0% drift



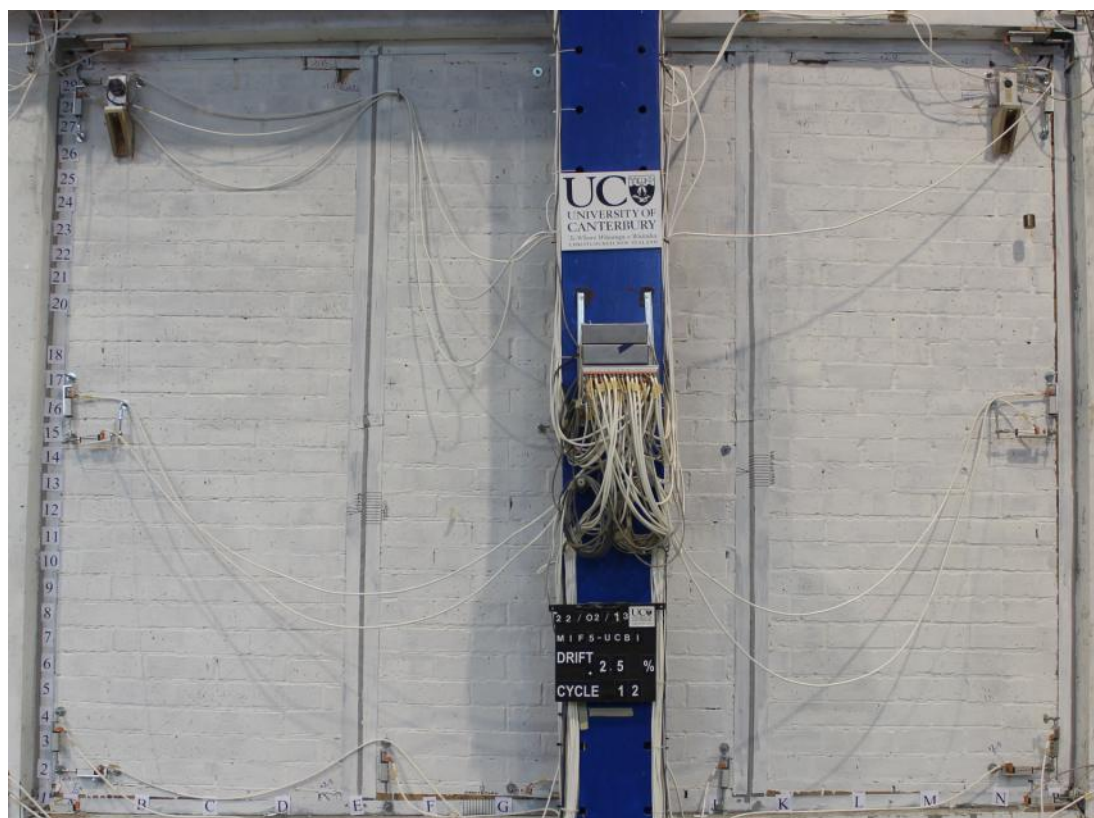


**Figure 0.56.** Low damage unreinforced clay brick infill wall specimen MIF5-UCBI at +2.5% drift

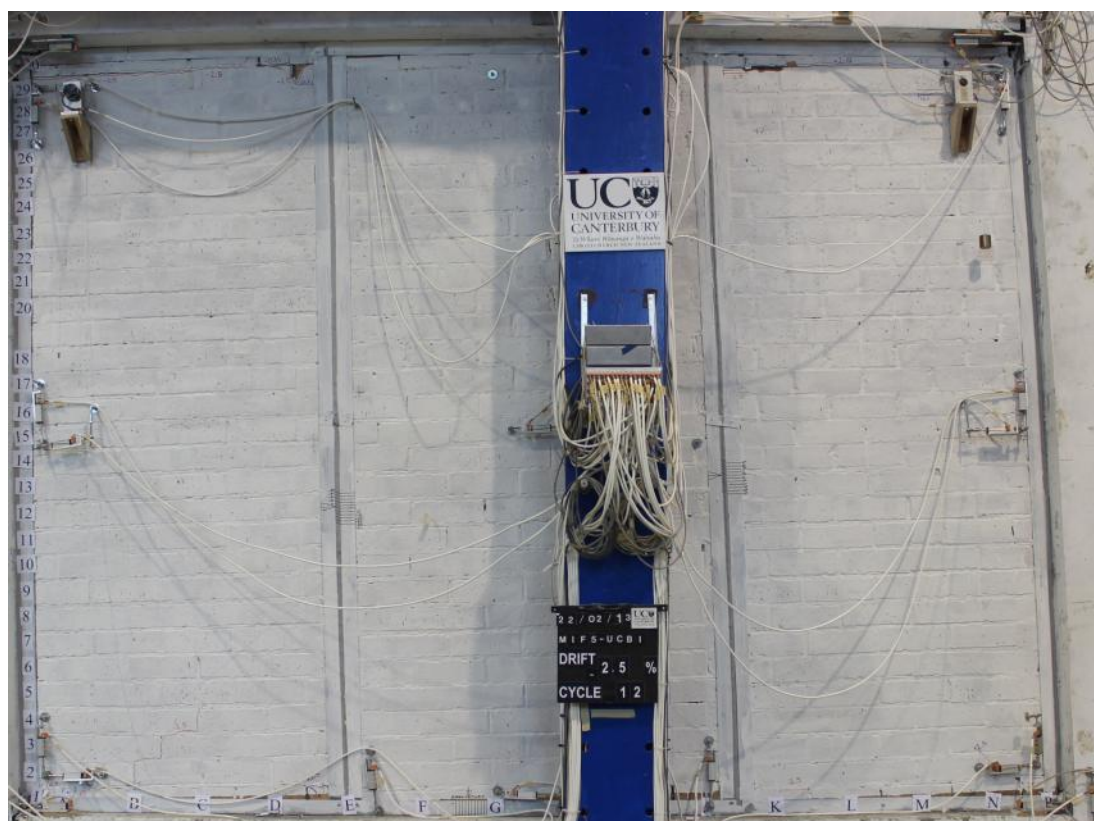


**Figure 0.57.** Low damage unreinforced clay brick infill wall specimen MIF5-UCBI at -2.5% drift



## ***H-Numerical Model of the Case Study Building in Ruaumoko 2D with As Built Steel Frame Struts***

The strut models previously given for the tested non-structural wall types can be assigned to the existing bare frame model directly by modifying the related hysteresis rule.

1	1 DESCRIPTION OF THE ANALYSIS													
1	10 STOREY RED BOOK BUILDING WITH AS BUILT STEEL FRAMED DRYWALL STRUTS													
1	UNITS: KN,M													
1	DATE: FEB 2011													
1	2 PRINCIPAL ANALYSIS OPTIONS													
1	IPANAL	IFMT	IPLAS	IPCONM	ICTYPE	IPVERT	INLGeo	IPNF	IZERO	ORTHO	IMODE			
1	2	0	1	0	2	0	1	0	0	0	0			
1	3 FRAME CONTROL PARAMETERS													
1	NNP	NMEM	NTYPE	M	MODE1	MODE2	GRAV	C1	C2	DT	TIME	FACTOR		
1	190	240	8	4	1	1	9.81	5	5	0.001	50	1		
1	4 OUTPUT INTERVALS AND PLOTTING CONTROL PARAMETERS													
1	KP	KPA	KPLOT	JOUT	DSTORT	DFACT	XMAX	YMAX	NLEVEL	NUP	IRESID	KDUMP		
1	0	500	500	0	1	2	1	1	11	2	0	0		
1	5 ITERATION CONTROL AND WAVE VELOCITIES													
1	MAXIT	MAXCIT	FTEST	WAVEX	WAVEY	THETA	DXMAX	DYMAX	D	OMEGA	F			
1	10	5	0.0001	0	0	0								
1	7 NODAL POINT INPUT													
1	NODAL POINT INPUT													
1	N	X(N)	Y(N)	NF1	NF2	NF3	KUP1	KUP2	KUP3	IOUT				
1	1	0	-3.6	1	1	1	0	0	0	0				
1	2	1	-3.6	1	1	1	0	0	0	0				
1	3	6.35	-3.6	1	1	1	0	0	0	0				
1	4	7.35	-3.6	1	1	1	0	0	0	0				
1	5	8.35	-3.6	1	1	1	0	0	0	0				
1	6	13.7	-3.6	1	1	1	0	0	0	0				
1	7	14.7	-3.6	1	1	1	0	0	0	0				
1	8	15.7	-3.6	1	1	1	0	0	0	0				
1	9	21.05	-3.6	1	1	1	0	0	0	0				
1	10	22.05	-3.6	1	1	1	0	0	0	0				
1	11	0	-2.6	0	0	0	0	0	0	0				
1	12	7.35	-2.6	0	0	0	0	0	0	0				
1	13	14.7	-2.6	0	0	0	0	0	0	0				
1	14	22.05	-2.6	0	0	0	0	0	0	0				
1	15	0	-1	0	0	0	0	0	0	0				
1	16	7.35	-1	0	0	0	0	0	0	0				
1	17	14.7	-1	0	0	0	0	0	0	0				
1	18	22.05	-1	0	0	0	0	0	0	0				
1	19	0	0	0	0	0	0	0	0	0				
1	20	1	0	0	0	0	0	0	0	0				
1	21	6.35	0	0	0	0	0	0	0	0				
1	22	7.35	0	0	0	0	0	0	0	0				
1	23	8.35	0	0	0	0	0	0	0	0				
1	24	13.7	0	0	0	0	0	0	0	0				
1	25	14.7	0	0	0	0	0	0	0	0				
1	26	15.7	0	0	0	0	0	0	0	0				
1	27	21.05	0	0	0	0	0	0	0	0				
1	28	22.05	0	0	0	0	0	0	0	0				
1	29	0	1	0	0	0	0	0	0	0				
1	30	7.35	1	0	0	0	0	0	0	0				
1	31	14.7	1	0	0	0	0	0	0	0				
1	32	22.05	1	0	0	0	0	0	0	0				
1	33	0	2.6	0	0	0	0	0	0	0				
1	34	7.35	2.6	0	0	0	0	0	0	0				
1	35	14.7	2.6	0	0	0	0	0	0	0				
1	36	22.05	2.6	0	0	0	0	0	0	0				
1	37	0	3.6	0	0	0	0	0	0	0				
1	38	1	3.6	0	0	0	0	0	0	0				
1	39	6.35	3.6	0	0	0	0	0	0	0				
1	40	7.35	3.6	0	0	0	0	0	0	0				
1	41	8.35	3.6	0	0	0	0	0	0	0				
1	42	13.7	3.6	0	0	0	0	0	0	0				
1	43	14.7	3.6	0	0	0	0	0	0	0				
1	44	15.7	3.6	0	0	0	0	0	0	0				
1	45	21.05	3.6	0	0	0	0	0	0	0				
1	46	22.05	3.6	0	0	0	0	0	0	0				
1	47	0	4.6	0	0	0	0	0	0	0				
1	48	7.35	4.6	0	0	0	0	0	0	0				
1	49	14.7	4.6	0	0	0	0	0	0	0				
1	50	22.05	4.6	0	0	0	0	0	0	0				

51	0	6.2	0	0	0	0	0	0	0
52	7.35	6.2	0	0	0	0	0	0	0
53	14.7	6.2	0	0	0	0	0	0	0
54	22.05	6.2	0	0	0	0	0	0	0
55	0	7.2	0	0	0	0	0	0	0
56	1	7.2	0	0	0	0	0	0	0
57	6.35	7.2	0	0	0	0	0	0	0
58	7.35	7.2	0	0	0	0	0	0	0
59	8.35	7.2	0	0	0	0	0	0	0
60	13.7	7.2	0	0	0	0	0	0	0
61	14.7	7.2	0	0	0	0	0	0	0
62	15.7	7.2	0	0	0	0	0	0	0
63	21.05	7.2	0	0	0	0	0	0	0
64	22.05	7.2	0	0	0	0	0	0	0
65	0	8.2	0	0	0	0	0	0	0
66	7.35	8.2	0	0	0	0	0	0	0
67	14.7	8.2	0	0	0	0	0	0	0
68	22.05	8.2	0	0	0	0	0	0	0
69	0	9.8	0	0	0	0	0	0	0
70	7.35	9.8	0	0	0	0	0	0	0
71	14.7	9.8	0	0	0	0	0	0	0
72	22.05	9.8	0	0	0	0	0	0	0
73	0	10.8	0	0	0	0	0	0	0
74	1	10.8	0	0	0	0	0	0	0
75	6.35	10.8	0	0	0	0	0	0	0
76	7.35	10.8	0	0	0	0	0	0	0
77	8.35	10.8	0	0	0	0	0	0	0
78	13.7	10.8	0	0	0	0	0	0	0
79	14.7	10.8	0	0	0	0	0	0	0
80	15.7	10.8	0	0	0	0	0	0	0
81	21.05	10.8	0	0	0	0	0	0	0
82	22.05	10.8	0	0	0	0	0	0	0
83	0	11.8	0	0	0	0	0	0	0
84	7.35	11.8	0	0	0	0	0	0	0
85	14.7	11.8	0	0	0	0	0	0	0
86	22.05	11.8	0	0	0	0	0	0	0
87	0	13.4	0	0	0	0	0	0	0
88	7.35	13.4	0	0	0	0	0	0	0
89	14.7	13.4	0	0	0	0	0	0	0
90	22.05	13.4	0	0	0	0	0	0	0
91	0	14.4	0	0	0	0	0	0	0
92	1	14.4	0	0	0	0	0	0	0
93	6.35	14.4	0	0	0	0	0	0	0
94	7.35	14.4	0	0	0	0	0	0	0
95	8.35	14.4	0	0	0	0	0	0	0
96	13.7	14.4	0	0	0	0	0	0	0
97	14.7	14.4	0	0	0	0	0	0	0
98	15.7	14.4	0	0	0	0	0	0	0
99	21.05	14.4	0	0	0	0	0	0	0
100	22.05	14.4	0	0	0	0	0	0	0
101	0	15.4	0	0	0	0	0	0	0
102	7.35	15.4	0	0	0	0	0	0	0
103	14.7	15.4	0	0	0	0	0	0	0
104	22.05	15.4	0	0	0	0	0	0	0
105	0	17	0	0	0	0	0	0	0
106	7.35	17	0	0	0	0	0	0	0
107	14.7	17	0	0	0	0	0	0	0
108	22.05	17	0	0	0	0	0	0	0
109	0	18	0	0	0	0	0	0	0
110	1	18	0	0	0	0	0	0	0
111	6.35	18	0	0	0	0	0	0	0
112	7.35	18	0	0	0	0	0	0	0
113	8.35	18	0	0	0	0	0	0	0
114	13.7	18	0	0	0	0	0	0	0
115	14.7	18	0	0	0	0	0	0	0
116	15.7	18	0	0	0	0	0	0	0
117	21.05	18	0	0	0	0	0	0	0
118	22.05	18	0	0	0	0	0	0	0
119	0	19	0	0	0	0	0	0	0
120	7.35	19	0	0	0	0	0	0	0
121	14.7	19	0	0	0	0	0	0	0



122	22.05	19	0	0	0	0	0	0	0
123	0	20.6	0	0	0	0	0	0	0
124	7.35	20.6	0	0	0	0	0	0	0
125	14.7	20.6	0	0	0	0	0	0	0
126	22.05	20.6	0	0	0	0	0	0	0
127	0	21.6	0	0	0	0	0	0	0
128	1	21.6	0	0	0	0	0	0	0
129	6.35	21.6	0	0	0	0	0	0	0
130	7.35	21.6	0	0	0	0	0	0	0
131	8.35	21.6	0	0	0	0	0	0	0
132	13.7	21.6	0	0	0	0	0	0	0
133	14.7	21.6	0	0	0	0	0	0	0
134	15.7	21.6	0	0	0	0	0	0	0
135	21.05	21.6	0	0	0	0	0	0	0
136	22.05	21.6	0	0	0	0	0	0	0
137	0	22.6	0	0	0	0	0	0	0
138	7.35	22.6	0	0	0	0	0	0	0
139	14.7	22.6	0	0	0	0	0	0	0
140	22.05	22.6	0	0	0	0	0	0	0
141	0	24.2	0	0	0	0	0	0	0
142	7.35	24.2	0	0	0	0	0	0	0
143	14.7	24.2	0	0	0	0	0	0	0
144	22.05	24.2	0	0	0	0	0	0	0
145	0	25.2	0	0	0	0	0	0	0
146	1	25.2	0	0	0	0	0	0	0
147	6.35	25.2	0	0	0	0	0	0	0
148	7.35	25.2	0	0	0	0	0	0	0
149	8.35	25.2	0	0	0	0	0	0	0
150	13.7	25.2	0	0	0	0	0	0	0
151	14.7	25.2	0	0	0	0	0	0	0
152	15.7	25.2	0	0	0	0	0	0	0
153	21.05	25.2	0	0	0	0	0	0	0
154	22.05	25.2	0	0	0	0	0	0	0
155	0	26.2	0	0	0	0	0	0	0
156	7.35	26.2	0	0	0	0	0	0	0
157	14.7	26.2	0	0	0	0	0	0	0
158	22.05	26.2	0	0	0	0	0	0	0
159	0	27.8	0	0	0	0	0	0	0
160	7.35	27.8	0	0	0	0	0	0	0
161	14.7	27.8	0	0	0	0	0	0	0
162	22.05	27.8	0	0	0	0	0	0	0
163	0	28.8	0	0	0	0	0	0	0
164	1	28.8	0	0	0	0	0	0	0
165	6.35	28.8	0	0	0	0	0	0	0
166	7.35	28.8	0	0	0	0	0	0	0
167	8.35	28.8	0	0	0	0	0	0	0
168	13.7	28.8	0	0	0	0	0	0	0
169	14.7	28.8	0	0	0	0	0	0	0
170	15.7	28.8	0	0	0	0	0	0	0
171	21.05	28.8	0	0	0	0	0	0	0
172	22.05	28.8	0	0	0	0	0	0	0
173	0	29.8	0	0	0	0	0	0	0
174	7.35	29.8	0	0	0	0	0	0	0
175	14.7	29.8	0	0	0	0	0	0	0
176	22.05	29.8	0	0	0	0	0	0	0
177	0	31.4	0	0	0	0	0	0	0
178	7.35	31.4	0	0	0	0	0	0	0
179	14.7	31.4	0	0	0	0	0	0	0
180	22.05	31.4	0	0	0	0	0	0	0
181	0	32.4	0	0	0	0	0	0	0
182	1	32.4	0	0	0	0	0	0	0
183	6.35	32.4	0	0	0	0	0	0	0
184	7.35	32.4	0	0	0	0	0	0	0
185	8.35	32.4	0	0	0	0	0	0	0
186	13.7	32.4	0	0	0	0	0	0	0
187	14.7	32.4	0	0	0	0	0	0	0
188	15.7	32.4	0	0	0	0	0	0	0
189	21.05	32.4	0	0	0	0	0	0	0
190	22.05	32.4	0	0	0	0	0	0	0

DRIFT	A	10	28	46	64	82	100	118	136	154	172	190
!	8 MEMBER TOPOLOGY/GEOMETRY											
ELEMENTS	0											
!	N	MT	NODE1	NODE2	NODE3	NODE4	IOUT					
	1	7	1	11	0	0	0					
	2	2	11	15	0	0	0					
	3	3	15	19	0	0	0					
	4	7	4	12	0	0	0					
	5	2	12	16	0	0	0					
	6	3	16	22	0	0	0					
	7	7	7	13	0	0	0					
	8	2	13	17	0	0	0					
	9	3	17	25	0	0	0					
	10	7	10	14	0	0	0					
	11	2	14	18	0	0	0					
	12	3	18	28	0	0	0					
	13	1	19	29	0	0	0					
	14	2	29	33	0	0	0					
	15	3	33	37	0	0	0					
	16	1	37	47	0	0	0					
	17	2	47	51	0	0	0					
	18	3	51	55	0	0	0					
	19	1	55	65	0	0	0					
	20	2	65	69	0	0	0					
	21	3	69	73	0	0	0					
	22	1	73	83	0	0	0					
	23	2	83	87	0	0	0					
	24	3	87	91	0	0	0					
	25	1	91	101	0	0	0					
	26	2	101	105	0	0	0					
	27	3	105	109	0	0	0					
	28	1	109	119	0	0	0					
	29	2	119	123	0	0	0					
	30	3	123	127	0	0	0					
	31	1	127	137	0	0	0					
	32	2	137	141	0	0	0					
	33	3	141	145	0	0	0					
	34	1	145	155	0	0	0					
	35	2	155	159	0	0	0					
	36	3	159	163	0	0	0					
	37	1	163	173	0	0	0					
	38	2	173	177	0	0	0					
	39	3	177	181	0	0	0					
	40	1	22	30	0	0	0					
	41	2	30	34	0	0	0					
	42	3	34	40	0	0	0					
	43	1	40	48	0	0	0					
	44	2	48	52	0	0	0					
	45	3	52	58	0	0	0					
	46	1	58	66	0	0	0					
	47	2	66	70	0	0	0					
	48	3	70	76	0	0	0					
	49	1	76	84	0	0	0					
	50	2	84	88	0	0	0					
	51	3	88	94	0	0	0					
	52	1	94	102	0	0	0					
	53	2	102	106	0	0	0					
	54	3	106	112	0	0	0					
	55	1	112	120	0	0	0					
	56	2	120	124	0	0	0					
	57	3	124	130	0	0	0					
	58	1	130	138	0	0	0					
	59	2	138	142	0	0	0					
	60	3	142	148	0	0	0					
	61	1	148	156	0	0	0					
	62	2	156	160	0	0	0					
	63	3	160	166	0	0	0					
	64	1	166	174	0	0	0					
	65	2	174	178	0	0	0					
	66	3	178	184	0	0	0					

67	1	25	31	0	0	0
68	2	31	35	0	0	0
69	3	35	43	0	0	0
70	1	43	49	0	0	0
71	2	49	53	0	0	0
72	3	53	61	0	0	0
73	1	61	67	0	0	0
74	2	67	71	0	0	0
75	3	71	79	0	0	0
76	1	79	85	0	0	0
77	2	85	89	0	0	0
78	3	89	97	0	0	0
79	1	97	103	0	0	0
80	2	103	107	0	0	0
81	3	107	115	0	0	0
82	1	115	121	0	0	0
83	2	121	125	0	0	0
84	3	125	133	0	0	0
85	1	133	139	0	0	0
86	2	139	143	0	0	0
87	3	143	151	0	0	0
88	1	151	157	0	0	0
89	2	157	161	0	0	0
90	3	161	169	0	0	0
91	1	169	175	0	0	0
92	2	175	179	0	0	0
93	3	179	187	0	0	0
94	1	28	32	0	0	0
95	2	32	36	0	0	0
96	3	36	46	0	0	0
97	1	46	50	0	0	0
98	2	50	54	0	0	0
99	3	54	64	0	0	0
100	1	64	68	0	0	0
101	2	68	72	0	0	0
102	3	72	82	0	0	0
103	1	82	86	0	0	0
104	2	86	90	0	0	0
105	3	90	100	0	0	0
106	1	100	104	0	0	0
107	2	104	108	0	0	0
108	3	108	118	0	0	0
109	1	118	122	0	0	0
110	2	122	126	0	0	0
111	3	126	136	0	0	0
112	1	136	140	0	0	0
113	2	140	144	0	0	0
114	3	144	154	0	0	0
115	1	154	158	0	0	0
116	2	158	162	0	0	0
117	3	162	172	0	0	0
118	1	172	176	0	0	0
119	2	176	180	0	0	0
120	3	180	190	0	0	0
121	4	19	20	0	0	0
122	5	20	21	0	0	0
123	6	21	22	0	0	0
124	4	22	23	0	0	0
125	5	23	24	0	0	0
126	6	24	25	0	0	0
127	4	25	26	0	0	0
128	5	26	27	0	0	0
129	6	27	28	0	0	0
130	4	37	38	0	0	0
131	5	38	39	0	0	0
132	6	39	40	0	0	0
133	4	40	41	0	0	0
134	5	41	42	0	0	0
135	6	42	43	0	0	0
136	4	43	44	0	0	0
137	5	44	45	0	0	0

138	6	45	46	0	0	0
139	4	55	56	0	0	0
140	5	56	57	0	0	0
141	6	57	58	0	0	0
142	4	58	59	0	0	0
143	5	59	60	0	0	0
144	6	60	61	0	0	0
145	4	61	62	0	0	0
146	5	62	63	0	0	0
147	6	63	64	0	0	0
148	4	73	74	0	0	0
149	5	74	75	0	0	0
150	6	75	76	0	0	0
151	4	76	77	0	0	0
152	5	77	78	0	0	0
153	6	78	79	0	0	0
154	4	79	80	0	0	0
155	5	80	81	0	0	0
156	6	81	82	0	0	0
157	4	91	92	0	0	0
158	5	92	93	0	0	0
159	6	93	94	0	0	0
160	4	94	95	0	0	0
161	5	95	96	0	0	0
162	6	96	97	0	0	0
163	4	97	98	0	0	0
164	5	98	99	0	0	0
165	6	99	100	0	0	0
166	4	109	110	0	0	0
167	5	110	111	0	0	0
168	6	111	112	0	0	0
169	4	112	113	0	0	0
170	5	113	114	0	0	0
171	6	114	115	0	0	0
172	4	115	116	0	0	0
173	5	116	117	0	0	0
174	6	117	118	0	0	0
175	4	127	128	0	0	0
176	5	128	129	0	0	0
177	6	129	130	0	0	0
178	4	130	131	0	0	0
179	5	131	132	0	0	0
180	6	132	133	0	0	0
181	4	133	134	0	0	0
182	5	134	135	0	0	0
183	6	135	136	0	0	0
184	4	145	146	0	0	0
185	5	146	147	0	0	0
186	6	147	148	0	0	0
187	4	148	149	0	0	0
188	5	149	150	0	0	0
189	6	150	151	0	0	0
190	4	151	152	0	0	0
191	5	152	153	0	0	0
192	6	153	154	0	0	0
193	4	163	164	0	0	0
194	5	164	165	0	0	0
195	6	165	166	0	0	0
196	4	166	167	0	0	0
197	5	167	168	0	0	0
198	6	168	169	0	0	0
199	4	169	170	0	0	0
200	5	170	171	0	0	0
201	6	171	172	0	0	0
202	4	181	182	0	0	0
203	5	182	183	0	0	0
204	6	183	184	0	0	0
205	4	184	185	0	0	0
206	5	185	186	0	0	0
207	6	186	187	0	0	0
208	4	187	188	0	0	0

```

209      5      188      189      0      0      0
210      6      189      190      0      0      0
211      8      1      22      0      0      0
212      8      4      25      0      0      0
213      8      7      28      0      0      0
214      8      19      40      0      0      0
215      8      22      43      0      0      0
216      8      25      46      0      0      0
217      8      37      58      0      0      0
218      8      40      61      0      0      0
219      8      43      64      0      0      0
220      8      55      76      0      0      0
221      8      58      79      0      0      0
222      8      61      82      0      0      0
223      8      73      94      0      0      0
224      8      76      97      0      0      0
225      8      79      100     0      0      0
226      8      91      112     0      0      0
227      8      94      115     0      0      0
228      8      97      118     0      0      0
229      8     109      130     0      0      0
230      8     112      133     0      0      0
231      8     115      136     0      0      0
232      8     127      148     0      0      0
233      8     130      151     0      0      0
234      8     133      154     0      0      0
235      8     145      166     0      0      0
236      8     148      169     0      0      0
237      8     151      172     0      0      0
238      8     163      184     0      0      0
239      8     166      187     0      0      0
240      8     169      190     0      0      0

!
! 9 MEMBER PROPERTY TABLES
!
! PROPS
!
! N      MTYPE LABEL
!      1 FRAME Column_c1
!
! 11A BASIC SECTION PROPERTIES
!
! ITYPE IPIN ICOND IHYST ILOS IDAMG ICOL IGA IDUCT
!      2      0      0      4      0      0      0      0      0
!
! 11B ELASTIC SECTION PROPERTIES
!
! E      G      A      AS      I      WGT      END1      END2      FJ1      FJ2
!      2.80E+07 1.17E+07 0.414 0.345 1.96E-02 9.729 0.45 0 0 0
!
! 11C MEMBER BILINEAR FACTORS
!
! RA      RF      H1      H2      H3      H4      H5      H6      H7
!      0.005 0.005 0.484 0
!
! 11G CONCRETE BEAM COLUMN YIELD SURFACE AT END1 OF MEMBER
!
! PYC      PB      MB      M1B      M2B      MO      PYT      IEND
!      -18736 -6831 2058.6 1905.5 1505.1 849.64 2073.5 0
!
! HYSTERESIS MODEL
!
! ALFA      BETA      NF      KKK
!      0.5      0.3      1      1 !
!      TAKEDA
!
!      2 FRAME Column_c2
!      1      0      0      0      0      0      0      0
!      2.80E+07 1.17E+07 0.414 0.345 1.96E-02 9.729 0 0 0
!
!      3 FRAME Column_c3
!      2      0      0      4      0      0      0      0
!      2.80E+07 1.17E+07 0.414 0.345 1.96E-02 9.729 0 0.45 0
!      0.005 0.005 0 0.484
!      -18736 -6831 2058.6 1905.5 1505.1 849.64 2073.5 0
!      0.5 0.3 1 1 !
!      TAKEDA
!
!
! N      MTYPE LABEL
!      4 FRAME Beam_b1
!
! 11A BASIC SECTION PROPERTIES
!
! ITYPE IPIN ICOND IHYST ILOS IDAMG ICOL IGA IDUCT
!      1      0      0      4      7      1      0      0      0

```

```

! 11B ELASTIC SECTION PROPERTIES
! E      G      A      AS      I      WGT      END1      END2      FJ1      FJ2
! 2.80E+07 1.17E+07 0.414 0.345 1.96E-02 9.729 0.45 0 0 0
! 11C MEMBER BILINEAR FACTORS
! RA      RF      H1      H2      H3      H4      H5      H6      H7
! 0.005 0.005 0.005 0.484 0
! 11G CONCRETE BEAM COLUMN YIELD SURFACE AT END1 OF MEMBER
! PYC      PB      MB      M1B      M2B      MO      PTT      IEND
! -18736 -6831 2058.6 1905.5 1505.1 849.64 2073.5 0
! HYSTERESIS MODEL
! ALFA      BETA      NF      KKK
! 0.5 0.3 1 1 ! TAKEDA

! 2 FRAME Column_c2
! 1 0 0 0 0 0 0 0 0
! 2.80E+07 1.17E+07 0.414 0.345 1.96E-02 9.729 0 0 0 0
! 3 FRAME Column_c3
! 2 0 0 4 0 0 0 0 0
! 2.80E+07 1.17E+07 0.414 0.345 1.96E-02 9.729 0 0.45 0 0
! 0.005 0.005 0 0.484
! -18736 -6831 2058.6 1905.5 1505.1 849.64 2073.5 0
! 0.5 0.3 1 1 ! TAKEDA

! N      MTYPE LABEL
! 4 FRAME Beam_b1
! 11A BASIC SECTION PROPERTIES
! ITYPE      IPIN      ICOND      IHYST      ILOS      IDAMG      ICOL      IGA      IDUCT
! 1 0 0 0 4 7 1 0 0 0
! 11B ELASTIC SECTION PROPERTIES
! E      G      A      AS      I      WGT      END1      END2      FJ1      FJ2
! 2.80E+07 1.17E+07 0.36 0.3 9.72E-03 8.46 0.45 0 0.00E+00 0.00E+00
! 11C MEMBER BI-LINEAR FACTORS AND HINGE PROPERTIES
! RA      RF      H1      H2      H3      H4      H5      H6      H7
! 0.001 0.001 0.363 0
! 11F BEAM YIELD CONDITIONS
! PTT      PYC      MY1+      MY1-      MY2+      MY2-      MY3+      MY3-      MY4+      MY4-
! 1295.9 -11512 544 -544 544 -544
! 11L STRENGTH DEGRADATION PARAMETERS (ONLY IF ILOS>0)
! DUCT1      DUCT2      RDUCT      DUCT3      RCYC
! 16.59 46.27 0
! 11M STIFFNESS DEGRADATION PARAMETERS (ONLY IF IHYST>0)
! ALFA      BETA      NF      KKK
! 0.3 0.2 1 1
! 11N DAMAGE INDEX DATA (ONLY IF IDAMG>0)
! MUT      MUC      MU1+      MU1-      MU2+      MU2-      MU3+      MU3-      MU4+      MU4-      BETA1      BETA2
! 100 100 16.59 16.59 16.59 16.59

! 5 FRAME Beam_b2
! 1 0 0 0 0 0 0 0 0
! 2.80E+07 1.17E+07 0.36 0.3 9.72E-03 8.46 0 0 0.00E+00 0.00E+00
! 6 FRAME Beam_b3
! 1 0 0 4 7 1 0 0 0
! 2.80E+07 1.17E+07 0.36 0.3 9.72E-03 8.46 0 0.45 0.00E+00 0.00E+00
! 0.001 0.001 0 0.363
! 1295.9 -11512 544 -544 544 -544
! 16.59 46.27 0
! 0.3 0.2 1 1
! 100 100 16.59 16.59 16.59
! 7 FRAME Column_c1
! 2 0 0 4 0 0 0 0 0
! 2.80E+07 1.17E+07 0.414 0.345 1.96E-02 9.729 0 0 0 0
! 0.005 0.005 0.484
! -18736 -6831 2058.6 1905.5 1505.1 849.64 2073.5 0
! 0.5 0.3 1 1

! N      MTYPE LABEL
! 8 SPRING STRUT
! 12A BASIC SECTION PROPERTIES
! ITYPE      IHYST      ILOS      IDAMG      KX      KY      GJ      WGT      RF      RT      PSX      PSY      PSZ      THETAITRUSS      IOP
! 1 9 0 0 15000 0 0 0 0 0.001 0 0 0 0 0 0
! 12C YIELD SURFACE
! FX+      FX-      FY+      FY-      MZ+      MZ-
! 45 -40 0 0 0 0
! FU      FI      PTRI      PUNL      GAP+      GAP-      BETA      ALPHA      LOOP
! 45 0 0 2 0 0 1.04 0.2 1

! 21 LUMPED WEIGHTS AT NODES
WEIGHTS
! N      WX      WY      WM
! 1 0 0 0
! 2 0 0 0
! 3 0 0 0
! 4 0 0 0
! 5 0 0 0
! 6 0 0 0
! 7 0 0 0
! 8 0 0 0
! 9 0 0 0
! 10 0 0 0
! 11 0 0 0
! 12 0 0 0
! 13 0 0 0
! 14 0 0 0
! 15 0 0 0
! 16 0 0 0
! 17 0 0 0
! 18 0 0 0
! 19 650 0 0
! 20 0 0 0

```

STRUT MODEL

21	0	0	0
22	650	0	0
23	0	0	0
24	0	0	0
25	650	0	0
26	0	0	0
27	0	0	0
28	650	0	0
29	0	0	0
30	0	0	0
31	0	0	0
32	0	0	0
33	0	0	0
34	0	0	0
35	0	0	0
36	0	0	0
37	650	0	0
38	0	0	0
39	0	0	0
40	650	0	0
41	0	0	0
42	0	0	0
43	650	0	0
44	0	0	0
45	0	0	0
46	650	0	0
47	0	0	0
48	0	0	0
49	0	0	0
50	0	0	0
51	0	0	0
52	0	0	0
53	0	0	0
54	0	0	0
55	650	0	0
56	0	0	0
57	0	0	0
58	650	0	0
59	0	0	0
60	0	0	0
61	650	0	0
62	0	0	0
63	0	0	0
64	650	0	0
65	0	0	0
66	0	0	0
67	0	0	0
68	0	0	0
69	0	0	0
70	0	0	0
71	0	0	0
72	0	0	0
73	650	0	0
74	0	0	0
75	0	0	0
76	650	0	0
77	0	0	0
78	0	0	0
79	650	0	0
80	0	0	0
81	0	0	0
82	650	0	0
83	0	0	0
84	0	0	0
85	0	0	0
86	0	0	0
87	0	0	0
88	0	0	0
89	0	0	0
90	0	0	0
91	650	0	0

92	0	0	0
93	0	0	0
94	650	0	0
95	0	0	0
96	0	0	0
97	650	0	0
98	0	0	0
99	0	0	0
100	650	0	0
101	0	0	0
102	0	0	0
103	0	0	0
104	0	0	0
105	0	0	0
106	0	0	0
107	0	0	0
108	0	0	0
109	650	0	0
110	0	0	0
111	0	0	0
112	650	0	0
113	0	0	0
114	0	0	0
115	650	0	0
116	0	0	0
117	0	0	0
118	650	0	0
119	0	0	0
120	0	0	0
121	0	0	0
122	0	0	0
123	0	0	0
124	0	0	0
125	0	0	0
126	0	0	0
127	650	0	0
128	0	0	0
129	0	0	0
130	650	0	0
131	0	0	0
132	0	0	0
133	650	0	0
134	0	0	0
135	0	0	0
136	650	0	0
137	0	0	0
138	0	0	0
139	0	0	0
140	0	0	0
141	0	0	0
142	0	0	0
143	0	0	0
144	0	0	0
145	650	0	0
146	0	0	0
147	0	0	0
148	650	0	0
149	0	0	0
150	0	0	0
151	650	0	0
152	0	0	0
153	0	0	0
154	650	0	0
155	0	0	0
156	0	0	0
157	0	0	0
158	0	0	0
159	0	0	0
160	0	0	0
161	0	0	0
162	0	0	0



163	650	0	0
164	0	0	0
165	0	0	0
166	650	0	0
167	0	0	0
168	0	0	0
169	650	0	0
170	0	0	0
171	0	0	0
172	650	0	0
173	0	0	0
174	0	0	0
175	0	0	0
176	0	0	0
177	0	0	0
178	0	0	0
179	0	0	0
180	0	0	0
181	650	0	0
182	0	0	0
183	0	0	0
184	650	0	0
185	0	0	0
186	0	0	0
187	650	0	0
188	0	0	0
189	0	0	0
190	650	0	0

EXTERNAL NODAL STATICAL LOADS				
LOADS	N	FX	FY	FM
1		0	0	0
2		0	0	0
3		0	0	0
4		0	0	0
5		0	0	0
6		0	0	0
7		0	0	0
8		0	0	0
9		0	0	0
10		0	0	0
11		0	0	0
12		0	0	0
13		0	0	0
14		0	0	0
15		0	0	0
16		0	0	0
17		0	0	0
18		0	0	0
19		0	-260	0
20		0	0	0
21		0	0	0
22		0	-260	0
23		0	0	0
24		0	0	0
25		0	-260	0
26		0	0	0
27		0	0	0
28		0	-260	0
29		0	0	0
30		0	0	0
31		0	0	0
32		0	0	0
33		0	0	0
34		0	0	0
35		0	0	0
36		0	0	0
37		0	-260	0
38		0	0	0
39		0	0	0

40	0	-260	0
41	0	0	0
42	0	0	0
43	0	-260	0
44	0	0	0
45	0	0	0
46	0	-260	0
47	0	0	0
48	0	0	0
49	0	0	0
50	0	0	0
51	0	0	0
52	0	0	0
53	0	0	0
54	0	0	0
55	0	-260	0
56	0	0	0
57	0	0	0
58	0	-260	0
59	0	0	0
60	0	0	0
61	0	-260	0
62	0	0	0
63	0	0	0
64	0	-260	0
65	0	0	0
66	0	0	0
67	0	0	0
68	0	0	0
69	0	0	0
70	0	0	0
71	0	0	0
72	0	0	0
73	0	-260	0
74	0	0	0
75	0	0	0
76	0	-260	0
77	0	0	0
78	0	0	0
79	0	-260	0
80	0	0	0
81	0	0	0
82	0	-260	0
83	0	0	0
84	0	0	0
85	0	0	0
86	0	0	0
87	0	0	0
88	0	0	0
89	0	0	0
90	0	0	0
91	0	-260	0
92	0	0	0
93	0	0	0
94	0	-260	0
95	0	0	0
96	0	0	0
97	0	-260	0
98	0	0	0
99	0	0	0
100	0	-260	0
101	0	0	0
102	0	0	0
103	0	0	0
104	0	0	0
105	0	0	0
106	0	0	0
107	0	0	0
108	0	0	0
109	0	-260	0
110	0	0	0

111	0	0	0
112	0	-260	0
113	0	0	0
114	0	0	0
115	0	-260	0
116	0	0	0
117	0	0	0
118	0	-260	0
119	0	0	0
120	0	0	0
121	0	0	0
122	0	0	0
123	0	0	0
124	0	0	0
125	0	0	0
126	0	0	0
127	0	-260	0
128	0	0	0
129	0	0	0
130	0	-260	0
131	0	0	0
132	0	0	0
133	0	-260	0
134	0	0	0
135	0	0	0
136	0	-260	0
137	0	0	0
138	0	0	0
139	0	0	0
140	0	0	0
141	0	0	0
142	0	0	0
143	0	0	0
144	0	0	0
145	0	-260	0
146	0	0	0
147	0	0	0
148	0	-260	0
149	0	0	0
150	0	0	0
151	0	-260	0
152	0	0	0
153	0	0	0
154	0	-260	0
155	0	0	0
156	0	0	0
157	0	0	0
158	0	0	0
159	0	0	0
160	0	0	0
161	0	0	0
162	0	0	0
163	0	-260	0
164	0	0	0
165	0	0	0
166	0	-260	0
167	0	0	0
168	0	0	0
169	0	-260	0
170	0	0	0
171	0	0	0
172	0	-260	0
173	0	0	0
174	0	0	0
175	0	0	0
176	0	0	0
177	0	0	0
178	0	0	0
179	0	0	0
180	0	0	0
181	0	-260	0
182	0	0	0
183	0	0	0
184	0	-260	0
185	0	0	0
186	0	0	0
187	0	-260	0
188	0	0	0
189	0	0	0
190	0	-260	0
! EXCITATION FLAG			
! EQUAKE			
IBERG	ISTART	DELTAT	ASCALE
6	1	0.005	1
END	VEL	DIS	TSCALE
-1	0	0	1

